SPIE.

OPTICAL GLASS

Peter Hartmann

OPTICAL
GLASS

OPTICAL GLASS

Peter Hartmann

SPIE PRESS
Bellingham, Washington USA

Library of Congress Preassigned Control Number: 2014942744

for

Optical glass (ISBN 9781628412925).

Published by
SPIE
P.O. Box 10
Bellingham, Washington 98227-0010 USA
Phone: +1 360.676.3290
Fax: +1 360.647.1445
Email: books@spie.org
Web: http://spie.org

Copyright © 2014 Society of Photo-Optical Instrumentation Engineers (SPIE)

All rights reserved. No part of this publication may be reproduced or distributed in any form or by any means without written permission of the publisher.

The content of this book reflects the work and thought of the author. Every effort has been made to publish reliable and accurate information herein, but the publisher is not responsible for the validity of the information or for any outcomes resulting from reliance thereon.

Printed in the United States of America.
First printing

Contents

Preface ix
Acknowledgments xi
List of Symbols xiii

Chapter 1 Optical Glass: Significance and Definitions 1
1.1 Key Enabling Material 1
1.2 The History of Optical Glass 3
1.3 General Glass Properties 7
1.4 Optical Glass: Definition 8
1.5 Optical Glass Types 9
1.6 Optical Glass Types: Denominations 10
1.7 Optical Glass Types: Glass Codes 10
1.8 Optical Glass Types: Portfolio 11
1.9 Optical Glass Types: Availability 14
1.10 Selected Types of Optical Glass 15
References 16

Chapter 2 Production of Optical Glass 19
2.1 Melting 19
2.2 Annealing 23
2.3 Reheat Pressing 28
2.4 Precision Molding 29
References 31

Chapter 3 Refractive Index and Dispersion 33
3.1 Snell's Law of Refraction 33
3.2 Dispersion: Abbe Number 33
3.3 Characteristic Light Wavelengths 35
3.4 Partial Dispersion 36
3.5 Dispersion Formulas 40
3.6 Refractive Index Tolerances 43
3.7 Refractive Index Variation Tolerances 43
3.8 Abbe Number Tolerances 44
3.9 Annealing Influence on Refractive Index and Dispersion 45
3.10 Annealing Influence on Different Glass Types 49
3.11 Annealing Schedule 52
3.12 Refractive Index Measurement: V-Block 54

3.13 Standard Test Certificate: V-Block 55
3.14 Test Certificate for a Delivery Lot 56
3.15 Refractive Index Measurement: Prism Goniometer 57
3.16 Sellmeier Data Fit Quality 59
3.17 Test Certificate: Prism Goniometer 60
3.18 Refractive Index: Temperature Influence 61
3.19 Temperature Coefficient Measurement Reproducibility and Melt Variations 64
3.20 Temperature Coefficients of the Refractive Index 67
3.21 Thermo-optical Coefficient 74
References 76

Chapter 4 Homogeneity 77
4.1 Optical Homogeneity versus Striae 77
4.2 Optical Homogeneity: Tolerances 78
4.3 Wavefront Measurement 79
4.4 Optical Homogeneity: Measurement of Glass Items 80
4.5 Optical Homogeneity in Glass Items 82
4.6 Optical Homogeneity of Glass Types 86
4.7 Striae Appearance 88
4.8 Striae Measurement: The Shadowgraph Method 89
4.9 Striae Specification 90
4.10 Stress Birefringence: Refractive Index Homogeneity in Polarized Light 91
4.11 Stress-Optical Coefficient 92
4.12 Stress Birefringence: Limit Values for Typical Applications 94
4.13 Stress Birefringence: Size Effect 95
4.14 Transient Stress Birefringence 96
4.15 Birefringence Measurement 98
4.16 Bubbles and Other Inclusions 99
4.17 Bubbles and Inclusions: Inspection 100
4.18 Bubbles and Inclusions: Specification 101
References 103

Chapter 5 Transmittance 105
5.1 Internal Transmittance 105
5.2 Measurement of Internal Transmittance 106
5.3 Overall Internal Transmittance of Optical Glass 106
5.4 Internal Transmittance: Color Code 110
5.5 Internal Transmittance Tolerances and High Transmittance Quality Grade 111
5.6 Fluorescence 114
5.7 Solarization 115

5.8 Ionizing-Irradiation-Induced Transmittance Loss: Radiation Damage........116
5.9 Use of Optical Glass in the UV and IR Wavelength Ranges........118
References........119

Chapter 6 Chemical Resistance........121
6.1 General Remarks on Chemical Resistance of Optical Glasses...... 121
6.2 Chemical Resistance: Measurement and Classification........121
6.3 Chemical Resistance of the Optical Glass Types: Overview Diagrams........123

Chapter 7 Mechanical Properties........127
7.1 Density........127
7.2 Elasticity: Young's Modulus........128
7.3 Knoop Hardness........129
7.4 Grindability........130
7.5 Bending Strength........131
7.6 Mechanical Properties of Selected Optical Glass Types........133

Chapter 8 Thermal Properties........135
8.1 Viscosity........135
8.2 Thermal Expansion........135
8.3 Transformation Temperature........137
8.4 Thermal Conductivity and Heat Capacity........138
8.5 Thermally Induced Stress........139
8.6 Thermal Properties of Selected Glass Types........139

Chapter 9 Environmental Properties........141
References........143

Chapter 10 Specification of Optical Elements: Recommendations for Optical Glass Properties and Optical Element Manufacturing........145
10.1 Small, Thin Lenses........146
10.2 Medium-Sized Lenses and Prisms........146
10.3 Large Lenses and Prisms........146
References........149

Chapter 11 Other Optical Materials........151
11.1 General Requirements on Materials for Optical Elements........151
11.2 Other Materials Used for Optical Elements........151
References........154

Standards........155
Bibliography........157
Index........159

Preface

Very few books on optical glass are available in the literature. Especially lacking is a compilation of the basic properties of optical glass for readers who are not specialists in glass but need some information for their work with optical glass elements. For example, ISO has plans to write a new part (Part 18) of the international standard ISO 10110 (Optics and Photonics—Preparation of Drawings for Optical Elements and Systems) that will replace Parts 2, 3, and 4 on material imperfections. Providing only the formal specification tolerances for material properties of optical elements leaves the user with the problem of how to translate these requirements into the optical raw glass delivery forms needed for the production of optical elements. Such a translation needs to include some information about optical glass, its properties, and its production. A number of specific issues are encountered when dealing with optical glass that, if ignored, can easily lead to problems in daily practice. These problems result in, for example, unexpected availability difficulties, long delivery times, and high prices for special tolerances, sizes, and shapes.

In the past, such problems have originated from the fact that instructions in the way of optical element drawings, alone, have been simply copied to glass purchase orders. The example of the zero-bubble requirement for a small lens transferred to an entire large strip of 800-mm length may seem odd, but this actually happened. The question, "Will you throw away an entire 800-mm strip just because there is a single bubble inside?" solved the problem instantly. But such an incident illustrates the need for information on optical glass and its properties that also relates to glass item sizes. This book is meant to reduce communication problems between the glass supplier and the customers.

Many years of responding to customer's questions on optical glass has led to the *SCHOTT Technical Information Exchange* (TIE) series, which treats special aspects in a set of articles. However, it is not possible to simply assemble these exchanges and publish them as a book. A considerable amount of additional information is needed to provide a general overview, which this book provides.

Another observation is that optical glass is deemed to be a commodity product in the view of many people, even leaders in the optics industry. Therefore, a short chapter points out the key enabling character of this material for science and technology as a whole. Optical glass manufacturing needs outstanding capabilities; it is not a technology for which one can simply purchase a standard production plant and begin delivery.

Optical glass is a material with a high leverage effect. As a rule, the value of optical systems is 100 times higher than that of the glass used in the systems.

Thus, there is little room for cost-cutting strategies. On the other hand, each dollar of missing optical glass will lead to the loss of $100 in turnover. Delivery of a glassless microscope is a 99% deal for the system supplier and a 100% loss for his customer. Optical glass purchasing strategies should take this fact into account.

Optical glass is a high-tech product. Its main property, refractive index, is specified and monitored to the fifth decimal place, whereas technical glasses need only one to three digits in their refractive indices. Everyone who has ever improved production tolerances or has related measurement methods knows that each digit or each factor of ten of higher accuracy means not only another digit to be read from the display but also a factor of ten of more precise equipment and stabilization, a more highly mastered environment, and more highly skilled personnel. Optical glass is two orders of magnitude away from the highest-quality technical glass; thus, its production and quality assurance is in another category altogether.

Chemistry plays the decisive role in melting. This is especially the case for the most sought-after extreme glass types, which present particular challenges during the melting and casting process. If these challenges are not overcome, the material can end up as polycrystalline pieces that are useless for optics. A variety of melting facilities must be maintained in high standards in order to produce the many different optical glass types. Even though optical glasses end up looking very much the same as technical glasses, their production requires different setups with different resistances of the facilities against high temperature and highly chemically aggressive melts. This involves developing high-precision chemistry under adverse conditions.

But even these mastered processes can define refractive index only to the third decimal place. Therefore, it is not only the melting processes that must be mastered, but also the subsequent heat treatment, the so-called fine annealing. During this annealing process, the refractive index is adjusted to the required fifth decimal place.

Optical glass without the data given in a test report is useless. For reliable provision of actual test results from glass items, sophisticated sample logistics are necessary to obtain melt-specific glass data. These data must be determined with precise measurement methods. For fine control of annealing processes, carefully determined typical glass data are needed.

Optical homogeneity is another critical requirement on optical glass items. High homogeneity becomes an increasing challenge with larger sizes of glass pieces. This holds not only for production but also for measurement. Generally, size increase exacerbates issues pertaining to many optical glass properties such as stress birefringence, striae, and transmittance. Detrimental effects not only increase linearly with size but also grow stronger for most properties. This will be pointed out accordingly.

For a set of other properties, overview diagrams similar to the one at the end of this Preface are provided that rank glass types with respect to these properties. The last chapter of the book gives practical advice for transferring material requirements on optical elements to the raw glass forms to be purchased from the glass supplier.

This book concentrates on optical glass and its principal purpose of imaging with visible light. Other materials with core applications outside of the visible light range, such as fused silica and calcium fluoride, or infrared light materials such as chalcogenides, zinc sulfide, zinc selenide, sapphire, and germanium, are outside the scope of this book. These materials are very different from optical glasses in many aspects. Of these materials, only fused silica and chalcogenides are also classified as glasses. However, these two materials consist of only a few components (3 or fewer) in contrast to optical glasses, which consist of 6–12 components. The other materials are crystals or microcrystalline materials. In any case, the production processes and properties of the mentioned materials are very different from those of optical glasses.

Acknowledgments

The author thanks Ralf Reiter for his continuous support in writing this book and Ralf Jedamzik for his contributions to this field.

Without the enduring, creative, and careful work of numerous people at SCHOTT, the current, outstanding level of melting, annealing, and optical metrology would not have been reached.

Thanks are also due to the users of the glass, who ask many questions that lead to further progress in a field that, even after 130 years, is still vividly developing.

Finally, the author is grateful to optical glass itself, which has decisively influenced technical civilization and will continue to do so for a long time to come.

Peter Hartmann
August 2014

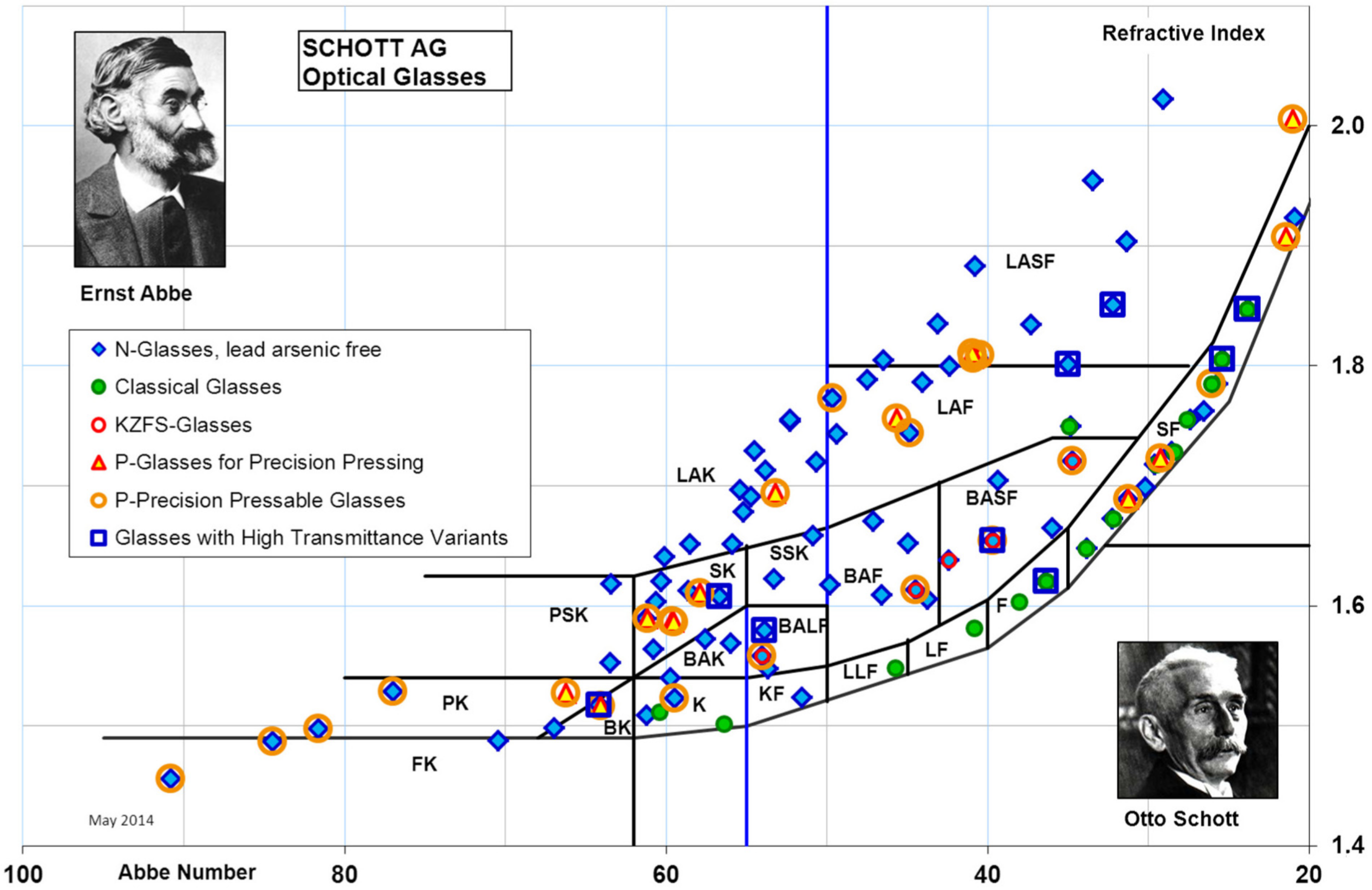

SCHOTT Optical glass program of 2014: Abbe diagram.

List of Symbols

A	grade number = square root of a bubble's cross-section area
$A_0, \ldots, A_5$	glass-melt-specific coefficients of Laurent series expansion dispersion formula
$B_1, \ldots, C_3$	glass-melt-specific coefficients of Sellmeier dispersion formula
$D_0, D_1, D_2,$ $E_0, E_1, \lambda_{\mathrm{TK}}$	glass-type-specific coefficients of the dispersion formula for the temperature coefficients
dn_{abs}/dT	temperature coefficient for the absolute refractive index
dn_{rel}/dT	temperature coefficient for the refractive index relative to air
E	Young's modulus
$G(\lambda,T)$	thermo-optical coefficient
HG	grindability according to ISO 12844
HK	Knoop hardness according to ISO 9385
$K_{\parallel}$	stress optical coefficient for light polarized parallel to the stress direction
$K_{\perp}$	stress optical coefficient for light polarized perpendicular to the stress direction
$K = K_{\parallel} - K_{\perp}$	glass-type-specific stress optical coefficient
$K_{\Delta T}$	figure of merit ranking optical glasses with respect to the amount of birefringence related to temperature gradients within the glass
m_{nd}	annealing parameter for refractive index change with annealing rate
m_{vd}	annealing parameter for Abbe number change with annealing rate
n	refractive index
$n_{\parallel}$	refractive index for light polarized parallel to the stress direction
$n_{\perp}$	refractive index for light polarized perpendicular to the stress direction
$n_{\mathrm{abs}}(\lambda,T)$	absolute refractive index at wavelength λ and temperature T

n_d	refractive index at the wavelength of the helium d line
$n_\mathrm{F} - n_\mathrm{C}$	principal dispersion for mercury F and C lines
$n_{\mathrm{F}'} - n_{\mathrm{C}'}$	principal dispersion for cadmium F′ and C′ lines
$n_\mathrm{rel}(\lambda,T)$	refractive index relative to air at wavelength λ and temperature T
$P_{x,y}$	relative partial dispersion for the wavelengths x and y related to principal dispersion for mercury F and C lines
$P'_{x,y}$	relative partial dispersion for the wavelengths x and y related to principal dispersion for cadmium F′ and C′ lines
$P(\lambda)$	reflection factor = ratio between transmittance and internal transmittance
$\mathrm{T}_{10}{}^{4}$	characteristic viscosity temperature: working point
$\mathrm{T}_{10}{}^{7.6}$	characteristic viscosity temperature: softening point
$\mathrm{T}_{10}{}^{13.2}$	characteristic viscosity temperature: annealing point
$\mathrm{T}_{10}{}^{14.5}$	characteristic viscosity temperature: strain point
T_g	transformation temperature
UVC 80/10	UV cutoff edge according to ISO 12123
$\alpha_{-30/+70\,^\circ\mathrm{C}}$	coefficient of thermal expansion in the temperature range of –30 °C to +70 °C
$\Delta s = K\sigma d$	optical path difference at stress σ and glass thickness d, and with stress optical coefficient K
$\Delta n_\mathrm{rel}(\lambda,T,T_0)$	difference of the refractive indices relative to air at target temperature T and at room temperature $T_0 = 20\,^\circ\mathrm{C}$ for wavelength λ
$\Delta P_{x,y}$	deviation of the partial dispersion $P_{x,y}$ from Abbe’s rule: $P_{x,y} = a_{x,y} + b_{x,y} \times \nu_\mathrm{d}$
ΔW	optical path length change or wavefront deformation
λ	wavelength
μ	Poisson’s ratio
ν_d	$= (n_\mathrm{d} - 1)/(n_\mathrm{F} - n_\mathrm{C})$ Abbe number referring to the helium d line
ν_e	$= (n_\mathrm{e} - 1)/(n_{\mathrm{F}'} - n_{\mathrm{C}'})$ Abbe number referring to the mercury e line
ν_k	annealing rate: temperature change rate in Kelvin per hour (K/h)

τ	transmittance = transmitted light intensity / incident light intensity
τ_i	internal transmittance = light transmitted without reflection losses
$\varphi = \alpha E/(1 - \mu)$	thermal stress factor

Chapter 1
Optical Glass: Significance and Definitions

1.1 Key Enabling Material

Optical glass is a very important material in the development of technology and thus of the history of mankind as a whole. It first allowed access to the micro- and macrocosm, when, about 400 years ago, the microscope and the telescope were invented at almost the same time and location in the town Middelburg in the Netherlands (Fig. 1.1). Although glass lenses were known before this time, only the combination of two or more lenses forming optical instruments could increase magnification to such an extent that new worlds were opened to human vision and investigation.

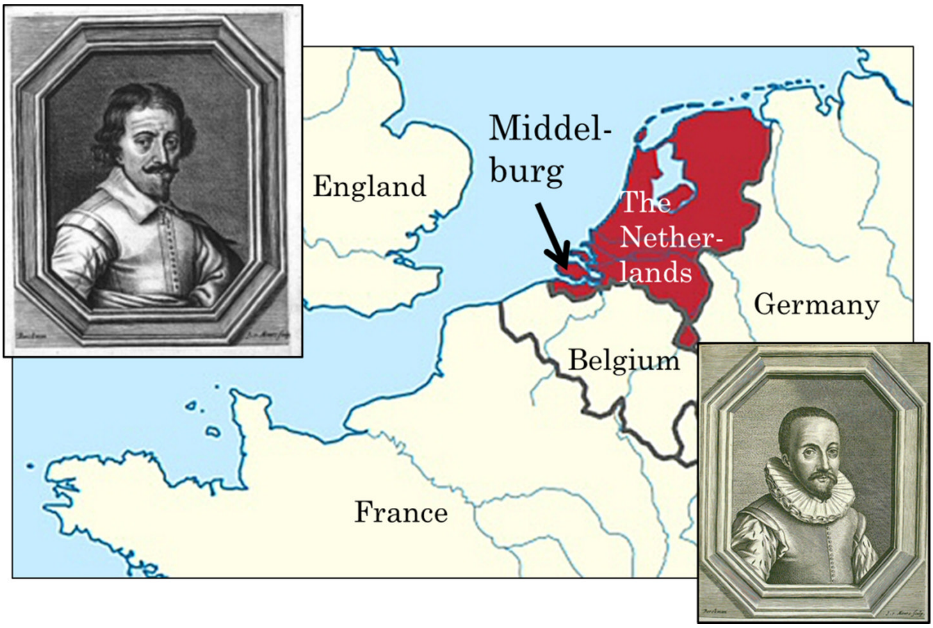

Figure 1.1 The invention of the microscope (Zacharias Janssen, left) and the telescope (Hans Lippershey, right) at almost the same time (ca. 1600) and location (Middelburg in the Netherlands) marks one of the great milestones in technology development. (Courtesy of Wikipedia.)

Glass was the only bulk material capable of changing the direction of light rays without impairing them by absorption or scattering that could be produced in large volume with comparatively low cost. This property is still the basis of a vast variety of optical systems in use today, not only for imaging but for light management in general. Today's microscopes are highly sophisticated instruments with outstanding precision mechanics, computer control, and software assistance. But without the glass inside of them, they are worthless.

Quite obvious is the use of optical glass in consumer products such as photography cameras, camcorders, and binoculars. The general public is also familiar with applications in movie cameras and projectors. Much less known is the fact that optical systems have widespread use in metrology, which is the necessary precondition process in any manufacturing. The automotive industry uses stationary, computer-numerical controlled 3D (CNC 3D) measurement machines, which appear to work mechanically. However, a closer look shows that these machines work with glass–ceramic-scale readout using small lenses. Mobile machines provide 3D measurement directly at the workshop floor. In the aviation- and ship-building industries, very large elements need to precisely fit one another. This is also achieved with 3D measurement machines, so-called laser trackers. In general industry, quite often large machines need to be precisely aligned; this is achieved with optical systems. Products will be quality controlled with telecentric optical lens systems. Machine vision systems are ubiquitous nowadays. Theodolites are workhorses for civil engineering. Land surveying, the application that boosted the development of optics 200 years ago, uses earth-bound, airborne, and spaceborne optical systems.

Optical glass is of high strategic importance in military applications. The best and most precise weapons are useless without accurate aiming devices. Submarines need high-performance periscopes with large optical elements of the highest quality. In 1917, when the U.S. entered World War I, they were cut off from the German glass supply and had to invent the production of the most essential optical glass types within six months.

The progress in information technology is unthinkable without optical glass, which was the pioneering material for pattern transfer of integrated circuits on silicon chips via optical imaging. Microbiology owes its tremendous progress mainly to microscopy (Fig. 1.2). Medicine uses optical systems for research, diagnosis, and therapy. A large part of the 20-year prolongation of the average human lifespan between 1880 and 1950 is due to the fight against infectious diseases, where high-resolution microscopes played a decisive role. Optical spectrographs were the key instruments for the foundation of quantum mechanics, and telescopes were key in the development of general relativity theory.

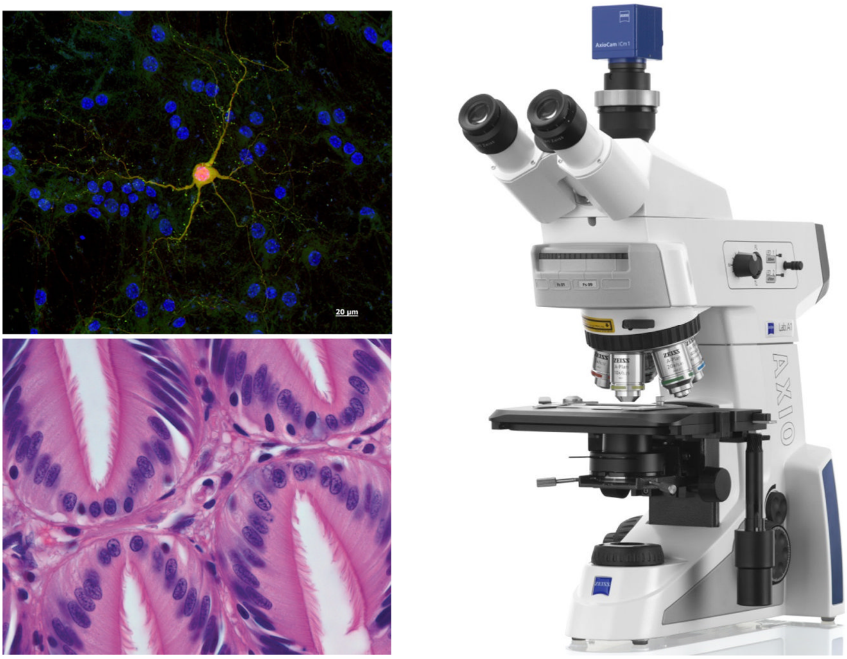

Figure 1.2 Microscopes (right) have opened human vision for the micro-world (left top: neuron, left bottom: liver tissue) and are absolutely essential tools for many science and technology fields.

Optical systems that use highly sophisticated optical glasses fulfilling narrowest tolerances are key enabling systems throughout all technology. There have been times in history when general technical progress was delayed or even prevented because suitable optical glasses were not available. In most applications, the glass items are not directly visible. And even if it is so, they are taken for granted and not recognized as high-tech materials that have required 400 years of development and that are continuously challenging their producers.[1]

1.2 The History of Optical Glass

Glass is one of the oldest manmade materials. In most of its more than 5000-year history, it was used only for decorative purposes as vases, goblets, and drink ware. Its use as an optical material began with the development of spectacles about 700 years ago.

The first milestone on the way to present-day quality was around 1450, when Angelo Barovier, a Venetian glass maker of decorative household glass, made clear white glass. It was not until 150 years later that white glass was used in the first optical instruments: the telescope by Hans Lippershey and the microscope by Zacharias Janssen.

Before long it became obvious that further progress beyond magnification of about 10 was limited by chromatic aberration. Only one color could be focused, while the others remained blurred. The refractive index's dependence on wavelength as the cause of this effect seemed to be the same for all glasses. Around 1670, Isaac Newton began using mirror telescopes because he believed that none of the glasses with deviating dispersion were suitable for compensating color aberration.

Just at this time, George Ravenscroft, an English glass manufacturer, managed to produce lead flint glass with color dispersion differing considerably from that of the soda or potash lime glasses known to that point.[2,3] This glass was not used for optical lenses but for vases and goblets. A long time passed before Chester Moore Hall, an English lawyer and hobby astronomer, first combined a soda lime crown glass and a lead silicate flint glass to form an achromate doublet lens with much reduced color aberration. Contrary to Hall, who wanted to keep this invention secret, around 1760, John Dollond (Fig. 1.3) marketed the first color-corrected telescopes. His firm dominated this technology for more than 50 years. His optical systems, however, continuously suffered from poor and strongly varying glass quality.

Further progress in optics took place in Bavaria in the early 19th century. Newly gained territories as allies of Napoleon made it necessary to perform precise land surveying as a basis of taxation. Joseph von Utzschneider, a Bavarian entrepreneur also working in state administration, hired Joseph von Fraunhofer and Pierre Guinand (Fig. 1.4) in order to provide the required optical instruments.[4] Guinand had already improved glass homogeneity by stirring melts. Fraunhofer further developed the glass-melting process, achieving lenses with diameters larger than 20 cm. He was the first to melt from well-defined recipes and to measure refractive index and dispersion of glasses at well-defined wavelengths, in what is known as the Fraunhofer lines of the solar spectrum. His telescopes were the largest and highest quality of their time.

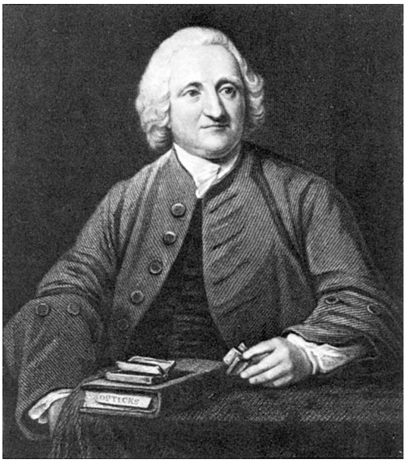

Figure 1.3 John Dollond introduced achromatic lenses for wide application. Color aberrations were corrected by the use of two glass types with different dispersion properties. (Courtesy of Wikipedia.)

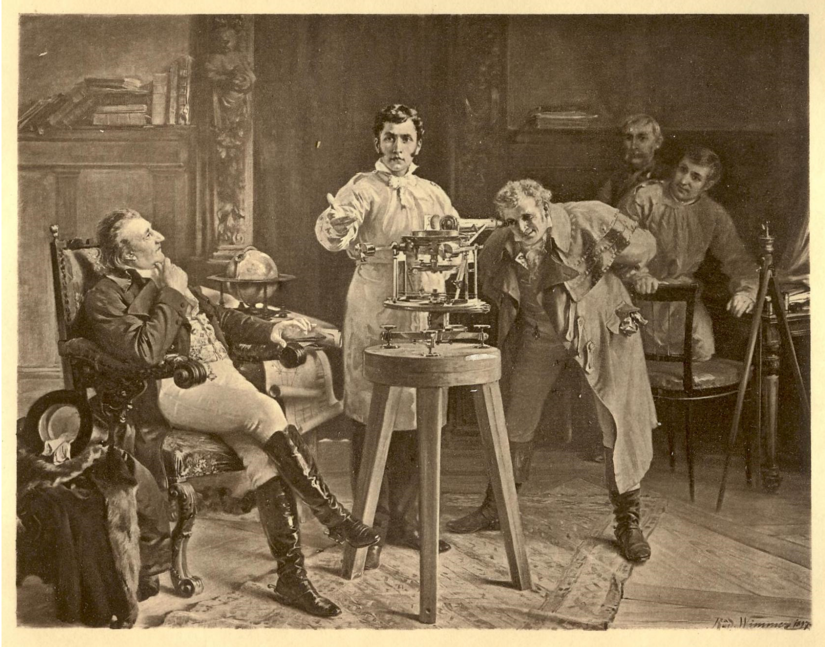

Figure 1.4 Joseph von Fraunhofer (together with P. Guinand) revolutionized glass manufacturing by introduction of raw-material recipes, measurement of glass properties (Fraunhofer lines and diffraction gratings as wavelength references), and improvement of transmittance and homogeneity. (Courtesty of Wikipedia.)

Fraunhofer also tried to melt new glass types with properties different from the existing ones by introducing new chemical elements in glass composition. However, he was not successful; chemistry was still in its foundation phase as science.

Fraunhofer's direct successors produced optical glass only for their own purposes. For decades, the companies of Guinand's grandson Charles Feil in Paris, France and of the Chance Brothers in Birmingham, England were the only glass suppliers. However, these two companies worked only with established glass types.

William Vernon Harcourt, an English scientist and clergyman, tried to melt glass types with different compositions. However, his samples were small and unsuitable for determining their optical properties with sufficient precision.

Until the late 19th century, optics in general suffered from the lack of glass types with widely varying properties and from poor reproducibility of optical properties and quality. In the 1880s, the needed breakthrough was achieved. It was initiated by Carl Zeiss (Fig. 1.5), then a manufacturer of microscopes, who was not content with the fact that the performance of his microscopes was not predictable and reproducible. Ernst Abbe, a professor at the University of Jena, whom Zeiss asked for assistance, proved that, in principle, performance predictability and reproducibility should be possible. Microscopes of even much higher performance than the existing ones could be built if adequate optical glasses would be available. Finally Otto Schott, a descendant of a glass-maker family, joined them, providing his expertise in chemistry and glass-melting technology. Within a short time Schott developed a considerable number of new glass types, for which Ernst Abbe could directly measure and appraise whether they had favorable optical properties.[5,6]

Otto Schott extended his very systematic approach for development not only to finding new glass types but also to mastering the melting process. The availability of new glass types with much improved and reproducible quality marked the beginning of optical design. Now, optical systems could be reliably designed and manufactured. Shortly thereafter, Schott's research initiated widespread progress in all optical applications. Microscopes could be built with diffraction-limited performance, enabling immeasurable progress in most sciences, including medicine.

Milestones in optical glass development in the 20th century are: the extension of the glass-type range with the high-index, low-dispersion, lanthanum glass types by George W. Morey; the very low-dispersion fluoro-phosphate glass types and the continuous melting tank technology in the 1950s and 1960s by Schott; the precise molding technology with adapted glass types and the introduction of lead- and arsenic-free glass types by Hoya Co. in Japan in the 1980s; and the glass types with extreme quality requirements, needed for i-line microlithography, by Schott in the 1990s.

The general trends of the past also hold for the future. Requirements on resolution and color trueness will continue to grow. For example, television with 4K and 8K resolution needs cameras capable to produce images worthwhile to be watched on screens with such outstanding quality. In industrial optical systems increasing resolution is accompanied by extension of the wavelength range into the near UV and IR.

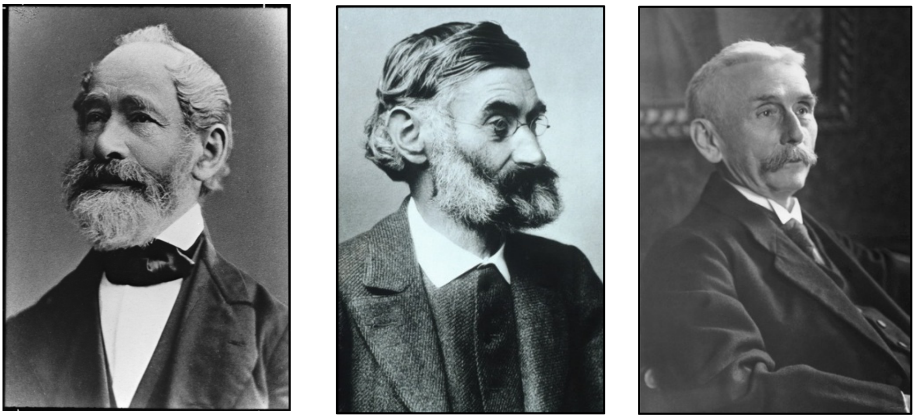

Figure 1.5 (left to right) Carl Zeiss, initiator, Ernst Abbe, inventor, and Otto Schott, enabler of optical design. (Courtesy of SCHOTT AG.)

Optical glass will continue to be a key enabling material with ever-increasing requirements on variety, quality, and reproducibility.

1.3 General Glass Properties

There are some essential general properties of glass that one should be aware of in order to understand the more-specific properties of optical glass, which can appear to be different from the properties expected in other materials.

In general terms, glass is a material that is cooled down from a melt and that fails to crystallize. During cooling, viscosity rises by many orders of magnitude until glass becomes a rigid body. Its atomic structure is very similar to that of crystals, but the positions of the atoms in space are not regular; glass consists of a disordered network. Because the ordered crystal structure would be the state with lowest energy, glasses are substances that are not in thermal equilibrium. Therefore, unlike crystals, their properties are not determined only by their composition but also by their actual deviation from thermal equilibrium. A glass that cools down slowly from transformation temperature is closer to thermal equilibrium than a glass that cools down rapidly; i.e., the slowly cooled glass has atoms that are packed more closely and hence acquires a higher density. As a consequence, refractive index and dispersion depend not only on the glass composition but also on its cooling history or, to use a more common expression in glass manufacturing, its annealing history.

Glasses are low-thermal-conducting materials. Therefore, large temperature differences may occur during tempering processes between the inner part of a piece and its outer volume, depending on the temperature change rate and thickness of samples. Temperature gradients are linearly proportional to temperature change rate and rise with the square of the thickness. Rapid annealing of optical glass pieces with thickness of 4 mm and below will lead to negligible temperature differences. However, thicker pieces require a limiting of the annealing rate. Because of the quadratic dependence, the annealing rate limit drops very fast for pieces with higher thicknesses. With 200 mm or more thickness, annealing will last for weeks or even months. Optical glass annealing rates in practice are a compromise between quality and economic requirements.

Temperature gradients lead to annealing rate variations in different partial volumes. As a result, properties determined by annealing rate such as refractive index and dispersion will be different for each partial volume and will end up in different values throughout the volume. In other words, inhomogeneity results.

Moreover, mechanical stress will arise while cooling to room temperature. The inner volume reaches room temperature later than the outer volume. Its thermal length shrinkage is hindered by the rigid outer volume, leading to tensile stress in the inner part and compressive stress in the outer part. This stress is not only bad for precision polishing of optical elements, but it also introduces an additional optical inhomogeneity, the stress birefringence, which is the dependence of refractive index on light polarization.

Unlike crystals, glasses have no specific composition preferred by nature. For table salt, the relation of sodium and chlorine atoms is exactly one to one. A chemical reaction with one substance in abundance will not lead to salt with a different composition. The abundant component will remain unbound. Glasses prepared from raw materials with composition differing from the nominal material will become glasses with different compositions and properties. Glass compositions can vary continuously in wide ranges. The task of a glass manufacturer is to define special compositions together with technically reasonable annealing conditions to form glass types as elements of their portfolio of optical glasses. These glass types must be reproducible with high quality in narrow tolerances in reasonable sizes and quantities.

1.4 Optical Glass: Definition

Optical glass is a technical material, meaning that it is specified by a set of properties that can be reproduced in narrow tolerances within reasonable volumes. In the following list, these properties are first given as general requirements and then as physical properties (in parentheses):

- high light transmission (internal transmittance);
- precise light deflection (index of refraction and its dependence on wavelength: dispersion);
- high uniformity in light deflection throughout the volume (optical homogeneity, stress birefringence);
- high material homogeneity and clarity (content of bubbles, inclusions, single crystals, clouds of submicroscopic crystals: haze, crystallization); and
- suitable behavior in grinding and polishing processes and under environmental influences (mechanical and chemical resistance).

All of these properties must be

- well defined, preferably as a physical quantity,
- measureable with sufficient accuracy,
- reproducible, and
- constant in minimum piece size and lot size.

A sufficient number of glass types with different indices of refraction and with dispersions complementing each other must be available for long time periods. Some properties are well defined and can be measured with high accuracy, e.g., refractive index and optical homogeneity. Other properties, e.g., striae content, are not sufficiently well defined. For many years, striae have been inspected against reference samples denominated with grades A to D, indicating the varying striae content. Efforts have been undertaken to develop a measurement method based on the physically meaningful quantity wavefront deformation. However, a practicable method could not be established until now. Also problematic are mechanical and chemical-resistance properties. Additionally, some classifications of optical glasses are based on measurement methods. However, their reproducibility is only moderate, and their relevance for practice is restricted.

1.5 Optical Glass Types

Optical glass is the general term for a large set of individual optical glass types. Such a glass type has an individual name, which usually is a trademark of the manufacturer (Fig. 1.6). Its properties are given in a detailed data sheet, which lists its optical properties and some additionally needed data, such as density, coefficient of thermal expansion, transformation temperature, elasticity, chemical resistance, and so on.

In contrast to crystals, the properties of optical glass types are not given solely from their chemical composition, but also from individual annealing histories. For calcium fluoride, refractive index varies only in the sixth decimal place, most likely due mainly to the limited measurement accuracy. With optical glass, refractive index varies even in the third decimal place for the same chemical composition, but depending on the annealing history of the material. The given example for the optical glass type N-BK7 (Table 1.1) shows that ten times faster or slower annealing leads to refractive index values violating the range of even the standard tolerance, which is 1.51630 to 1.51730.

Figure 1.6 Optical glass blocks.

Table 1.1 Refractive index and Abbe number both change significantly due to different annealing rates.

N-BK7	Index of Refraction	Abbe Number	Annealing rate K/h
	1.51587	64.09	20
Catalog	1.51680	64.17	2
	1.51773	64.25	0.2

It should be noted that only a small fraction of properties given in the data sheets are actually guaranteed values. These properties can be recognized in manufacturers' catalogs as those that are specified with tolerance ranges. The other properties are typical values that are not subject to quality assurance procedures, in order to keep costs within reasonable limits. Due to close monitoring of such sensitive properties as refractive index and dispersion, during production any deviations from catalog values for typical values can be deemed negligible.

1.6 Optical Glass Types: Denominations

Initially, optical glass types of SCHOTT were named by their fabrication number and a serial number. When these numbers reached five decimal places and became tedious in daily practice, SCHOTT introduced a new denomination system with the 1923 catalog edition.[7] Glass types were divided into groups with similar chemical composition and marked with respect to important chemical elements used to achieve special optical properties, their belonging to crown or flint types, and their density. BaSF1, for example, expresses that barium is an important constituent, F denotes the glass to be of the flint type, and S stands for "dense," coming from the original German word "Schwer." The two main denominations are for

- Crowns K (from the German "Kron"): FK (fluorine), PK (phosphate), PSK (phosphate dense), BK (boron), BaLK (barium light), K (crown), ZK (zinc), BaK (barium), SK (dense), SSK (extra-dense), and LaK (lanthanum);
- Flints F: BaLF (barium light), LLF (extra-light), BaF (barium), LF (light), F (flint), SF (dense), BaSF (barium dense), LaF (lanthanum), LaSF (lanthanum dense), and KzFS (short flint special glass; the abbreviation "Kz" is from the German "Kurz," meaning "short").

With the introduction of computer databases, glass names have been simplified by using only capital letters and omitting empty spaces.

Since 1998, optical glass family names have partially lost their relation to their chemical composition. On the occasion of introducing lead- and arsenic-free glass types, all glass types formerly containing lead were changed significantly in their composition; this is especially true for the lead flint glass families LLF, LF, F, and SF. Up to 75% of lead oxide had to be replaced by oxides of other metals such as titanium and niobium. Thus, a present-day N-SF glass type (the N stands for "No" lead and arsenic) is still called "dense flint glass," even though its composition is far from its classical lead oxide predecessor glass type.

1.7 Optical Glass Types: Glass Codes

Another way to specify a glass type is by the glass code. The glass code uses the refractive index n_d, with index d referring to the wavelength of the helium d line, which lies in the middle of the visible light spectrum at 587 nm, and the Abbe number $\nu_d = (n_d - 1)/(n_F - n_C)$ as a measure for dispersion, which relates n_d with the main dispersion $(n_F - n_C)$, a measure of the refractive index change from the blue mercury F line at 486 nm to the mercury C line at 656 nm. The glass code as described in the international standard ISO 12123 "Optics and photonics—Specification of raw optical glass" uses a six-digit number. The first three digits give the refractive index n_d, omitting the leading "1," and the second three digits give the Abbe value ν_d. The code is not unique for a glass type. Lead- and arsenic-free glass types have been developed with the very aim to have the same optical position as their classical predecessors. Therefore, with only the glass code, they are indistinguishable because the same refractive indices and Abbe numbers lead to the same code, even though they may have very different chemical compositions as well as physical properties. SCHOTT removed this ambiguity for its glass types by adding three digits that indicate the density of the glass. Table 1.2 shows the values for the lead- and arsenic-free glass type N-SF6 and its classical lead silicate predecessor SF6.

Table 1.2 Glass code of optical glasses extended by density code.

Glass Type	n_d	ν_d	Density	Glass Code
N-SF6	1.80518	25.36	3.37	805254.337
SF6	1.80518	25.43	5.18	805254.518

Some manufacturers provide lists indicating equivalency of glass types from different manufacturers. Such lists should be used with some caution. The intended equivalency applies only to that of the optical position, i.e., the refractive index n_d and Abbe number ν_d. Identical optical positions can be achieved with different chemical compositions. It should be checked how closely these values and other properties match each other. So-called equivalent glass types, even with identical optical positions, might behave much differently during processing in the optical workshop.

1.8 Optical Glass Types: Portfolio

Before the groundbreaking work of Otto Schott, there had been only two families of about 20 optical glass types: soda lime crown glasses with low refractive index and moderately low dispersion, and higher-index lead silicate flint glasses with higher dispersion. Together with the then-notorious variations in quality, the two classifications were not sufficient as material basis for precision optics.

With the 1886 SCHOTT catalog, the number of available glasses doubled due to the introduction of new glass types containing chemical elements such as boron, barium, phosphor, and zinc. Two years later, the number of glass types was even tripled. The main goals of the re-engineered traditional glass types and the new glass types were to match dispersion of crown and flint glasses better than previous matching, and to provide glass types with different dispersions at the same refractive index level, and vice versa. This glass portfolio providing an enlarged range of optical properties led to the breakthrough of precision optics and the possibility of optical design.

Since that time, the number of glass types rose continuously due to the introduction of additional elements such as fluorine and especially lanthanum by the Kodak Company, until it reached a summit in 1967, when 273 glass types were listed in the catalog (Fig. 1.7).

In the years following 1967, some glass types were abandoned due to low usage. In 1998, a further strong reduction together with a wide exchange of glass types led to a dramatic change in the number of available glass types.

The consumer-optics-dominated Asian market now accepted only lead- and arsenic-free glass types and refused to use single-supplier glass types. Many special glass types used only by U.S. and European customers became uneconomic and were thus abandoned. A large number of glass types had to be redeveloped to achieve the same optical performance as the lead- and arsenic-containing glass types. In many cases this was possible, even though other properties changed. However, the high transmittance of lead oxide flint glasses in the blue to ultraviolet (UV) spectral range in combination with the high refractive index could not be preserved with any replacement composition.

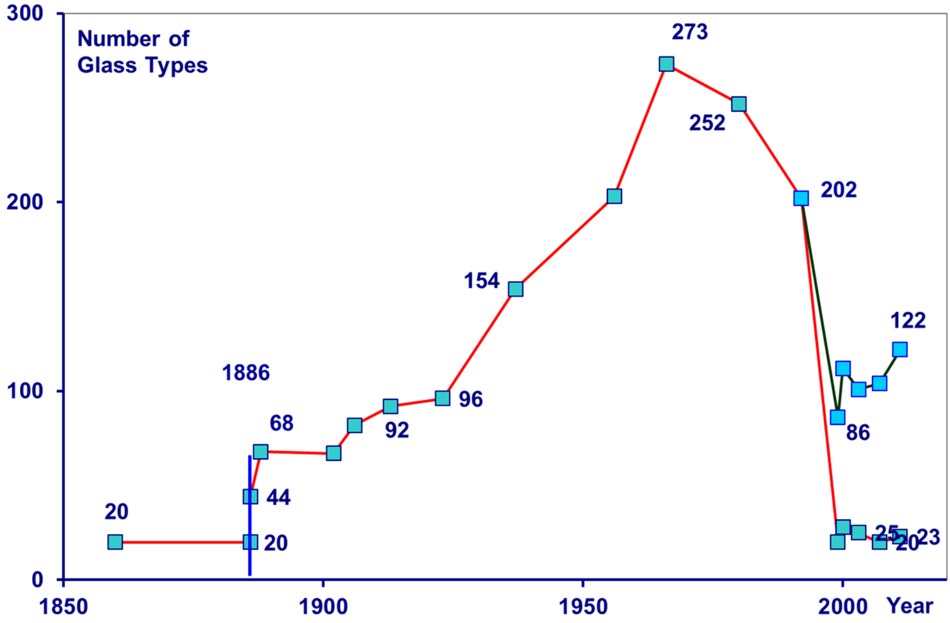

Figure 1.7 History of the optical glass types portfolio of SCHOTT. Red line: classical glass types, black line: total number. Note the sharp rise with the beginning of glass-type development and the sharp drop due to the change to lead- and arsenic-free glass types and economic restructuring.

Another trend in consumer optics, the low-cost production of small and especially aspheric lenses (the so-called precision-molding process), is to use glass types that have been adapted to process requirements. These glasses have to be moldable at the lowest possible temperature, maintaining the highly polished surface quality of preforms and avoiding sticking to press mold surfaces. The number of specially developed glass types together with process-qualified existing glass types is still growing.

The 2014 portfolio of SCHOTT contains 105 glass types, including 17 classical lead- and arsenic-containing glasses. 26 of the lead- and arsenic-free glasses are precision moldable, and 15 of these 26 were developed especially for this purpose.

Traditionally, an overview of the optical glass portfolio is given in the so-called Abbe diagram (Fig. 1.8). Here, the glass types are plotted in the *x* axis according to their Abbe number. Unlike most diagrams, the numbers grow larger moving to the left. This format is chosen to reflect the rise of dispersion to the right. High values of the Abbe number reflect low dispersion, and vice versa. The refractive index is given on the *y* axis.

Glass types are grouped in families defined by regions with fixed border lines containing the denomination part that they have in common (the family name); for example, BK for boron crown and LASF for lanthanum dense flint. The numbers indicating individual glass types are sequential and have no special meaning.

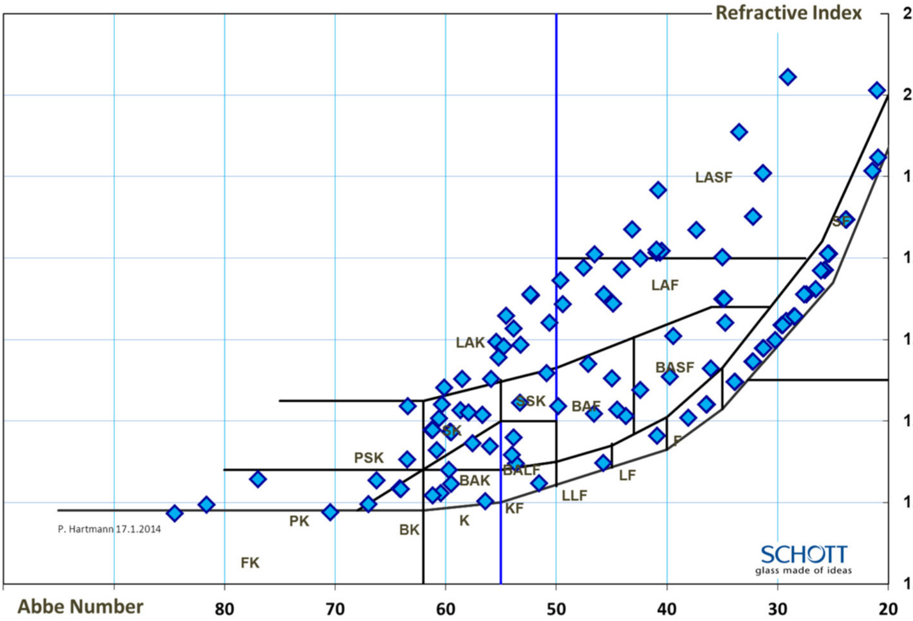

Figure 1.8 Abbe diagram as an overview for available glass types with glass family border lines and names as introduced with the 1923 edition of the SCHOTT catalog. Note: Abbe number rises to the left, but dispersion rises to the right.

The area populated with glasses looks like an elongated island with high-refractive-index, high-dispersion glass types in the upper right corner, and low-refractive-index, low-dispersion glass types in the lower left corner. The glass types in highest demand are those that lie in the corners and along the imaginary border lines. These glasses allow best optical performance but, on the other hand, are the more expensive. Most of the glass types that have been abandoned fall in the middle of the island. Generally, optical designers' requirements direct them to the upper left portion, all along the border line. This border line is set by the materials' tendency to crystallize while cooling down from melt. As mentioned, glasses are substances that failed to crystallize upon cooling. The classical glasses have such a small tendency toward crystallization that they end up as glass in any circumstance. The glass types along the border line to the upper left need to be prevented from crystallization. This is done by rapidly quenching them during casting.

Melts leading to optical positions beyond the border line crystallize so fast that it is impossible to cast pieces of reasonable minimum volumes. The border line to the lower right can be surpassed to a certain extent. However, glass types with high dispersion at lower refractive index are not required by optical companies, with the exception of high-index glasses with Abbe numbers lower than 20; these glass types are used in some special optical designs.

1.9 Optical Glass Types: Availability

The number of glass types in a company portfolio is the result of a compromise between opposing requirements. Optical companies prefer to have a large number of glass types available for an unlimited time in the future.[8] A large number of available glass types facilitates design and provides higher adjustability to the desired performance. New designs of optical systems need two or more years between initial concept and initial glass purchase. During product sales and later during warrantee periods, all of the glass types that have been used in a design must be available for purchase. In optical companies, a legacy of designs and process knowledge grows with time. Discontinuing a glass type will result in high damages to the company. This is due, first of all, to high turnover losses. As a rule, for $1 lost from a discontinued glass, $50 to 100 dollars in turnover is lost. Secondly, a large amount of time and effort is needed to accommodate for changes in optical design, production processes, and tools after discontinuation of a glass type that was initially used in the design.

For glass manufacturers, a large number of optical glass types results in a considerable variety of processes needed to enable the melting and casting of glasses with highly varying chemical and physical properties. This requires a wide variety of expensive melting facilities and casting equipment. The demand for different sizes and shapes as well as quality grades increases the number of products to be inspected, administered, and stored by a large factor, from roughly 100 initial glass types to many thousands of components in daily practice.

Considering the production volume per year, which spans from 1 ton to more than 100 tons, the task of maintaining sound company economics proves to be challenging.

As mentioned, glass manufacturers commit to keeping the glass types in their portfolios ready for delivery and available for many years. For high-sales-volume glass types, the task is usually not very difficult. Small-sales-volume type glasses might be sold out in a very short time if one customer buys the entire inventory, which was expected to be sufficient for a total year. Then, it might be that the glass type will not be available for months, as a glass manufacturer is not necessarily always free to produce any glass in any melting facility at any time. In addition to the general restriction of producing glass types only in dedicated facilities, the production series has its own restrictions. One cannot melt any arbitrary glass type after a given predecessor type has been melted. Chemical properties and purity requirements must be compliant.

Glass types that will not be economical for a long time into the future and that have no prospects for increased sales will be removed from the glass portfolio. This measure is necessary in order for a glass manufacturer to survive in the market for the long term. Such a removal should be indicated years in advance. This gives customers the opportunity to buy the inventory sufficient for future needs in special products, to change designs in due time, or to discuss waiving the removal because their sales projections indicate future higher consumption of the glass type in question.

Other glass types in a portfolio can sometimes be regarded as long term, even when a glass manufacturer cannot guarantee long-term demand. Market requirements and regulatory conditions may change such that even well-proven, high-volume glass types might become endangered. For example, SCHOTT F2 is more than 150 years old. This is possible because a glass with very similar composition and optical values existed even before SCHOTT was founded. In the 1990s consumer optics discarded the glass because of its lead content, and in the 2000s it was nearly forbidden by the European Restriction of Hazardous Substances (RoHS) Directive-based restrictions of hazardous substances in electronic devices. However, it is still a very important glass type, especially for endoscopy.

1.10 Selected Types of Optical Glass

N-BK7 is a classical borosilicate glass type that is available in all delivery forms, from preforms for precision molding in its variant P-BK7 over thick strip glass and block glass to large blanks of more than 1-m diameter and 300-mm thickness. Generally a glass with high homogeneity, N-BK7 has the highest proven homogeneity with a proven refractive index variation peak-to-valley of 1×10^{-7} in block glass with test volume diameter of 100 mm and thickness of 137 mm, and better than 1×10^{-6} refractive index variation peak-to-valley within the full volume of a $217 \times 217 \times 100\ \text{mm}^3$ block in all directions. It is frequently used for prisms with long light paths.

N-FK51A, N-PK52A, and N-FK58 are high-value, extreme fluorophosphate glass types with very low dispersion and with dispersion strongly differing from normal glasses. They are used in high-performance optics for outstanding color trueness in imaging. These glass types, when used in binoculars, are advertised as “fluorite glass,” indicating outstanding color trueness. The term fluorite refers to calcium fluoride, a well-known, high-performance, but very expensive and sensitive material. These glasses extend not only most deeply into the UV spectrum with respect to transmittance but also into the infrared (IR) spectrum because of their low content of residual water.

N-KZFS2, N-KZFS4, and N-KZFS11 are tantalum borosilicate short flint special glasses and are the best partners of extreme fluorophosphate glass types because they combine to render the best color trueness in imaging. They are precisely moldable. N-KZFS4 has the special property that its Abbe number is not at all affected by variation in annealing rates.

N-LASF44 is a high-refractive-index, low-dispersion lanthanum borate glass.

SF57 is a high-lead-containing classical dense flint glass with high transmittance in the blue to UV spectral range. This glass does not react to thermal gradients with birefringence and is therefore best suited for color cubes in digital projection. In this respect, it is called a $K = 0$ glass since its stress optical constant K is very close to 0, as opposed to almost all other glass types, for which K is not close to 0. Its special-quality grade SF57HTUltra is the best transmitting glass in the near-UV spectral range at high refractive index and dispersion.

N-SF57 is a lead- and arsenic-free barium niobium titanium silicate dense flint glass with the same refractive index and Abbe number as SF57 but with much better chemical resistance, higher hardness, better workability, and much lower density. Processing temperatures for pressing are much higher, blue transmission is lower, and its optical properties are much more sensitive to annealing rate changes than SF57 and other glasses. Due to its high reactivity with birefringence on thermal gradients, it is one of the worst glasses in this respect.

References

1. P. Hartmann, “Optical glass: past and future of a key enabling material,” *Adv. Opt. Techn.* **1**, 5–10, (2012).

2. P. Hartmann, R. Jedamzik, S. Reichel, and B. Schreder, “Optical glass and glass ceramic historical aspects and recent developments: a Schott view,” *Appl. Optics* **49**(16), D157–D176 (2010).

3. C. R. Kurkjian and W. R. Prindle, “Perspectives on the history of glass Composition,” *J. Am. Ceram. Soc.* **81**(4), 795–813 (1998).

4. W. Jahn, “He brought us closer to the stars,” in *Fraunhofer in Benediktbeuern*, Fraunhofer Gesellschaft, pp. 4–15 (2008).

5. D. Kappler and J. Steiner, *SCHOTT 1884–2009 Vom Glaslabor zum Technologiekonzern*, SCHOTT AG (2009).
6. SCHOTT Optical Glass Catalog, "Productions- und Preis-Verzeichnis," Glastechnisches Laboratorium Scott & Gen. (1886).
7. Catalog: "Jenaer Glas für die Optik," Jenaer Glaswerk Schott & Genossen, Jena (1923).
8. W. Besenmatter, "How many glass types does a designer really need?" *Proc. SPIE* **3482**, 294–305 (1998) [doi: 10.1117/12.322017].

Chapter 2
Production of Optical Glass

2.1 Melting

Several of the special aspects of optical glass properties can only be understood with some knowledge about the production processes and their restrictions. The traditional way, introduced more than 100 years ago, is to melt optical glass in a clay pot (Fig. 2.1). A raw material batch consisting of precisely weighed and carefully mixed compounds is put in the clay pot. When the batch is molten, the next batch follows, until the pot is filled with molten glass.

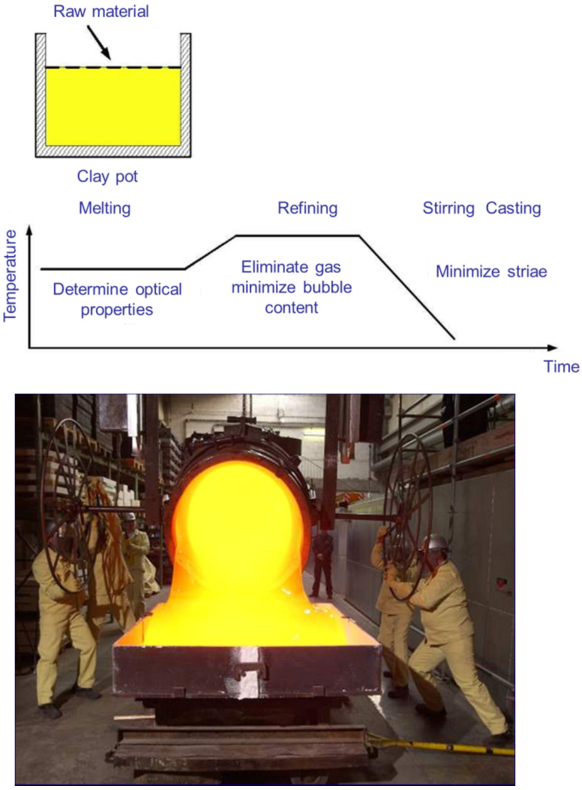
Raw material
Clay pot
Melting
Refining
Stirring
Casting
Temperature
Determine optical properties
Eliminate gas minimize bubble content
Minimize striae
Time

Figure 2.1 Clay pot melting process. (top) Temperature-versus-time diagram and (bottom) casting from a clay pot melt. (Courtesy of SCHOTT AG.)

Although compositions of optical glasses are usually given in the form of the oxides used, in reality, many needed elements are introduced as different compounds. The reason for this is that many oxides have high melting temperatures that would require high energy. These temperatures might even be higher than that of the refractory material used. The compounds actually used, such as carbonates and hydro-carbonates, release gas when being incorporated into the glass melt. In order to eliminate resulting gas bubbles, the temperature is raised considerably above the melting temperature. This so-called glass refining leads to higher gas pressure, enlarging existing bubbles and lowering the melt viscosity, thus, allowing these bubbles to leave the melt via buoyancy forces.

Bubbles that are too small to leave the melt will be dissolved by integrating their gas atoms into the glass matrix with the help of refining agents. These agents are elements that change their valence from three to five while cooling down. After refining, the melt will be stirred for improved homogeneity. The contents of the clay pot are cast in a very short timeframe into a large mold. The mold is moved into a preheated furnace. Then starts the process of cooling down the glass to room temperature. The cooling must happen slowly in order to prevent breakage caused by internal temporal stresses.

This method has the advantage that all glass properties are very constant throughout the total volume. Maximum refractive index changes are in the range of 1×10^{-5}. The main disadvantage, which has led to almost complete abandonment of the method, is the high cost per amount of good glass produced.

With the continuous tank melting method (Fig. 2.2) introduced for optical glass in the 1950s, costs could be cut by 70 to 80%, while saving energy and valuable raw materials. The process performed for pot production in the single vessel is only now evolving to include several vessels.

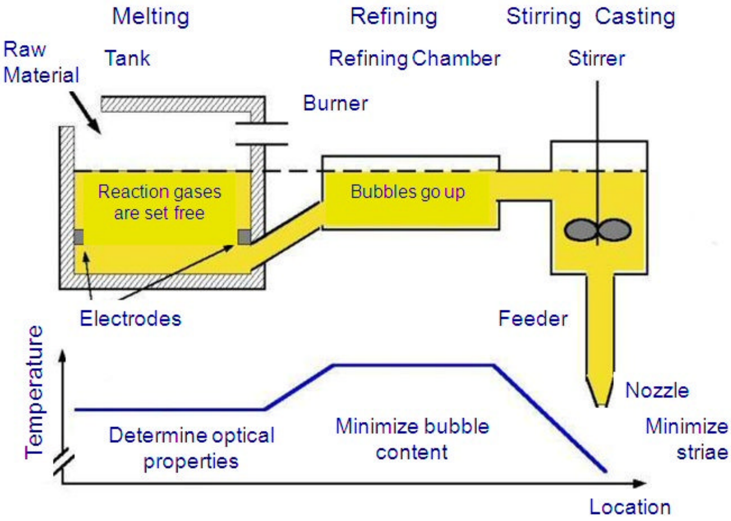
Melting
Refining
Stirring
Casting
Raw Material
Tank
Refining Chamber
Stirrer
Burner
Reaction gases are set free
Bubbles go up
Electrodes
Feeder
Nozzle
Temperature
Determine optical properties
Minimize bubble content
Minimize striae
Location

Figure 2.2 Continuous tank melting-temperature-versus-time diagram.

Like clay pot melting, tank melting has been optimized for high glass homogeneity also. However, even with careful monitoring and control, changes in refractive index over time cannot be kept within a narrow tolerance over long production time, sometimes days and even weeks. Therefore, a material administration system was established to make essential glass data available for all production batches. The batch volume is chosen such that properties can be considered to be constant within the batches. Although delivery lots for continuous melting tanks (see example in Fig. 2.3) are not constant in their properties to the same level as in pot melts, they are in tolerance and can be assembled to larger total delivery lots than can be assembled from pot melts.

Not all present-day melts are done in continuous tanks. Special glass types with outstanding properties or with comparatively low consumption are made in discontinuous platinum pots (Fig. 2.4).

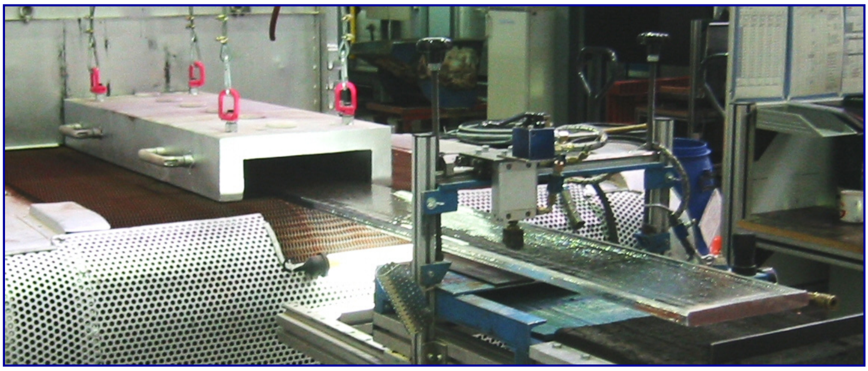

Figure 2.3 Continuous tank melting: strip glass leaving an annealing lehr (a conveyor belt that moves continuous glass strips through long furnaces with a small temperature gradient along the travelling direction).

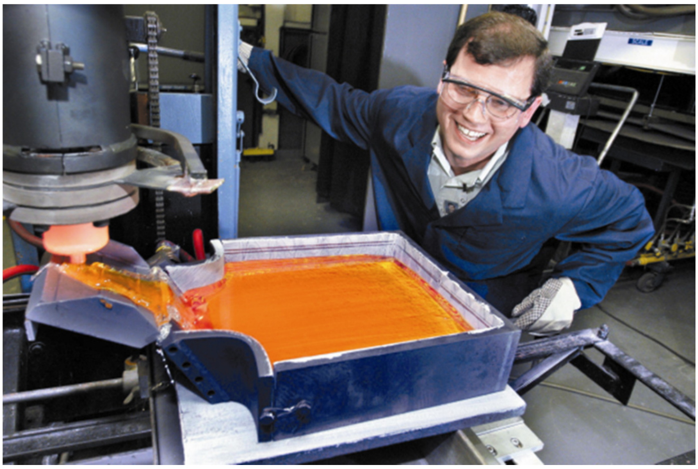

Figure 2.4 Platinum pot melting: casting of a glass block.

Generally, for a wide variety of optical glass types, one has to operate a considerable number of facilities with different melting volumes and with different components, in order to fulfill all requirements from chemistry, technology, and economics. Not every glass type can be produced in any aggregate, nor can they be produced in arbitrary sequence. Changing from one glass type to the next requires similar chemical composition in the glass types. Otherwise, the change might become time consuming and costly. Consequently, there are assigned time slots for glass types to be molten, and even a sudden rise in demand for a special glass type might not directly lead to the initiation of its production.

Additionally, casting formats need to be taken into account, especially for large-sized production formats, where special equipment for heat forming may be needed, and even larger setups require special casting molds. Generally, large formats take a longer time to produce than small formats of the same glass type (see example in Fig. 2.5).

The production processes presented in this chapter are used, with some variations, by several glass manufacturers. Some Japanese companies use a variation for strip glass production, which consists of a two-step melting process. They first melt glass in clay pots and then crush the pots' contents to cullets, which will be re-melted to form continuous strips. The optical values of such clay pot batches are highly constant within a batch and can be precisely determined. A combination of cullets from batches with different optical values can be used to control the resulting optical values of the strip glass. Disadvantages are the required double melting with high energy consumption and the need for additional material and data logistics.

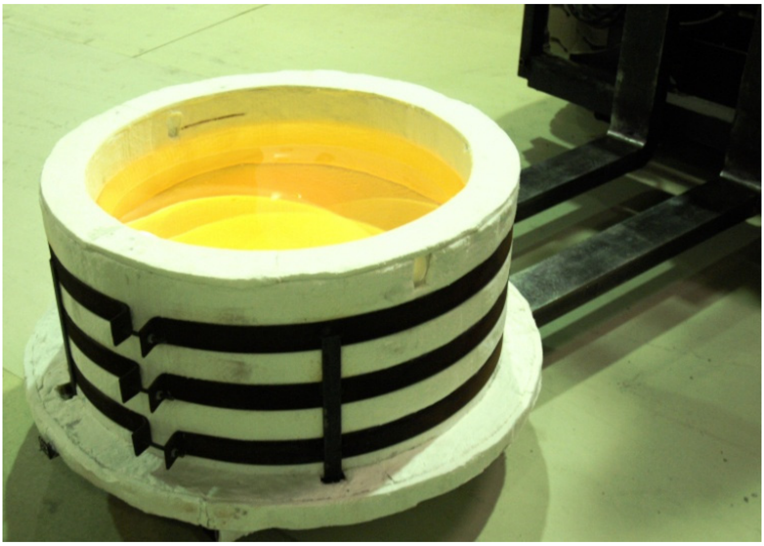

Figure 2.5 N-BK7 600-mm casting.

2.2 Annealing

The glass-melting process decisively determines the degree of light transmission and the content of bubbles, inclusions, and striae. The melt also influences refractive index, dispersion, and optical homogeneity, but, of course, not to the degree of precision needed for final application. Final adjustment requires an additional production step called fine annealing. This process takes refractive index dispersion homogeneity and stress birefringence to their tolerance limits.

For a better explanation of the annealing process, it is necessary to give some general information about glass properties in different temperature ranges. Since glass is generated by melting, its life starts at high temperatures of 1000 °C or above. At this temperature, they are low-viscosity liquids. While cooling down, they will remain a liquid for a large temperature range and will gradually become more and more viscous. In a specific temperature range called the transformation range, the liquid becomes a solid. This is not a sharp transition, as in the phase transition from liquid to solid that occurs with crystal formation. It is rather a matter of attaining a certain viscosity value, at which the material can be considered to be stiff, and where, in practice, bulk pieces will no longer deform under their own weight. The transformation range for any given glass is the range in which the glass's viscosity values span from 10^{13} to 10^{15} dPas (deci-Pascal-seconds). Below 10^{15} dPas, glass is the brittle elastic solid as known in daily practice. Cooling it down further will just simply lead to shrinking according to the glass's coefficient of thermal expansion.

In the two temperature ranges above and below the transformation range, nothing happens that will consistently influence glass properties. However, the special circumstances the glass is subject to while passing through the transformation range will influence the glass's properties. These circumstances could even lead to the destruction of molten pieces by breakage.

In order to understand this breakage, another fundamental property of glass needs to be recalled: Its thermal conductivity is low. This is a favorable property of window panes in winter time. On the other hand, it is the reason that many measures and precautions are taken in glass manufacturing. Bulk pieces of materials with low thermal conduction react to fast temperature changes by exhibiting high temperature differences within their volume. The following formula for temperature difference holds for a glass plate, in which the length and width are much larger than the thickness such that the influence of the edges can be ignored:[1]

$$\Delta T = \frac{\nu_{\mathrm{K}}}{8k} d^2, \tag{2.1}$$

and

$$k = \lambda / c_{\mathrm{p}} \rho, \tag{2.2}$$

where ν_{K} is the temperature change rate in the unit K/h (Kelvin per hour), d is the thickness, k is the material constant calculable from its thermal conductivity λ in the unit W/m·K (watt per meter per Kelvin), c_p is its heat capacity in the unit J/m·K (joule per meter per Kelvin), and ρ is its density in g/cm^3.

The most important message from these formulas is that temperature differences rise with the square of the thickness. So differences that might occur in a 5-mm-thick glass sheet will be 100 times higher in a 50-mm-thick piece. In practice, thickness up to 4 mm is not critical for temperature processes with optical glass. At higher thickness, temperature differences will be so high that special measures have to be applied in production.

The transformation range can be seen in a plot of the relative length change with respect to temperature (see Fig. 2.6). It is the portion of the plot that lies between two straight lines with different slopes. The transformation temperature given in data sheets is the point where the two extrapolated lines meet. Note that the upper line has a much higher slope than the lower line. (The direction change at highest temperatures is due to the push rod measurement, with the samples becoming too soft.)

Now consider a bulk piece of glass at a temperature that is above the transformation range and that is consistent throughout the total volume. Being cooled down first, the outer faces will become rigid and will contract according to the line with the lower slope. At this instant, the internal parts are still at higher temperatures, thus, following the curved part or even the line with the higher slope. However, the outer faces can no longer contract freely because the shape of the piece is now defined by the rigid outer faces. So, until the inner portion becomes rigid, it should contract more strongly than the outer part; however, it cannot do this any longer. This causes tensile stress to develop, and as a mechanical reaction, the outer layers come into compressive stress. Such stress will not relax even at equilibrium at room temperature.

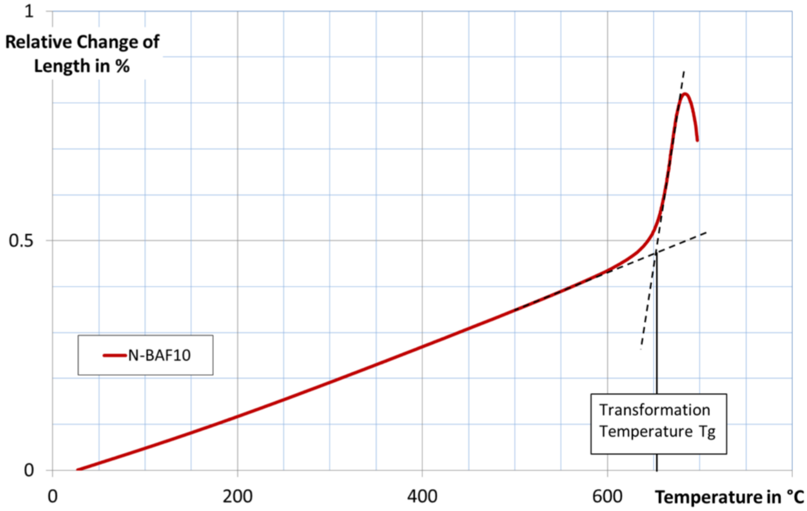

Figure 2.6 Relative length change of the optical glass N-BAF10 with temperature.

The resulting permanent stress is further increased by another typical characteristic of glass. Different cooling rates shift the lower line parallel to the line given in Fig. 2.6. For faster cooling, the line is shifted upward, resulting in lower glass density; for slower cooling, the opposite occurs (see Fig. 2.7).

The inner part of a bulk piece of glass not only follows the outer part later but also more slowly due to the low thermal conductivity. Hence it stays longer on the line with the higher slope, increasing the different contraction behaviors and the resulting stress.

Such stress leads to birefringence, which is very disturbing in optical glass. For high-end applications, stress birefringence must be kept very low. Two ways to achieve this are (1) cooling down very slowly or (2) keeping at least one dimension small, i.e., using thin elements. This is the reason that precise molding elements for optical imaging are restricted to thicknesses of around 4 mm. Thicker pieces would be possible but require much longer annealing times, thus destroying the economic advantage of this process.

The different densities in the outer and inner part of a bulk piece of glass—a result of rapid cooling—lead to another unwanted effect for optical glass. The refractive index of optical glass is strongly correlated with its density. Therefore, density inhomogeneity means refractive index inhomogeneity as well. This is the second reason that low annealing rates are necessary for high-quality optical glass.

Figure 2.8 shows the temperature history of a glass, from melting to cooling down to the subsequent additional heat treatment the fine annealing.

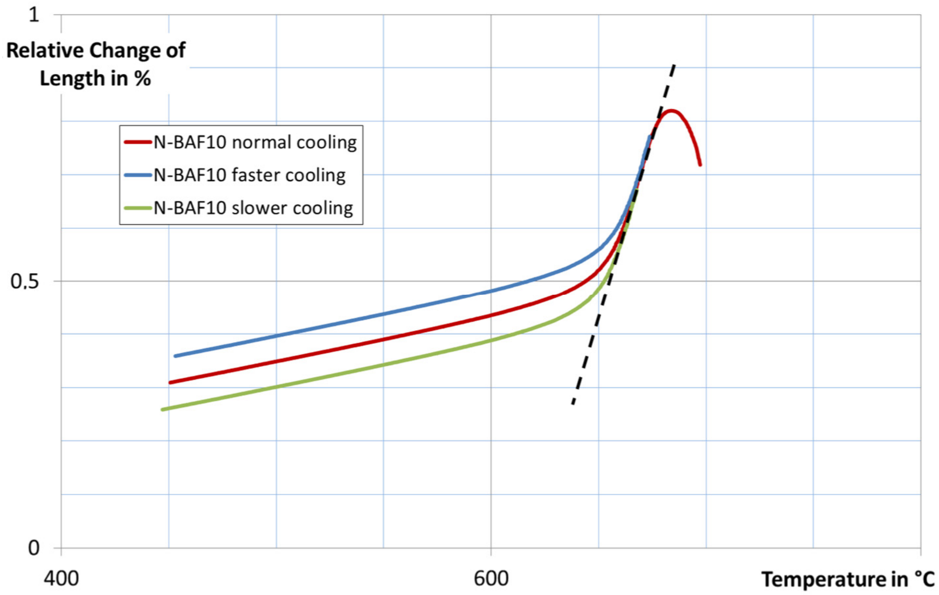

Figure 2.7 Relative length change of the optical glass N-BAF10 with temperature for different cooling rates.

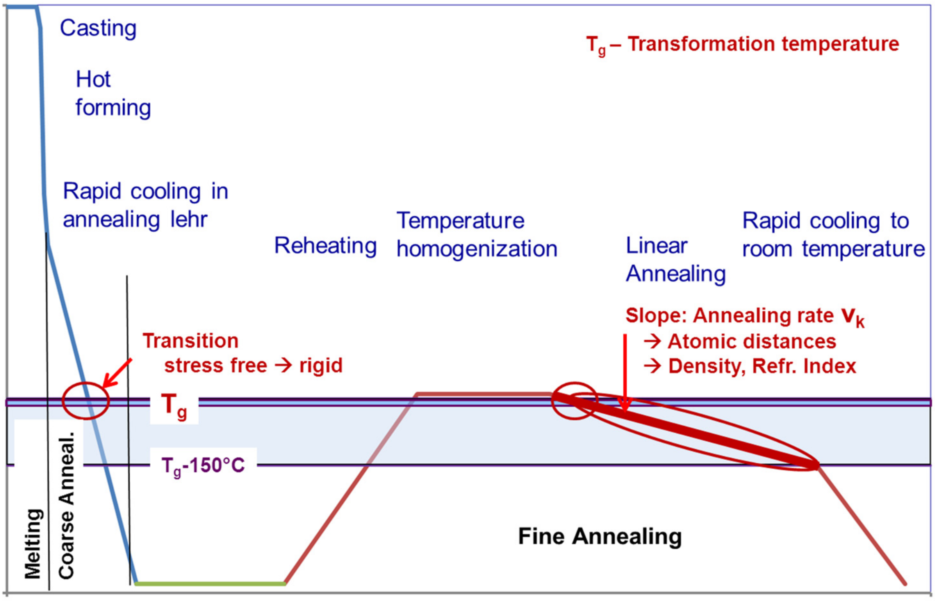
Casting
Hot forming
Rapid cooling in annealing lehr
Reheating
Temperature homogenization
Linear Annealing
Rapid cooling to room temperature
T_g – Transformation temperature
Transition stress free → rigid
Slope: Annealing rate v_k
→ Atomic distances
→ Density, Refr. Index
T_g
T_g-150°C
Melting
Coarse Anneal.
Fine Annealing

Figure 2.8 Temperature-versus-time diagram for coarse and fine annealing.

While cooling down from melting to room temperature, the transformation range must always be crossed. In principle, it is possible to do this in a way that is controlled to the extent that no further thermal treatment will be necessary. Stress birefringence must be kept low, and refractive index within the required tolerance range. This could be achieved with slow cooling directly after melting, e.g., with especially long annealing lehrs. However, this is not done in common practice. It is questionable whether temperature could be controlled precisely enough to reliably achieve narrow refractive index tolerances. The necessary reduction of the traveling speed would reduce the overall glass throughput to an uneconomic level.

Thus, the practical method that is used for the largest (by far) number of optical glasses involves a rapid cool down after the melt, at speeds that are just limited to prevent high stress levels. Stress must be kept low enough to allow the strips to be broken into short pieces of, e.g., 300 mm with straight edges. Most glass types will be heated again later to be pressed to preforms of lenses and prisms. Such rapid stress-reducing cooling is called coarse annealing. Coarse annealed strips have stress birefringence that is too high for precision optical application as well as unknown and inhomogeneous refractive indices.

For removal of stress and homogenization of the refractive index, and for obtaining an absolute value in the desired tolerance range, it is necessary to apply another thermal treatment called fine annealing.[2–4]

Fine annealing requires furnaces with precise temperature control and homogeneous temperature volume. The process starts with heating the glass items to a temperature at which they lose all internal stress within a short time. This relaxation temperature is called the annealing point and is given by the temperature at which the glass has a viscosity of $10^{13.2}$ dPas. By definition, at this viscosity, residual stress relaxes completely within 15 min. For most glass types, $T_{10^{13.2}}$ lies very close to the transformation temperature T_g. For thick pieces, it is important to maintain a temperature slightly higher than the relaxation temperature long enough to ensure that also the inner part of the volume is completely relaxed. The next step is to cool the item down to about 150 °C below T_g with a linear slope. In this temperature range, density and thus refractive index will be established. At lower temperatures, there is no further influence on glass properties. The cooling rate is restricted only to prevent breakage due to transient stress caused by the temperature differences within the glass volume. These stresses vanish with the temperature differences at room temperature.

The applicable annealing rate in the constant slope range is limited by the refractive index and dispersion tolerances, and by the stress birefringence limits to be fulfilled. For glass items with small thickness, even fast annealing rates will not introduce high stress. In this case, rate limits are set by economic factors. With high rates, annealing cycles are short, and furnaces can be used more frequently.

For thicker pieces, annealing rate will be strongly limited to avoid stress birefringence out of tolerance. For reheat pressings, rates of 4–10 °C/h are acceptable, depending on their thickness; glass blocks require rates of 1 °C/h and below; and large disks require about 0.2 to 0.1 °C/h, which ultimately leads to annealing periods of up to three months.

The degree of change in refractive index and dispersion with annealing rate is specific for any individual optical glass type. With the actual chemical composition given for a specific melt, the resulting optical properties can be influenced only in a restricted range given by the so-called annealing line (see Section 3.9), but not arbitrarily. This may lead to a situation in which narrower tolerance ranges are not accessible via annealing for a specific melt. More details on this topic will be given in Section 3.9, which discusses the influence of annealing on the refractive index and on the Abbe number.

A press shop receives optical glass for reheat pressing only in a coarse annealed state, together with a prescription for the rate at which glass batches can be annealed in order to attain the required tolerance ranges. The delivery of fine annealed glass to press shops would be a waste of time and money because in the pressing process the fine annealed status of the glass will be lost again due to the glass being heated to a much higher temperature than the transformation temperature for pressing. Fine annealing of pressings is performed by press shops, which also issue test certificates with optical data of delivery lots.

Strip glass, block glass (Fig. 2.9), or large glass items for cold processing in optical companies will leave glass manufacturers' factories fine annealed and ready for use together with their optical data recorded in a test certificate.

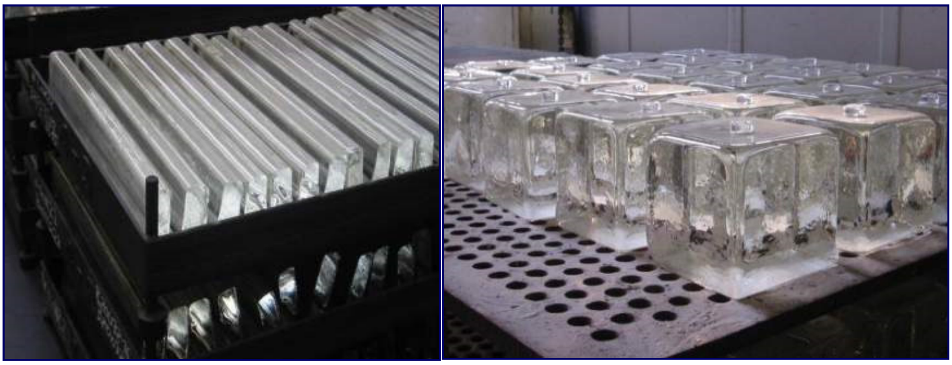

Figure 2.9 (left) Strip glass and (right) block glass arranged for fine annealing.

2.3 Reheat Pressing

Reheat pressing is the primary process used for converting strip glass to near-net-shape preforms for optical elements in an economic manner. This process prevents glass wastage and saves time by avoiding expensive shaping by cutting and grinding. The resulting shape precision is still far from the specifications for finished optical elements. This lack of precision in shape, together with the dull surfaces of the pressings, make the subsequent grinding and polishing required steps in the process.

Reheat pressing begins with carving and breaking strip glass into cubes with volumes as needed for the final pressing. The cubes will be tumbled in silicon carbide grain slurry to round off sharp edges, possibly leading to press folds or trapped air bubbles. After heating to the temperature range that enables easy deformation, the cubes are placed into press molds, pressed, and moved to an annealing lehr for fast cooling to room temperature again. In order to attain refractive index and Abbe number tolerances, and to achieve high optical homogeneity and low stress birefringence, it is necessary to reheat the pressings again for fine annealing. They are collected into batches and annealed in precision-controlled, temperature-homogeneous furnaces (Fig. 2.10).

The applicable annealing rate depends on several factors. From an economic standpoint, the annealing should take place as quickly as possible. The upper limit, however, is set by the glass item's thickness, which determines its sensitivity to thermal gradients that lead to stress birefringence and inhomogeneity. Moreover, the change in refractive index and Abbe number with different annealing rates must be taken into account. In order to assess this with high precision, the optical values must be closely and accurately monitored during melting. This requires a reliable system for taking samples, preparing them for measurement at room temperature in short time, measuring them with high accuracy, and providing the data in an operational database. With these operational data and glass-type-specific annealing parameter prescriptions, so-called annealing schedules (see Fig. 3.19) are calculated and provided to the press shops.

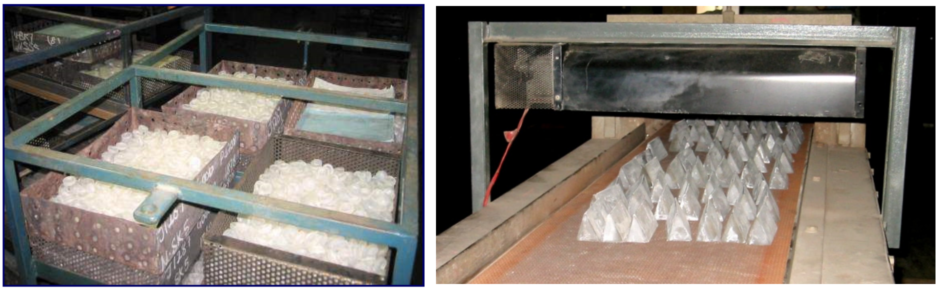

Figure 2.10 Reheat pressings: (left) Lenses in trays waiting for fine annealing and (right) prism bars coarse annealed on an annealing lehr.

Fulfilling narrow tolerances in refractive index and Abbe number is possible only when the annealing parameters, i.e., the changes of these quantities with annealing rate, are precisely determined. This is done when a new glass type is introduced to the optical glass program. At the same time, its capability is tested to withstand press temperature without crystallization.

The advantages of reheat pressing are:

- Large items of up to 300-mm diameter are possible with high homogeneity and low stress birefringence.
- Refractive index and Abbe number can be very precisely controlled.
- It slightly improves internal transmission.
- With very few exceptions, almost all glass types can be pressed.
- Low-cost molds enable small, economical pressings of even less than 10,000 pieces per lot.

The disadvantages are:

- Processing time is comparatively long (two days or longer).
- Heating glass twice means higher energy consumption.
- It requires subsequent grinding and polishing.

2.4 Precision Molding

Precision molding is a glass-shaping process that is capable of producing optical elements that do not need any further grinding and polishing. After centering and antireflection coating, the optical elements are ready for use. The introduction of this process in the 1980s by Hoya Co. of Japan led to swift progress in consumer optics applications. Together with digitization, precision molding made photography and video recording with high image quality accessible to a continuously growing user community.

Just as with reheat pressing, the main goal is cost reduction. Precision molding enables the production of aspheric optical elements with dramatically reduced costs, so much so that, since its introduction, application of such elements has become the standard, whereas, before, applications of aspheric elements was a rare exception. With these aspheric lenses, existing optical systems have gained outstanding performance improvements, and altogether new optical systems have become possible.

Precise molding starts from preforms that already have highly smooth polished surfaces, such as polished spheres or fire-polished precision gobs that are directly produced from glass melts (Fig. 2.11). Fire polish is the surface condition that glass acquires directly from casting. The main challenge here is to reshape these preforms to lenses while maintaining the high surface quality. For this reason, the preforms are heated to the lowest possible temperature that enables deformation by pressing. High-precision shaping while withstanding high pressure and wear puts strict requirements on the press molds. These molds are very precisely produced from hard metal and are therefore very expensive. This fact restricts application of precise molding to the production of series with a minimum number of parts ranging from 10,000 to 100,000, which is typical for consumer optics (see product examples in Fig. 2.12) but is rare in industrial optics applications or with high-end consumer optics.

The precise molding process puts requirements on the glass types, such that not all glass types are suitable for this process. They must have a low transformation temperature and should not stick to the mold material. Glass manufacturers have introduced sets of new glass types developed to fulfill these requirements. Such glasses are frequently called low-T_g glasses. However, existing glass types have been tested and have proven to be suitable for precise molding. For specific information, refer to the manufacturer catalogs.

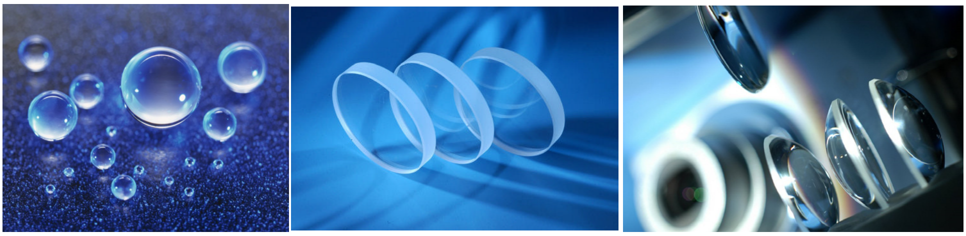

Figure 2.11 Precise molding of preforms: (left to right) spheres, disks, and gobs (courtesy of SCHOTT AG).

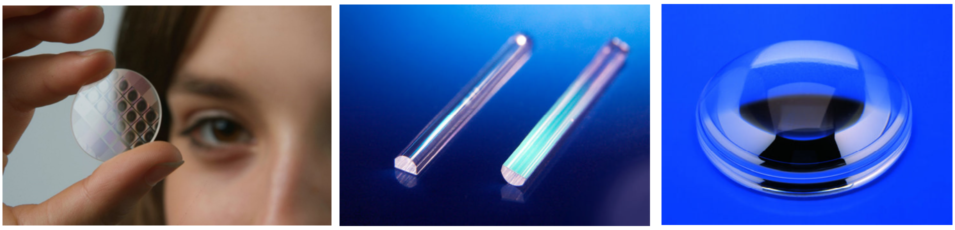

Figure 2.12 Precise molding products: (left to right) Diffractive optical elements, LED fast axis collimating lenses, and aspheric lenses (courtesy of SCHOTT AG).

Another restriction is due to the short processing cycles for single items that is necessary for maintaining low costs. Cycle periods are typically 20 min. This time period includes heating, pressing, and annealing of the glass. The restriction results specifically from the very short time available for annealing. Such cycle times are equivalent to annealing rates much higher than 1000 K/h, which is more than a factor of 100 higher than the rates used for fine annealing. Such temperature change rates will lead to high thermal gradients when glass thickness exceeds about 4 mm. The strongly rising inhomogeneity of refractive index and stress birefringence precludes using precise molding for applications with thicker lenses.

Moreover, with such annealing rates, refractive index and Abbe number are significantly different from values determined for standard data sheets. The so-called index drop and the change of the Abbe number cannot be determined and controlled with the same precision as with reheat pressing. Therefore, the usability of precision molding for optical systems with high specifications should be carefully checked.

Advantages of precise molding are:

- low-cost production of polished lenses;
- low-cost production of aspheric polished lenses.

Disadvantages are:

- High mold costs require large series in order to be economic.
- Only a restricted number of glass types can be precision molded.
- Thickness of items is restricted to about 4 mm.

References

1. H. R. Lillie and H. N. Ritland, “Fine annealing of optical glass,” *J. Amer. Ceram. Soc.* **37**, 466–473 (1954).

2. H. Rötger and H. Besen, “Ein rationelles Kühlverfahren zur Toleranzeinengung des Brechungverhältnisses optischer Gläser,” *Feingerätetechnik* **12**, 1–8 (1961).

3. H. Rötger and H. Besen, “Brechzahlbeeinflussung durch Feinkühlung bei Jenaer optischen Gläsern,” *Zeitschrift Silikattechnik* **13**(12), 424–427 (1962).

4. H. E. Hagy, “Fine annealing of optical glass for low residual stress and refractive index homogeneity,” *Appl. Opt.* **7**(5), 833–835 (1968).

Chapter 3

Refractive Index and Dispersion

3.1 Snell's Law of Refraction

The ISO 9802 Raw Optical Glass–Vocabulary and ISO 12123 Specification of Raw Optical Glass define refractive index as follows: "Ratio of the velocity of the electromagnetic waves at a specific wavelength in a vacuum to the velocity of the waves in the medium." From a more practical point of view, one may define it with Snell's law of refraction:

$$\frac{\sin \alpha_1}{\sin \alpha_2} = n, \tag{3.1}$$

with α_1 being the angle of an incident light ray coming from vacuum and α_2 the angle of the ray refracted in the medium with refractive index n. The angles are taken with respect to the surface's normal at the point where the light rays enters the medium (see Fig. 3.1). More generally, the law reads as

$$\frac{\sin \alpha_1}{\sin \alpha_2} = \frac{n_2}{n_1}, \tag{3.2}$$

for two media with different refractive indices. In the following discussion, if not otherwise stated, refractive indices of optical glasses will always be given with respect to standard air, which has a refractive index related to vacuum of 1.000272 at wavelength 589 nm and normal pressure of 1013 mbar.

3.2 Dispersion: Abbe Number

Dispersion denotes the effect that refractive index changes with wavelength. For optical glasses, refractive index changes more strongly in the blue–violet range than in the red range of the visible (VIS) spectrum (see Fig. 3.2). The dispersion curve is not linear and is also not a simple function of the wavelength. In order to easily characterize glass types with respect to their dispersion behavior, one uses different simplifying quantities in practice.

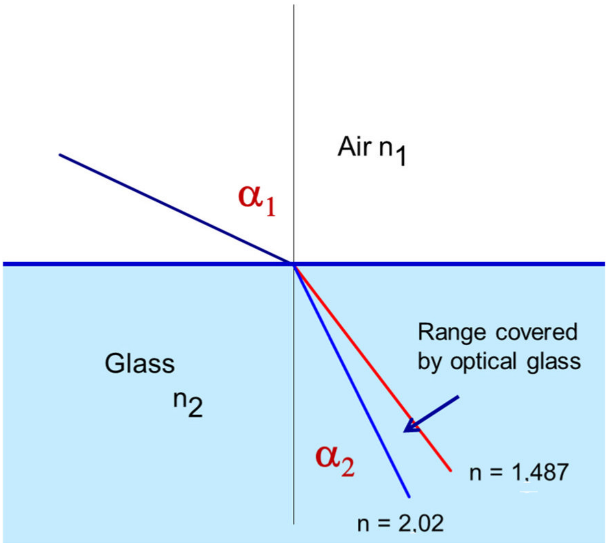

Figure 3.1 Refraction of light at an air–glass border.

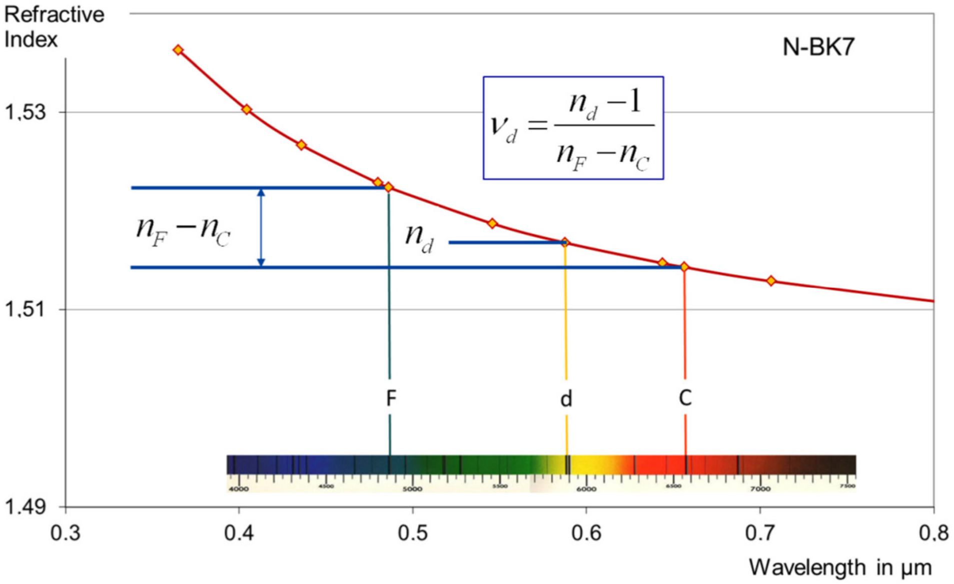

Figure 3.2 Dispersion: principal dispersion and Abbe number.

The first quantity is simply the difference between the refractive index at a blue light wavelength and a red light wavelength. This is called the principal dispersion and defined by the difference between the refractive indices at 486 nm and 656 nm (Fraunhofer's F and C lines): $n_F - n_C$. Most commonly used as a quantity for description of dispersion is the Abbe number, which relates the center refractive index at the d line (588 nm) to the principal dispersion as follows:

$$\nu_{\mathrm{d}} = \frac{n_{\mathrm{d}} - 1}{n_{\mathrm{F}} - n_{\mathrm{C}}}. \tag{3.3}$$

Because the principal dispersion is in the denominator, a high Abbe number corresponds to low dispersion.

A long-standing debate among optical designers is on whether the d, F, and C lines are the right choices for characterization of an optical glass. Many designers prefer the refractive index and Abbe number referring to the e, F′ and C′ lines, which are the mercury e line at 546.07 nm, and the two cadmium lines C′ at 643.85 and F′ at 479.99 nm. Historically, human vision opticians preferred the d-, F- and C-line set, and the device opticians preferred the e-, F′- and C′-line set. A vote in a large optical company resulted in one-third promoting the d line and two-thirds promoting the e line. Optical glass manufacturers wisely quote values for both sets in their catalogs. In ISO 10110, the standards series on optical elements, the reference set is the e-, F′- and C′-line set, and in the optical glass specification standard, both sets are given. The Abbe number based on the e-, F′- and C′-line set reads as follows:

$$\nu_{\mathrm{e}} = \frac{n_{\mathrm{e}} - 1}{n_{\mathrm{F'}} - n_{\mathrm{C'}}}. \tag{3.4}$$

3.3 Characteristic Light Wavelengths

Traditionally, a set of specific wavelengths is used for characterizing optical glasses with respect to refractive index and dispersion. These wavelengths belong to spectral lines of chemical elements. Most of them were introduced by Fraunhofer from his observation of absorption lines in the solar spectrum, and his designations are still in use. Table 3.1 gives the wavelengths of frequently used spectral lines with the current best accuracy. In order to obtain best refractive index data, it is important to enter the wavelengths with best available accuracy into the Sellmeier equation. Highlighted are the spectral lines that are the most common in specifying optical glasses.

Table 3.1 Characteristic light wavelengths used for characterizing optical glass properties. Bold: Most often used wavelength. FDes means Fraunhofer designation.

Wavelength (nm)	FDes	Element	Wavelength (nm)	FDes	Element	Wavelength (nm)	FDes	Element
2325.42		Hg	643.8469	C′	Cd	404.6561	h	Hg
1970.09		Hg	632.8		He-Ne	365.0146	i	Hg
1529.582		Hg	589.2938	D	Na	334.1478		Hg
1060.0		Nd	**587.5618**	**d**	**He**	312.5663		Hg
1013.98	t	Hg	**546.0740**	**e**	**Hg**	296.7278		Hg
852.11	s	Cs	**486.1327**	**F**	**H**	280.4		Hg
706.5188	r	He	479.9914	F′	Cd	248.3		Hg
656.2725	**C**	**H**	435.8343	g	Hg			

3.4 Partial Dispersion

Refractive index at the wavelength range center of visible light and Abbe number are only first approximations describing the refraction behavior of an optical glass. For high-quality optical systems, more precise characterization is needed. The next step is a more detailed look at refractive index changes over partial wavelength ranges that are related to the principal dispersion: relative partial dispersions.

The relative partial dispersion $P_{x,y}$ (d line) and $P'_{x,y}$ (e line) for the wavelengths x and y are defined by the equations

$$P_{x,y} = \frac{n_x - n_y}{n_\mathrm{F} - n_\mathrm{C}}, \quad P'_{x,y} = \frac{n_x - n_y}{n_{\mathrm{F}'} - n_{\mathrm{C}'}}. \tag{3.5}$$

Most frequently used are partial dispersions in the blue–violet range, based on the g (436 nm) and F line, where dispersion is strongest, and in the red range with the C and s (852 nm) line:

$$P_\mathrm{g,F} = \frac{n_\mathrm{g} - n_\mathrm{F}}{n_\mathrm{F} - n_\mathrm{C}}, \quad P'_\mathrm{g,F} = \frac{n_\mathrm{g} - n_\mathrm{F}}{n_{\mathrm{F}'} - n_{\mathrm{C}'}}; \tag{3.6a}$$

and

$$P_\mathrm{C,s} = \frac{n_\mathrm{C} - n_\mathrm{s}}{n_\mathrm{F} - n_\mathrm{C}}, \quad P'_\mathrm{C,s} = \frac{n_\mathrm{C} - n_\mathrm{s}}{n_{\mathrm{F}'} - n_{\mathrm{C}'}}. \tag{3.6b}$$

As Ernst Abbe observed, many optical glasses follow an approximately linear relationship between partial dispersions and the Abbe number as follows:

$$P_{x,y} \approx a_{xy} + b_{xy} \nu_\mathrm{d}, \tag{3.7}$$

where a_{xy} and b_{xy} are specific constants for the given relative partial dispersion. Concrete formulas for some partial dispersions are:

$$\begin{aligned} P_\mathrm{C,t} &= 0.5450 + 0.004743 \cdot \nu_\mathrm{d} \\ P_\mathrm{C,s} &= 0.4029 + 0.002331 \cdot \nu_\mathrm{d} \\ P_\mathrm{F,e} &= 0.4884 - 0.000526 \cdot \nu_\mathrm{d} \\ P_\mathrm{g,F} &= 0.6438 - 0.001682 \cdot \nu_\mathrm{d} \\ P_\mathrm{i,g} &= 1.72541 - 0.008382 \cdot \nu_\mathrm{d} \end{aligned} \tag{3.8}$$

Glass types that lie on straight lines are called normal glasses. In order to correct color in images for more than two wavelengths, glasses are required that do not obey this rule. Therefore, glass types with partial dispersion deviating from Abbe's empirical rule are needed, and indeed, much effort in glass development has concentrated on finding such glasses.

The deviation of the partial dispersion $P_{x,y}$ from Abbe's rule is given by $\Delta P_{x,y}$. With this extension, the relation between partial dispersion and Abbe number now reads as follows:

$$P_{x,y} = a_{xy} + b_{xy}\nu_{\mathrm{d}} + \Delta P_{x,y}, \tag{3.9}$$

with $\Delta P_{x,y}$ providing a numerical value for the deviation of the glass from the "iron straight line" of the normal glasses, as Otto Schott called it.

Optical glass data sheets list the partial dispersion $P_{x,y}$ for five relative partial dispersions for each glass type in the data sheets. The positions of the normal lines for each of the partial dispersions $\Delta P_{x,y}$ are determined based on value pairs of the glass types K7 and F2. The explicit formulas for the deviations of the above-mentioned five relative partial dispersions are:

$$\Delta P_{\mathrm{C,t}} = \frac{n_{\mathrm{C}} - n_{\mathrm{t}}}{n_{\mathrm{F}} - n_{\mathrm{C}}} - \left(0.5450 + 0.004743 \cdot \nu_{\mathrm{d}}\right),$$

$$\Delta P_{\mathrm{C,s}} = \frac{n_{\mathrm{C}} - n_{\mathrm{s}}}{n_{\mathrm{F}} - n_{\mathrm{C}}} - \left(0.4029 + 0.002331 \cdot \nu_{\mathrm{d}}\right),$$

$$\Delta P_{\mathrm{F,e}} = \frac{n_{\mathrm{F}} - n_{\mathrm{e}}}{n_{\mathrm{F}} - n_{\mathrm{C}}} - \left(0.4884 - 0.000526 \cdot \nu_{\mathrm{d}}\right),$$

$$\Delta P_{\mathrm{g,F}} = \frac{n_{\mathrm{g}} - n_{\mathrm{F}}}{n_{\mathrm{F}} - n_{\mathrm{C}}} - \left(0.6438 - 0.001682 \cdot \nu_{\mathrm{d}}\right),$$

$$\Delta P_{\mathrm{i,g}} = \frac{n_{\mathrm{i}} - n_{\mathrm{g}}}{n_{\mathrm{F}} - n_{\mathrm{C}}} - \left(1.7241 - 0.008382 \cdot \nu_{\mathrm{d}}\right). \tag{3.10}$$

It should be noted that the deviations of the relative partial dispersions might be slightly different between different glass manufacturers because the parameters of the straight lines are not standardized.

Data on partial dispersions (see Figs. 3.3–3.5) have lost quite a lot of importance since computers with optical design software started allowing the use of full dispersion curves in calculations of optical systems. Nowadays, these plots are mainly used for an initial selection of glass types for a design.

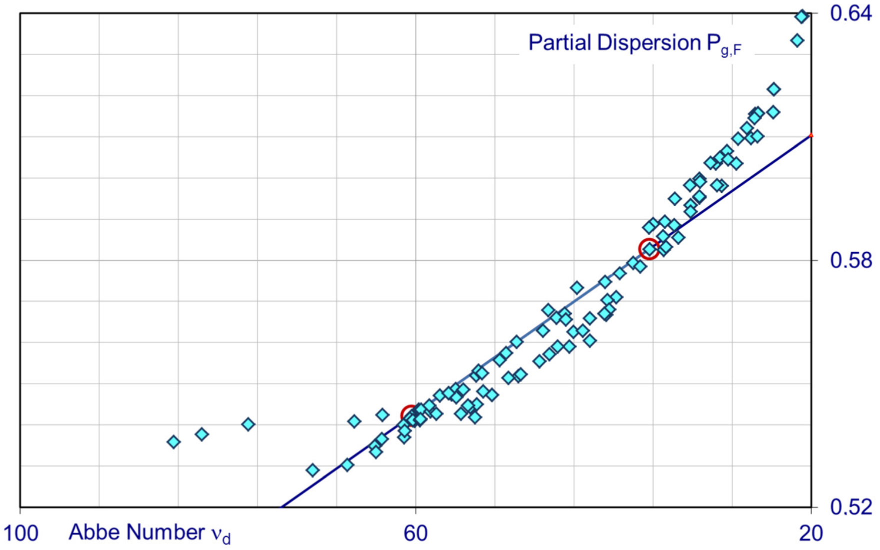

Figure 3.3 Partial dispersion $P_{g,F}$ in the blue light of optical glasses plotted against the Abbe number with the normal-glass line defined by the values of the glass types K7 and F2 (marked with circles).

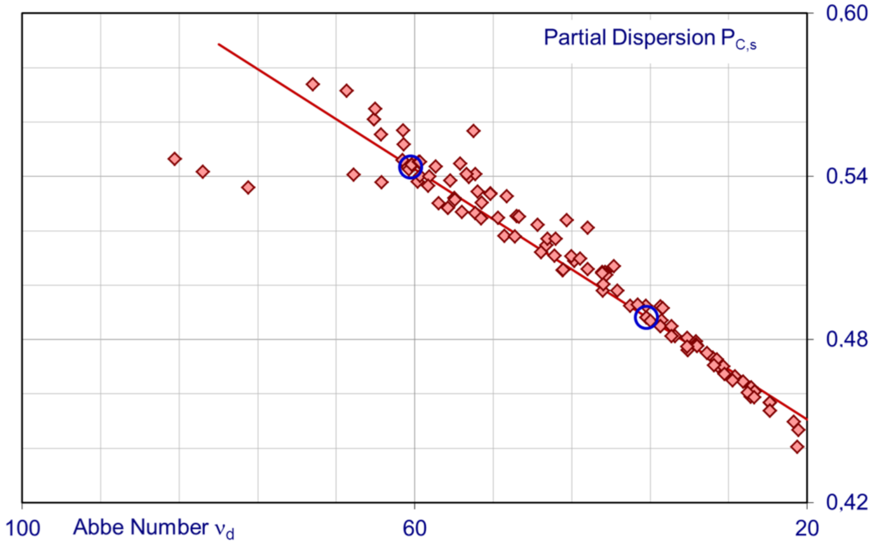

Figure 3.4 Partial dispersion $P_{C,s}$ in the red light of optical glasses plotted against the Abbe number with the normal-glass line defined by the values of the glass types K7 and F2 (marked with circles).

If one categorizes the optical glass types according to their deviation of the partial dispersion $\Delta P_{g,F}$ from the normal line, the Abbe diagram shows the ranges in which glasses are located with special dispersion properties (see Fig. 3.6). High positive deviations can be found in the lower left with the fluoro-phosphate glass types and in the upper right corner with the dense flint glasses. Glasses with negative deviations are concentrated in the upper left region, with the highest deviations at the very edge of the diagram's population. An exception forms a set with the shape of a curved line at much lower refractive index. These are the special short flint KZFS glass types. The categorization according to the deviation of the partial dispersion $\Delta P_{C,s}$ from the normal line (Fig. 3.7) is the complement of the one for $\Delta P_{G,f}$ to a great extent, but not entirely.

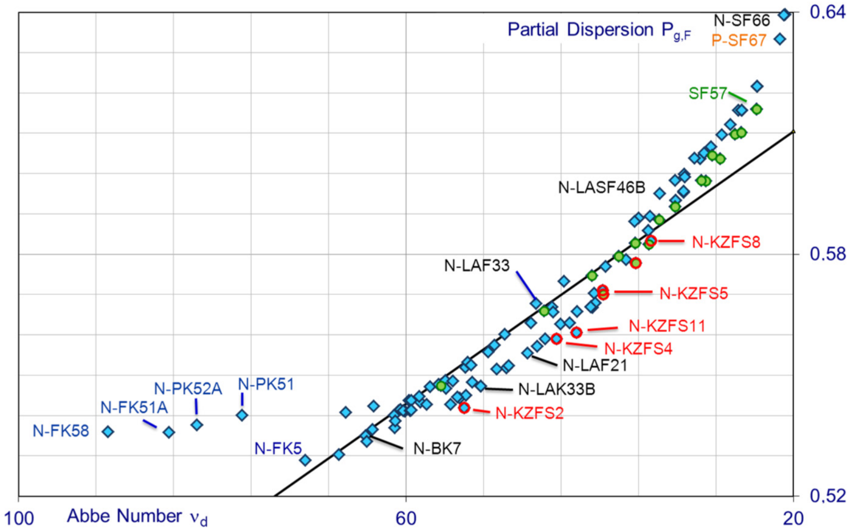

Figure 3.5 Partial dispersion $P_{g,F}$ of selected optical glass types.

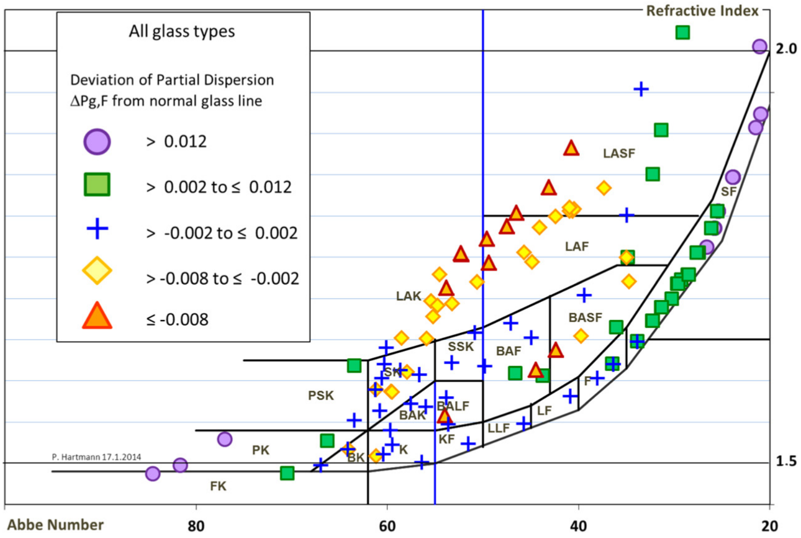

Figure 3.6 Optical glass types categorized according to their deviation of the partial dispersion $\Delta P_{g,F}$ from the normal line.

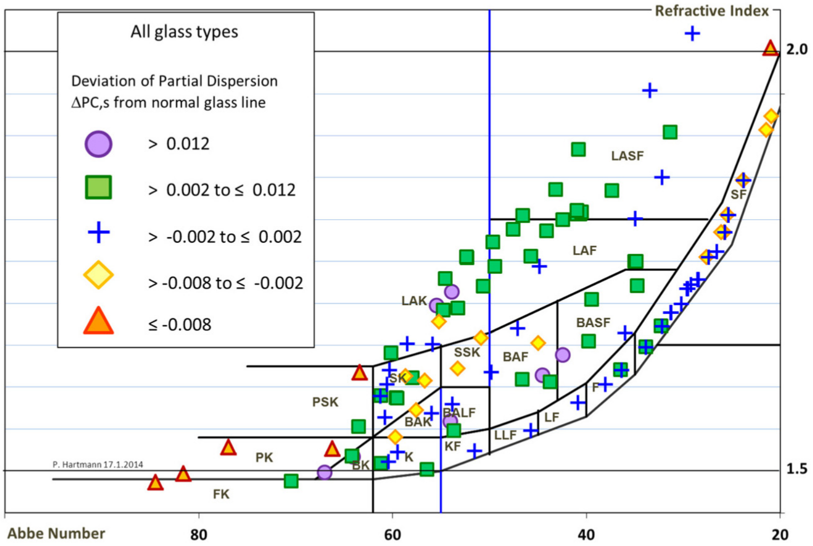

Figure 3.7 Optical glass types categorized according to their deviation of the partial dispersion $\Delta P_{C,s}$ from the normal line.

3.5 Dispersion Formulas

The most accurate and complete description of dispersion is done with dispersion formulas extending from the UV absorption edge to IR light, where most glasses start to absorb significantly: around 2.5 μm. A requirement for a dispersion formula is that the refractive index values must be calculated over a wide range of wavelengths with the same precision as the best measurement devices can achieve, which is below 3×10^{-6}. Moreover, this should be accomplished with a restricted number of coefficients.

In the past, a Laurent series expansion formula was used:

$$n^2 = A_0 + A_1\lambda^2 + A_2\lambda^{-2} + A_3\lambda^{-4} + A_4\lambda^{-6} + A_5\lambda^{-8}, \tag{3.11}$$

with the wavelength λ and the glass-type specific coefficients $A_0, \ldots, A_5$ quoted in the optical glass catalog. The accuracy of this formula was $\pm 3 \times 10^{-6}$ in the VIS range and $\pm 5 \times 10^{-6}$ in the neighboring ranges of down to 365 nm and up to 1014 nm. In the 1980s, the demand for higher accuracy and applicability over a wider wavelength span increased. The Laurent series turned out to be incapable of adequately representing the glass dispersion. Therefore, with the 1992 catalog,[1] SCHOTT replaced it with a Sellmeier-type formula with three absorption terms derived from the general dispersion formula:

$$n(\lambda)=\left(\frac{B_1\lambda^2}{\lambda^2-C_1}+\frac{B_2\lambda^2}{\lambda^2-C_2}+\frac{B_3\lambda^2}{\lambda^2-C_3}+1\right)^{1/2}. \tag{3.12}$$

The better physical foundation leads to more accurate values beyond 1 μm and better interpolation values between the measured wavelengths, as careful tests have demonstrated.[2–4]

The Sellmeier coefficients are given for each optical glass type in its data sheet for the temperature of 22 °C and air pressure of 1013 mbar. For calculations with the coefficients given in the SCHOTT data sheets, the wavelength must be entered with the unit of microns. With precision measurement, they can be determined for individual pieces of glass.

The range of validity for given coefficients may extend between 300 and 2325 nm but depends on the position of the UV transmission edge, which, for optical glass, is travelling from 300 nm to the VIS light range, with increasing refractive index (see Section 5.3). In precision test certificates, the validity range is given explicitly for each measurement.

The Sellmeier formula with its three absorption terms does not accurately describe dispersion outside of the given validity range and it is not meant to do so. Close to the UV absorption band, refractive index rises very fast (see Fig. 3.8), such that deviations also rise fast. The third term represents an IR absorption band in the region of 10 μm. In reality, absorption starts soon after 2 μm (depending on the glass type); beyond 4.5 μm, glass absorbs strongly. The Sellmeier formula should be seen as a fit formula working very well in the specified validity range with a reasonable number of parameters, the six Sellmeier coefficients. Other dispersion formulas with only a few coefficients give values that are less accurate or have restricted application ranges.

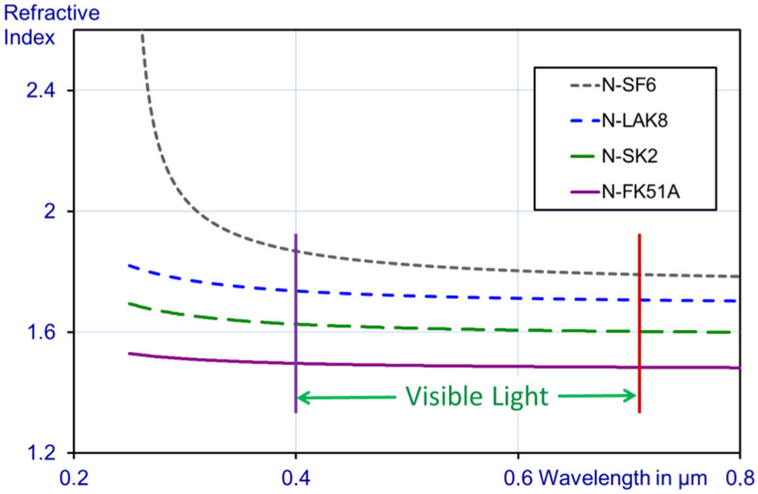

Figure 3.8 Refractive index curves for four optical glasses covering a wide range of dispersion.

As an example of calculating refractive index and dispersion quantities from Sellmeier coefficients, the data sheet of N-BK7 is shown in Fig. 3.9. All entries in the cells marked by dark, full frames are calculated from the six Sellmeier coefficients marked by the dashed frame in the lower left corner. All refractive index and dispersion data are redundant and are given only for convenience; for optical design software, the Sellmeier coefficients are sufficient. All of these coefficients are given to a precision of eight digits. In principle, this would not be necessary for all coefficients for all glass types. Some coefficients could be given with lower precision. However, doing so would introduce the need for detailed data control, which would not provide a real benefit but might cause confusion and errors.

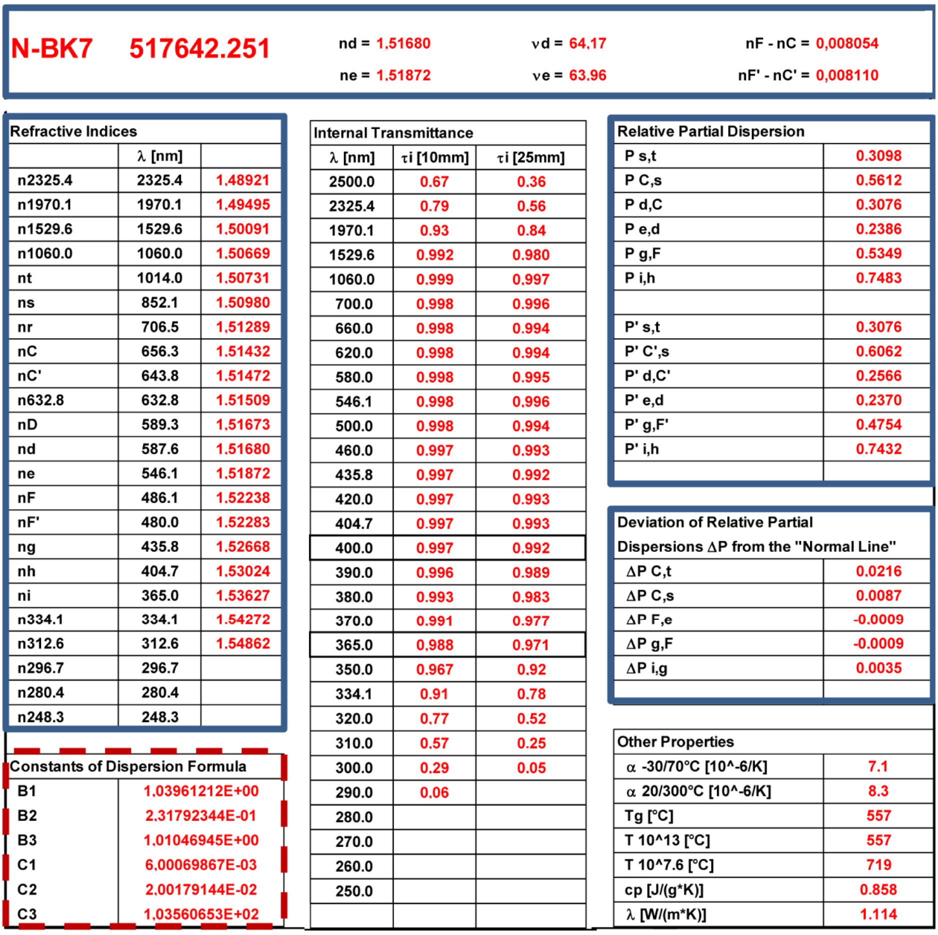

N-BK7 517642.251

nd = 1,51680
νd = 64,17
nF - nC = 0,008054

ne = 1,51872
νe = 63.96
nF' - nC' = 0,008110

Refractive Indices		
	λ [nm]	
n2325.4	2325.4	1,48921
n1970.1	1970.1	1,49495
n1529.6	1529.6	1,50091
n1060.0	1060.0	1,50669
nt	1014.0	1,50731
ns	852.1	1,50980
nr	706.5	1,51289
nC	656.3	1,51432
nC'	643.8	1,51472
n632.8	632.8	1,51509
nD	589.3	1,51673
nd	587.6	1,51680
ne	546.1	1,51872
nF	486.1	1,52238
nF'	480.0	1,52283
ng	435.8	1,52668
nh	404.7	1,53024
ni	365.0	1,53627
n334.1	334.1	1,54272
n312.6	312.6	1,54862
n296.7	296.7	
n280.4	280.4	
n248.3	248.3	

Constants of Dispersion Formula	
B1	1,03961212E+00
B2	2,31792344E-01
B3	1,01046945E+00
C1	6,00069867E-03
C2	2,00179144E-02
C3	1,03560653E+02

Internal Transmittance		
λ [nm]	τi [10mm]	τi [25mm]
2500.0	0.67	0.36
2325.4	0.79	0.56
1970.1	0.93	0.84
1529.6	0.992	0.980
1060.0	0.999	0.997
700.0	0.998	0.996
660.0	0.998	0.994
620.0	0.998	0.994
580.0	0.998	0.995
546.1	0.998	0.996
500.0	0.998	0.994
460.0	0.997	0.993
435.8	0.997	0.992
420.0	0.997	0.993
404.7	0.997	0.993
400.0	0.997	0.992
390.0	0.996	0.989
380.0	0.993	0.983
370.0	0.991	0.977
365.0	0.988	0.971
350.0	0.967	0.92
334.1	0.91	0.78
320.0	0.77	0.52
310.0	0.57	0.25
300.0	0.29	0.05
290.0	0.06	
280.0		
270.0		
260.0		
250.0		

Relative Partial Dispersion	
P s,t	0.3098
P C,s	0.5612
P d,C	0.3076
P e,d	0.2386
P g,F	0.5349
P i,h	0.7483
P' s,t	0.3076
P' C',s	0.6062
P' d,C'	0.2566
P' e,d	0.2370
P' g,F'	0.4754
P' i,h	0.7432

Deviation of Relative Partial Dispersions ΔP from the "Normal Line"	
ΔP C,t	0.0216
ΔP C,s	0.0087
ΔP F,e	-0.0009
ΔP g,F	-0.0009
ΔP i,g	0.0035

Other Properties	
α -30/70°C [10^-6/K]	7.1
α 20/300°C [10^-6/K]	8.3
Tg [°C]	557
T 10^13 [°C]	557
T 10^7.6 [°C]	719
cp [J/(g*K)]	0.858
λ [W/(m*K)]	1.114

Figure 3.9 Data sheet of N-BK7 (excerpt) with refractive index and dispersion data. The data marked by solid-line frames are calculated from the six Sellmeier coefficients given in the dashed-line frame. For checking calculations, note that wavelengths must be entered into the Sellmeier equation in the unit of micrometers.

3.6 Refractive Index Tolerances

One of the most important requirements on the properties of any material to be used technically is that the properties are reproducible and have constant values within certain given volumes. As a consequence, there must be tolerances for absolute values and for changes of these values.

The absolute tolerance for the refractive index of optical glasses refers to limits around their nominal catalog values. Possible grades according to the standard ISO 12123 Specification of Raw Optical Glass are shown in Table 3.2.

Table 3.2 Principal refractive index tolerances (* denotes a new grade introduced by SCHOTT in 2013).

Refractive index	SCHOTT grade denominations
n.a.	±0.0020
n.a.	±0.0010
3	±0.0005
2	±0.0003
1	±0.0002
0.5*	±0.0001*

The principal refractive index, as shown in the table, is the refractive index in the middle range of the VIS spectrum and is commonly used to characterize an optical glass. Traditionally, two variants are in use: n_d, the refractive index at the wavelength 587.56 nm, and n_e, the refractive index at 546.07 nm. The tolerance limits are valid for both variants. The table additionally contains the SCHOTT grade denominations. ISO 12123 allows a variation width of ±0.0020 and ±0.0010 for the widest tolerances. In practice, high-quality optical glass suppliers guarantee ±0.0005 as a normal tolerance without the need for special requirements. In contrast to regulations used in the past, the given limits hold for all glass types of any refractive index values.

With respect to tolerances on refractive index changes, it is essential to distinguish between changes within two different reference volumes. Refractive index variation means the change of the refractive index among different pieces of glass of a delivery lot. Homogeneity describes the change within a given individual piece.

3.7 Refractive Index Variation Tolerances

The refractive index variation applies to a delivery lot, which is a set of production batches assembled according to a customer's order requirement. Production batches are the smallest amount of material subject to material management and consist of several strip cuts or single glass blocks. They are denominated with a batch number and represent a short production period, usually one hour or less. Such batches are assembled to form a delivery lot based on the tolerances according to ISO 12123 (see Table 3.3). ISO 12123 allows a variation width of $\pm 30 \times 10^{-5}$ for the widest tolerance. However, in practice, high-quality optical glass suppliers guarantee $\pm 10 \times 10^{-5}$ as a normal tolerance without the need for special requirements.

Table 3.3 Refractive index variation tolerance limits for delivery lots.

n.a.	$\pm 30 \times 10^{-5}$
SN	$\pm 10 \times 10^{-5}$
S0	$\pm 5 \times 10^{-5}$
S1	$\pm 2 \times 10^{-5}$

The delivery lots may be selected according to the tolerance limits from different parts of production sequences; thus, smooth variation in the lot's glass properties cannot be expected in all cases. Moreover, the glass from different lots may have different fine-annealing histories. This is of no importance for a normal end customer. Re-annealing of such delivery lots, however, may lead to increasing the refractive index variation. If parts of the delivery lots had been annealed with different annealing rates in order to fit in the same tolerance range, a re-annealing with a new rate being the same now for all parts will lead to diverging resulting values. For reheat pressings, the variation tolerance limits are twice as wide as those for fine annealed cut pieces or blocks.

3.8 Abbe Number Tolerances

Dispersion variation is limited by means of Abbe number intervals. Table 3.4 lists the preferred quality grades according to ISO 12123. They hold for both Abbe numbers, either referred to the d line or to the e line. Schott's standard tolerance of the Abbe number is ±0.5%. The Abbe number variation within delivery lots may extend over the same spans as those given for the absolute value while these limits will be kept anyway. The fulfilling of the tolerance is reported in test certificates providing actual values for delivery lots.

Table 3.4 Abbe number tolerance limits (* denotes a new grade introduced by SCHOTT in 2013).

4	±0.8%
3	±0.5%
2	±0.3%
1	±0.2%
0.5*	$\pm 0.1\%^{*}$

3.9 Annealing Influence on Refractive Index and Dispersion

Generally, two processes can be used for adjusting refractive index and dispersion with fine annealing: soak annealing (or quenching) and constant-rate annealing. In both processes, the first step involves heating the glass to a temperature higher than the glass's transformation temperature, and staying at that temperature long enough to assure complete stress relaxation throughout the total volume.

The first method, soak annealing, adjusts the optical properties of glass by keeping it at a constant temperature in the transformation range for a minimum time period to reach equilibrium, and then cooling it rapidly. Refractive index is determined by the specific constant soaking temperature chosen.

With the second method, the constant rate annealing method, the glass is cooled from the relaxation temperature to about 150 °C below the transformation temperature, with a constant cooling rate. Refractive index and dispersion can be adjusted by changing the cooling rate.

The soak method needs longer process times and leads to a lower homogeneity quality. This method is not at all suited to thicker pieces of glass because inhomogeneity and stress birefringence will be too high. For this reason, the constant-rate method is used almost exclusively in common practice.

With the constant-rate method, the refractive index n_d and Abbe number ν_d of fine annealed batches can be calculated very precisely in advance. The formulas provide changes in refractive index and Abbe number caused by annealing with a rate ν_k that is different from a predetermined reference rate ν_{k0}:

$$n_\mathrm{d}\left(\nu_\mathrm{k}\right) = m_{n_\mathrm{d}} \cdot \log_{10}\left(\frac{\nu_\mathrm{k}}{\nu_\mathrm{k0}}\right) + n_\mathrm{d}\left(\nu_\mathrm{k0}\right), \tag{3.13a}$$

$$\nu_\mathrm{d}\left(\nu_\mathrm{k}\right) = m_{\nu_\mathrm{d}} \cdot \log_{10}\left(\frac{\nu_\mathrm{k}}{\nu_\mathrm{k0}}\right) + \nu_\mathrm{d}\left(\nu_\mathrm{k0}\right). \tag{3.13b}$$

Preconditions for using the constant-rate method are:

- careful control of the annealing rates employed,
- precisely determined annealing parameters m_{nd} and $m_{\nu d}$ for each glass type, and
- accurate reference values for refractive index and Abbe number of the glass batches to be annealed determined with samples taken routinely during production. SCHOTT uses 2 K/h as reference annealing rate.

The annealing parameters m_{nd} and $m_{\nu d}$ are determined for a glass type on the occasion of its introduction to the optical glass program with high-precision refractive index measurements on samples cooled with different rates. In practice, the annealing rate cannot be chosen arbitrarily. The first limit is set by stress birefringence, which forbids fast rates, depending on the glass item's size and geometry. The smaller the item is, the faster it can be cooled down. With increasing size, especially increasing thickness, the cooling rate must be strongly reduced, as follows:

- for small reheat pressings with thickness of a few centimeters, 4–10 K/h is acceptable;
- for thick strips or blocks with thickness around 10 cm, rates around 1 K/h are acceptable; and
- for large castings of 1-m diameter and 200-mm thickness or more, 0.2–0.15 K/h is acceptable.

The lower limit of the annealing rate is set by economics in order not to occupy annealing furnaces longer than actually needed. These limits might be further narrowed by the requirement of fulfilling the tolerance for refractive index and Abbe number.

Refractive index and Abbe number changes with annealing have some consequences in everyday practice. The most important consequence is that, even if there is material available on stock, it might not be suitable for annealing to the tolerances required. This will be explained in Figs. 3.10–3.13, which are called annealing line diagrams. These diagrams show the changes in refractive index and Abbe number with respect to the absolute tolerances for N-BK7. The boxes represent different refractive index and Abbe number grades, with the narrowest being in the middle around the catalog value, marked with a cross. The optical position at reference annealing rate of 2 K/h coincides with the catalog value.

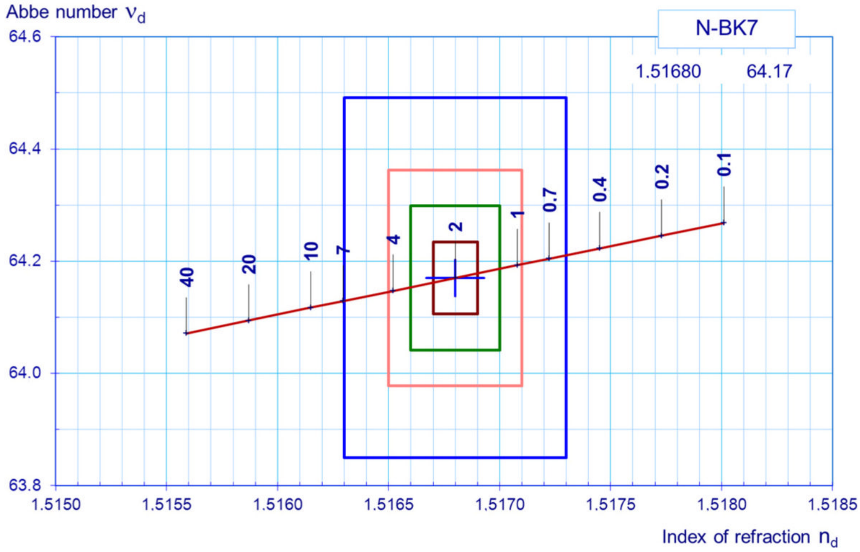

Figure 3.10 Annealing line diagram for the glass type N-BK7 with boxes representing tolerance grades 3/3, 2/2, 1/1, and 05/05 and with reference sample annealed at 2 K/h, coinciding with the catalog value of the glass. The numbers on the annealing line give annealing rates in K/h.

Fine annealing can change refractive index and Abbe number only along the straight line, the so-called annealing line. The actual optical position of a specific melt at 2 K/h annealing rate is given by the melt's individual chemical composition, which will vary slightly from melt to melt. A melt with catalog position at 2 K/h, as shown in the Fig. 3.10, is not well suited for reheat pressing. The narrowest tolerances can be achieved, but, for economic reasons, only with rates that are slower than desired. Annealing at 4 to 10 K/h will lead to pressings lying only in the coarsest tolerance range of refractive index or will even violate tolerance. Large items, which cannot be annealed faster than 0.5 K/h due to stress birefringence, will generally lie outside of the refractive index tolerance.

Thus, in practice, chemical composition will be adjusted to shift the 2 K/h position to higher refractive indices for glass meant for pressings production, as shown in Fig. 3.11. Here the 2 K/h position lies directly at the border of the tolerance range. However, annealing of pressings with a rate between 4 K/h and 10 K/h will lead to fulfilling the narrowest tolerance range, as shown in Fig. 3.11. For large glass items, the shift must be exactly in the opposite direction (see Fig. 3.12.) As a consequence, in practice, one must use three different N-BK7 recipes in order to cover the requirements for producing items of different size.

Furthermore, chemical composition will vary to a certain extent. Some scatter in the 2 K/h values has to be expected. This can result in a given melt that might be not suitable to be annealed to the narrowest tolerance ranges. Figure 3.13 shows such a case. With that specific melt, only grade 3/3 will be reliably achieved. In order to achieve grade 2/2, the annealing rate must be between 7 and 10 K/h. It is not possible to reach the narrowest tolerance range, regardless of which annealing rate will be applied.

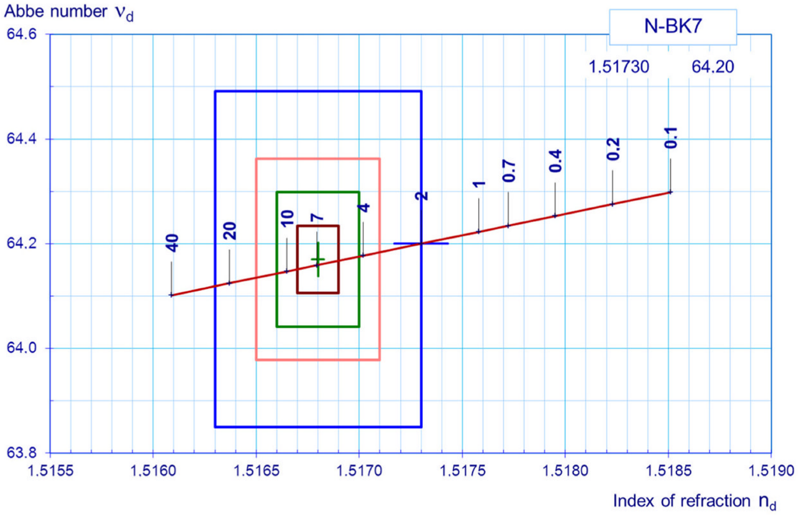

Figure 3.11 Annealing line diagram for the glass type N-BK7 with reference annealing rate shifted to the right by slightly adjusting its composition to be perfectly suited for reheat pressing production within the annealing rate range of 4 to 10 K/h.

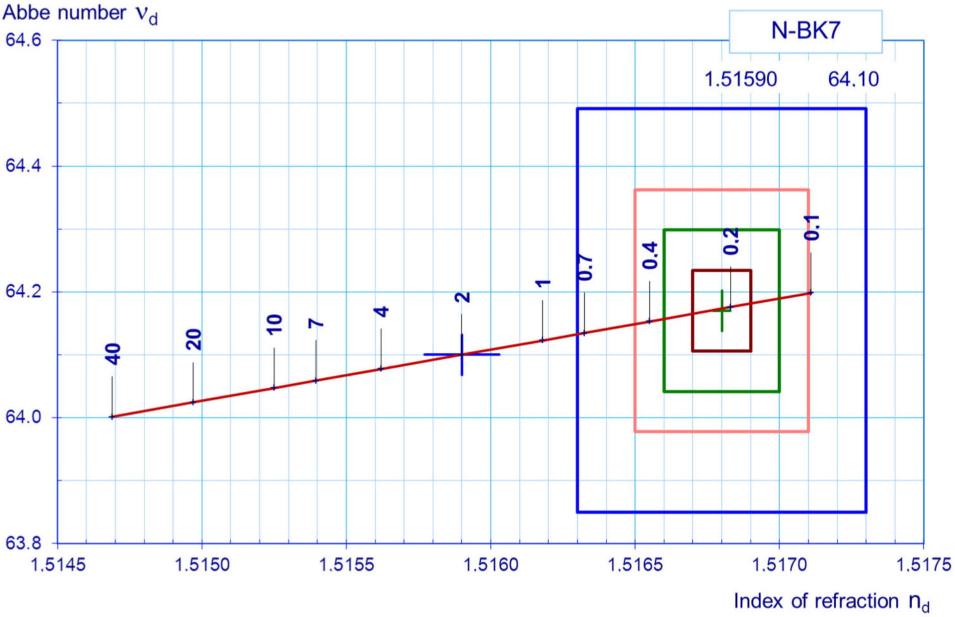

Figure 3.12 N-BK7 adjusted in chemical composition for the production of large glass blanks with a 2 K/h value far below the refractive index's lower tolerance.

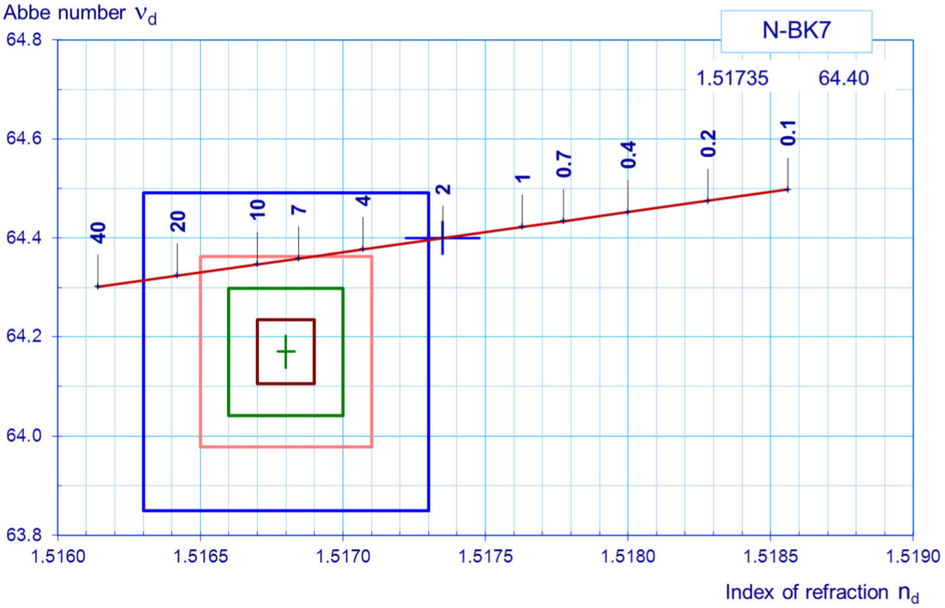

Figure 3.13 N-BK7 with chemical composition leading to a 2 K/h reference annealing rate value, resulting in the annealing line being located out of reach for the narrowest tolerances. Only grades 3/3 and 2/2 are accessible.

This property of optical glass causes enhanced complexity in material management and sometimes leads to the odd situation in which sufficient glass might be on stock, but cannot be delivered because the required optical position is not reachable. For large sales volume glasses, such a situation is not very likely, but for small-sales-volume glasses this property must be considered.

3.10 Annealing Influence on Different Glass Types

The slope of the annealing line and the width of the range between 40 K/h and 0.1 K/h is typical for a given glass type. There is a wide variation among the optical glasses of the catalog program. N-BK7 has a moderate sensitivity of the refractive index against annealing rate changes, that of the Abbe number being even lower (Fig. 3.10).

Stronger influence on the annealing rate change is observed for all lead- and arsenic-free glass types replacing the old lead silicate flints such as N-F2, which is, in fact, the most sensitive glass types of all (see Fig. 3.14). Its 40 K/h to 0.1 K/h interval spreads far outside the tolerance ranges, and its annealing line slope is negative.

The earlier lead-containing variant F2 is much less sensitive (see Fig. 3.15). The slope is positive, and the optical position width limited by the annealing rates of 40 K/h to 0.1 K/h almost completely covers the normal tolerance range of the refractive index. This also holds for the extremely low-dispersion glass type N-FK51A (see Fig. 3.16).

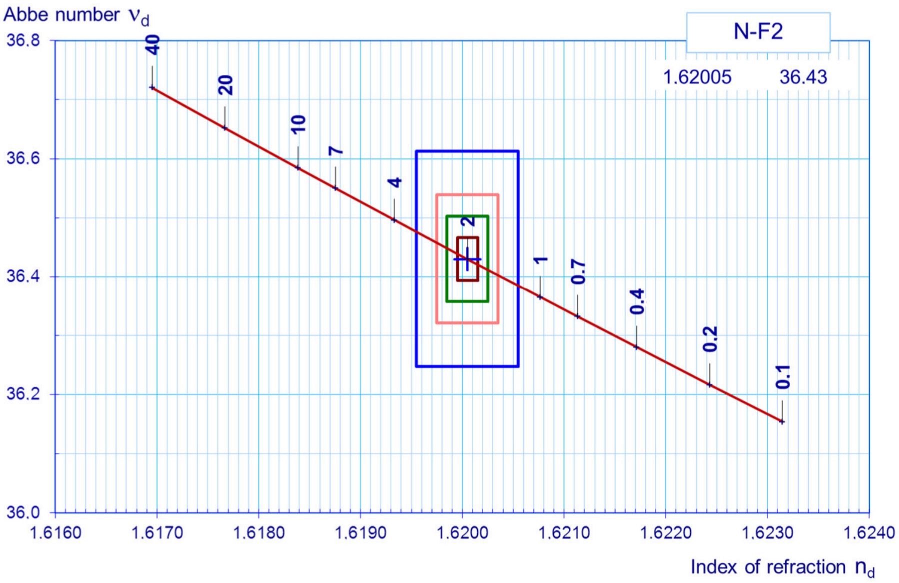

Figure 3.14 The lead-free flint glass type N-F2 is very sensitive to annealing rate changes. The slope of the annealing line and the ranges it spans relative to the tolerance widths are extraordinary.

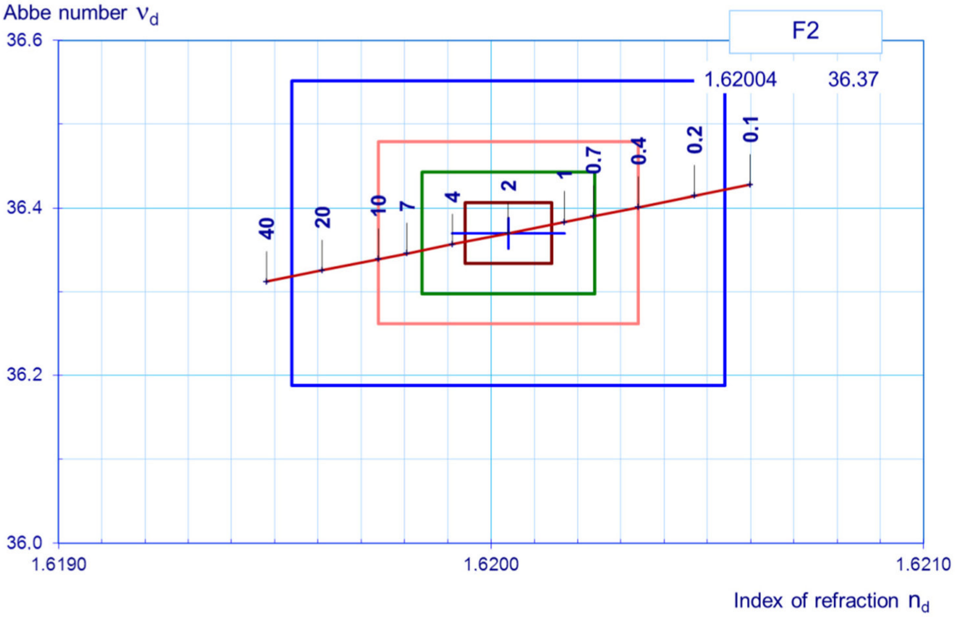

Figure 3.15 The lead-containing classical flint glass type F2 is far less sensitive to annealing rate changes. The slope and range of the annealing line show that this glass is much easier to anneal than N-F2.

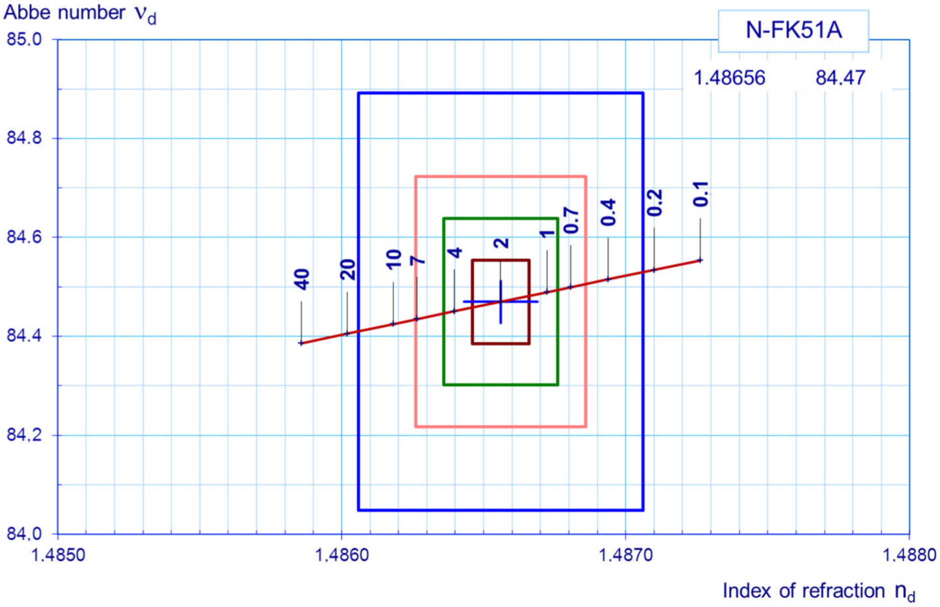

Figure 3.16 The very low-dispersion fluoro-phosphate glass type N-FK51A is also not very sensitive to annealing rate changes.

Another outstanding glass type is N-KZFS4, the lead- and arsenic-free variant of the short flint special glass KZFS4. Its slope is very close to zero (Fig. 3.17). Regardless of which annealing rate is applied, the Abbe number will always be the same.

Figure 3.18 shows the change of refractive index Δn_d and Abbe number $\Delta \nu_d$ in the case where glass is annealed ten times faster than with the reference annealing rate, meaning that the annealing rate ratio ν_k/ν_{k0} = 10:1. The changes are given relative to the width of the normal tolerance of the refractive index Δn_d (G3) = $\pm 5 \times 10^{-4}$ (x axis) and Abbe number $\Delta \nu_d$ (G3) = ±0.5% (y axis). (G3 means standard tolerance grade 3). For example, a ten-times-faster annealing for N-F2 means that the refractive index will decrease by almost –150% of the standard tolerance width, and the Abbe number will increase by about +60% of the standard tolerance. For the glass type F2, it is about –25% for the refractive index and –10 % for the Abbe number.

Classical glass types tend to have lower dependence of refractive index and Abbe number on the change in annealing rates than the lead- and arsenic-free glass types; compare, for example, the pairs F2 and N-F2 and SF6 and N-SF6. Most of the glass types with highest sensitivity located in the upper left part of Fig. 3.18 are lead-free flint glass types. Such glass types require careful control of their annealing processes, i.e., temperature absolute values and temperature homogeneity of annealing furnaces must be controlled and monitored with great care.

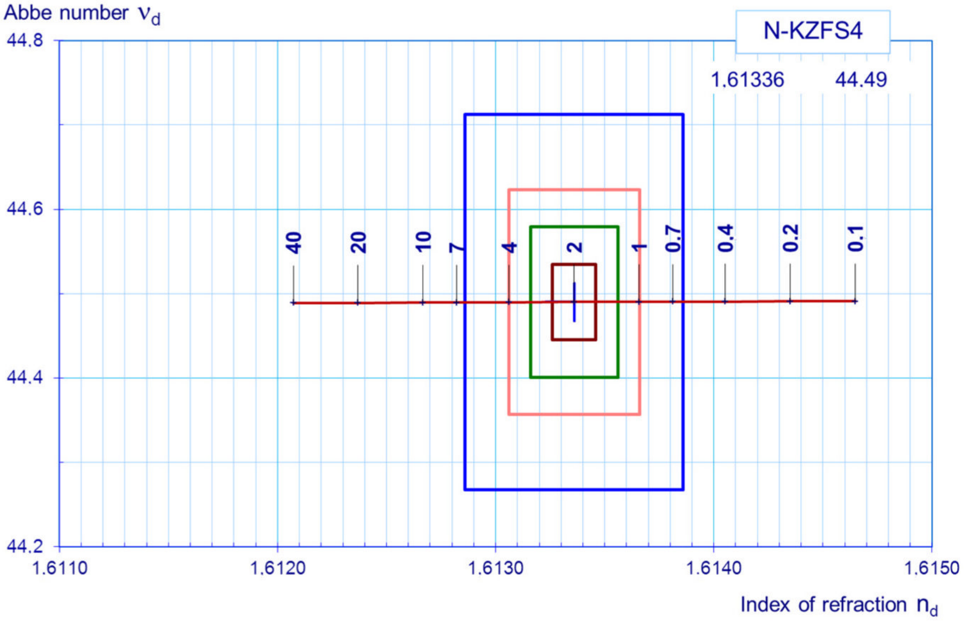

Figure 3.17 Annealing line of the short flint special glass N-KZFS4, with the slope being very close to zero.

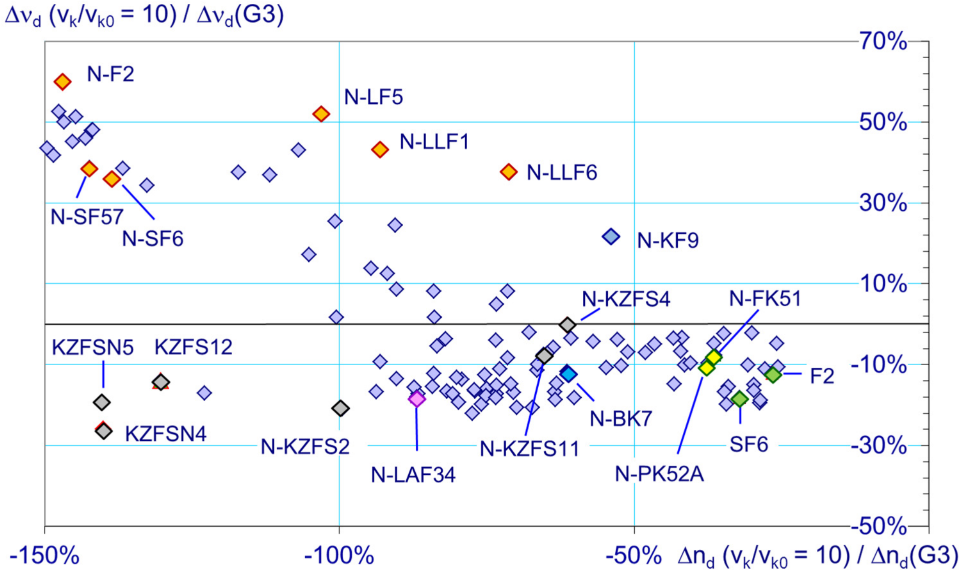

Figure 3.18 Change of refractive index Δn_d and Abbe number $\Delta \nu_d$ for annealing that is ten times faster than that using the reference annealing rate (ν_k/ν_{k0} = 10:1).

3.11 Annealing Schedule

By far, the highest volume of optical glass is produced as coarse annealed strip glass, and is reheat pressed later to the shape specified by customers. The pressings will be fine annealed according to a prescription called an annealing schedule (see Fig. 3.19). This certificate provides the reference annealing rate values for refractive index and Abbe number for the production batches used, together with the annealing parameters of the glass type. Additionally, it contains ranges for the annealing rate to be used in order to reach different refractive index and Abbe number tolerance grades.

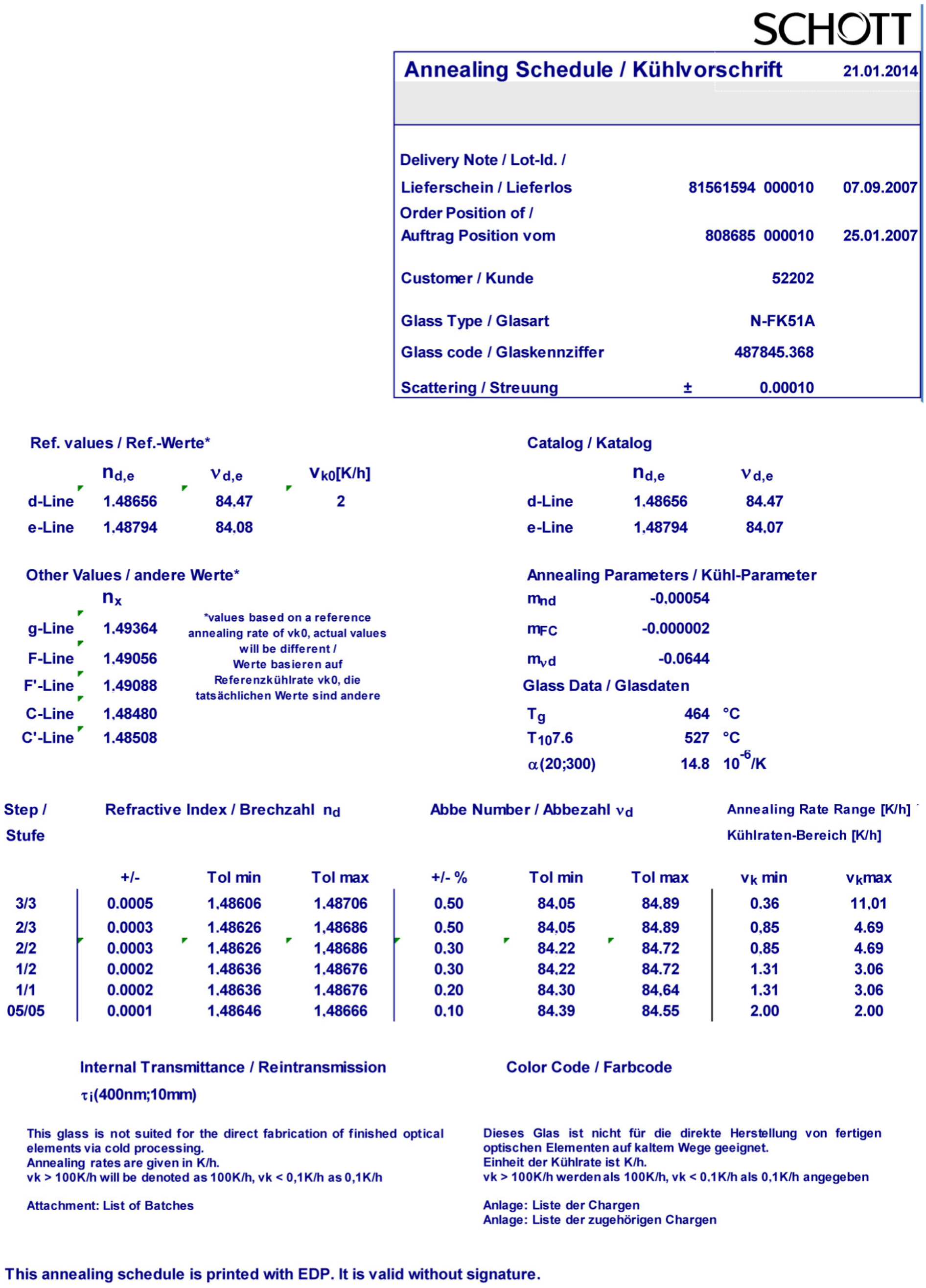

SCHOTT

Annealing Schedule / Kühlvorschrift 21.01.2014

Delivery Note / Lot-Id. / Lieferschein / Lieferlos	81561594 000010	07.09.2007
Order Position of / Auftrag Position vom	808685 000010	25.01.2007
Customer / Kunde	52202	
Glass Type / Glasart	N-FK51A	
Glass code / Glaskennziffer	487845.368	
Scattering / Streuung	± 0.00010	

Ref. values / Ref.-Werte*

	$n_{d,e}$	$\nu_{d,e}$	ν_{k0}[K/h]
d-Line	1.48656	84.47	2
e-Line	1.48794	84.08	

Catalog / Katalog

	$n_{d,e}$	$\nu_{d,e}$
d-Line	1.48656	84.47
e-Line	1.48794	84.07

Other Values / andere Werte*

	n_x
g-Line	1.49364
F-Line	1.49056
F'-Line	1.49088
C-Line	1.48480
C'-Line	1.48508

*values based on a reference annealing rate of vk0, actual values will be different / Werte basieren auf Referenzkühlrate vk0, die tatsächlichen Werte sind andere

Annealing Parameters / Kühl-Parameter

m_{nd}	-0.00054
m_{FC}	-0.000002
$m_{\nu d}$	-0.0644

Glass Data / Glasdaten

T_g	464	°C
$T_{10^{7.6}}$	527	°C
α(20;300)	14.8	10^{-6}/K

Step / Stufe	Refractive Index / Brechzahl n_d			Abbe Number / Abbezahl ν_d			Annealing Rate Range [K/h] / Kühlraten-Bereich [K/h]	
	+/-	Tol min	Tol max	+/- %	Tol min	Tol max	ν_k min	$\nu_k$max
3/3	0.0005	1.48606	1.48706	0.50	84.05	84.89	0.36	11.01
2/3	0.0003	1.48626	1.48686	0.50	84.05	84.89	0.85	4.69
2/2	0.0003	1.48626	1.48686	0.30	84.22	84.72	0.85	4.69
1/2	0.0002	1.48636	1.48676	0.30	84.22	84.72	1.31	3.06
1/1	0.0002	1.48636	1.48676	0.20	84.30	84.64	1.31	3.06
05/05	0.0001	1.48646	1.48666	0.10	84.39	84.55	2.00	2.00

Internal Transmittance / Reintransmission

τ_i(400nm;10mm)

Color Code / Farbcode

This glass is not suited for the direct fabrication of finished optical elements via cold processing.
Annealing rates are given in K/h.
vk > 100K/h will be denoted as 100K/h, vk < 0,1K/h as 0,1K/h

Attachment: List of Batches

Dieses Glas ist nicht für die direkte Herstellung von fertigen optischen Elementen auf kaltem Wege geeignet.
Einheit der Kühlrate ist K/h.
vk > 100K/h werden als 100K/h, vk < 0.1K/h als 0,1K/h angegeben

Anlage: Liste der Chargen
Anlage: Liste der zugehörigen Chargen

This annealing schedule is printed with EDP. It is valid without signature.

Figure 3.19 SCHOTT annealing schedule for a delivery lot of the glass type N-FK51A.

3.12 Refractive Index Measurement: V-Block

The v-block method for measuring the refractive index is well suited to combine high precision with a high throughput of samples. With the many measurements needed for monitoring production and provision of reliable data for test certificates and annealing schedules, a simple and cost-effective preparation of the samples is needed. Time-consuming and tedious sample adjustments and alignments must be avoided.

The key element is a glass block with a rectangular v-shaped groove and with refractive index values known from best-possible precision measurement. The sample will be located in the groove. Its dull surfaces will be made transparent with immersion oil. When the refractive indices of the sample and v-block match perfectly, an incident light ray will travel straight through the set without any deflection. If the sample's refractive index is higher than that of the v-block, the ray will be deflected upward in the system, as shown in Fig. 3.20, and vice versa for the opposite case. From the deflection angle one can calculate the difference of the relative indices.

As a rule, the refractive index will be measured at seven spectral lines: g, F′, F, e, d, C′, and C. The VIS light range is covered in this way between the wavelengths of 436 and 656 nm. In order to obtain the refractive index n_d and Abbe number ν_d with the lowest possible measurement errors, a dispersion curve is fitted to the data for all wavelengths. Refractive index n_d and Abbe number ν_d will be calculated from this dispersion curve. The accuracy of measurements obtained in this way for standard test certificates is $\pm 3 \times 10^{-5}$ for refractive index and $\pm 2 \times 10^{-5}$ for dispersion $n_F - n_C$. Extending the wavelength range to 365–1014 nm by measuring the four spectral lines i, h, r, and t additionally improves accuracy to $\pm 2 \times 10^{-5}$ for refractive index and $\pm 1 \times 10^{-5}$ for dispersion $n_F - n_C$.

In practice, a set of up to ten samples will be cemented together. Measuring the resulting bar in one process eliminates systematic errors when concentrating on the relative changes between the samples. This allows comparison between samples with considerably better accuracy than measuring absolute values.

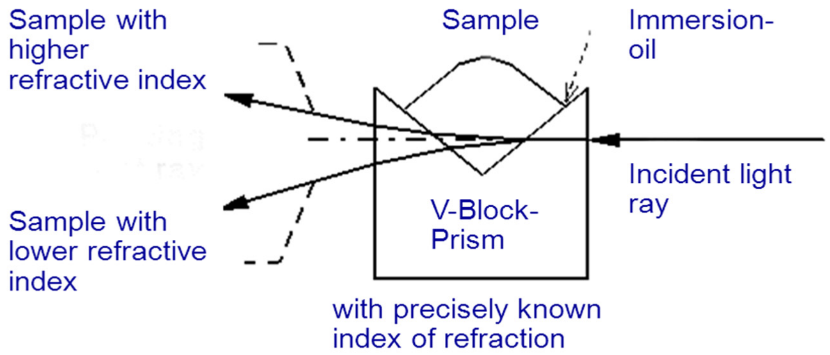
Sample with higher refractive index
Sample
Immersion-oil
Incident light ray
Sample with lower refractive index
V-Block-Prism
with precisely known index of refraction

Figure 3.20 V-block method for measuring refractive index.

3.13 Standard Test Certificate: V-Block

The standard test certificate is issued together with a delivery lot of optical glass based on v-block measurement data. Typical information given in the test certificate header (Fig. 3.21) consists of the type of certificate according to the ISO standard 10474-2.2, glass type, and glass code. The quality grades (n_d/ν_d step) referring to the absolute refractive index and Abbe number are the actual values of the delivery lot. The variation range is not the actual variation of the delivery lot but the confirmation of the specification range ordered.

The test certificate (Fig. 3.22) gives the refractive index and Abbe number referring to the d line and e line as well as the offset from the nominal catalog values. Additionally, some selected dispersions are listed. All values are valid only for the delivery lot consisting of the set of batches that are listed on the test certificate. Refractive index values $n_{x\mathrm{L}}$ in the VIS spectral range can be calculated for the delivery lot (index L) from test certificate data for n_{dL} and ν_{dL} using catalog partial dispersion (index Cat) with the following formula:

$$n_{x_{\mathrm{L}}} = \frac{n_{x_{\mathrm{Cat}}} - n_{\mathrm{d}_{\mathrm{Cat}}}}{n_{\mathrm{F}_{\mathrm{Cat}}} - n_{\mathrm{C}_{\mathrm{Cat}}}} \cdot \frac{1}{\nu_{\mathrm{d}_{\mathrm{L}}}} \cdot \left(n_{\mathrm{d}_{\mathrm{L}}} - 1\right) + n_{\mathrm{d}_{\mathrm{L}}}. \tag{3.14}$$

As a rule, results deviate from measured values by not more than 1×10^{-5} or 2×10^{-5} in the blue–violet range.

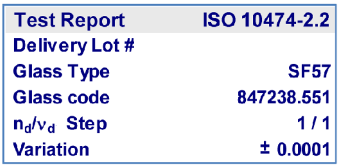

Test Report	ISO 10474-2.2
Delivery Lot #	
Glass Type	SF57
Glass code	847238.551
n_d/ν_d Step	1 / 1
Variation	± 0.0001

Figure 3.21 Standard test certificate header.

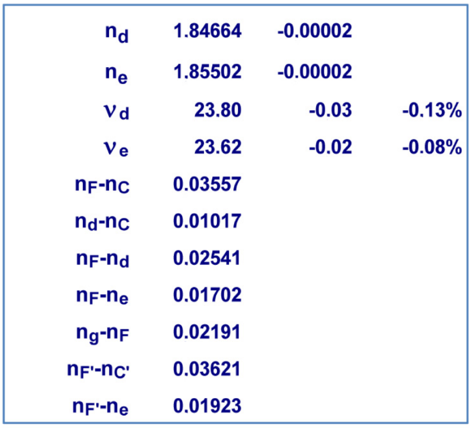

n_d	1.84664	-0.00002	
n_e	1.85502	-0.00002	
ν_d	23.80	-0.03	-0.13%
ν_e	23.62	-0.02	-0.08%
n_F-n_C	0.03557		
n_d-n_C	0.01017		
n_F-n_d	0.02541		
n_F-n_e	0.01702		
n_g-n_F	0.02191		
$n_{F'}$-$n_{C'}$	0.03621		
$n_{F'}$-n_e	0.01923		

Figure 3.22 Standard test certificate glass data.

3.14 Test Certificate for a Delivery Lot

Delivery lots of optical glasses come with test certificates, which provide actual values for delivery lots. Figure 3.23 shows a delivery lot consisting of subsequent production batches, which is not a general requirement and in practice is not always given. The refractive index values for individual batches come either directly from monitoring measurements or from interpolations. Delivery lots will be assembled according to the refractive index variation tolerance being ±1 × 10^{-4} (±2 × 10^{-4} for pressings lots) as standard or narrower on request. Homogeneity of individual pieces will be better by at least a factor of ten.

The reported values for refractive index and Abbe number represent the middle position of the delivery lot's batch values, i.e., the position equally far from maximum and minimum values. This should not be confused with the average values. A delivery lot is not guaranteed to consist of batches having a consistent annealing rate. For normal users, this is of no consequence. However, if someone wants to perform a fine annealing on his own for adjusting refractive index to special desired values, this may lead to an increase in the lot's variation. In order to avoid this, special lots consisting of batches with the same annealing rate may be ordered.

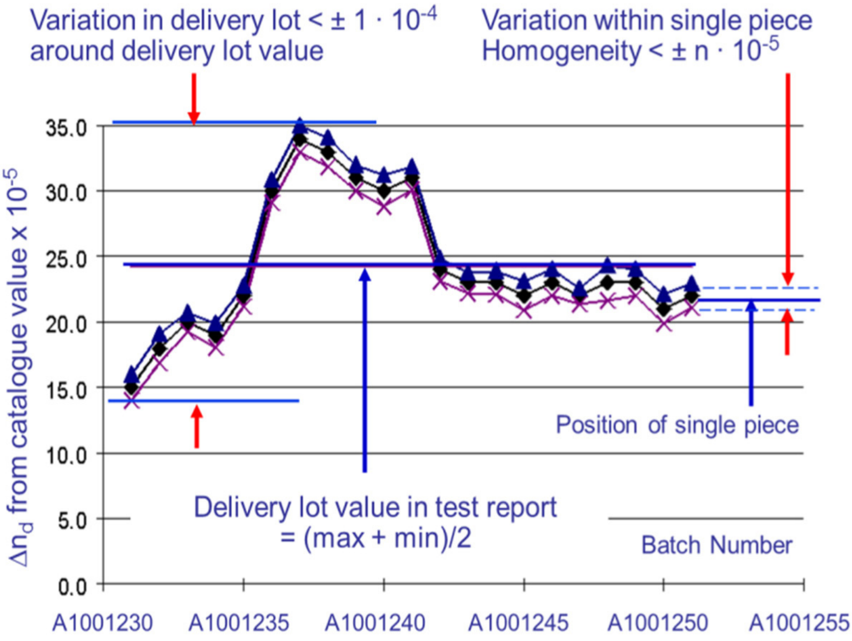

Figure 3.23 Refractive index variation within a delivery lot. The batch-to-batch variation is limited according the variation tolerance (see Section 3.7) (usually ±1 × 10^{-4}). The nominal refractive index for the delivery lot represents the mean value between minimum and maximum, not to be confused with the average or median value. Homogeneity within one piece is much better.

3.15 Refractive Index Measurement: Prism Goniometer

Refractive index measurements with the highest accuracy are performed with a classical Newton prism goniometer setup[5] (Fig. 3.24). The method of minimum angle deviation determination allows for an absolute measurement without a reference (see Fig. 3.25). The wavelength range extends from the vacuum UV border at 185 nm through the total VIS spectrum up into the NIR at 2325 nm. This is a wavelength where many glass types begin to absorb light again. Standard measurement uncertainty for refractive index as reported in the precision test certificate is $\pm 1 \times 10^{-5}$ and for dispersion is $\pm 3 \times 10^{-6}$. With special effort (very narrow angle and flatness tolerances for the prism faces, and extreme temperature stabilization) it is possible to achieve $\pm 1.3 \times 10^{-6}$, and $\pm 0.7 \times 10^{-6}$ for refractive index and dispersion (one standard deviation each).

Disadvantages of this measurement method are the comparatively large size of the prisms needed ($>35 \times 35 \times 25$ mm^3), the high flatness and angle precision requirements, and the need for very stable temperature. This makes using a high-precision goniometer an expensive and time-consuming method.

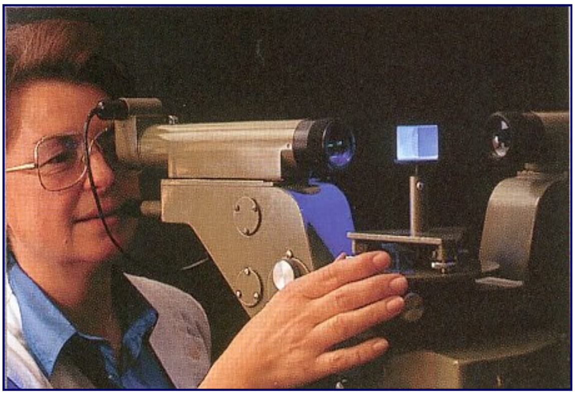

Figure 3.24 Refractive index measurement with a precision goniometer (courtesy of SCHOTT AG).

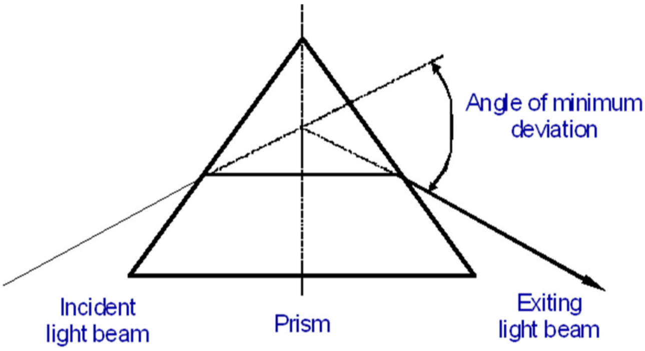

Figure 3.25 Principle of refractive index measurement with a precision goniometer.

Reproduction measurements taken over a long time span show the very low measurement uncertainty of the precision goniometer method[4] (see Fig. 3.26). The standard deviation of 20 measurements covering a ten-year period stays below 1 × 10^{-6} over the total wavelength range. The increase at 300 nm is due to the transmittance reduction of BK7 at the UV edge. FK5 (also after 20 measurements), with a better transmittance at 300 nm, remains below 1 × 10^{-6}.

Figure 3.27 shows results for the glass types PK50 and LAK8 (after 17 measurements each) in comparison to BK7. In the VIS range, PK50 with a refractive index almost the same as that of BK7, shows results comparable to BK7. The IR standard deviations increase because of its transmittance reduction in the IR. The higher-index glass LAK8 shows somewhat higher uncertainty. The high-index glass type SF57 lies considerably higher, partly due to its high dispersion, since its prism angle is not optimum for all measured wavelengths.

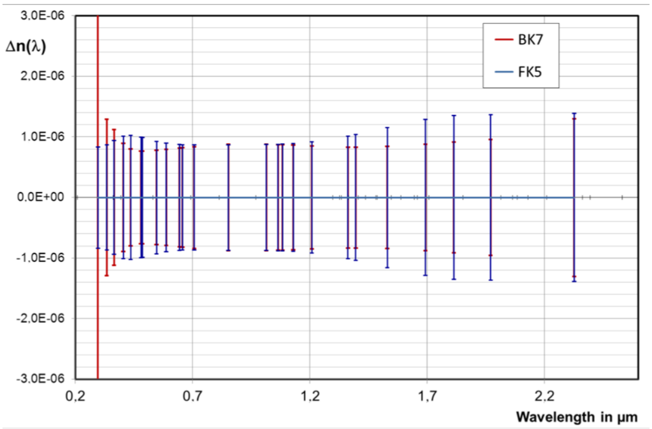

Figure 3.26 Refractive index measurement reproducibility per wavelength for the glass types BK7 and FK5 with ±1 standard deviation.

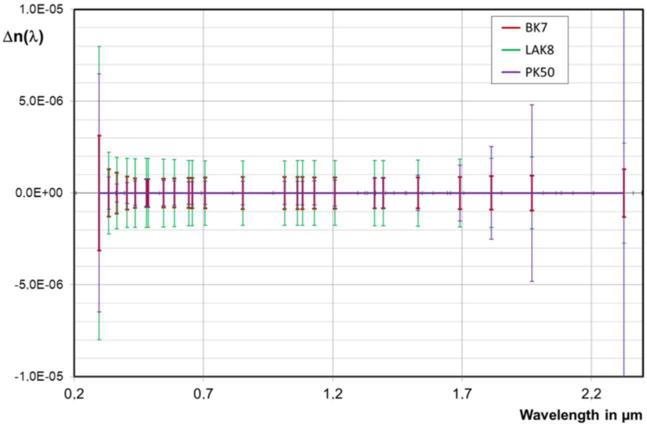

Figure 3.27 Refractive index measurement reproducibility per wavelength for the glass types LAK8 and PK50 with ±1 standard deviation together with that of BK7 serving as a reference.

3.16 Sellmeier Data Fit Quality

For precision measurements of optical glasses, refractive index is measured for at least 15 wavelengths from 297 to 2326 nm. Fitting the Sellmeier equation with the least-squares method delivers the Sellmeier coefficients. Figures 3.28 and 3.29 show deviations of measured values from fit values. The error bars in the diagrams represent the standard deviations of each set of differences from the fit values at the measured wavelengths.

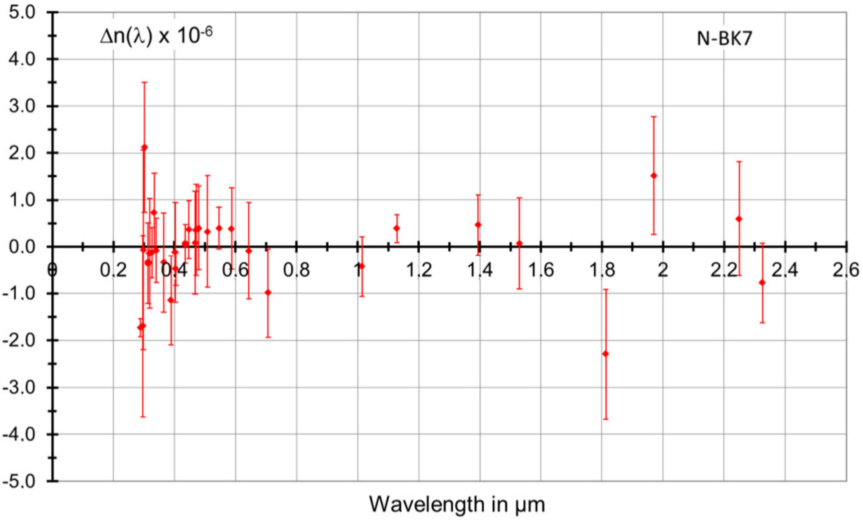

Figure 3.28 Differences in measured data from Sellmeier fit values for N-BK7 (±1 standard deviation; 14 data sets).

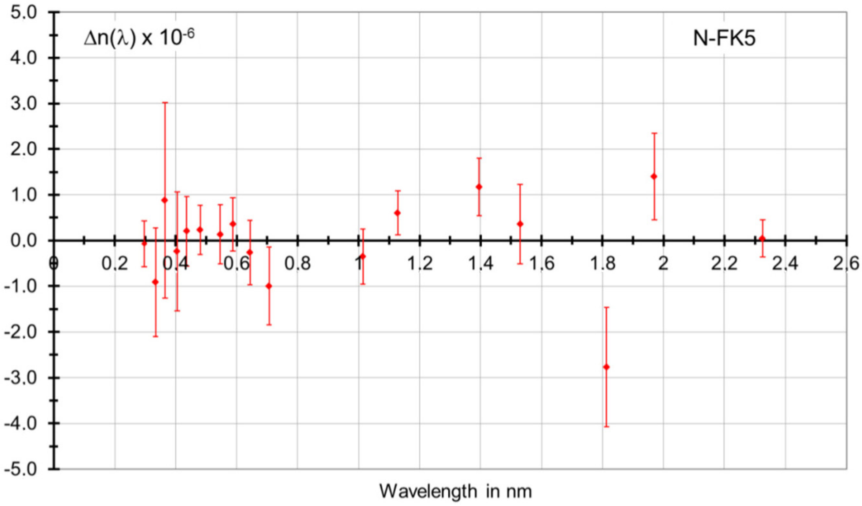

Figure 3.29 Differences in measured data from Sellmeier fit values for N-FK5 (±1 standard deviation; 31 data sets).

For BK7 and FK5, the standard deviations of the differences between measured and fitted values are in good agreement with reproducibility results of around 1×10^{-6}, as presented in Chapter 2. The symmetric scattering around the zero line confirms that the Sellmeier formula represents the refractive index changing with wavelength very well within the statistical variations of the precision measurement.

3.17 Test Certificate: Prism Goniometer

The results of the goniometer refractive index measurements are reported in a precision test certificate comprising a large set of data (Fig. 3.30). The most important data given on the precision test certificate are the six constants for the Sellmeier formula: B_1, B_2, B_3, C_1, C_2, and C_3. All other refractive index and dispersion values are calculated from these constants. The constants are given explicitly for convenience to make these values directly available without the need for calculation. The wavelength range applicable for the given sample is given in the certificate (in the example above, 0.326–2.325 µm). The UV transmittance cutoff edge varies with different optical glass types. Therefore, the Sellmeier constants are valid only in the wavelength range where transmittance is high enough to enable suitable refractive index measurements.

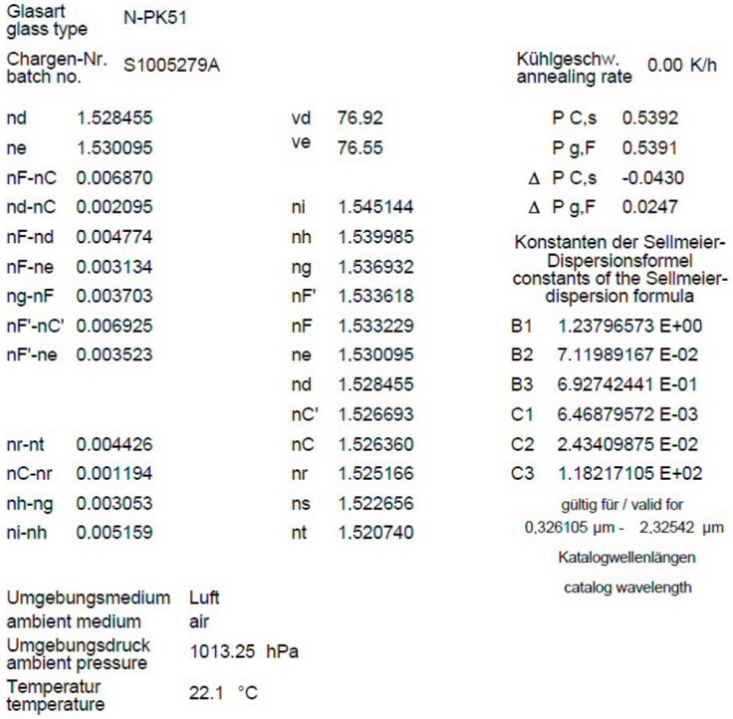

Glasart glass type N-PK51

Chargen-Nr. batch no. S1005279A

Kühlgeschw. annealing rate 0.00 K/h

nd	1.528455	vd	76.92	P C,s	0.5392
ne	1.530095	ve	76.55	P g,F	0.5391
nF-nC	0.006870			Δ P C,s	-0.0430
nd-nC	0.002095	ni	1.545144	Δ P g,F	0.0247
nF-nd	0.004774	nh	1.539985	Konstanten der Sellmeier-Dispersionsformel constants of the Sellmeier-dispersion formula	
nF-ne	0.003134	ng	1.536932		
ng-nF	0.003703	nF'	1.533618		
nF'-nC'	0.006925	nF	1.533229	B1	1.23796573 E+00
nF'-ne	0.003523	ne	1.530095	B2	7.11989167 E-02
		nd	1.528455	B3	6.92742441 E-01
		nC'	1.526693	C1	6.46879572 E-03
nr-nt	0.004426	nC	1.526360	C2	2.43409875 E-02
nC-nr	0.001194	nr	1.525166	C3	1.18217105 E+02
nh-ng	0.003053	ns	1.522656	gültig für / valid for	
ni-nh	0.005159	nt	1.520740	0,326105 µm - 2,32542 µm	

Katalogwellenlängen
catalog wavelength

Umgebungsmedium ambient medium Luft air

Umgebungsdruck ambient pressure 1013.25 hPa

Temperatur temperature 22.1 °C

Figure 3.30 Precision goniometer refractive index test certificate. As in the data sheet of N-BK7 in Fig. 3.9, all refractive indices and dispersion values are calculated from the six Sellmeier coefficients given in the column on the right side.

The environmental medium (which is air for optical glass types) is reported. If not required otherwise, the measurement temperature is 22 °C. All data are corrected for standard atmospheric air pressure. The measured values always refer only to the specific individual piece of optical glass from which the sample was taken. Refractive index values may change by amounts larger than the measurement uncertainty, even among glass parts in close proximity to each other in the production time line.

It is possible to transfer the high accuracy for absolute refractive index values to such neighboring parts by means of additional v-block measurements performed on samples taken from these parts and from the part where the precision measurement sample was taken. With this method it is possible to combine the high reproducibility of the v-block method with the high absolute accuracy of the goniometer method.

3.18 Refractive Index: Temperature Influence

Refractive index depends on temperature. For example, the refractive index n_e of N-BK7 changes with temperature by 1.6×10^{-6} per Kelvin at room temperature. Values for other glass types lie within the limits set by the extreme glass types N-PK51 with -8.1×10^{-6} /K and SF57 with $+10.9 \times 10^{-6}$ /K, most of them being within 0 and $+5 \times 10^{-6}$ /K.

These values refer to the refractive index related to vacuum and are denoted with the index "abs" as absolute. For practical purposes the refractive index related to air is more important and is denoted with the index "rel" for relative. The refractive index change relative to air with temperature differs noticeably from the absolute value. The corresponding values at room temperature for the three glasses mentioned above (at room temperature) are given in Table 3.5.

Table 3.5 Refractive index change absolute and relative to air for three selected glass types.

Glass Type	$\Delta n_{eabs}/\Delta T$ 1/K	$\Delta n_{erel}/\Delta T$ 1/K
N-BK7	1.6×10^{-6}	3.0×10^{-6}
N-PK51	-8.1×10^{-6}	-6.7×10^{-6}
SF57	10.9×10^{-6}	12.5×10^{-6}

The temperature dependence of the refractive index becomes important with imaging systems that are expected to have high performance throughout a wide temperature range. Such optical designs will be optimized with respect to the different behaviors of the employed glass types, which can even have opposite directions, as can be seen from the values of N-PK51.

With large optical elements, refractive index inhomogeneity induced by temperature gradients becomes a serious concern. For example, consider a 500-mm-diameter, 100-mm-thick disk of N-BK7 with perfect refractive index homogeneity. A temperature difference slightly larger than only 0.3 K within this disk would result in surpassing the limits of homogeneity tolerance grade H4 of 2×10^{-6}. Expressed differently, this means that in order not to degrade the quality of an H4 disk of this size due to temperature gradients, the gradients need to be kept considerably below 0.3 K. This is far from easy for a large disk of a material with temperature conduction as low as that of glass.

The 1966 edition of the SCHOTT optical glass catalog provided the first data on the temperature dependence of the refractive index for specific glass types. With the 1992 edition SCHOTT introduced the Sellmeier dispersion formula as a precise representation of the refractive indices' dependence on wavelength.[1–3,6] Along with this, SCHOTT provided a dispersion formula for the refractive indices' dependence on temperature and wavelength derived from the Sellmeier equation. This formula allows for calculation of refractive index changes with temperature in the VIS spectral range and the temperature range of –40 °C to +80 °C. Some years ago, wavelength and temperature ranges were extended to the near UV and IR (365 to 1014 nm) and –100 °C to +140 °C. Reference temperature is 20°C, and reproducibility is better than $\pm 5 \times 10^{-7}$/K. The measurement setup is shown in Fig. 3.31.

The dispersion formula for the refractive index depending on temperature is somewhat involved and becomes even more complicated when calculating its dependence on wavelength relative to air. This is because the refractive index of air must also be calculated taking into account its dependence on wavelength, temperature, and pressure.

The difference in the refractive indices relative to air at target temperature T and at reference temperature T_0 = 20 °C for wavelength λ is

$$\Delta n_{\text{rel}}\left(\lambda, T, T_0\right) = \frac{n_{\text{abs}}\left(\lambda, T\right)}{n_{\text{air}}\left(\lambda, T\right)} - \frac{n_{\text{abs}}\left(\lambda, T_0\right)}{n_{\text{air}}\left(\lambda, T_0\right)}, \tag{3.15}$$

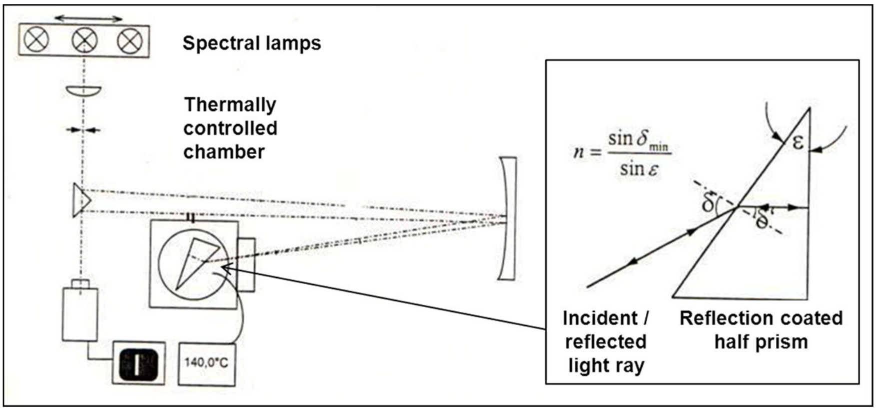
Spectral lamps
Thermally controlled chamber
140,0°C
$n = \frac{\sin \delta_{\min}}{\sin \varepsilon}$
ε
δ
δ
Incident / reflected light ray
Reflection coated half prism

Figure 3.31 Measurement setup for the temperature dependence of the refractive index. The glass sample is prepared as a reflection-coated half-prism. The reflection angle is determined for different temperatures and light wavelengths.

where

$$n_{\text{abs}}(\lambda, T) = n_{\text{abs}}(\lambda, T_0) + \Delta n_{\text{abs}}(\lambda, T), \tag{3.16}$$

$$n_{\text{abs}}(\lambda, T_0) = n_{\text{rel}}(\lambda, T_0) \cdot n_{\text{air}}(\lambda, T_0), \tag{3.17}$$

and $n_{\text{rel}}(\lambda, T_0)$ is the data sheet value.

The difference in the absolute refractive indices at the different temperatures is given by the following formula:

$$\Delta n_{\text{abs}}(\lambda, T) = \frac{n^2(\lambda, T_0) - 1}{2n(\lambda, T_0)} \cdot \left[D_0 \Delta T + D_1 \Delta T^2 + D_2 (\Delta T)^3 + \frac{E_0 \Delta T + E_1 \Delta T^2}{\lambda^2 - \lambda_{\text{TK}}^2} \right], \tag{3.18}$$

which is derived from the dispersion formula for the temperature coefficients for the refractive index introduced by Hoffmann, Jochs, and Westenberger in 1990:

$$\frac{dn_{\text{abs}}(\lambda, T)}{dT} = \frac{n^2(\lambda, T_0) - 1}{2n(\lambda, T_0)} \cdot \left[D_0 + 2D_1 \Delta T + 3D_2 (\Delta T)^2 + \frac{E_0 + 2E_1 \Delta T}{\lambda^2 - \lambda_{\text{TK}}^2} \right]. \tag{3.19}$$

The constants D_0, D_1, D_2, E_0, E_1, and λ_{TK} are specific for each optical glass type and are listed in the data sheets. From dn/dT_{abs} it is possible to calculate the temperature coefficients of the refractive index relative to air:

$$\frac{dn_{\text{rel}}(\lambda, T)}{dT} = \frac{\dfrac{dn_{\text{abs}}(\lambda, T)}{dT} - n_{\text{rel}}(\lambda, T) \cdot \dfrac{dn_{\text{air}}(\lambda, T)}{dT}}{n_{\text{air}}(\lambda, T, p)}, \tag{3.20}$$

with the temperature coefficient for air dn/dT_{air} being

$$\frac{dn_{\text{air}}(\lambda, T, p)}{dT} = -0.00367 \cdot \frac{n_{\text{air}}(\lambda, T, p) - 1}{1 + 0.00367 \dfrac{1}{°\text{C}} T}. \tag{3.21}$$

The refractive index of air at a given wavelength and standard conditions (T = 15 °C and pressure p_0 = 1013.25 hPa) is

$$n_{\text{air}}(\lambda, T = 15\ °\text{C}, p_0 = 1013.25\ \text{hPa}) = 1 + \left[6432.8 + \frac{2949810 \cdot \lambda^2}{146 \cdot \lambda^2 - 1} + \frac{25540 \cdot \lambda^2}{41 \cdot \lambda^2 - 1} \right] \cdot 10^{-8}. \tag{3.22}$$

Depending on temperature and pressure, the refractive index of air can be calculated (see Fig. 3.32) as follows:

$$n_{\text{air}}\left(\lambda, T, P\right) = 1 + \frac{n_{\text{air}}\left(\lambda, T = 15\ °\text{C}, p_0\right) - 1}{1 + 3.4785 \cdot 10^{-3} \cdot \left[T\left(°\text{C}\right) - 15\right]} \cdot \frac{p}{p_0}. \tag{3.23}$$

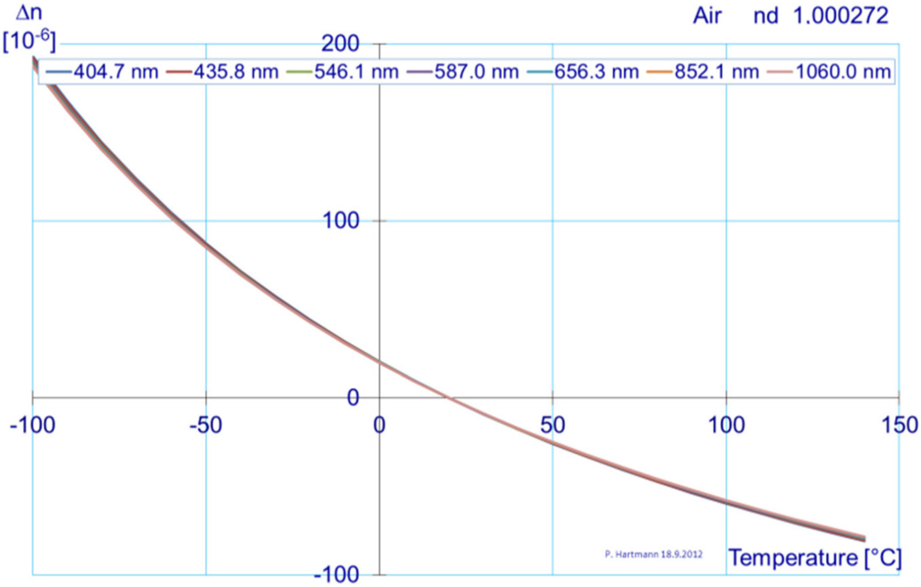

Figure 3.32 Refractive index change of air with temperature for different wavelengths.

3.19 Temperature Coefficient Measurement Reproducibility and Melt Variations

Based on 22 reproduction measurements of BK7 over 13 years, it is possible to value the measurement uncertainty of the temperature coefficient measurement.[4] Figure 3.33 shows changes in the absolute refractive index of BK7 for three wavelengths. It is an excerpt of the diagram in Fig. 3.35. Figure 3.33 shows error bars representing the standard deviations of the reproducibility measurements.

Figure 3.34 shows the same standard deviations as in Fig. 3.33, but now related to their measured values. The relative standard deviations grow with falling temperature and increasing wavelength. This is mainly due to the change effect being smaller in these directions. The overall reproducibility for the long time period is outstanding.

Figure 3.35 shows results for five different melts of N-BK7. The error bars representing one standard deviation are the same as those in Fig. 3.26 and are centered at the melt that was used for the reproducibility measurements. Table 3.6 lists the intermelt variation spans of four materials for which at least four measurements were available. These spans are related to the relative standard deviations found for N-BK7 reproducibility. If such a span equals or is greater than 3 standard deviations, it is considered to be a significant effect caused by material variation and not by statistics.

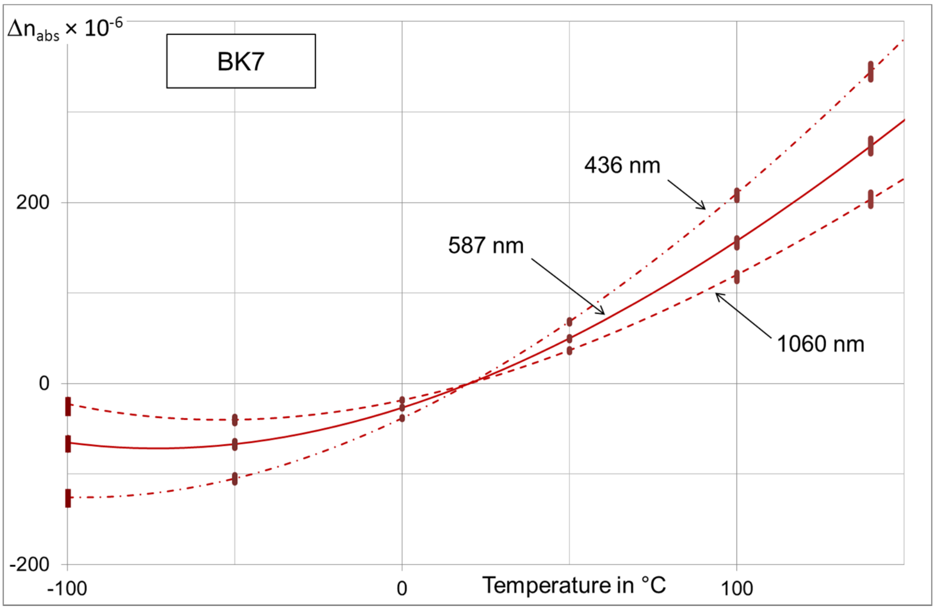

Figure 3.33 Change of the absolute refractive index of the optical glass BK7 for temperature intervals for three wavelengths of a measurement representing the middle position of a set of 22 reproduction measurements. The error bars denote the standard deviations of the reproducibility measurements.

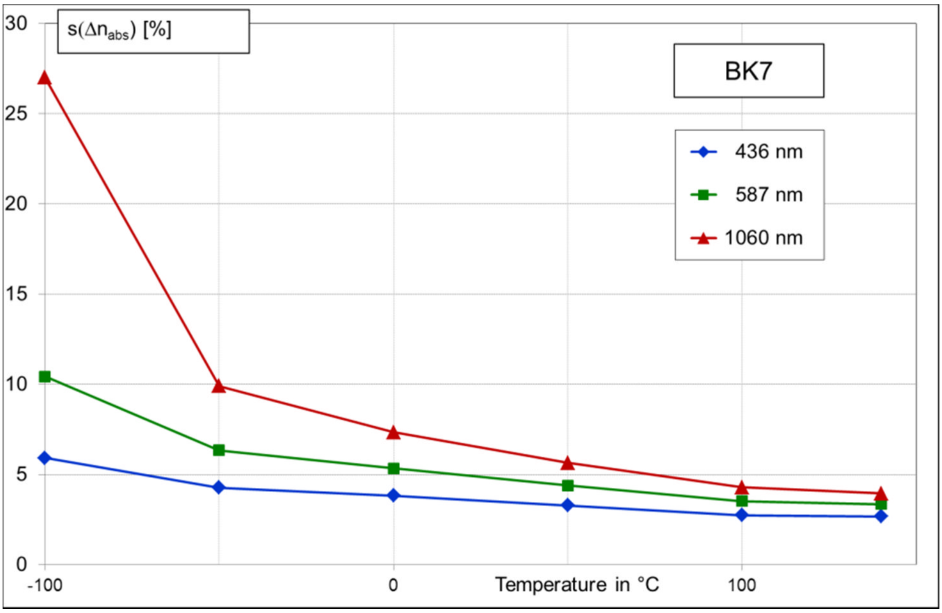

Figure 3.34 Relative standard deviations (in percent) of 22 reproducibility measurements of the absolute refractive index change for BK7.

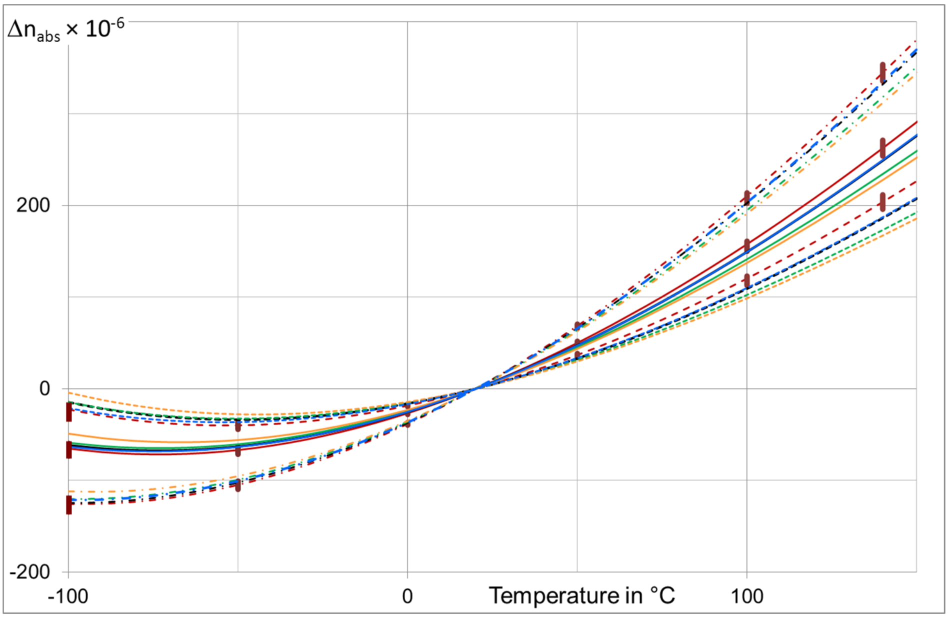

Figure 3.35 Refractive index change with temperature for five melts of N-BK7.

Table 3.6 Intermelt variation spans of four optical materials divided by the standard deviations of the reproducibility standard deviations. Variations exceeding three standard deviations are in bold. The numbers of data per set are given in parentheses after the material names.

Temp. inter-val [°C]	IRG2 (12)			N-LAF21 (5)			CAF2 (4)			N-BK7 (5)		
	Wavelength in nm											
	436	587	1060	436	587	1060	436	587	1060	436	587	1060
–100	1.6	1.2	0.7	0.9	0.9	0.5	0.1	0.0	0.0	1.8	2.3	2.8
–50	2.5	1.5	1.4	0.9	0.9	0.6	0.1	0.1	0.1	2.1	2.6	**3.0**
0	2.7	2.1	2.5	0.9	1.0	0.6	0.1	0.1	0.1	2.2	2.6	**3.0**
50	2.8	2.5	**3.3**	0.9	1.0	0.7	0.2	0.1	0.2	2.6	**3.0**	**3.4**
100	2.6	2.4	**3.7**	0.8	1.0	0.7	0.4	0.4	0.4	**3.3**	**3.7**	**4.3**
140	1.9	2.2	**3.1**	0.6	0.9	0.5	0.7	0.6	0.6	**3.6**	**4.0**	**4.7**

For calcium fluoride, the material variations are very small, as is expected for a crystal with its precisely defined atomic structure underlining the high measurement reproducibility. The optical glass N-LAF21 shows maximum differences of 1.0 standard deviation at 587 nm, which is in agreement with no detectable material variations from melt to melt. For N-BK7, differences exceed three standard deviations for all three wavelengths but at different temperature interval sizes and thus have to be considered as significant. The IR glass type IRG2 is a borderline case. Only at 1060 nm at temperature intervals higher than 50 °C do significant differences occur. The data evidence it is not sufficient for deciding definitively whether the differences are significant.

3.20 Temperature Coefficients of the Refractive Index

The diagrams in this section show the temperature coefficients of the absolute refractive index dn/dT_{abs} and of the relative refractive index dn/dT_{rel}. The curves of N-BK7 (Figs. 3.36–3.39) are typical for many optical glass types.

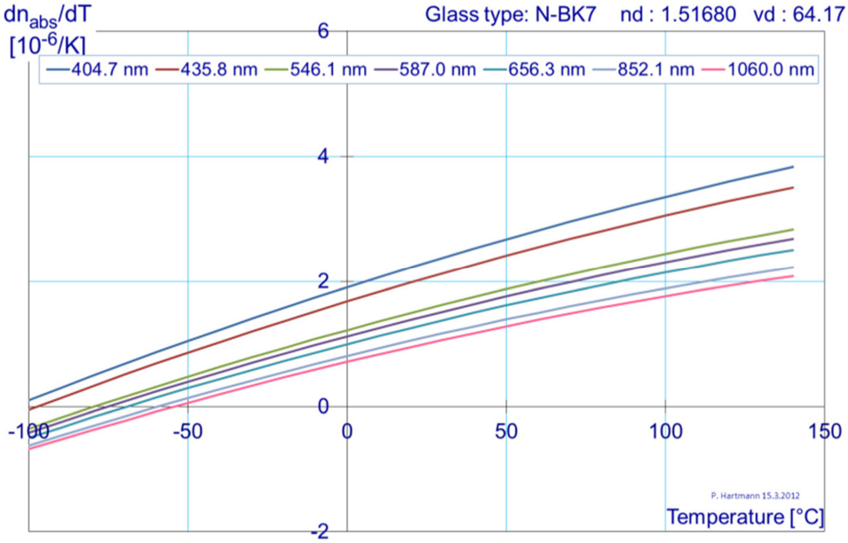

Figure 3.36 Temperature coefficients of the absolute refractive index *dn*/*dT*abs for N-BK7 for different wavelengths.

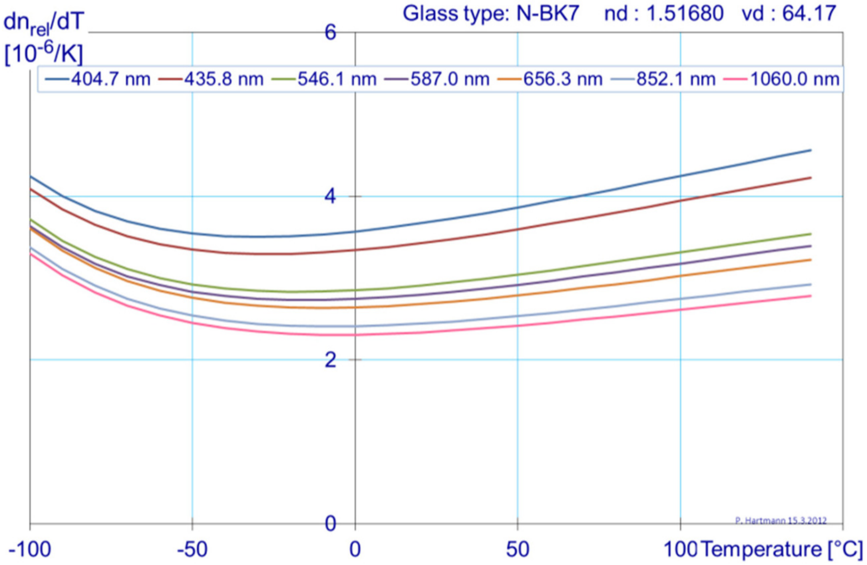

Figure 3.37 Temperature coefficients of the relative refractive index *dn*/*dT*rel for N-BK7 for different wavelengths.

For practical purposes, the change intervals of the refractive index may be more interesting. First the intervals for the absolute refractive index are given and second those relative to air.

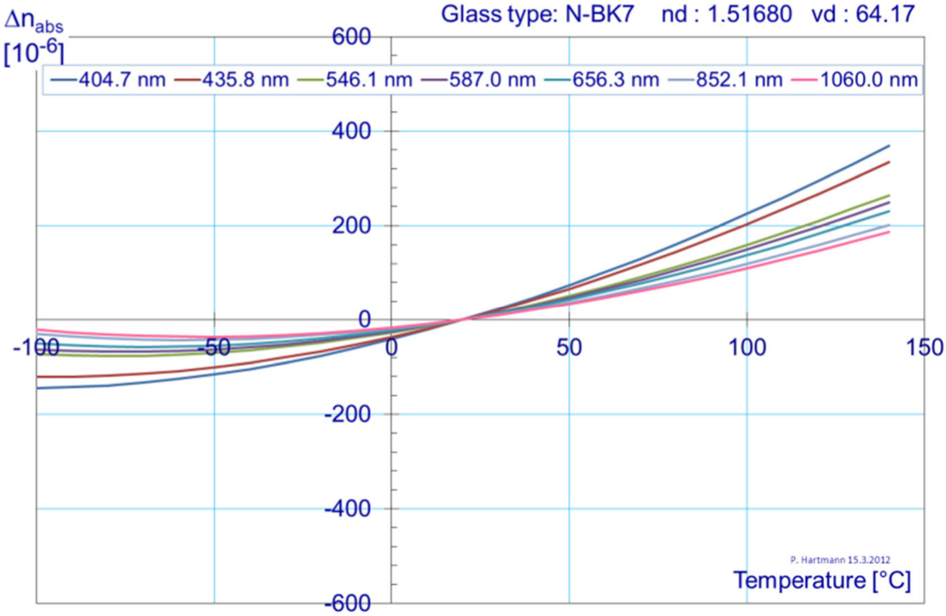

Figure 3.38 Absolute refractive index change of N-BK7 for different wavelengths (T_{ref} = 20 °C).

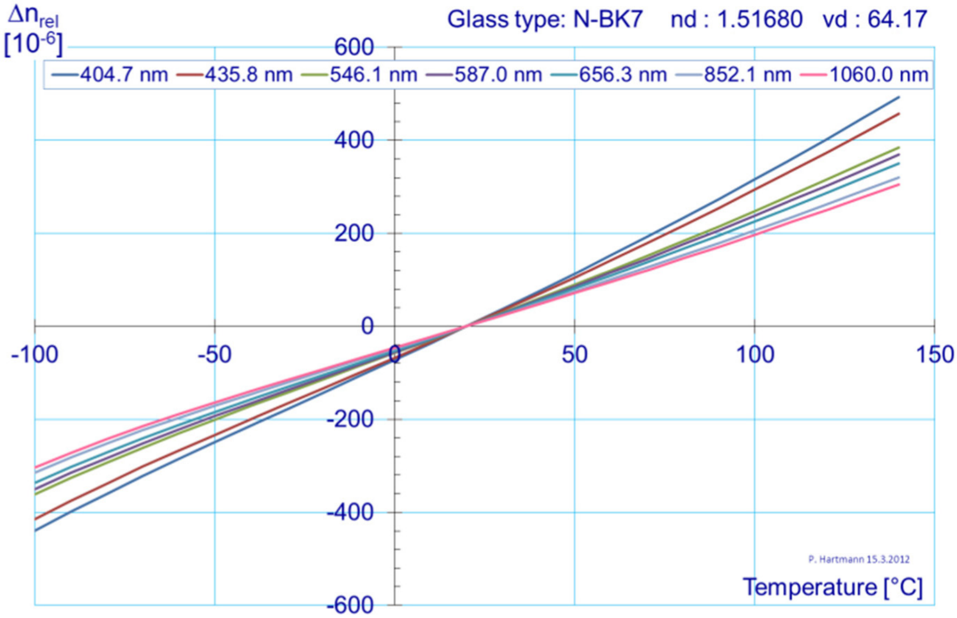

Figure 3.39 Relative refractive index change of N-BK7 for different wavelengths (T_{ref} = 20 °C).

N-PK51 (Figs. 3.40–3.43) is the extreme glass type with the highest negative change of refractive index with temperature. This holds for the absolute index as well as for the relative index.

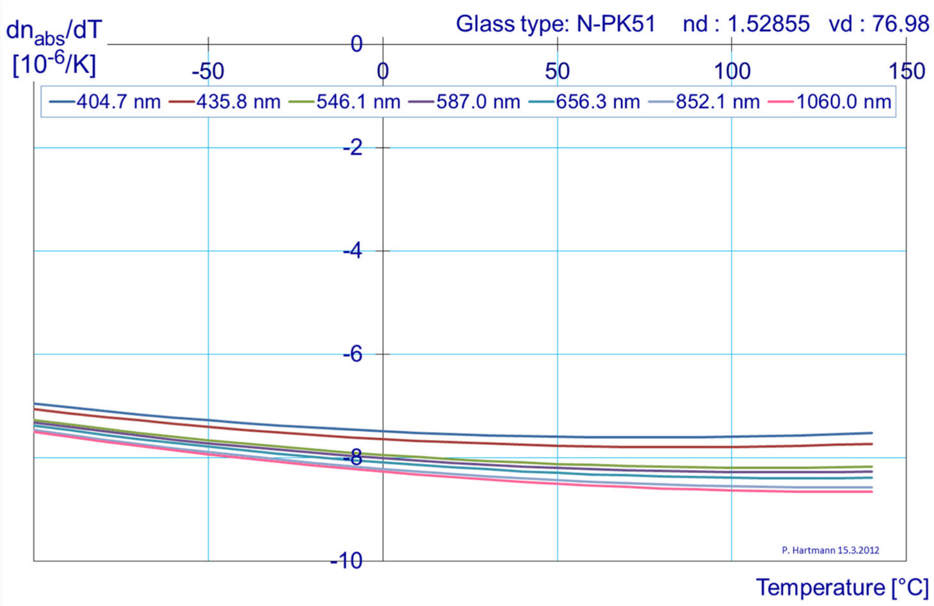

Figure 3.40 Temperature coefficients of the absolute refractive index *dn*/*dT*abs for N-PK51 for different wavelengths.

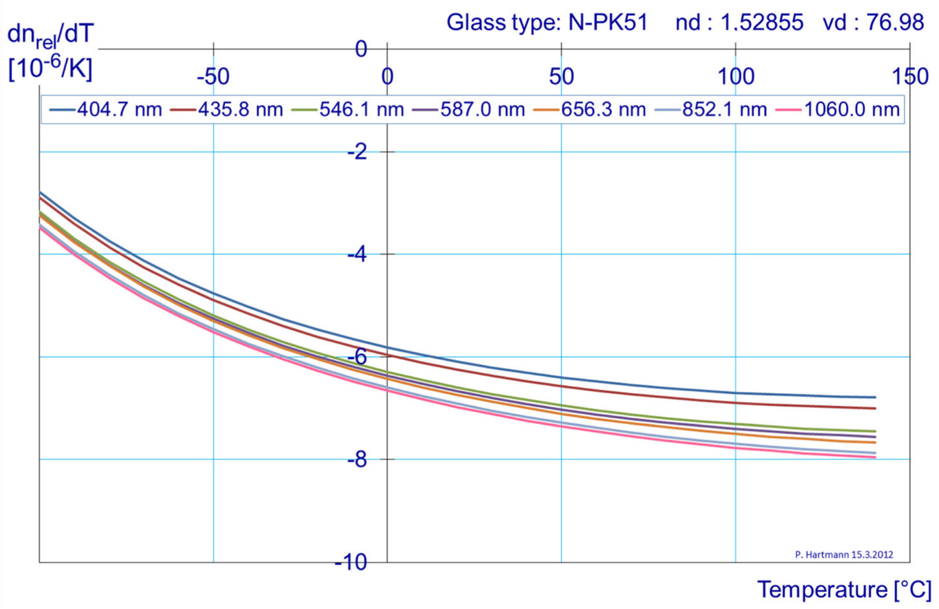

Figure 3.41 Temperature coefficients of the relative refractive index *dn*/*dT*rel for N-PK51 for different wavelengths.

The differences of the absolute and relative refractive indices with temperature changes of N-PK51 show the strong negative effect. Wavelength is of no great influence with this glass, being generally of low dispersion.

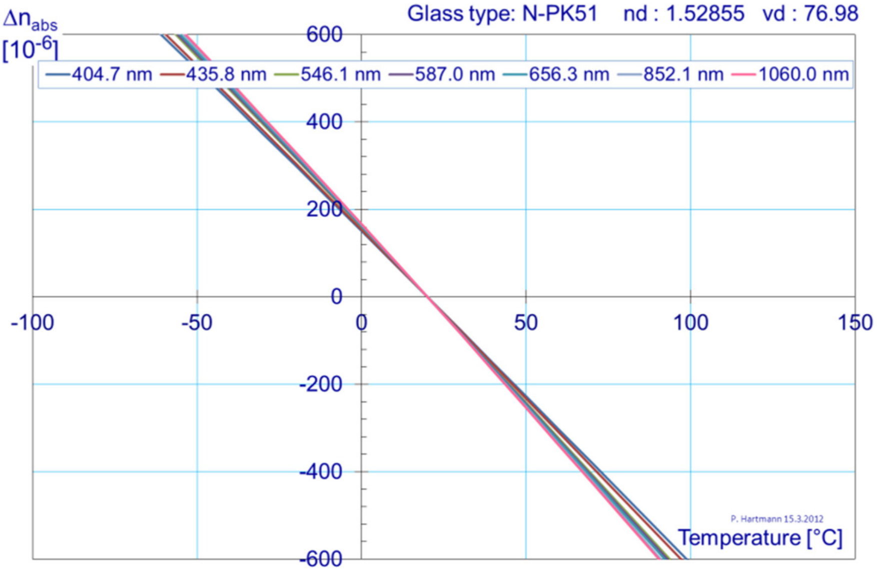

Figure 3.42 Absolute refractive index change of N-PK51 for different wavelengths (T_{ref} = 20 °C).

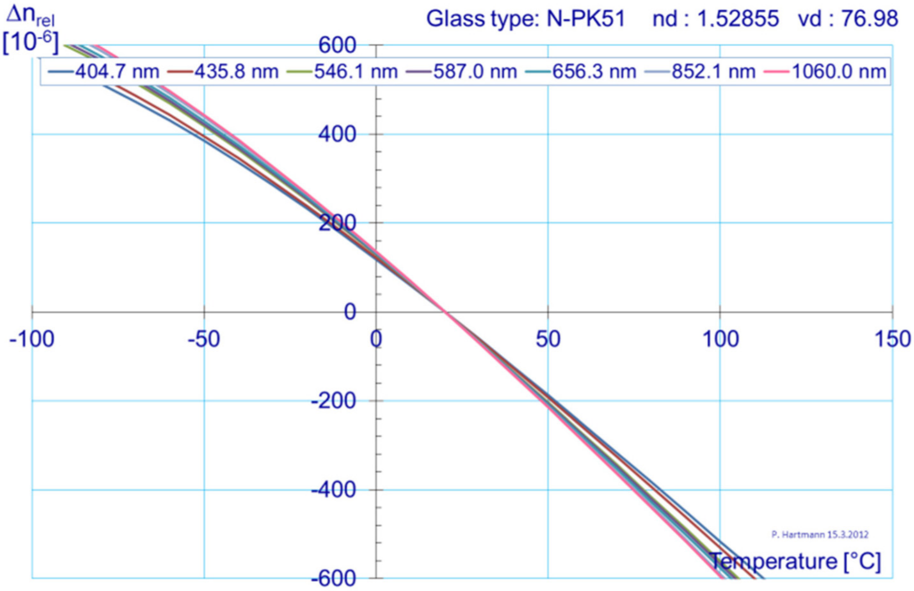

Figure 3.43 Relative refractive index change of N-PK51 for different wavelengths (T_{ref} = 20 °C).

The opposite extreme is the classical lead flint glass SF57 (Figs. 3.44–3.47), with very pronounced positive temperature dependence.

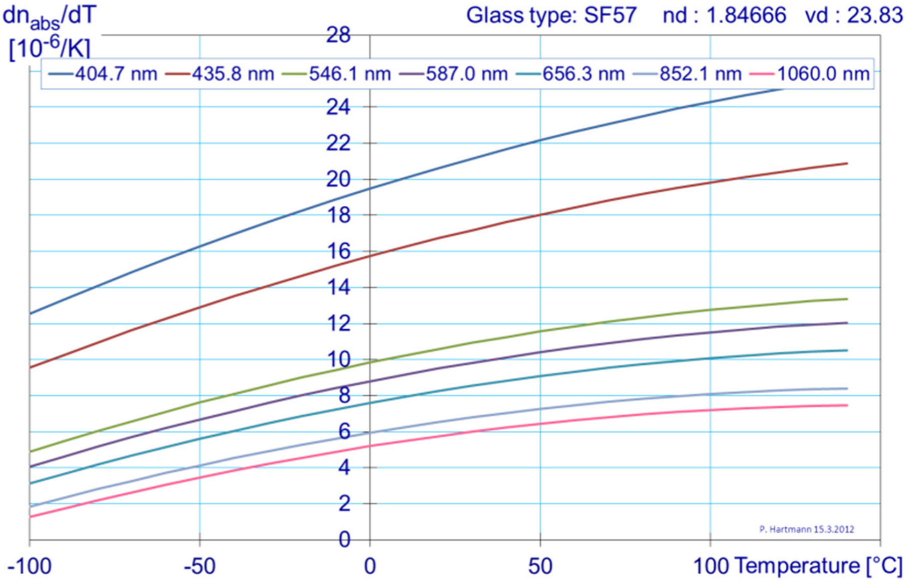

Figure 3.44 Temperature coefficients of the absolute refractive index *dn*/*dT*abs for SF57 for different wavelengths.

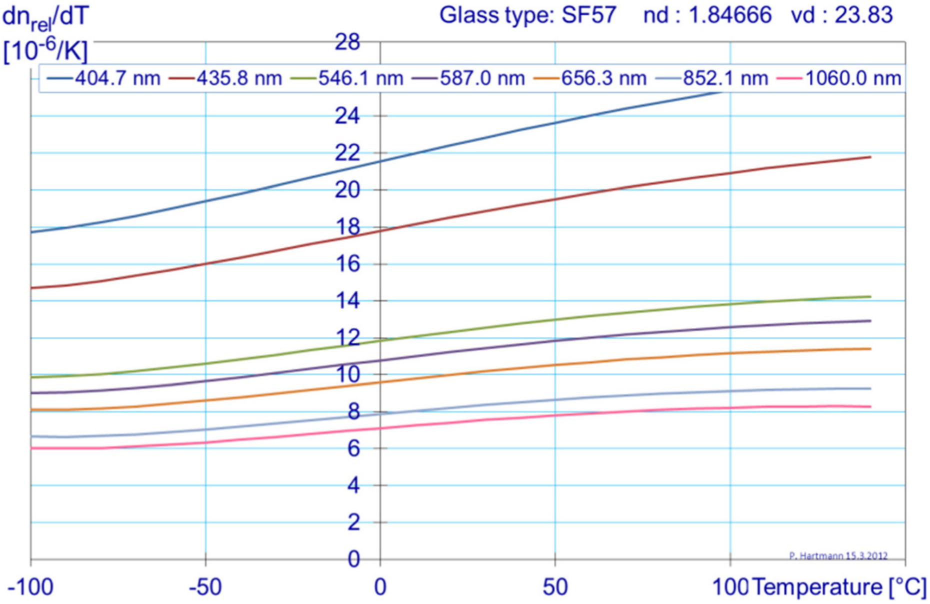

Figure 3.45 Temperature coefficients of the relative refractive index *dn*/*dT*rel for SF57 for different wavelengths.

The large change intervals also strongly depend on wavelength with this generally high-dispersion glass type.

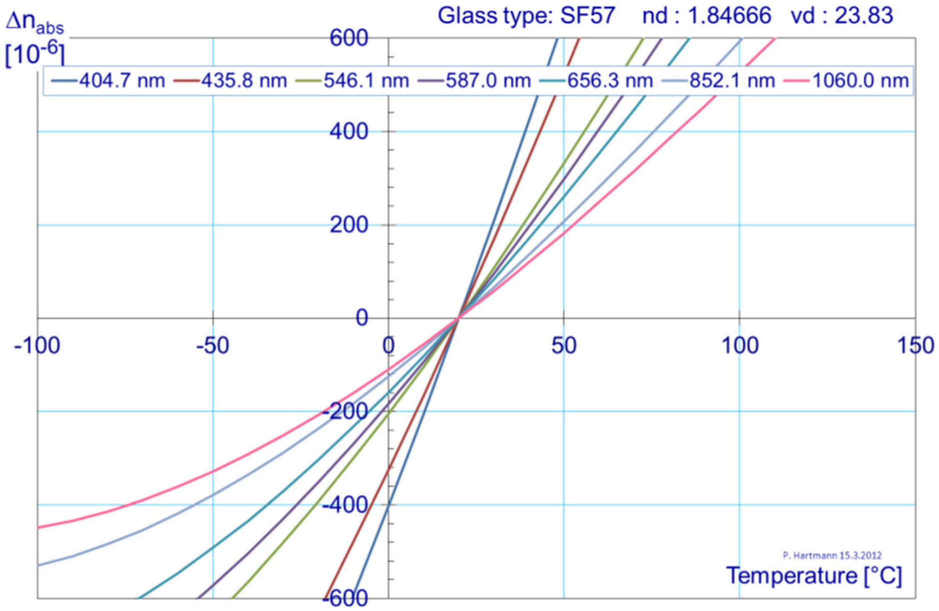

Figure 3.46 Absolute refractive index change of SF57 for different wavelengths (T_{ref} = 20° C).

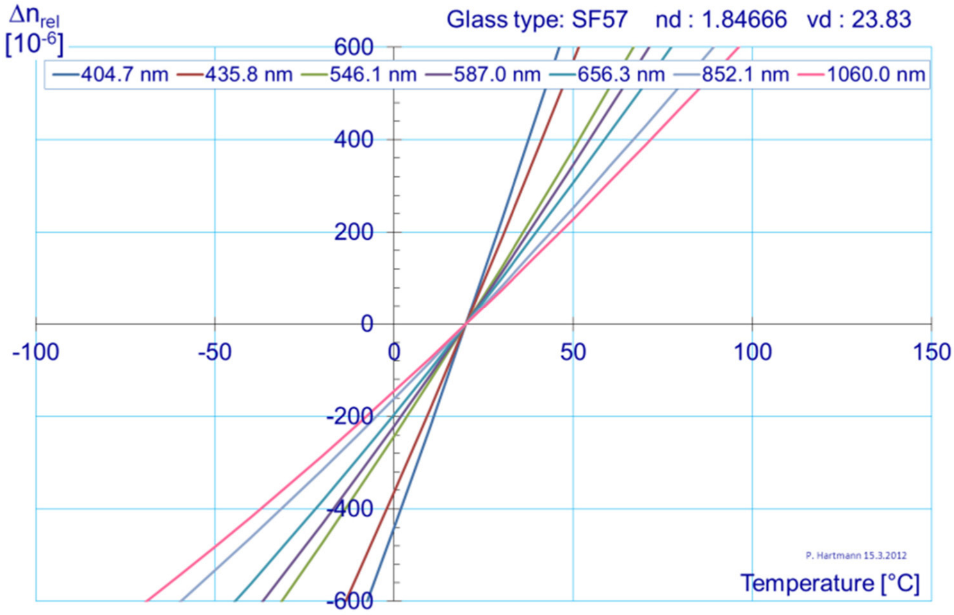

Figure 3.47 Relative refractive index change of SF57 for different wavelengths (T_{ref} = 20 °C).

Figure 3.48 shows the variety of relative refractive index changes for different glass types with moderate and strong slopes of positive and negative signs. Table 3.7 lists numerical values of refractive index change for three different glass types, three temperature intervals, and three light wavelengths.

A calculation example for the relative refractive index change of SF57 at 546.1 nm for the full interval +20 to +40 °C is as follows: $12.5 \times 10^{-6}/\text{K} \times 20\ \text{K} = 250 \times 10^{-6}$ or 1.88504 → 1.88529.

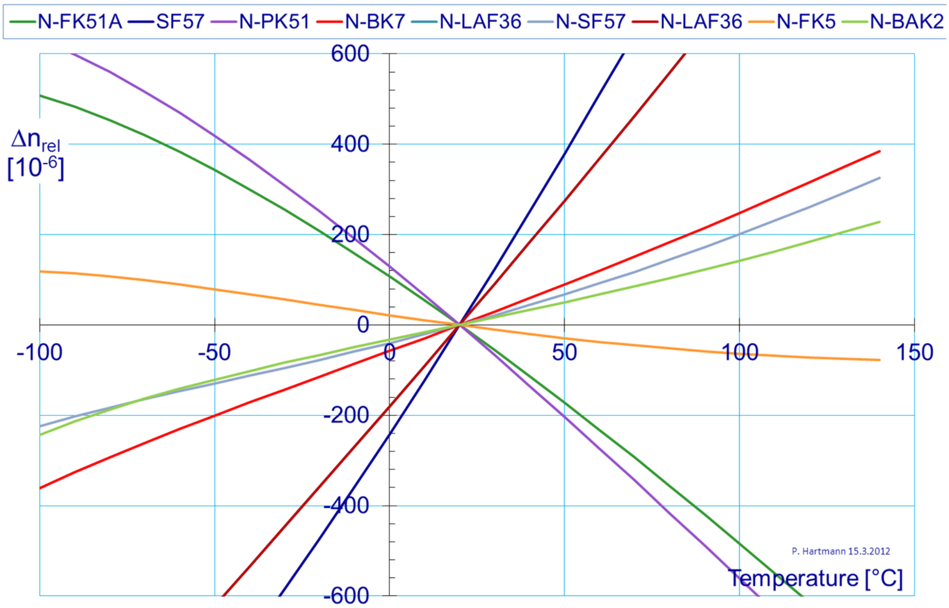

Figure 3.48 Relative refractive index change of selected glass types at 546.1 nm wavelength (T_{ref} = 20 °C).

Table 3.7 Refractive index change for three different glass types relative to air and absolute as given in the optical glass data sheets.

	ΔT	$\Delta n_{rel}/\Delta T$ [10^{-6}/K]			$\Delta n_{abs}/\Delta T$ [10^{-6}/K]		
λ [nm]	[°C]	1060.0	546.1	435.8	1060.0	546.1	435.8
N-BK7	–40/–20	2.4	2.9	3.3	0.3	0.8	1.2
	+20/+40	2.4	3.0	3.5	1.1	1.6	2.1
	+60/+80	2.5	3.1	3.7	1.5	2.1	2.7
N-PK51	–40/–20	–6.0	–5.7	–5.4	–8.1	–7.8	–7.5
	+20/+40	–7.1	–6.7	–6.4	–8.4	–8.1	–7.7
	+60/+80	–7.5	–7.1	–6.7	–8.6	–8.2	–7.8
SF57	–40/–20	6.6	11.1	16.7	4.2	8.6	14.1
	+20/+40	7.6	12.5	18.9	6.0	10.9	17.2
	+60/+80	8.0	13.4	20.1	6.8	12.1	18.8

3.21 Thermo-optical Coefficient

The influence of the refractive index change with temperature on wavefront distortion does not depend only on the temperature coefficients *dn*/*dT*. The overall change of the optical light path includes also the length change due to thermal glass expansion.

For plane light waves of wavelength λ passing along a defined distance *t* through an optical element of glass, the change of the optical path length Δ*W* resulting from temperature variation Δ*T* is

$$\Delta W = t\left\{\alpha\left[n(\lambda)-1\right]+\frac{dn}{dT_{\text{rel}}}(\lambda,T)\right\}\Delta T, \tag{3.24}$$

where α is the thermal coefficient of expansion, and *n* is the refractive index. The expression in the curly brackets in Eq. (3.24) is called the thermo-optical coefficient *G*(λ,*T*):

$$G(\lambda,T)=\alpha\left[n(\lambda)-1\right]+\frac{dn}{dT_{\text{rel}}}(\lambda,T). \tag{3.25}$$

Table 3.8 lists thermo-optical coefficients of some selected glass types. Together with the coefficient of thermal expansion, the relative temperature coefficient at room temperature and the refractive index are given for the spectral e line at 546 nm. Glass thickness is assumed to be 20 mm, and temperature change 1 K. The last column shows the values for resulting wavefront deformation. The first three glass types are N-BK7 together with the two extreme glass types N-PK51 and SF57.

Table 3.8 Thermo-optical coefficients of some selected glass types.

	t in mm:	20		ΔT in K:	1
	alpha	dn$_e$/dT rel	n$_e$	G	ΔW
Material	(-30/70°)	(20/40°)			
	K^{-1}	K^{-1}		10^{-6} K^{-1}	nm
N-BK7	7.10E-06	3.00E-06	1.51872	6.68	133.7
N-PK51	1.24E-05	-6.70E-06	1.53019	-0.15	-3.0
SF57	8.30E-06	1.25E-05	1.85504	19.60	391.9
N-SF57	8.46E-06	2.20E-06	1.85504	9.43	188.7
N-FK5	9.20E-06	-1.00E-06	1.48914	3.50	70.0
N-FK51A	1.27E-05	-5.70E-06	1.48794	0.52	10.3
N-PK52A	1.30E-05	-6.40E-06	1.49845	0.08	1.7
N-SK2	6.00E-06	4.50E-06	1.60994	8.16	163.2
N-LAF7	7.30E-06	4.30E-06	1.75459	9.81	196.2
N-LAK9	6.30E-06	3.70E-06	1.69401	8.07	161.4
N-LASF31A	6.74E-06	4.90E-06	1.88815	10.89	217.7
N-KZFS4	7.30E-06	3.70E-06	1.61664	8.20	164.0
CaF2	1.67E-05	-1.06E-05	1.43495	-3.34	-66.7
Vitreous Silica	5.10E-07	1.01E-05	1.46008	10.33	206.7
Zerodur	2.00E-08	1.48E-05	1.54470	14.81	296.2

One characteristic of some glass types such as N-PK51 and other low-index, low-dispersion glass types N-PK52A and N-FK51A is that they are very sensitive with regard to *dn*/*dT* alone. With respect to thermo-optical coefficient, however, they prove to be almost insensitive to wavefront distortions. With these glasses, the high coefficient of thermal expansion leads to a compensation of the first term with the negative *dn*/*dT* term. At the other extreme, SF57 remains highly sensitive. Its lead- and arsenic-free replacement glass type N-SF57 is much less sensitive and lies in the range where most other glass types can be found.

It is noticeable that materials with very low thermal expansion such as vitreous silica and ZERODUR® are highly sensitive with respect to temperature changes from a refractive index point of view. With their low thermal length expansion, the first term of G vanishes, and the second term dominates in full size.

Wavefront deformation due to temperature leads to strong requirements on thermal stabilization with homogeneity measurements.[7] The optical components of interferometers are subject to wavefront deformations, which may be partially compensated by calibration. However, thermal gradients within measured samples will result in false inhomogeneity values. For highly accurate homogeneity measurements, strict thermal stabilization of samples is indispensable.

For large lenses with very high wavefront deformation requirements, the thermo-optical effect sets the achievable limits. Environmental temperature cycling will prevent thermal stabilization to the level needed for very small wavefront distortion. Figure 3.49 shows thermo-optical coefficients of SCHOTT optical glasses at room temperature and 546 nm wavelength (e line).

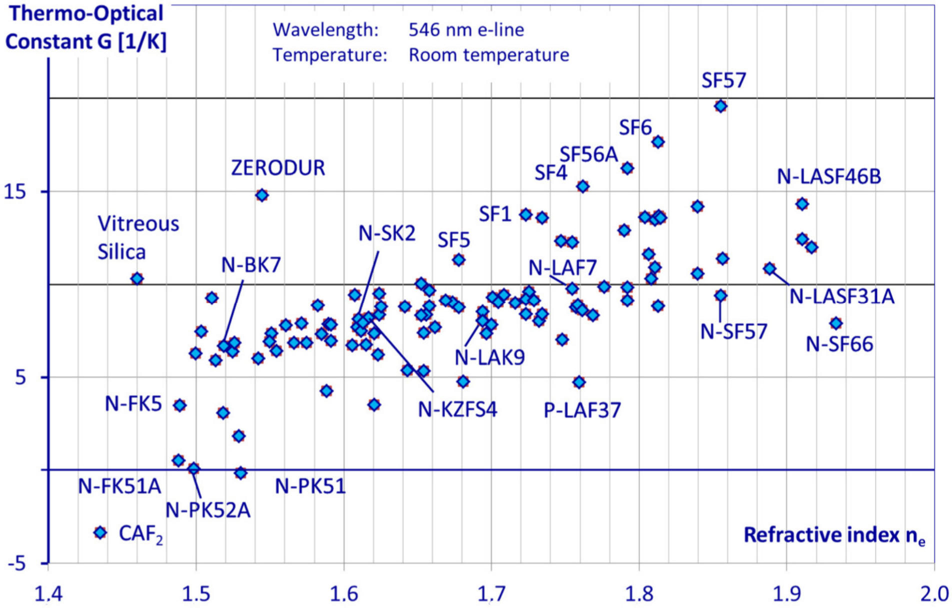

Figure 3.49 Thermo-optical coefficient for optical glasses.

References

1. SCHOTT Optical Glass Catalog 10.000 e 0992 (1992).
2. H. J. Hoffmann, W. W. Jochs, and G. Westenberger, “Use of the Sellmeier dispersion formula for optical glasses and practical implications,” *Proc. SPIE* **1780**, 303–314 (1992) [doi: 10.1117/12.142817].
3. H. J. Hoffmann, “A survey of isotropic and anisotropic modifications of the refractive index,” *J. Physique IV Colloque C2 Supplement J. de Physique III* **2**, C2-21–C2-30 (1992).
4. M. Englert, P. Hartmann, and S. Reichel, “Optical glass: refractive index change with wavelength and temperature,” *Proc. SPIE* **9131**, 91310H (2014) [doi: 10.1117/12.2052706].
5. A. Engel, G. Westenberger, L. Bartelmess, O. Sohr, R. Haspel, and E. Mörsen, “Advanced industrial metrology used for qualification of high-quality optical materials,” *Proc. SPIE* **4779**, 117–124 (2002) [doi: 10.1117/12.451741].
6. H. J. Hoffmann, W. W. Jochs, and G. Westenberger, “A dispersion formula for the thermo-optic coefficient of optical glasses,” *Proc. SPIE* **1327**, 219–230 (1990) [doi: 10.1117/12.22537].
7. P. Hartmann, R. Mackh, and H. Kohlmann, “Advances in the homogeneity measurement of optical glasses at the Schott 20-in. Fizeau interferometer,” *Proc. SPIE* **2775**, 108–114 (1996) [doi: 10.1117/12.246738].

Chapter 4
Homogeneity

The term *homogeneity* generally refers to the volume constancy of properties. This may be any property of a material, even the material itself. In local imperfections, different materials may be present, such as gas-filled bubbles or stones in glass. In, by far, the most cases, however, homogeneity means refractive index homogeneity in optical materials. So refractive index homogeneity, otherwise known as optical homogeneity, will be covered in the majority of this chapter. Bubbles and inclusions as material homogeneity defects will be discussed at the end of the chapter.

4.1 Optical Homogeneity versus Striae

General optical homogeneity can be subdivided into two aspects: global optical homogeneity and striae. Global optical homogeneity describes the refractive index changes over longer glass volume ranges, which means typically above several millimeters and extending to the total diameter of the optical element. The term striae refers to short-range changes from 1 mm down to 0.1 mm and below. This differentiation not only applies to the geometrical scales of refractive index changes but is also found in the variations that originate during production, the different measurement methods used for inspection, and the different effects these variations have on image quality.

For measurement and valuation of its effect in application, optical homogeneity is better expressed in terms of wavefront distortion, i.e., its effect on deforming plane wavefronts, rather than in terms of differences in refractive index. A collimated light beam may be considered as a series of plane wavefronts travelling in the direction of light propagation (Fig. 4.1). When one such wavefront hits a perfectly homogeneous piece of glass, it will travel through the glass without any distortion. The only effect is retardation because of the glass's refractive index. If the glass has a higher refractive index in the inner part than in its outer region, the wavefront will be retarded more strongly in the center. Thus, the wavefront leaving the glass will be curved.

Striae as a short-range refractive index variation will not only lead to distorted wavefronts as a result of different retardations along the different light paths but also to diffraction. This contribution will rise with shorter distances between neighboring refractive index gradients. The following chapters will treat global optical homogeneity first and then striae.

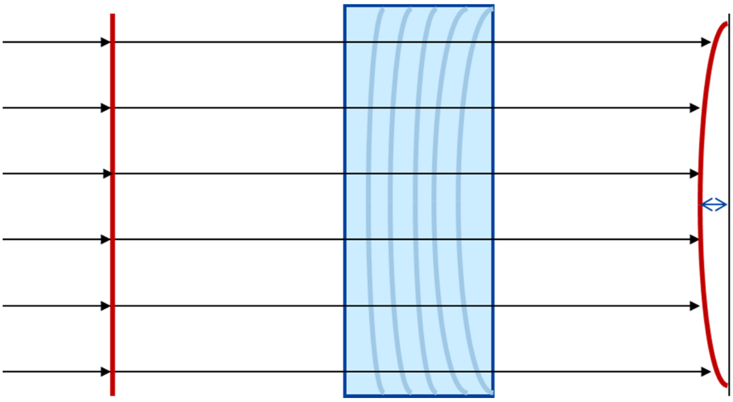

Figure 4.1 Wavefront distortion due to glass inhomogeneity. With a higher refractive index in the center of the glass plate, the wavefront is retarded in the middle.

4.2 Optical Homogeneity: Tolerances

Optical homogeneity as specified in a glass manufacturer's catalog is a measure of the refractive index variation within a single piece of optical glass. It is given by the peak-to-valley value, i.e., the difference between the maximum and minimum values of the refractive indices within the piece of optical glass. Table 4.1 gives the preferred homogeneity tolerances according to ISO 12123.

With the first edition of ISO 12123 in 2010, tolerance limits are given now in full ranges, contrary to previous references, where plus/minus ranges of half sizes were used. Plus/minus is adequate only around a given nominal value. For homogeneity, the target value is zero and cannot acquire negative values. Quoting the interval around the absolute refractive index value of a given piece of optical glass would require determination of this actual absolute value to a precision that is not possible and also not needed even in very high-quality optics. In practice, homogeneity is measured with interferometers, which can determine the variation only and not absolute values.

Table 4.1 Tolerances for the homogeneity of optical glass.

Homogeneity tolerance limits (peak-to-valley)		**Generally applicable for:**
n.a.	100×10^{-6}	common application sizes
H1	40×10^{-6}	
H2	10×10^{-6}	partial volumes of the raw glass
H3	4×10^{-6}	
H4	2×10^{-6}	partial volumes of the raw glass (not for all glass types)
H5	1×10^{-6}	

A standard homogeneity of 40×10^{-6} is provided by state-of-the-art suppliers. The achievable refractive index homogeneity depends on the glass type, glass item volume, and glass shape. The very general specification of optical homogeneity as a peak-to-valley value without any reference to glass dimensions has led to many communication errors. For adequate homogeneity specification, consideration of the information given in the next section is recommended.

4.3 Wavefront Measurement

Variations in the refractive index of the glass item lead to varying retardations and thus a wavefront no longer being flat but deformed. Such changes in retardation ΔW can be calculated using the formula

$$\Delta W = n \cdot d, \tag{4.1}$$

where n is the refractive index, and d is the glass thickness. This formula holds if light travels through the glass only once. In practice, wavefronts are measured using reflecting interferometers. Here, the light passes through the glass twice, requiring a factor of 2 to be added:

$$\Delta W = 2 \cdot n \cdot d. \tag{4.2}$$

The measurement of optical homogeneity requires highly sensitive interferometers, costly specimen preparation, a controlled and stable environment, and skilled personnel. The effect to be measured is very small, as a rule, below 100-nm wavefront deformation, and many of the influences that contribute to the errors may be as high as the wavefront distortion to be measured or even higher. Interferometers of the Fizeau type (Fig. 4.2) are commonly used for homogeneity measurement.[1,2]

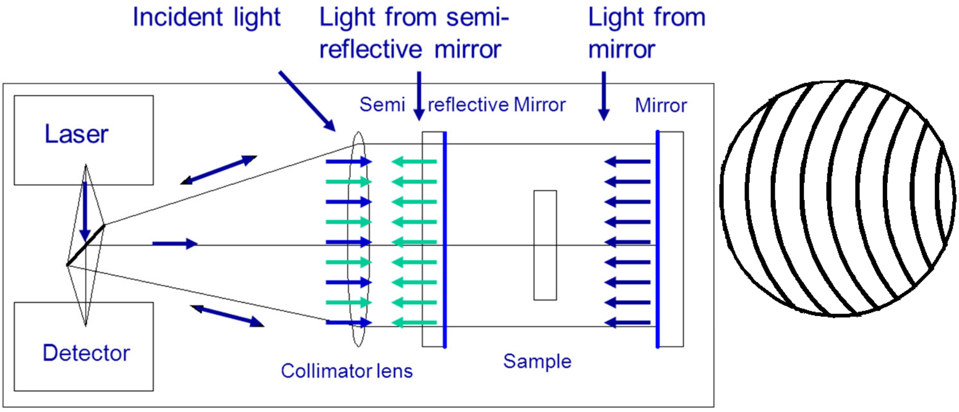

Figure 4.2 (left) Fizeau interferometer for homogeneity measurement and (right) resulting curved fringes.

The coherent light of a laser—generally, a helium-neon laser with 632-nm wavelength—travels through a lens collimator for beam expansion. The parallel light is partially reflected by the semi-transparent Fizeau mirror plate and partially transmitted. The autocollimation mirror reflects the transmitted light, which, after passing the collimator again, interferes with the light reflected by the semi-transparent mirror on the light detector. With the mirrors slightly tilted against each other, all conditions being perfect, and a perfectly homogenous medium between the mirrors, a set of straight interference fringes will arise. Placing a piece of glass with imperfect homogeneity into the interferometer will result in curved and locally deformed fringes.

Different methods can be used to acquire wavefront distortions from the fringes' deformation pattern. Progress in interferometer design and computer power has enabled high spatial resolution, high sensitivity, and reduced influence of the environment, such as vibrations.[2]

Temperature, however, must be kept as stable as possible (see Section 3.21).[3] The specimens to be measured must be very close to thermal equilibrium with their environment. Due to the temperature dependence of the refractive index, temperature variations in the glass will mimic optical inhomogeneity but are not caused by the glass itself. For example, a temperature variation of 0.3 °C in a 20-mm-thick N-BK7 disk results in the same wavefront deformation of 80 nm (double pass) as the refractive index variation allowed for homogeneity class H4 (2×10^{-6}).

4.4 Optical Homogeneity: Measurement of Glass Items

Two different methods are used for homogeneity measurement of optical glass plates. The first is the oil-on-plate method (Fig. 4.3). The sample is placed between two polished plates and is lapped to moderate flatness with matte surfaces. The flatness of the plates' surfaces should be 50 nm or better. Flatness imperfections and surface roughness of the sample will be compensated for with refractive-index-matched immersion oil filling the gaps between the sample and the oil-on plates. To obtain the sample's homogeneity, one measures the wavefront of the oil-on-plate sample assembly and subtracts the wavefront resulting from the oil-on plates with immersion oil alone, as determined in calibration position.

With the second method, one needs to acquire four wavefronts for a complete measurement.[4] Front and rear faces of the sample must be polished. Flatness requirements depend on the dynamic range of the interferometer. A complete measurement consists of wavefronts taken from reflections at the sample's front and rear face and at the autocollimation mirror with and without the sample. The method is sometimes called the Schwider method (after Johannes Schwider, a German physicist) (see Fig. 4.4).

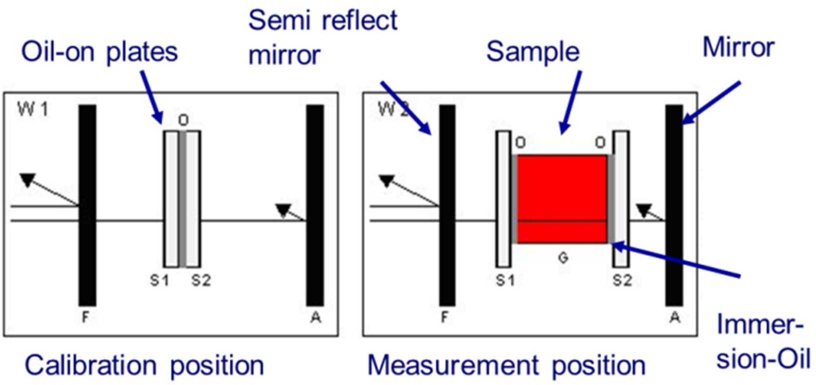
Oil-on plates
Semi reflect mirror
Sample
Mirror
W 1
O
S1 S2
F
A
W 2
O
O
G
S1
S2
F
A
Immer-sion-Oil
Calibration position
Measurement position

Figure 4.3 Oil-on method for measuring optical homogeneity of a glass plate.

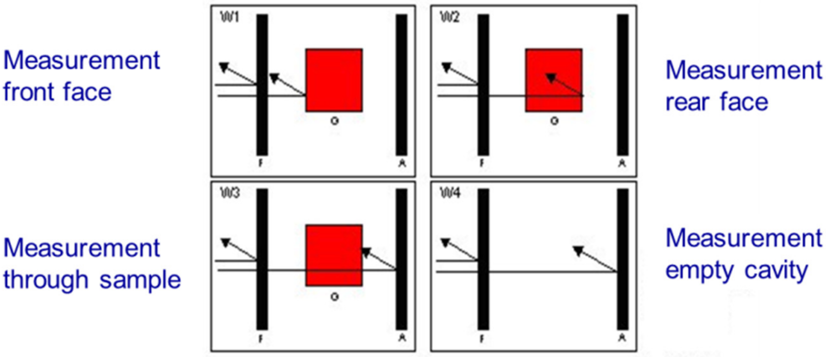
Measurement front face
W1
O
F
A
W2
O
F
A
Measurement rear face
Measurement through sample
W3
O
F
A
W4
F
A
Measurement empty cavity

Figure 4.4 Polished sample (Schwider) method for measuring optical homogeneity of a glass plate.

Advantages of the oil-on-plate method are the low-cost preparation of samples and the requirement of only one measurement for each sample, once the calibration has taken place. Disadvantages are the error sources that can be introduced by using immersion oil, such as refractive index mismatch, its high temperature dependence, and imperfections in the oil film's evenness (bubbles, edge effects, etc.). Immersion oils with high refractive index are toxic, a fact that restricts the method to low-refractive-index glasses.

The Schwider method removes all problems induced by immersion oil and allows measurements at all refractive indices. Hence, it is inherently more accurate. However, preparation of samples is more costly, and measurement requires a longer total time period during which all conditions must be kept stable. Disadvantages have been reduced since the newest interferometers can separate wavefronts from front and rear faces without the need of a wedge angle and without the need to adjust the sample accordingly. In any case, it is not possible to measure wavefront deformations up to the very edges of a glass item. It is necessary to allow a rim zone of about several millimeters with invalid data.

4.5 Optical Homogeneity in Glass Items

The definition of homogeneity as the maximum variation [peak-to-valley (p-v)] value is the most conservative way to specify homogeneity. In fact, this definition is more stringent than is usually needed. The effective homogeneity, which will be relevant inside a glass item, strongly depends on its size. In small thin lenses made from state-of-the-art optical glass, homogeneity is expected to be far better than required.

With increasing size (medium-sized lenses), residual variations begin to sum up but largely remain below a level that may be critical for common applications. Large optical elements, especially those with long light paths intended for precision optics, may become subject to individual specification requirements and verification by measurements. A rough measure for the expression "large optical elements" is a diameter larger than 100 mm or a light path in glass of more than 50 mm in prisms.

Within glass castings, refractive index changes smoothly in the inner part of the volume, while changes grow stronger approaching the natural cast surface. Very close to the surface, in about the last millimeters, homogeneity and striae quality may degrade because of contact with refractory materials during melting and casting or because of some evaporation of volatile constituents of the glass. Hence, staying clear of the very edge zones will significantly improve material quality. The final surfaces of large items should not lie closer than about 5 mm to the natural cast surfaces of the raw glass form (Fig. 4.5).

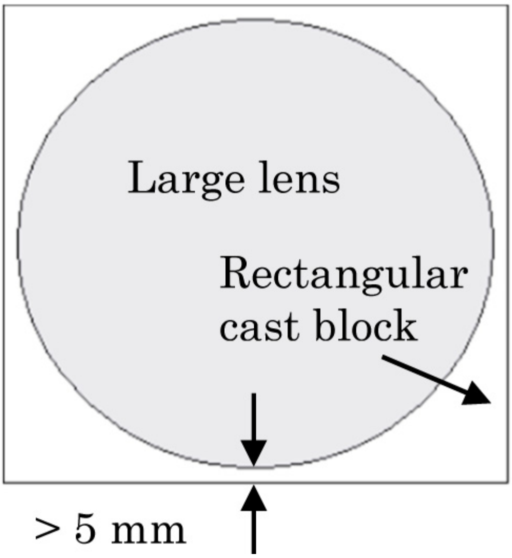

Figure 4.5 For highest homogeneity, net pieces should be placed at least several millimeters away from cast surfaces.

Smaller cut pieces have much better homogeneity than the total cast piece. Figure 4.6 shows a typical wavefront of a large block. The sample is an N-BK7 block with dimensions of 240 × 240 × 139 mm^3. Wavefront deformation is given in color-coded refractive index variation to allow better comparison with homogeneity tolerances. The first impression confirms the statement that stronger inhomogeneity is concentrated close to the surfaces. The inner part shows long-range, smooth changes. The highest peak and lowest valley lie close to each other at the rim zone and in the upper right corner. Appraisal of only the p-v value with 3.3×10^{-6} would result in a moderate overall homogeneity of the block. But this would obviously be a misjudgment. By far, the largest part of the volume shows much better homogeneity. The contiguous inner volume of 200 mm × 200 mm with blue and violet color represents an overall variation of 0.8×10^{-6}, fulfilling tolerance grade H5; yet the parts with the considerable size of 50-mm diameter show one-half the variation, corresponding to grade H6.

This observation might be considered to be self-evident. However, in practice, much trouble has occurred because customers order block glass with H4 tolerance without any reference to the glass element sizes for which the requirement should be valid. Thus, checking the availability based only on the p-v value results in discarding the block. If the element size corresponds to 50-mm diameter, the complete volume of the glass block would be suitable with

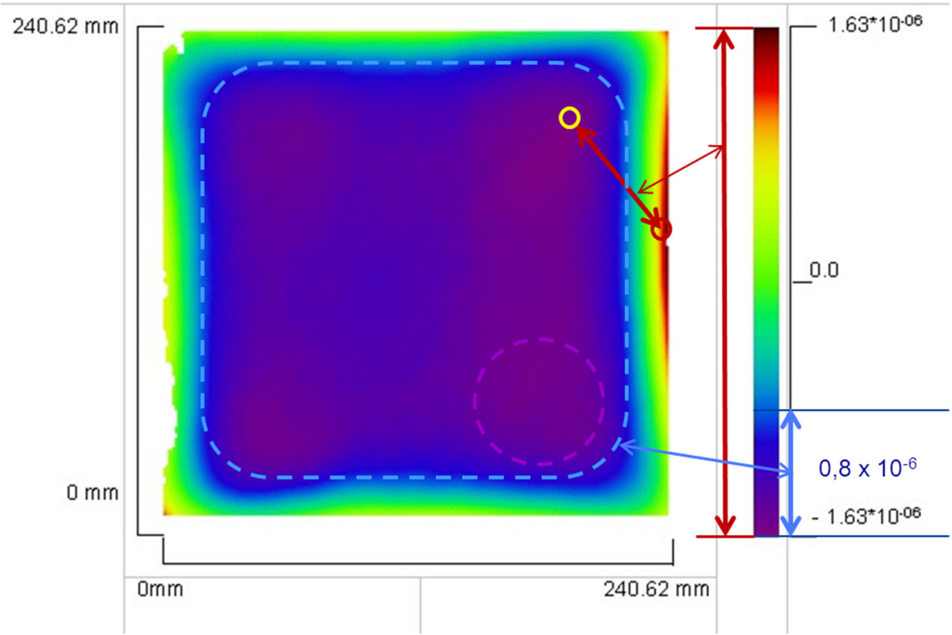

Figure 4.6 Color-coded wavefront of an N-BK7 block 240 × 240 × 139 mm^3 highlighting the scale dependence of homogeneity. The overall p-v value of 3.3×10^{-6} is not adequate for the block. The large inner part is much better with 0.8×10^{-6}, fulfilling tolerance grade H5 or even 0.4×10^{-6} (H6) in 50-mm diameter.

the exception of some few millimeters at the lateral surfaces, which would, in any case, be removed when cutting the element out of the block. Therefore, a customer should consider the sizes of the parts he wants to produce from the raw glass delivery form before ordering a piece of high-homogeneity glass. The homogeneity tolerance should be specified only for these sizes within a block.

The test report for homogeneity contains identification information of the glass item measured, its size, the aperture measured, the peak-to-valley and root-mean-square (rms) values, and the homogeneity grade valid for the complete aperture. The color-coded wavefront map comes together with the applicable color-code scale and a histogram. Additionally, the coefficients of the Zernike series expansions are given, which are related to aberration contributions with imaging. The coefficients C_1 and C_2 corresponding to wavefront shift and tilt, respectively, are omitted because C_1 is already given by the absolute value of the refractive index and C_2 cannot be determined with Fizeau interferometers. In principle, such measurements can be taken with a Loewe interferometer. With this method, usually four samples, staggered by 90 deg, are taken from the outer edge of the disk and polished and wringed to a polished reference sample. Tilt is calculated from the wavefront differences observed from fringe offsets among the samples.

One consideration needs to be taken into account when appraising the homogeneity of an optical glass disk. The Zernike coefficient C_3, equivalent to the parabolic focus term of wavefront distortion, usually forms a significant part of the p-v value. In the example test report of Fig. 4.7, it contributes 21% to the total wavefront distortion. In practice, it can easily be corrected by minimal refocusing and thus may be neglected in specification. Omitting this term explicitly from a p-v specification can determine whether or not raw glass items will be deliverable.

Figure 4.8 shows the homogeneity of an N-BK7 block representing best achievable quality.[5] The contiguous homogeneity over the complete 217 mm × 217 mm aperture is 1×10^{-6} p-v [0.18×10^{-6} rms (H5 grade)] (see left side of Fig. 4.8). The inner part with one-half of the lateral dimensions shows a refractive index variation of 3×10^{-7}, which is already outstanding. Truly remarkable, however, is that across the lateral faces of the block, homogeneity is at the same high level of 0.9×10^{-6} p-v (0.18×10^{-6} rms), again, contiguously across the complete measured aperture of 203.5 mm × 100.2 mm. This is the leading edge of optical glass manufacturing.

Also, in large blanks of SCHOTT BK7, homogeneity can be as good as 2×10^{-6} and even better. Figure 4.9 shows results of a 980-mm-diameter, 109-mm-thick disk measured in the center (2×10^{-6}) and at one position at the edge (1.7×10^{-6}). Stitching together six subapertures leads to 3.9×10^{-6} for the total disk. Considering that errors introduced by the stitching procedure and by temperature gradients are expected to be higher for such large items, the actual homogeneity will be noticeably better, as combined error contributions tend to make the result worse than reality.

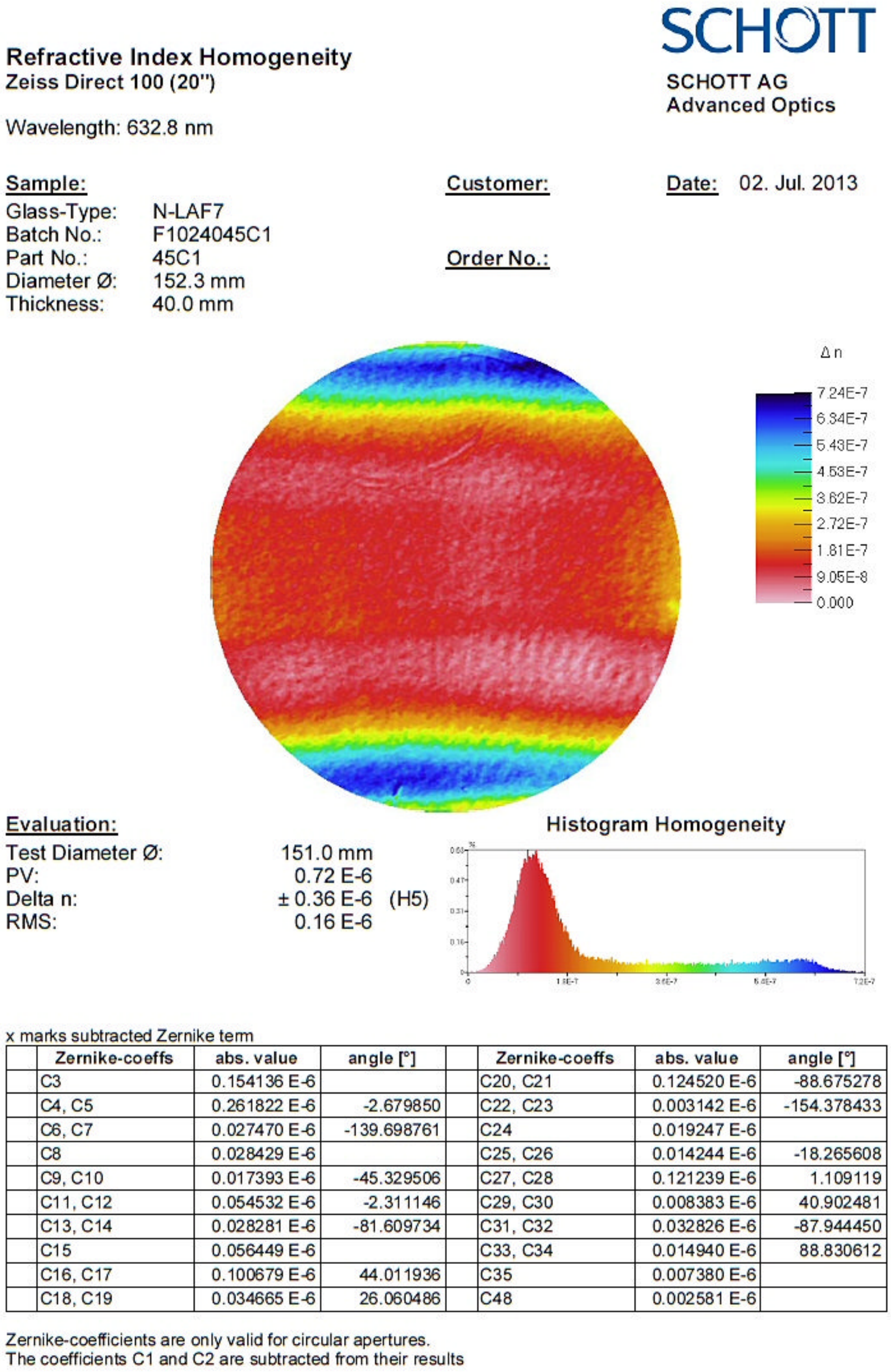
Δn
7.24E-7
6.34E-7
5.43E-7
4.53E-7
3.62E-7
2.72E-7
1.81E-7
9.05E-8
0.000
%
0.63
0.47
0.31
0.16
0
0
1.8E-7
3.6E-7
5.4E-7
7.2E-7

SCHOTT

SCHOTT AG
Advanced Optics

Refractive Index Homogeneity
Zeiss Direct 100 (20")

Wavelength: 632.8 nm

Sample:

Glass-Type:	N-LAF7
Batch No.:	F1024045C1
Part No.:	45C1
Diameter Ø:	152.3 mm
Thickness:	40.0 mm

Customer:

Order No.:

Date: 02. Jul. 2013

Evaluation:

Test Diameter Ø:	151.0 mm
PV:	0.72 E-6
Delta n:	± 0.36 E-6 (H5)
RMS:	0.16 E-6

Histogram Homogeneity

x marks subtracted Zernike term

	Zernike-coeffs	abs. value	angle [°]		Zernike-coeffs	abs. value	angle [°]
	C3	0.154136 E-6			C20, C21	0.124520 E-6	-88.675278
	C4, C5	0.261822 E-6	-2.679850		C22, C23	0.003142 E-6	-154.378433
	C6, C7	0.027470 E-6	-139.698761		C24	0.019247 E-6	
	C8	0.028429 E-6			C25, C26	0.014244 E-6	-18.265608
	C9, C10	0.017393 E-6	-45.329506		C27, C28	0.121239 E-6	1.109119
	C11, C12	0.054532 E-6	-2.311146		C29, C30	0.008383 E-6	40.902481
	C13, C14	0.028281 E-6	-81.609734		C31, C32	0.032826 E-6	-87.944450
	C15	0.056449 E-6			C33, C34	0.014940 E-6	88.830612
	C16, C17	0.100679 E-6	44.011936		C35	0.007380 E-6	
	C18, C19	0.034665 E-6	26.060486		C48	0.002581 E-6	

Zernike-coefficients are only valid for circular apertures.
The coefficients C1 and C2 are subtracted from their results

Figure 4.7 Optical glass homogeneity test report. Wavefront distortions are calculated back to refractive index variations.

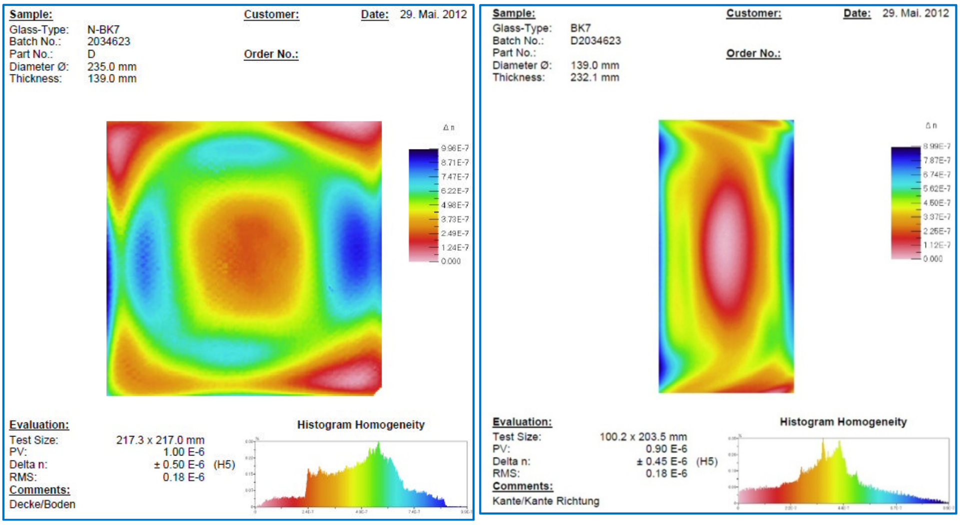

Sample:
Glass-Type: N-BK7
Batch No.: 2034623
Part No.: D
Diameter Ø: 235.0 mm
Thickness: 139.0 mm

Customer:

Order No.:

Date: 29. Mai. 2012

Evaluation:
Test Size: 217.3 x 217.0 mm
PV: 1.00 E-6
Delta n: ± 0.50 E-6 (H5)
RMS: 0.18 E-6

Comments:
Decke/Boden

Sample:
Glass-Type: BK7
Batch No.: D2034623
Part No.:
Diameter Ø: 139.0 mm
Thickness: 232.1 mm

Customer:

Order No.:

Date: 29. Mai. 2012

Evaluation:
Test Size: 100.2 x 203.5 mm
PV: 0.90 E-6
Delta n: ± 0.45 E-6 (H5)
RMS: 0.18 E-6

Comments:
Kante/Kante Richtung

Figure 4.8 (left) Interferogram of an N-BK7 block with a 217 mm × 217 mm aperture in the top-to-bottom direction. Homogeneity is 1 × 10^{-6} contiguously over the full aperture. (right) The same block measured in lateral direction with aperture 204 mm × 100 mm with homogeneity of 0.9 × 10^{-6} contiguously over the full aperture.

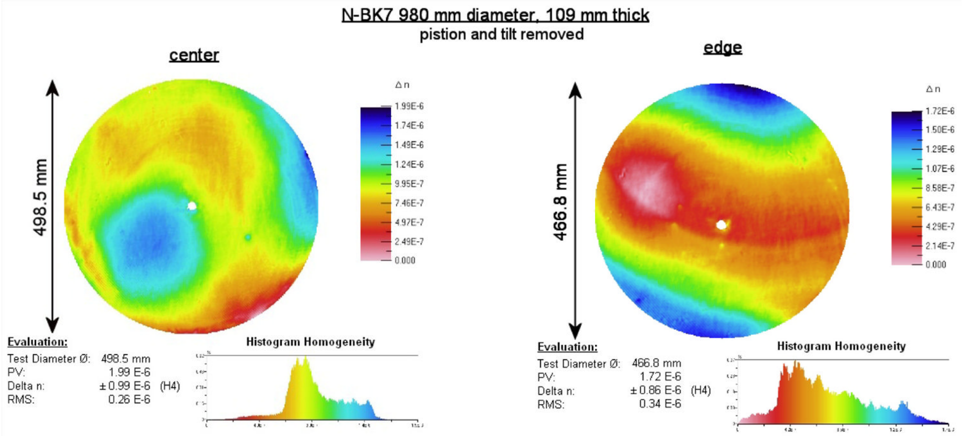

N-BK7 980 mm diameter, 109 mm thick
pistion and tilt removed

Evaluation:
Test Diameter Ø: 498.5 mm
PV: 1.99 E-6
Delta n: ± 0.99 E-6 (H4)
RMS: 0.26 E-6

Evaluation:
Test Diameter Ø: 466.8 mm
PV: 1.72 E-6
Delta n: ± 0.86 E-6 (H4)
RMS: 0.34 E-6

Figure 4.9 Homogeneity of a 980-mm-diameter N-BK7 blank (two subapertures of about 500-mm diameter): (left) central part and (right) edge portion. Total wavefront after stitching six subapertures is 430 nm, fulfilling H3 grade.

4.6 Optical Homogeneity of Glass Types

Optical glass is specially optimized with respect to its homogeneity. For most applications, it is far better than actually needed. Therefore, as a rule, it is necessary to perform interferometer measurements only in cases where extreme quality must be guaranteed. For small and thin lenses, it is neither necessary nor possible to measure their homogeneity, since this requires very high measurement accuracy down to single-digit-nanometer wavefront deformation. Homogeneity measurement of lenses has an additional difficulty: their curved faces. The curvature must be compensated for; this would have to be done with specially adjusted optical arrangements or with immersion oil cuvettes. In any case, the necessary accuracy in wavefront measurement would require extreme effort if it were possible at all. Optical distortion effects in imaging are small, even where the inhomogeneity was somewhat higher than expected. Therefore, for small lenses, homogeneity is of no concern.

With increasing lens size, and especially prism sizes with long light paths, the situation changes. For classical glass types from the borosilicate crown and lead flint glass families, which are production-friendly glass types without any crystallization tendencies, sizes up to 1 m with high homogeneity are possible and have been made. With such glasses, casting times of many hours for one piece can be mastered keeping variations of the refractive index in time very small and all production parameters as well as environmental conditions very stable.

Lanthanum-containing glasses, phosphate glasses, fluoro-phosphate glasses, and other glasses optimized for special dispersion properties use exotic compositions. Such glasses are restricted in size if the highest homogeneity is required. Evaporation of volatile components, delicate heat management to prevent crystallization, and low viscosity during casting (which tends to cause turbulence) all make it very difficult to maintain stability over long times.

Also, the homogeneity degradation close to cast surfaces will become more pronounced than in classical glass types. So, even if it would be possible to manufacture a larger lens from strip glass, due to geometrical considerations, sufficient surplus size must be given if homogeneity must be kept to the very edges of the lens. Also, special castings of such glass types must be made with much wider diameter than is finally needed. Glass types suited for larger, high-homogeneity disks are restricted to the classical families BK, FK, K, BAK, SK, KF, and LLF-SF lead oxide glasses (see Fig. 4.10).

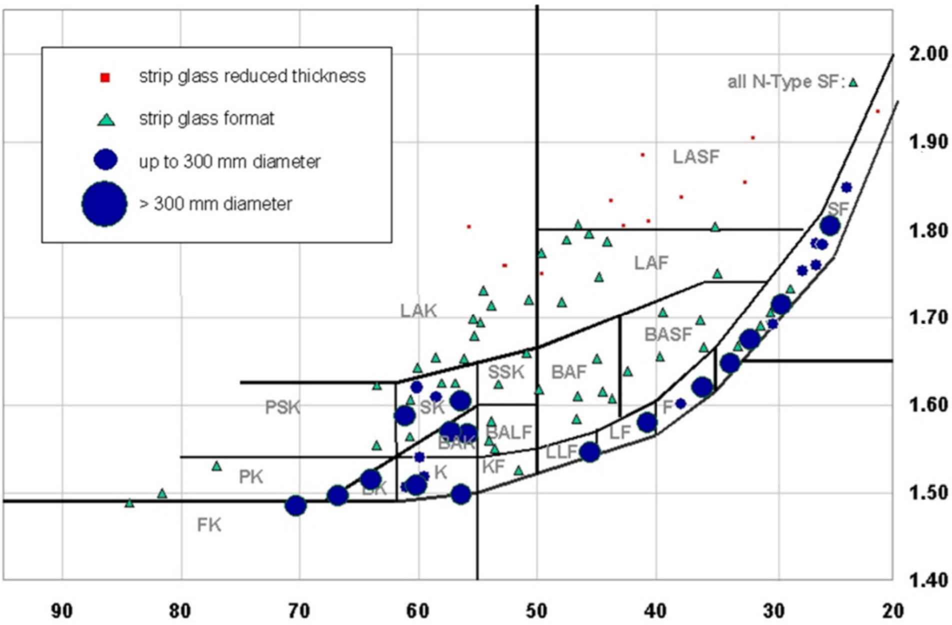

Figure 4.10 Optical glass types suitable for large casting with high homogeneity.

4.7 Striae Appearance

Striae are short-range variations in the refractive index in glass. In the historical production method of clay-pot melting, they appeared as filaments with about a millimeter and smaller thickness. With the modern tank melting process, the appearance has changed to bands extending along the drawing direction of strip glass, showing some refractive index variation periods also within the same size range (Fig. 4.11).

The origins of striae are mainly incomplete homogenization of the raw materials during melting and dissolved tank wall refractory material. Three homogenization steps in the melting process serve to minimize striae content: (1) convection in the tank, (2) convection in the refining chamber, and (3) a final stirring just before casting. Striae coming from tank wall material usually remain at the surfaces of the cast optical raw glass and are removed in the subsequent element production processes. Strip glass is inspected accordingly, and volume parts containing an exceedingly high content of striae will be cut or ground off.

Volume striae extending in the strip-drawing direction sum up over a long light path in this direction. For this reason, inspection is done with reference samples of 50-mm thickness. Tests have shown that with this kind of striae, the effects sum up roughly linearly with thickness. From the 50-mm inspection result, it is possible to estimate effects for smaller thicknesses with a high level of confidence because, in most cases, the results will lie far below any value that might affect the performance of the optical element.

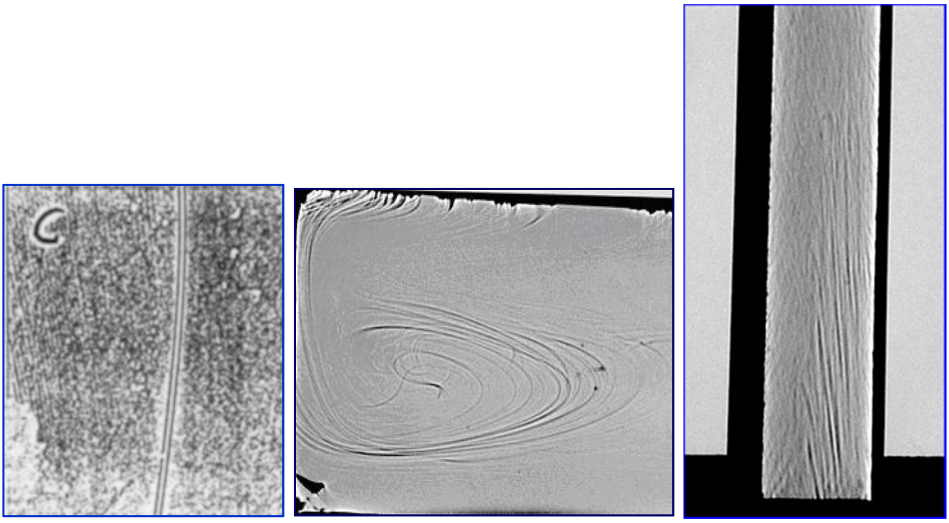

Figure 4.11 Striae in optical glass: (left) filament stria in clay-pot-molten glass, (middle) turbulence stria from casting of low-viscosity glass, and (right) band-like striae in strip glass.

4.8 Striae Measurement: The Shadowgraph Method

Even though the refractive index changes within striae are very small and their lateral extension also is minimal, there is a method available that has a simple setup without any complicated and delicate optical elements. The shadowgraph method needs only a point-like lamp and a screen (see Fig. 4.12). The sample to be measured must be polished but with only moderate surface flatness, far from the flatness of actual optically polished surfaces.

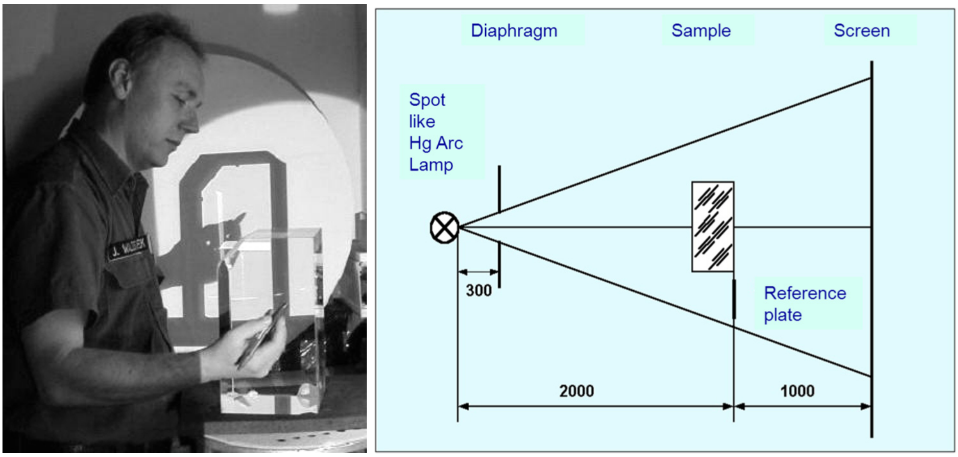

Figure 4.12 Shadowgraph setup with distances in millimeters (photograph courtesy of SCHOTT AG).

The setup consists of a 100-W mercury high-pressure short-arc lamp with a pinhole aperture, a sample holder on a turn table, and a white, opaque projection screen. Without a sample, the illumination pattern on the projection screen will show a constant bright area. Putting a sample with striae into the beam, the striae will become visible on the screen as gray or dark, straight or curved line patterns.

The disadvantage of the shadowgraph method is that it allows determination of striae quality only by visual comparison. In the past, striae grades have referred to standard samples provided by the U.S. National Institute of Standards and Technology (NIST). According to the expired military standard MIL-G-174B,[6] striae quality was subdivided into the grades A, B, C, and D.[7–9]

The supply of such samples ended long ago. The production method of clay-pot melting they refer to is no longer used. The type of striae these standard samples represented does not exist anymore. The grades have no relation to physical quantities that allow for appraising the effect of striae in optical systems. For these reasons, SCHOTT changed the specification of striae from A–D grades to wavefront-variation grades.

The SCHOTT reference samples were measured with a high-spatial-resolution and highly sensitive interferometer that was capable of identifying wavefront variations of about 10, 15, 30, and 60 nm for the A, B, C, and D samples, respectively.

Currently, glass plates with artificial striae are used as references. These artificial striae are made as gaps in coatings on a glass plate with varying thickness and gap width. The quantitative measurement of wavefront amplitudes together with their structural width from shadow contrasts is underway.[10]

4.9 Striae Specification

The effect of striae in an optical element depends on the fraction of aperture that is covered with striae, together with their strength. Older versions of standards for the quality of optical elements (expired DIN 3140 Part 3 and ISO 10110 Part 4) emphasized the fraction of aperture. If this fraction is small enough, striae are allowed to be very strong, even to the point of being opaque, thus becoming similar to bubbles and inclusions. The effects in images are loss of light and creation of stray light, which, in the end, means reduced contrast. If the fraction of aperture is in the small-percentage range, the loss of contrast in the image will be below one percent, which is acceptable for many applications.

However, if the strength of striae is below a certain limit, their effect on image contrast and distortion will be negligible, even when they cover the total aperture.[11,12] For many applications with moderate performance requirements, striae strength of 60-nm wavefront distortion summed up over a light path of 50 mm is sufficient, considering that a very large share of lenses used in everyday practice have thicknesses of only several millimeters.

The striae grades specified in the ISO standard 12123 on raw optical glass are 60 nm, 30 nm, 15 nm, and 10 nm, referred to a sample thickness of 50 mm. Schott has defined 30 nm per 50 mm as standard quality.

The approach of the older standards on optical elements (DIN 3140 Part 3 and ISO 10110 Part 4), referring to the fraction of aperture, is considered to be obsolete now. Due to the high degree of effort required to inspect single lenses in this way, the fraction-of-aperture standard was never really used. A new version replacing ISO 10110 Part 4 specifying striae without any reference to aperture is in preparation.

More attention must to be given to striae when handling large prisms. Light paths in prisms are long and may have directions that are perpendicular to each other. Therefore, a better-quality grade for striae may be needed. In this case, glass should be specified to a wavefront distortion smaller than 10 nm for the glass thickness to be inspected. If needed, this may be extended to two perpendicular inspection directions. Schott delivers optical glass with:

- standard quality 30-nm / 50-mm glass thickness,
  and on special request,
- VS1 enhanced quality with ≤10 nm / 50 mm, or
- VS2 enhanced quality with ≤10 nm / 50 mm inspected in two perpendicular directions.

4.10 Stress Birefringence: Refractive Index Homogeneity in Polarized Light

Each piece of glass has some residual permanent mechanical stress inside, depending on its cooling history. Stress induces anisotropy, which, in transparent media such as glass, can be seen in polarized light (Fig. 4.13).

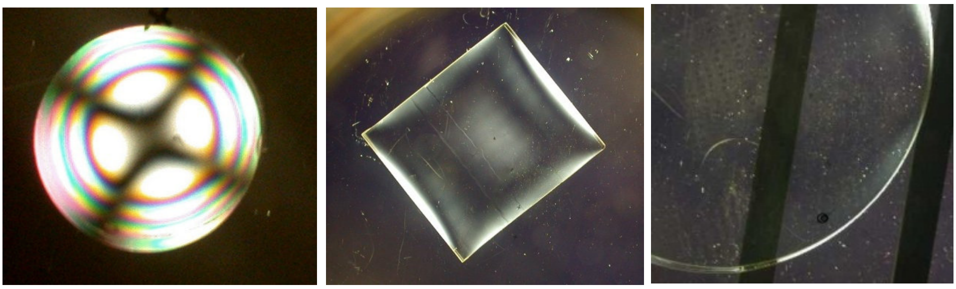

Figure 4.13 Glass items in polarized light: (left) a disk with high stress is recognizable from three circular fringes; (middle) a fine annealed glass block has some noticeable structure remaining; and (right) a fine annealed disk with very low stress is recognizable from its almost completely homogeneous dark image.

Mechanical stress in optical glass leads to birefringence. A piece of homogeneous and isotropic glass changes its refractive index under uniaxial stress depending on the angle of light polarization with respect to the stress direction. Imagine a polarized light ray entering the glass item perpendicularly to the stress direction. The refractive index will change by an amount of $\Delta n_{\parallel}$ if the polarization direction is parallel to the stress direction (Fig. 4.14):

$$n_{\parallel} = n + \Delta n_{\parallel} = n + \frac{dn_{\parallel}}{d\sigma}\sigma, \tag{4.3}$$

or it will change by an amount of $\Delta n_{\perp}$ if the polarization direction is perpendicular to the stress direction:

$$n_{\perp} = n + \Delta n_{\perp} = n + \frac{dn_{\perp}}{d\sigma}\sigma. \tag{4.4}$$

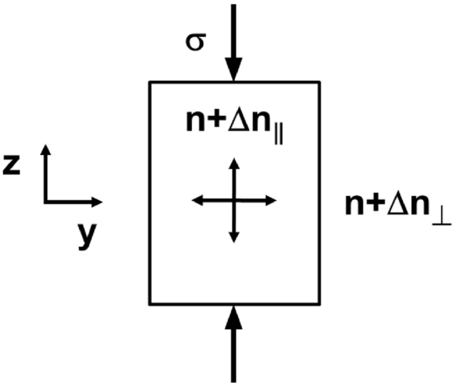

Figure 4.14 Refractive index changes in different directions relative to applied stress.

4.11 Stress-Optical Coefficient

The maximum optical path difference Δs that two perpendicularly polarized light rays travelling through glass thickness d can have is

$$\Delta s = \left(n + \frac{dn_{\parallel}}{d\sigma}\sigma - n + \frac{dn_{\perp}}{d\sigma}\sigma \right) d = \left(K_{\parallel} - K_{\perp} \right)\sigma d = K\sigma d\,. \tag{4.5}$$

The quantity $K = \left(K_{\parallel} - K_{\perp} \right)$ is called the stress-optical coefficient and is given in optical glass data sheets. Its unit is MPa^{-1}, however, some variations are common in practice: 10^{-6} MPa^{-1} or 0.1 nm/cm·MPa^{-1}. Table 4.2 lists stress-optical coefficient K for some glass types. The majority of glass types (about 80%) lie in the range between 1.5×10^{-6} MPa^{-1} and 3.5×10^{-6} MPa^{-1}. Classical flint glass types show a decrease in K with increasing lead content that crosses zero with glass type SF57 and then goes into the negative for even-more-lead-containing glasses (Fig. 4.15). SF57 is a unique glass type that does not react with birefringence on stress.

Table 4.2 Stress-optical coefficient for selected glass types.

Glass type	n_d	K (0.1 nm/cm/MPa)	Glass type	n_d	K (0.1 nm/cm/MPa)
N-KZFS4	1.61336	3.90	SF1	1.71736	1.80
N-FK5	1.48749	2.91	N-LASF44	1.80420	1.41
N-BAK4	1.56883	2.90	LASF35	2.02204	0.73
N-SF6	1.80518	2.82	N-FK51	1.48656	0.70
N-SF57	1.84666	2.78	N-PK52A	1.49700	0.67
N-BK7	1.51680	2.77	SF6	1.80518	0.65
N-SK2	1.60738	2.31	N-PK51	1.52855	0.54
N-LAK9	1.69100	1.83	SF57	1.84666	0.02

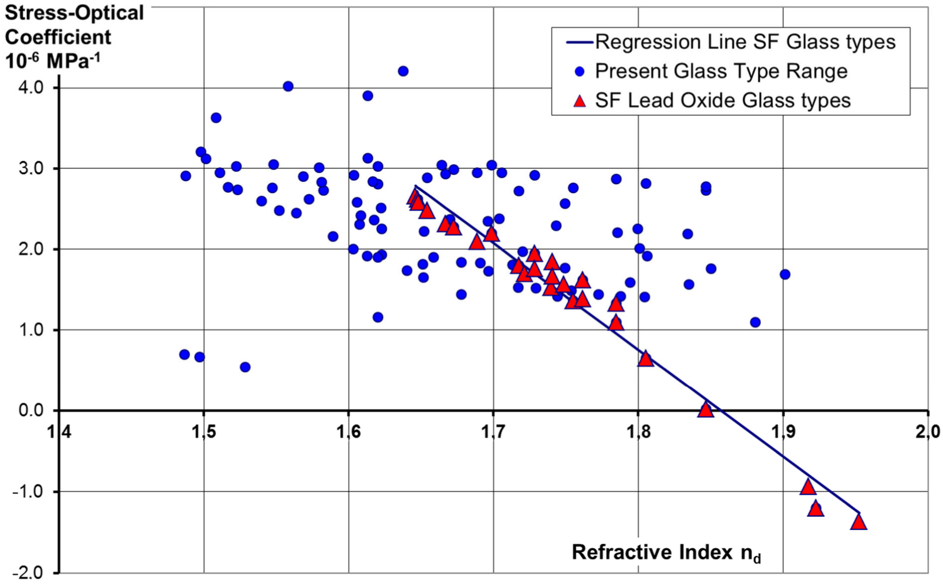

Figure 4.15 Stress-optical coefficient of optical glasses. Triangles correspond to lead silicate glass types. With these glasses, increasing the refractive index is achieved primarily by simply increasing the lead content; thus, refractive index and lead content can be considered to be proportional to each other. The diagram shows the uniqueness of high-lead-containing glasses with respect to the stress-optical coefficient and especially that of the glass type SF57 with the value zero.

The stress-optical coefficient measurement method involves the following: A defined mechanical stress will be introduced within the sample with a four-edge loading setup (Fig. 4.16). Polarized, monochromatic, parallel light of a halogen lamp travels through the loaded sample perpendicularly to the main stress direction, with the polarization direction 45 deg to the main stress direction. A lens focuses the lamp's image to the receiver of a CCD camera.

The induced birefringence, i.e., the phase difference between the ordinary and the extraordinary ray, will be measured by either:

- compensation with a rotating compensator according to Berek (compensation method), or
- determination of the fringe spacing (fringe frequency method).

The wavelength extends from 436 to 1014 nm. The stress-optical coefficient can be measured with an uncertainty of ±5%.

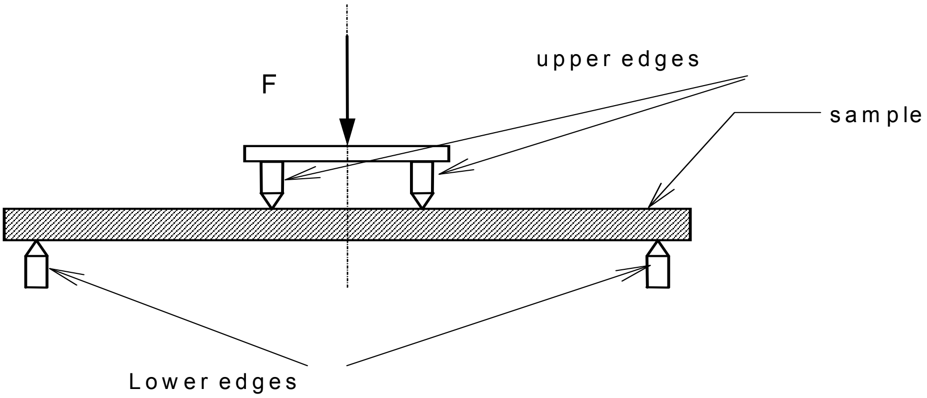

Figure 4.16 Four-edge loading setup for determining the stress-optical coefficient.

4.12 Stress Birefringence: Limit Values for Typical Applications

Inhomogeneity induced in optical elements by stress birefringence cannot be compensated by any means. Refractive index depends on the very position at which light rays enter the glass, its incidence angle, and polarization. Therefore inhomogeneity must be reduced to levels that are insignificant for the application of the optical system. Table 4.3 specifies limit values for stress birefringence for typical applications. Birefringence is given in nanometer wave retardation between two perpendicularly polarized light rays travelling through glass with thickness measured in centimeters.

Table 4.3 Stress birefringence limit values for typical applications.

Limit values	Typical application
<2 nm/cm	Polarization and interference instruments
5 nm/cm	Precision optics, astronomical optics
10 nm/cm	Photographic optics, microscope optics
20 nm/cm	Magnifying glasses, viewfinder optics
Unlimited	Illumination optics

4.13 Stress Birefringence: Size Effect

For small lenses with diameters smaller than about 30 mm and thicknesses smaller than 5 mm, stress birefringence is of no concern because stress is very small anyway. For larger items, stress birefringence should be considered if it is necessary to restrict it by an explicit specification. With large lenses and prisms with diameters or maximum edge lengths larger than 100 mm and thicknesses beyond 20 mm, careful stress birefringence specification becomes important.

There are two main control mechanisms for stress birefringence: cooling rate and the ratio between the gross raw glass size and that of the final optical element. In small thicknesses below 5 mm, thermal conduction prevents high thermal gradients, even in low-conducting material such as glass. Even very high cooling rates of more than 1000 K/h will result in only minute and acceptable stress and thus birefringence. Because of the quadratic dependence of thermal gradients on thickness, fine annealing becomes necessary for items above 5-mm thickness with annealing rates rapidly lowering for increasing thickness. Large items need lengthy and careful annealing processes.

Another method to reduce stress birefringence is simply cutting larger pieces to smaller ones (Fig. 4.17). A glass block of roughly 200 × 200 × 150 mm^3 with 13 nm/cm stress birefringence cut in half to 200 × 100 × 150 mm^3 leads to a reduction of stress birefringence to 4.5 nm/cm. A second cut to 200 × 100 × 75 mm^3 results in stress birefringence of 3 nm/cm.

Cutting prisms from block glass will reduce stress birefringence significantly if the ratio of the final size to the original size is more than 2. If the final optical element's size is only a little bit smaller than the original raw glass item, there is no way to avoid slow and lengthy fine annealing. A specification with a default tolerance value of 10 nm/cm or that requires fine annealing will work well with most small and medium-sized optical glass elements without causing increased and unnecessary effort.

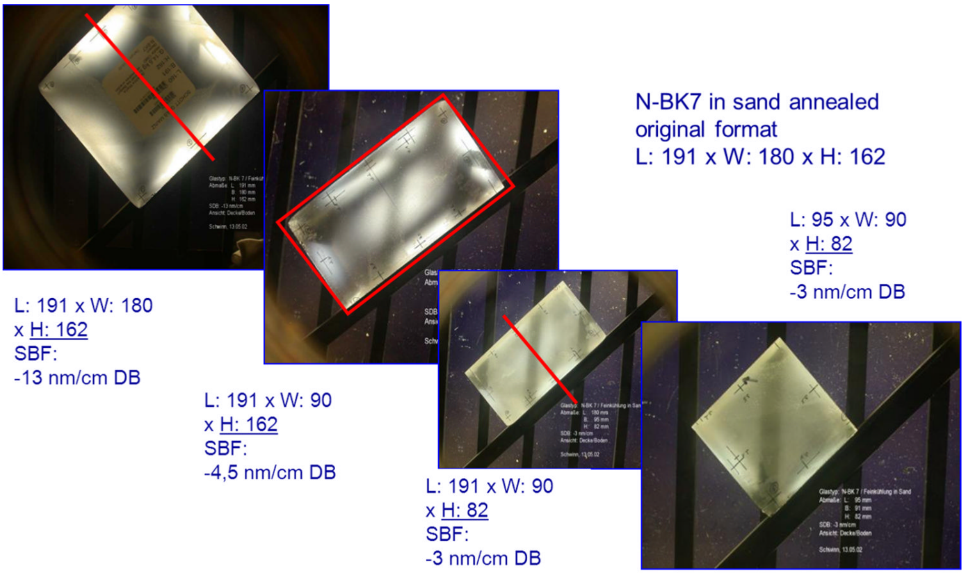
N-BK7 in sand annealed
original format
L: 191 x W: 180 x H: 162
L: 95 x W: 90
x H: 82
SBF:
-3 nm/cm DB
L: 191 x W: 180
x H: 162
SBF:
-13 nm/cm DB
L: 191 x W: 90
x H: 162
SBF:
-4,5 nm/cm DB
L: 191 x W: 90
x H: 82
SBF:
-3 nm/cm DB

Figure 4.17 A block of N-BK7 shows stress birefringence reduction due to cutting it down to smaller-sized pieces.

4.14 Transient Stress Birefringence

Stress birefringence as discussed in Chapter 3 is called permanent stress birefringence because it is introduced during the production process and cannot be changed unless the glass item is subjected to another annealing process.

Another type of stress birefringence called temporal or transient stress birefringence is caused by stress resulting from thermal gradients occurring in application. This could be from, for example, switching on a strong lamp in a digital projector, which imposes a sharp temperature rise in the color-combining prism cube.

Birefringence in such cases depends on three factors. First is the tendency to reduce thermal gradients to restore equilibrium, which can be described by the relaxation time t_r, formed by the ratio of thickness d squared to thermal diffusivity κ:

$$t_{\mathrm{r}} = \frac{d^2}{\kappa}. \tag{4.6}$$

κ contains the material-dependent quantities thermal conductivity λ, specific heat c_p and density ρ as follows:

$$\kappa = \frac{\lambda}{\rho \cdot c_{\mathrm{p}}}. \tag{4.7}$$

The second factor is the reaction of the glass items to thermal gradients with stress and is ruled by the geometrical factor f, the thermal stress coefficient φ, and the temperature difference ΔT:

$$\sigma = f \cdot \varphi \cdot \Delta T. \tag{4.8}$$

The thermal stress coefficient φ is another material-specific quantity governed by the coefficient of thermal expansion α, Young's modulus E, and Poisson's ratio μ:

$$\varphi = \frac{\alpha \cdot E}{1-\mu}. \tag{4.9}$$

The third factor determines how strongly a glass reacts to stress with birefringence. This is the stress-optical coefficient K.

Combining the three factors allows one to define a figure of merit $K_{\Delta T}$ that is useful for ranking optical glasses based on their sensitivity with respect to birefringence against thermally induced transient stress:

$$K_{\Delta T} = \frac{c_\mathrm{p}\rho}{\lambda} \cdot \frac{\alpha \cdot E}{1-\mu} \cdot K. \tag{4.10}$$

Figure 4.18 shows a ranking of glass types according to the figure of merit. The selection was made to demonstrate the variation and thus enhances the extreme regions. Most glasses by far lie within the range of 4000 to 6000. The exceptional position of SF57 is clearly noticeable. Its lead- and arsenic-free variant N-SF57 has a $K_{\Delta T}$ value that is about 200 times higher.

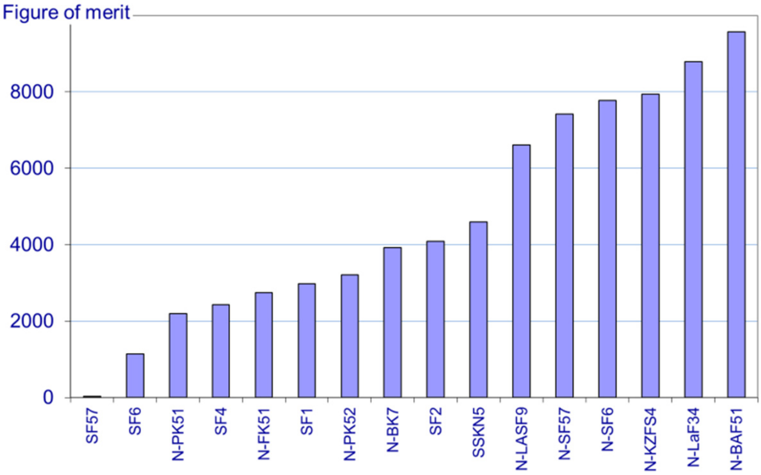

Figure 4.18 Glass type ranking according to their reaction on temperature differences with birefringence using the figure of merit quantity $K_{\Delta T}$.

Large optical glass disks sometimes are specified with high-refractive-index homogeneity. In such cases, it is not only the contribution of the refractive index that must be taken into account. Thermally induced stress birefringence can also introduce high wavefront distortion values. Consider a disk with 100-mm thickness. H4 homogeneity grade limits wavefront distortion to $2 \times 10^{-6} \times 100$ mm = 200 nm. Such wavefront distortion also results from thermally induced stress birefringence if the disk's center temperature differs from the edge temperature by only 1 °C. Many glasses react to temperature differences with 15–20 nm/cm·K^{-1} stress birefringence. For the highest-quality imaging performance, large lenses must be temperature stabilized to the best possible degree. For very critical applications, mirror optics should be considered as a preference over large lenses.[13]

4.15 Birefringence Measurement

The commonly used method for measuring stress birefringence is the de Sénarmont and Friedel[14] method (Fig. 4.19). A detailed description can be found in standard ISO 11455 Raw Optical Glass–Determination of Birefringence. Light with wavelength λ and polarization angle of 45 deg with respect to the stress direction is elliptically polarized after travelling through the glass sample of thickness d. The quarter-wave plate converts the elliptical polarization back to a linear one but rotated with respect to the polarization of the incident light. The rotation angle α is proportional to birefringence and is determined with the analyzer. Stress is calculated from the rotation angle employing the stress-optical coefficient of the glass being measured with the formula

$$\sigma = \frac{\alpha \cdot \lambda}{180} \cdot \frac{1}{K \cdot d}. \tag{4.11}$$

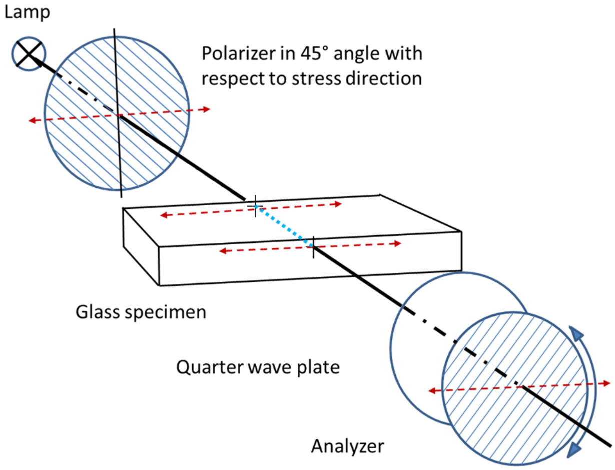

Figure 4.19 Birefringence measurement method of de Sénarmont and Friedel.

In order to simplify interpretation, measurements are usually taken at positions close to the edges, where the radial component of the stress tensor approaches zero and only the tangential component is effective. In the past, such measurements were quite tedious and could be made only at selected positions of the disks. Today, setups are commercially available that measure the total cross-section of the disk in one short measurement process, rendering high spatial resolution and high birefringence accuracy. Figure 4.20 shows such a measurement report with a color-coded scale. The measurement principle is the same as was explained earlier in this section. The field of view covers 300 mm × 225 mm with a spatial resolution of approximately 1–1.5 mm. Wavefront retardation accuracy is about ±1 nm absolute. The complete areal distribution of birefringence can be seen in a single view.

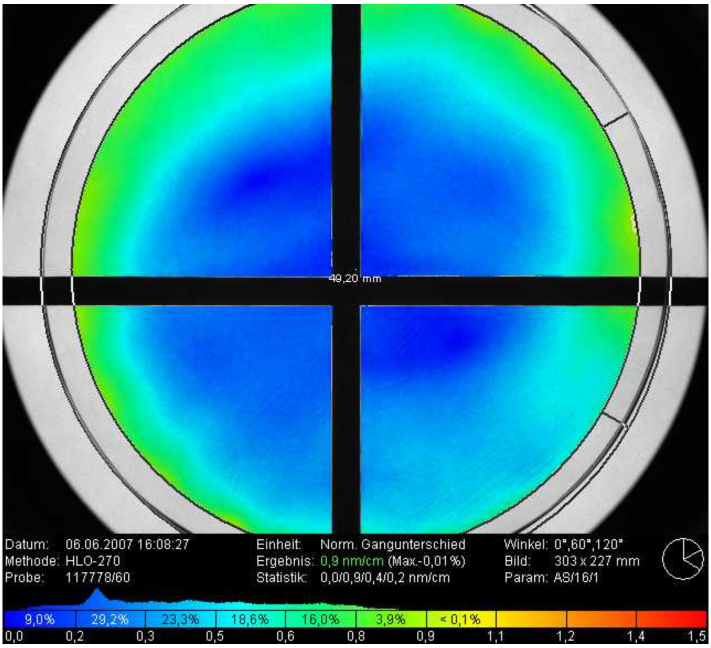

Datum: 06.06.2007 16:08:27
Methode: HLO-270
Probe: 117778/60
Einheit: Norm. Gangunterschied
Ergebnis: 0,9 nm/cm (Max.-0,01 %)
Statistik: 0,0/0,9/0,4/0,2 nm/cm
Winkel: 0°,60°,120°
Bild: 303 x 227 mm
Param: AS/16/1

Figure 4.20 Birefringence report for a highly homogeneous glass disk used in i-line microlithography. The measurement principle used was that of de Sénarmont and Friedel. Field of view covers 303 mm x 227 mm, and maximum birefringence is 0.9 nm/cm.

4.16 Bubbles and other Inclusions

In general, the term *inclusion* comprises all localized material imperfections in optical glass. Bubbles, small spherical gas-filled voids, are the most common type of inclusion. Their cause is imperfect refining of glass melts. Solid inclusions coming from nonmolten raw material are scarce. The present-day quality of glass with respect to numbers of bubbles and inclusions has reached a high level; even in large items, only a very small number will occur.

For optical imaging quality, bubbles are only of little importance. They reduce transmitted light and contribute to stray light. The resulting contrast reduction will be negligible.[15] Since this effect is roughly proportional to their cross-section, bubble quality is traditionally specified by using their total cross-section within a reference volume. However, bubble quality in delivered glass is important not for technical reasons, but for esthetics. Bubbles can easily be seen in an optical system. Depending on their position, they can appear to be larger than they are due to magnification by curved surfaces. All technical arguments supporting individual test results for the very system are worthless if the customer is irritated by clearly visible inclusions in the glass. This holds especially if the optical system is very expensive. Customers expect glass without any visible imperfections. In the end, this results in a bubble quality level much higher than is technically needed.

4.17 Bubbles and Inclusions: Inspection

The setup for bubble and inclusion inspection is very simple (Fig. 4.21). The glass sample is located on a black cloth and illuminated from the side. An inspector determines the number and sizes of the bubbles in the volume by visual comparison with reference samples. If necessary, a microscope with long working distance can be used to increase accuracy (Fig. 4.22).

This setup is very sensitive. Inclusions with sizes of only few micrometers can be seen clearly. If the illumination is too strong, such tiny inclusions will be overestimated in size, which can result in discarding glass samples that would have worked perfectly well under the actual light conditions of its application. In order to specify the bubble and inclusion quality of optical glass, one uses the sum of the cross-sections of all inclusions (in millimeters squared) within a reference volume of 100 mm^3.

Cross-sections of nonspherical inclusions are calculated by multiplying their maximum length and width. All inclusions that are smaller than 0.03 mm will be disregarded. Smaller bubbles and inclusions are scarcely observed. From a technical point of view, this specification would be sufficient. However, esthetics requires the introduction of another characteristic: the number of bubbles per reference volume.

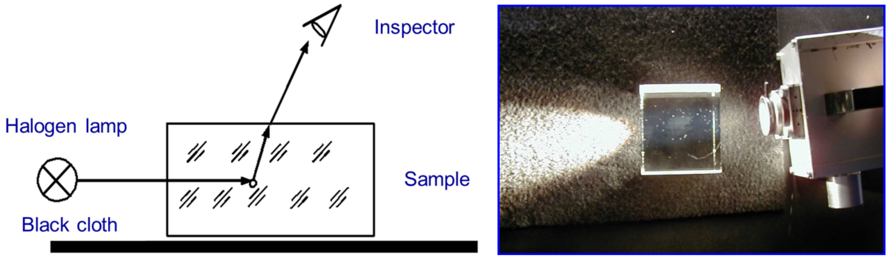

Figure 4.21 (left) Bubble and inclusion inspection setup using (right) lateral illumination with black background.

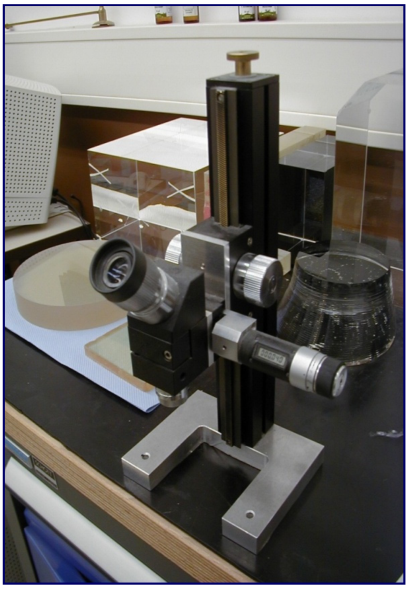

Figure 4.22 Microscope with long working distance for precision determination of inclusion sizes.

4.18 Bubbles and Inclusions: Specification

Formally specifying bubble and inclusion content only by restricting the total cross-section in a test volume cloud leads to the acceptance of a large number of very small bubbles. Such aggregations of even tiny inclusions are not acceptable to customers. Therefore, the number of bubbles per test volume is also restricted. The raw glass specification standard ISO 12123 sets limits only for the cross-section and the number per volume (Table 4.4). High-quality optical glass suppliers deliver glass with ≤0.1 mm^2 cross-section within 100 mm^3 volume or even better. SCHOTT defines 0.03 mm^2 cross-section as standard quality and 10 as maximum number of bubbles and inclusions in 100 mm^3. SCHOTT additionally offers two even-more-restricted grades numbers 4 and 2, of 0.02 and 0.006 mm^2, respectively.

Table 4.4 Bubble and inclusion specification according to ISO 12123.

Maximum permissible cross-section of any bubbles and inclusions per test volume (mm^2/100 cm^3)	**Maximum allowable number per test volume (N/100 cm^3)**
0.5	140
0.25	70
0.1	30
0.03	10

The specifications of Table 4.4 hold for raw optical glass. Designers of optical systems specify bubble and inclusion content in drawings for optical elements. Transferring tolerances for elements to raw glass delivery format, which is usually strip glass, is not as trivial as it might seem at first glance. This is especially true because, in most cases, a third party is involved in glass press shops. The requirement of no bubbles in small lenses transferred to the raw glass delivery format cannot simply mean no bubbles at all in the raw glass. Many thousands of small lenses can be produced from a single raw optical glass strip. A few small bubbles in the strip will lead to a few lenses with a bubble inside, which will just be thrown away. The raw glass format must have adequate quality to produce bubble-free lenses with high yield. For larger lenses, the zero-bubble requirement may lead to high losses. Here, a specification will be needed for the number and size of bubbles per lens.

ISO 10110 Part 3 gives a guideline for such a specification in the form $1/N \times A$ (example: 1/3 × 0.16). The leading "1" refers to bubbles and inclusions. N represents the number and A the grade of individual bubbles. The grade number is the square root of the bubble's area and is thus slightly smaller than its diameter (by 11%). Usually subdivision of the specified total area is possible. A multiplication factor table helps for this purpose by keeping the total area $N \times A^2$ constant. Table 4.5 is equivalent to that in ISO 10110 Part 3 with the exception that the cells with bubbles with grades smaller than 0.025 mm are omitted.

Table 4.5 Bubbles and inclusions allowed in subdivision according to ISO 10110 Part 3, with grades smaller than 0.025 mm omitted. Example: If the indication in a lens drawing is 1/2 × 0.25 (meaning 2 bubbles of grade number 0.25), then 2 × 2.5 = 5 bubbles of grade number 0.16 are allowed, or 2 × 6.3 ≈ 12 bubbles of grade number 0.10.

	Multiplication factors			
Grade numbers *A* in mm	**1**	**2.5**	**6.3**	**16**
	0.025			
	0.040	0.025		
	0.063	0.040	0.025	
	0.10	0.063	0.040	0.025
	0.16	0.10	0.063	0.040
	0.25	0.16	0.10	0.063
	0.40	0.25	0.16	0.10
	0.64	0.40	0.25	0.16
	1.0	0.64	0.40	0.25
	1.6	1.0	0.64	0.40
	2.5	1.6	1.0	0.64
	4.0	2.5	1.6	1.0

References

1. M. Küchel,” The new Zeiss interferometer,” *Proc. SPIE* **1332**, 655–663 (1990) [doi: 10.1117/12.51116].
2. P. Hartmann, R. Mackh, and H. Kohlmann, “Advances in the homogeneity measurement of optical glasses at the Schott 20 inch Fizeau interferometer,” *Proc. SPIE* **2775**, 108–114 (1996) [doi: 10.1117/12.246738].
3. F. Reitmayer and H. Schröder,” Effect of temperature gradients on the wave front aberration in athermal optical glasses,” *Appl. Opt.* **14**, p. 716–720 (1974).
4. J. Schwider, R. Burow, K.-E. Elssner, R. Spolaczyk, and J. Grzanna, “Homogeneity testing by phase sampling interferometry,” *Appl. Opt.* **24**(18), 3059–3061 (1985).
5. P. Hartmann, “110 years BK7: Optical glass type with long tradition and ongoing progress,” *Proc. SPIE* **8550**, 85500U (2012) [doi: 10.1117/12.981784].
6. U.S. Dept. of Defense, “Military specification, glass, optical,” MIL-G-174B, (1986).
7. J. S. Stroud, “Striae quality grades for optical glass,” *Opt. Eng.* **42**(6), 1618–1624 (2003) [doi: 10.1117/1.1571549].
8. J. R. Meyer-Arendt, Ed., *Selected Papers on Schlieren Optics*, *SPIE Milestone Series* MS61, SPIE Press, Bellingham, WA (1992).
9. V. S. Doladugina, “Evaluating the stria content in optical glass,” *J. Opt. Technol.* **71**, 836 (2004).
10. H. Gross, M. Hofmann, R. Jedamzik, P. Hartmann, and S. Sinzinger, “Measurement and simulation of striae in optical glass,” *Proc. SPIE* **7389**, 73891C (2009) [doi: 10.1117/12.827677].
11. R. Hild, G. Nietzsche, and J. Hebenstreit, “Influence of Schlieren on imaging properties of an optical system. II: Modulation transfer function (MTF),” *Optik* **85**, 177 (1990).
12. R. Hild, S. Kessler, and G. Nietzsche, “Influence of Schlieren on imaging properties of an optical system. I: Point spread function (PSF),” *Optik* **85**, 123 (1990).
13. P. Hartmann and R. Jedamzik, “Large optical glass lenses for ELTs,” *Proc. SPIE* **6273**, 62730H (2006) [doi: 10.1117/12.669939].
14. E. Werner, “Zur Bestimmung der Spannungsdoppelbrechung von optischem Glas,” *Silikattechnik* **18**(2), 45–49 (1967).

15. Zs. Nagya, P. Koppa, Gy. Nádudvari, E. Dirix, and P. Richter, "Modeling air inclusions in high performance objective lenses," *Proc. SPIE* **5249**, 703–709 (2004) [doi: 10.1117/12.513317].

Chapter 5
Transmittance

It is clear that high light transmission is the fundamental property of any glass that will be used as an optical material. Transmission is consistently high over the entire VIS wavelength range and even partially outside of this range.

The atomic bonds between the constituents of optical glass (silicon, oxygen, boron, sodium, potassium, lead, barium, lanthanum, and many others) are strong. In order to break them apart, photon energy higher than 3 eV is needed, corresponding to about 400-nm wavelength. Improved melting technology and raw materials of high purity enable a very low content of alien material that could introduce weaker bonds and thus absorption in VIS light.

Another essential property of glass is that it maintains its internal microstructure as a liquid while cooling down from melting until it becomes a rigid body. This means that no crystals or other types of micro-inhomogeneity of any size arise that could block, deflect, or scatter light and thus reduce clarity and transmission.

5.1 Internal Transmittance

One effect that reduces overall light transmission is Fresnel reflection, which is related to the refractive index of the glass. Since glass manufacturing cannot influence its contribution by any means, reflection-induced transmission reduction (Fig. 5.1) should be eliminated before appraising transmission quality of a glass melt. For this reason, specification of transmission refers to the internal transmittance τ_i, which is defined by the amount leaving the glass volume I_i relative to the amount entering I_{i0}:

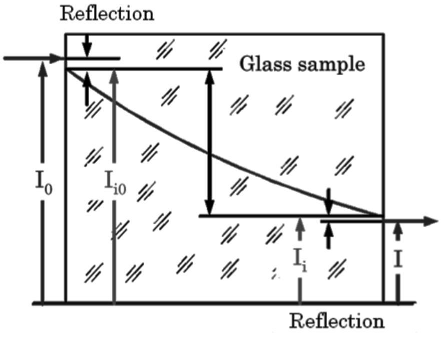

Figure 5.1 Reduction of light intensity while travelling through a piece of glass with reflection losses at the entrance and exit surface and absorption in between.

$$\tau = \frac{I}{I_0}, \text{ and } \tau_\mathrm{i} = \frac{I_\mathrm{i}}{I_{\mathrm{i}0}}. \tag{5.1}$$

5.2 Measurement of Internal Transmittance

Transmittance measurement is performed using a dual-beam spectral photometer covering the wavelength range from the UV to the NIR. The first beam travels through the sample, which is usually 25 mm thick. The second beam serves as a light intensity reference. The sample compartment allows a maximum length of 300 mm, which may become necessary for precision measurement close to an internal transmittance value of 1. High wavelength resolution is achieved with a setup of two monochromators arranged in series. The overall wavelength range is 190–3200 nm; with an integrating sphere, it reduces to 200–2500 nm. Wavelength can be resolved to within 1 nm.

The uncertainty of transmittance measurement is better than ±0.3% for UV–VIS and ±0.5% in the NIR. The uncertainty of wavelength measurement is better than ±0.08 nm (UV–VIS) and ±0.8 nm (NIR). Converting transmittance to internal transmittance is achieved by using the reflection factor $P(\lambda)$:

$$\tau(\lambda) = \tau_\mathrm{i}(\lambda) \cdot P(\lambda). \tag{5.2}$$

For calculating the wavelength-dependent reflection factor for multiple reflections,

$$P(\lambda) = \frac{2n(\lambda)}{n^2(\lambda)+1}, \tag{5.3}$$

it is necessary to have precise refractive index data available for the complete wavelength range of interest.

5.3 Overall Internal Transmittance of Optical Glass

The overall transmission curve for optical glass shows a steep UV absorption edge caused by ionization of bound atoms, a high transmission plateau in the VIS and NIR range, the IR edge caused by residual water, and a small transmission window around 3000 nm. At wavelengths longer than 4500 nm, optical glass is no longer transparent. Here, light is absorbed by transferring its energy to vibrations of the bound atoms.

The curves of Figs. 5.2 and 5.3 are typical for most glass types. The use of raw materials with higher impurity content will lead to decreased slopes extending farther into the VIS light range, leading to a yellowish appearance. For most NIR applications, the high transmission plateau extends far enough into the IR before reductions are observed. The residual water content causing the absorption at around 2700 nm can be greatly reduced by introducing drying measures while melting the glass. However, normally, this is not necessary and would only lead to higher costs. SCHOTT offers some glass types that have been melted in this way. Some glasses of the fluoro-phosphate crown family dry by themselves due to their high fluorine content, thus leading to high transmission extending farther into the IR.

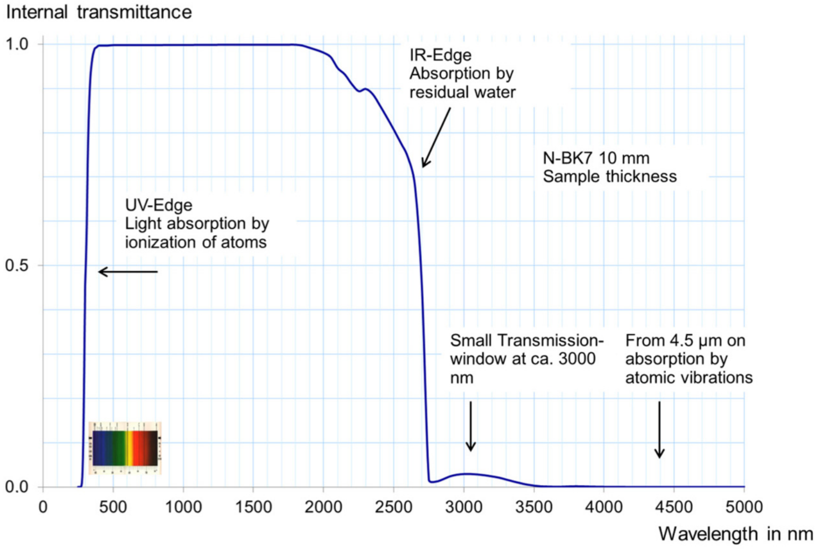

Figure 5.2 Internal transmission typical for an optical glass from UV to IR.

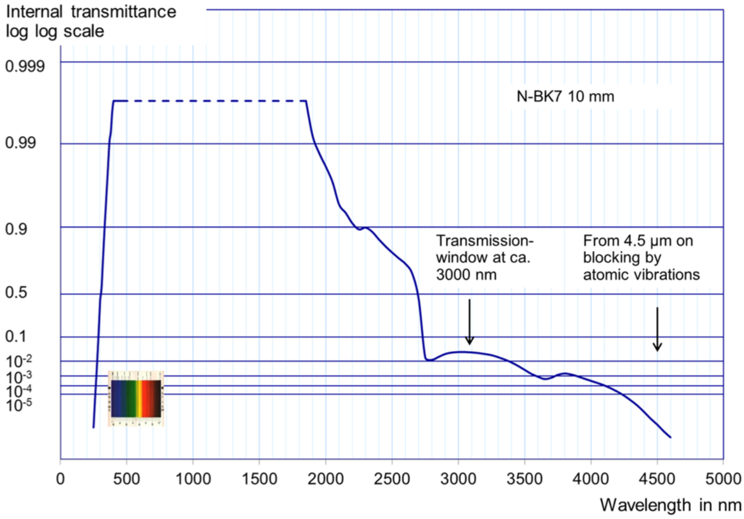

Figure 5.3 Internal transmission typical for an optical glass from UV to IR, the same curve as in Fig 5.2 but with double logarithmic transmittance scale allowing better recognition of IR transmittance.

General dispersion theory points to the fact that the higher the refractive index of a glass type, the closer the UV edge approaches the VIS light. For very high-index glasses, and especially for the lead-free variants, the absorption edge enters the VIS light range, introducing a yellowish tint, as can be seen in the right side of Fig. 5.4. The UV edge in Fig. 5.5. shifts from about 300 to 400 nm. Figure 5.6 ranks the glass types in the Abbe diagram according to their internal transmission at 400 nm and 25 mm sample thickness. The diagram demonstrates the trend of transmission at the UV edge to decrease with larger refractive index.

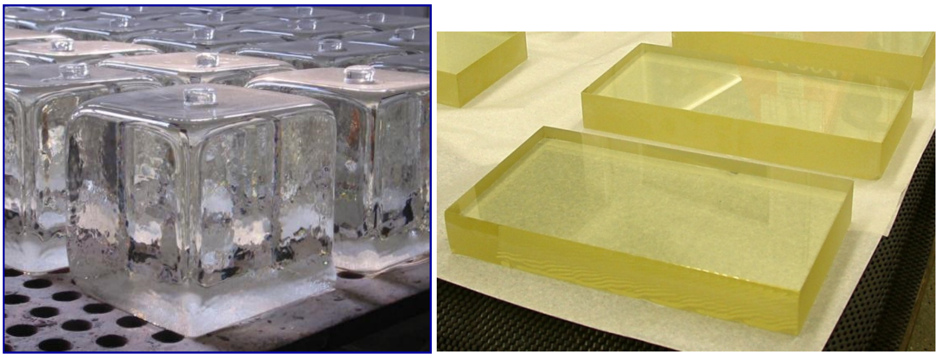

Figure 5.4 (left) White glass blocks of N-BK7 with high transmission in the VIS range. (right) Glass strips of N-SF4 with blue–violet transmission reduction and a yellowish tint.

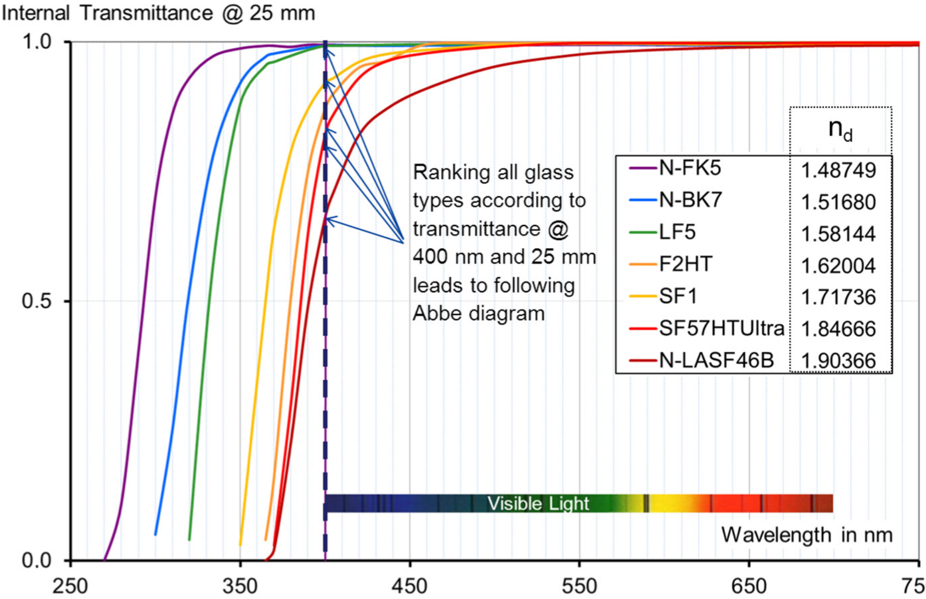

Figure 5.5 The internal transmittance UV edge for a set of optical glasses. The position shifts from UV to the VIS light range for higher-index glass types.

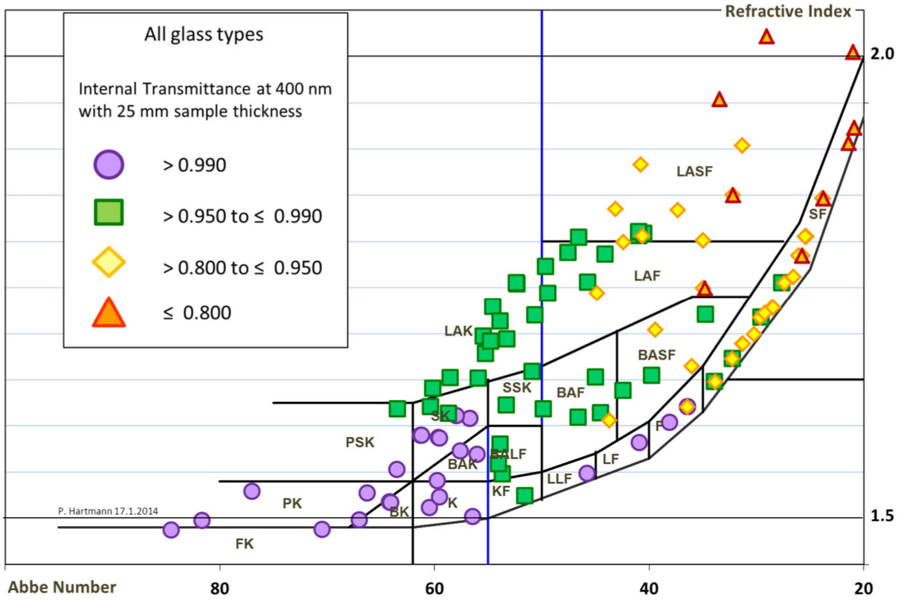

Figure 5.6 Abbe diagram with glass types categorized with respect to the internal transmittance directly at the UV–VIS light border of 400 nm, showing the trend of high UV transmittance for the low-refractive-index glass types and low UV transmittance for the high-refractive-index glass types.

Transmittance is measured using a spectrograph covering a wavelength range from 250 nm to 2500 nm with polished samples. The internal transmittance changes exponentially with glass thickness:

$$\tau_i\left(d_2\right)=\tau_i^{d_2/d_1}\left(d_1\right). \tag{5.4}$$

SCHOTT uses 25-mm-thick glass samples for measurement. Results for 10-mm thickness could already lie within the range of 1 minus measurement uncertainty. For extreme requirements, it is possible and practical to use 100-mm samples. The following table shows internal transmission values for 10- and 100-mm glass thickness, referring to 25-mm example values calculated with Eq. (5.4).

Table 5.1 Internal transmittance values for 10-mm and 100-mm thickness calculated from example values for 25 mm.

d (mm)	10	25	100
τ_i	0.998	0.995	0.980
	0.996	0.990	0.961
	0.980	0.950	0.815
	0.959	0.900	0.656
	0.915	0.800	0.410

5.4 Internal Transmittance: Color Code

The color code characterizes the position and slope of the transmission UV edge with two numbers, e.g., 30/27 for N-FK5. The numbers indicate the wavelengths at 80% and 5% transmittance for a glass type or a specific glass melt (Fig. 5.7). The wavelengths are given in rounded tens of nanometers. The use of transmittance including reflection losses is due to the fact that not all suppliers have dispersion curves available that are as precise as needed for removing these losses.

Unfortunately, this definition leads to problems with high-refractive-index glasses. There are glass types that barely surpass the 80% transmittance because of their high reflection factor. In order to cope with this problem, for such glasses, the upper border line is lowered to 70%. Color code data are marked accordingly, e.g., 42/37* for the glass type N-SF57. Other glass types with a slightly lower refractive index and therefore lower reflection factor may encounter quality acceptance problems for specific melts because of the flat slope of the transmittance curve when crossing the 80% line. Small changes in transmittance may lead to large changes in the wavelength determining the color code value for the 80% limit such that melts would be rejected due to an artificial formal deviation. To avoid this, ISO 12123 introduced another definition, the UV cutoff edge UVC 80/10, using the 80% and 10% limits for internal transmittance.

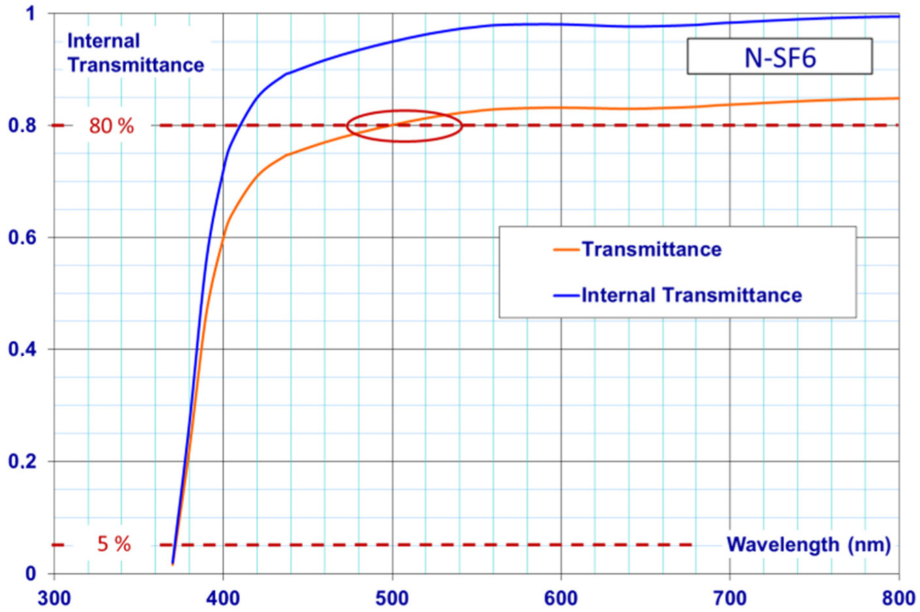

Figure 5.7 Color code definition values (5% and 80% transmittance) and the problem with the upper limit value for high-refractive-index glass types. Slight changes in transmittance at 500 nm result in a large change in wavelength values. The use of internal transmittance prevents this problem.

5.5 Internal Transmittance Tolerances and High Transmittance Quality Grade

Generally, glass supplier catalogs do not provide any tolerance limits for transmittance values but provide only typical values. In many optical systems, light intensity varies by large factors or even orders of magnitude. Variations in glass transmittance in the per mille range are hardly detected against such large variations. Defining tolerances would require enhanced effort for measurements and production surveillance beyond the present level of common practice, which would increase prices for glass without any additional benefit. This holds especially when the glass lenses have small thickness.

For special applications such as mesopic vision with binoculars, the highest light transmission is desired for optical elements with a long light path. In this case, catalog values can be specified as minimum values, or special high transmission (HT) grades for optical glasses will be used. Such grades are also used with optical systems with high white-light intensity from halogen or arc lamps. Glasses with enhanced transmission in blue–violet light not only increase light yield but also facilitate heat management. For the HT grades of SCHOTT, data are guaranteed minimum values in the VIS range. Transmittance gain can be very significant, especially for high-refractive-index glasses close to the border line at 400 nm that divides the VIS from the UV range (Fig. 5.8).

The HT grades were originally introduced for high-refractive-index glasses. Due to increasing market demand, HT grades have been introduced for glasses that are traditionally used for prisms: N-BK7, N-BAK4, and N-SK2 (Fig. 5.9). The high transmission grade of the classical flint glass F2 is indispensable for endoscopes. Figure 5.10 shows the gain in transmission for the HT grade of N-BK7. At first glance the improvement from 0.992 to 0.996 does not seem very interesting. However, from the point of view of heat absorption, it is a significant improvement; $(1 - 0.996)/(1 - 0.992) = 0.5$, which means that the amount of absorbed light is only half of the previous amount. High temperatures change the refractive index and thus may change the imaging performance of sensitive optical systems. This so-called thermal lensing effect can be reduced substantially by using HT-grade glass (see Fig. 5.10).

From the observation of a yellowish tint in old binoculars, some people deduced that they were subjected to solarization (refer to Section 5.7). This is most probably untrue. The white appearance of present-day binoculars mainly stems from the fact that transmission has been considerably improved in the last 50 years (see Fig. 5.11).

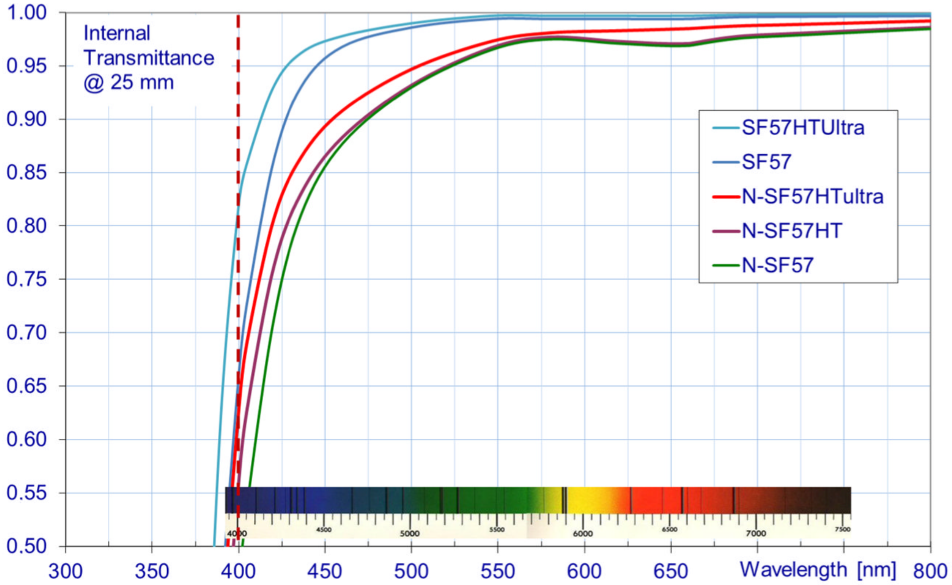

Figure 5.8 Improved internal transmittance with special quality grades HT and HTUltra for the two glass types SF57 and its lead- and arsenic-free counterpart N-SF57.

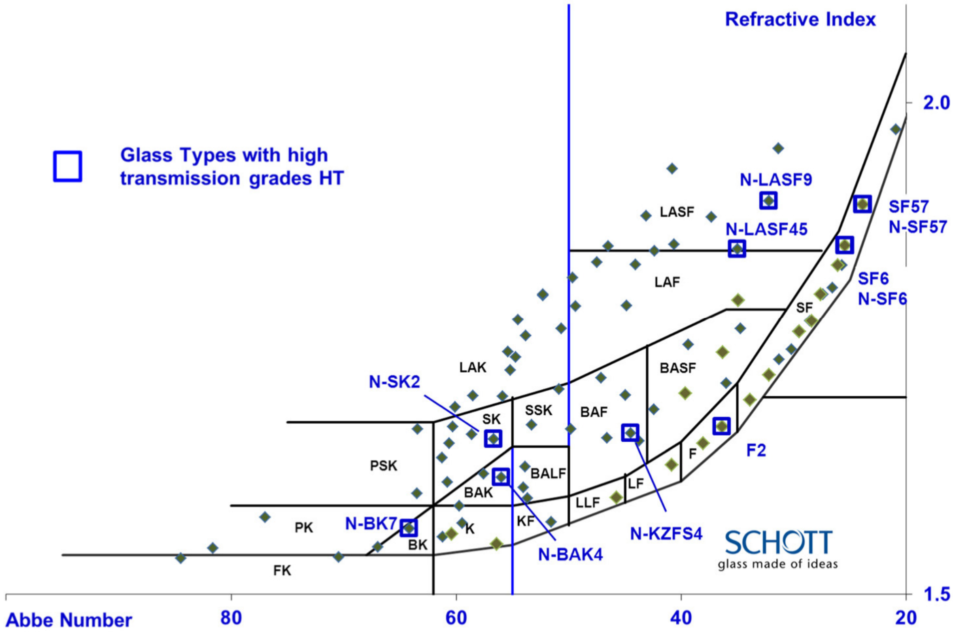

Figure 5.9 Abbe diagram showing glass types with improved internal transmittance marked with the special quality grades HT and HTUltra.

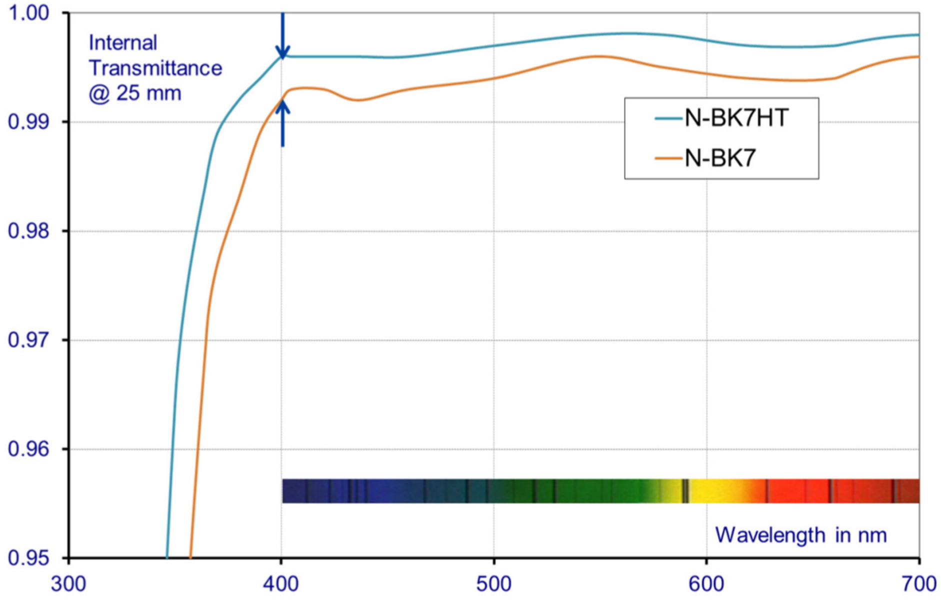

Figure 5.10 Internal transmittance of N-BK7 and its special quality grade N-BK7HT. The gain of transmittance corresponds to a reduction of absorption to one-half. This can be a considerable advantage when thermal lensing is a problem for the overall system performance.

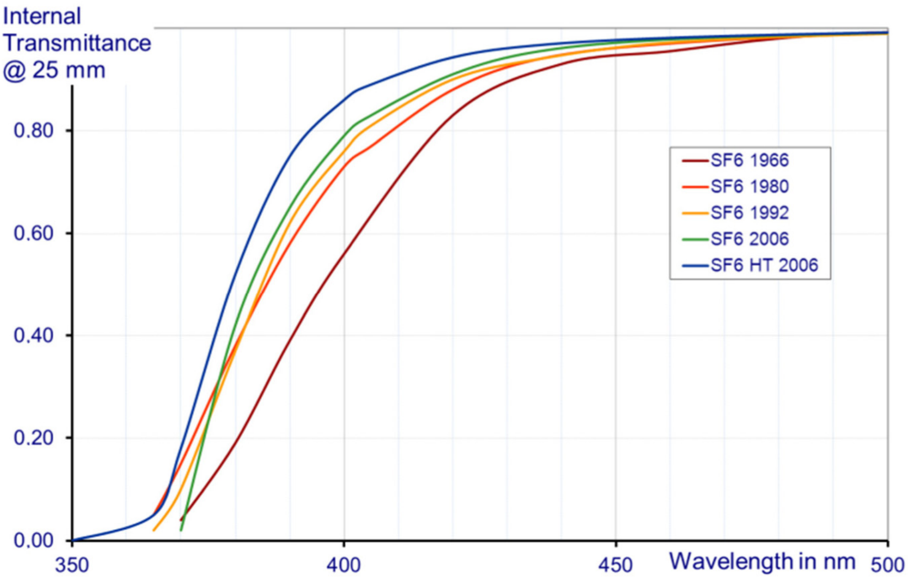

Figure 5.11 Historical development of the slope of the UV edge of the glass type SF6 showing the significant improvement in internal transmittance achieved between 1966 and 2006. Old binoculars with yellowish images do not suffer from solarization but from the lower transmittance quality of the past.

5.6 Fluorescence

By far, the highest share of light that is absorbed in glass will be converted to heat. A small fraction, however, may be re-emitted as light, leading to a glowing effect, which is called luminescence. If the light appears and vanishes almost instantaneously after starting or shutting off glass illumination, it is called fluorescence. A long-lasting afterglow is called phosphorescence. Because the intensity of phosphorescence is very low, if existent at all, it can be neglected.

Fluorescence of optical glass lenses can be disturbing in microscope applications, where fluorescence is excited in the objects to be observed and the glasses' background light reduces contrast. The usual method for measuring fluorescence intensity is observing the emitted light spectrum under excitation with the 365-nm spectral line of mercury.[1,2] The intensity integrated over the observed spectrum for a given sample will be related to that of a reference sample of the optical glass SF1. Figure 5.12 shows spectral emission intensity for different glass types excited at the 365-nm wavelength.

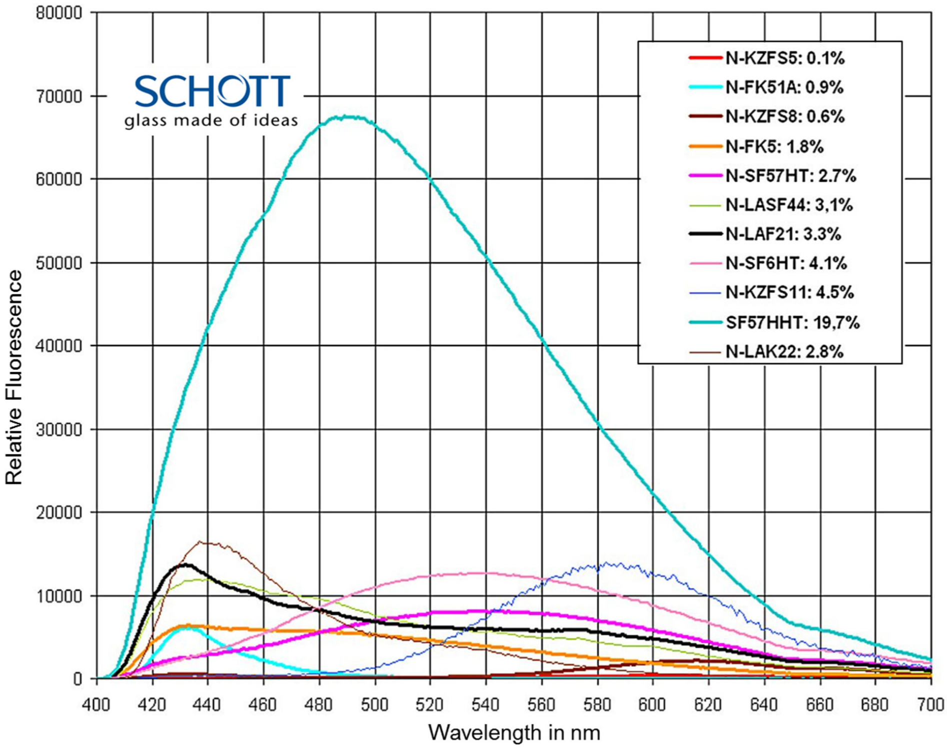

Figure 5.12 Fluorescence of optical glasses excited with 365-nm light (integral fluorescence is relative to standard glass type SF1).

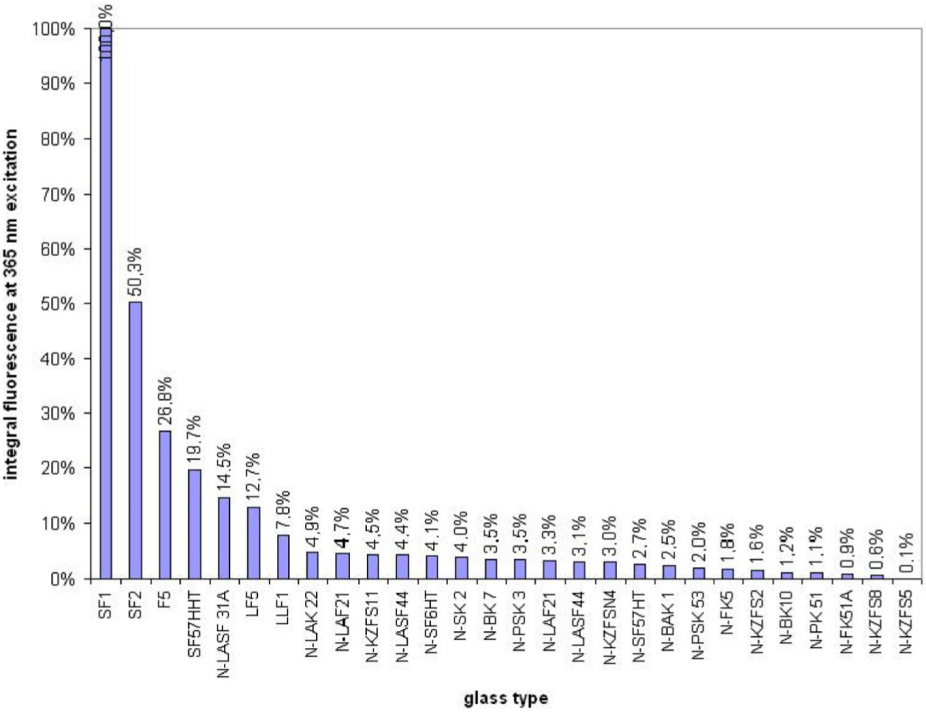

Figure 5.13 Fluorescence intensity of optical glasses excited with 365-nm light. The glass types above 5% fluorescence are almost exclusively lead-containing glasses.

The intensity of fluorescence depends on the presence and number of ions in the glass that are capable of emitting light. Almost all such ions are residual impurities of raw materials, with the exception of lead, which is a constitutive component in classical flint glasses. Lead ions absorb near-UV light and re-emit in the blue range. Hence, lead-containing optical glasses have higher fluorescence. Almost all glass types to the left of N-LAK22 in Fig. 5.13 contain lead (with the exception of N-LASF31A).

Excitation at longer wavelengths (e.g., 532 nm) as used, for example, in bio-analytic investigations, leads to much lower fluorescence. Generally, all glasses absorb much less at longer wavelengths. Since the atomic energy levels involved are different in this energy range from those in the range around 365 nm, there is no correlation to fluorescence with 365-nm excitation.

5.7 Solarization

If light absorbed in glass exceeds the energy level where it is capable of releasing electrons from atomic bonds, an absorbed photon will create an electron–hole pair. In most cases, such pairs will recombine in a short timeframe, converting their energy to heat or luminescence. Some pairs, however, may have their two parts separated sufficiently far from each other that a free electron and a hole will remain for a longer time and act as absorption centers. This effect is called solarization since it is observed as a yellow coloration with glass pieces exposed to the sun for long periods. Due to thermal movement of the electrons, electron–hole pairs will recombine as time passes. Thus, solarization reduces with time by itself. Elevated temperature strongly mobilizes the electrons and dramatically shortens this healing effect.

Optical glasses can be stabilized against solarization to a high degree using an absorbing ion such as titanium. Figure 5.14 shows transmission curves of a titanium-free test melt. The UV absorption edge of the nonirradiated sample lies furthermost in the short-wavelength range. However, it shows strong transmission loss even in the VIS range after 15 hours of strong irradiation with a HOK-4 lamp. The stabilized sample of N-BK7 from normal production has a UV edge closer to the VIS. However, it hardly reacts to the same amount of irradiation.

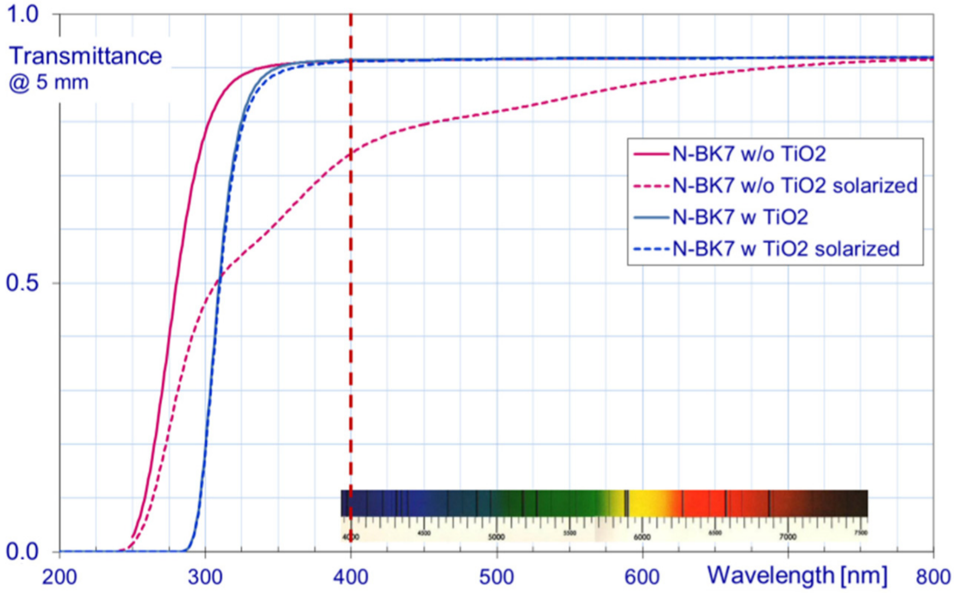

Figure 5.14 Solarization of N-BK7 with and without titanium oxide irradiated with the same amount of UV light.

5.8 Ionizing-Irradiation-Induced Transmittance Loss: Radiation Damage

In principle, transmittance losses due to ionizing irradiation are similar to those of solarization. The main effect is that such irradiation is capable of releasing electrons from their bound states in the glass matrix. Ionizing irradiation may be high-energy particles such as electrons and protons as found in the Van Allen radiation belt around the earth. Satellite optics must withstand such influences. High-energy gamma rays in nuclear power plants or research institutions may be the source of irradiation loads on optical glasses. Even though primary processes are quite different, any of these radiation types will result in creation of electron–hole pairs, with the number of pairs depending on the energy deposited in the glass. Just as with solarization, the free electrons and stationary holes will act as absorption centers; however, the effect of irradiation will be much stronger than that of solarization due to the much higher energy being converted to a very large number of electron–hole pairs.

The strong effect of gamma rays coming from the radioactive decay of cobalt 60 can be seen in Fig. 5.15. Cobalt 60 emits gamma photons of around 1.3 MeV, which is 300,000 times higher than the energy of photons causing solarization and is somewhat higher than 3 eV. Irradiation of normal BK7 glass with 100 Gy (Gray is the deposited energy dose of 1 J per kg of material) already leads to strong reduction of internal transmittance.

Doping optical glasses with cerium oxide, however, improves radiation resistance to a very large extent. Cerium-doped glass types can be recognized by the letter G attached to their name together with a two-digit number. The denomination G18 in the glass type BK7G18 stands for 1.8 weight % of cerium oxide CeO_2. The stabilization effect is very significant (see Fig. 5.15). BK7G18 maintains its internal transmittance almost completely, even with an 80,000 times higher dose than the dose that previously led to the strong reduction. One drawback to this doping is that the UV edge is shifted toward VIS light from the very beginning.

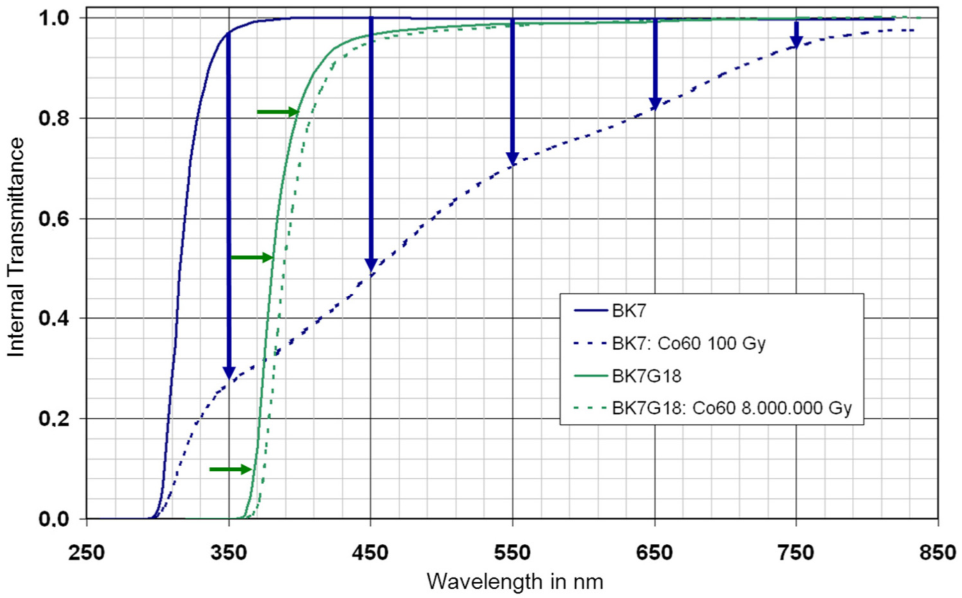

Figure 5.15 Solarization of N-BK7 with and without titanium oxide irradiated with the same amount of UV light.

Stabilization with cerium oxide can be done with most if not all optical glass types (see Fig. 5.16). However, due to low demand, it is not economic to offer all glass types with a stabilized variant. Traditionally, a selection of glass types has proven to be sufficient. The different glass types have different cerium oxide content. Each glass type is optimized between high stabilization and low initial transmittance reduction due to cerium coloring.

The glass types BK7G18, LF5G15, LF5G19, and SF6G05 are also used for radiation-shielding windows. Therefore, they have a higher probability of being available "off the shelf" than inquiry glass types, whose availability is not assured. All glass types are arsenic free. The flint glasses are classical flint glasses, which means that they contain lead. As a rule, it is recommended to use stabilized glass types when the expected final dose exceeds 10 Gy or the dose rate exceeds 0.05 Gy/h.

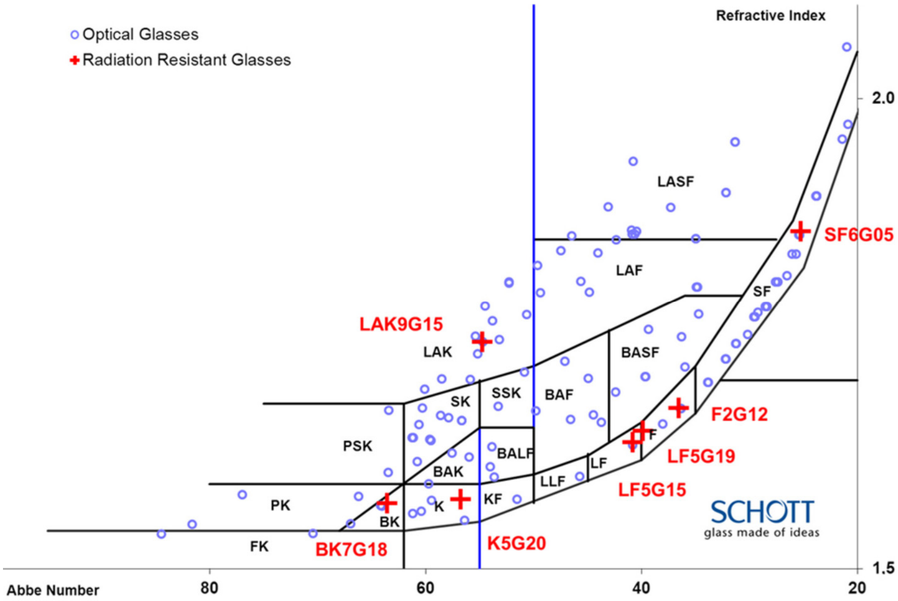

Figure 5.16 SCHOTT program of ionizing-irradiation-stabilized optical glass types enabling color-corrected optical systems for use in radioactive environments.

5.9 Use of Optical Glass in the UV and IR Wavelength Ranges

Figure 5.17 shows the transmittance curves of some selected glass types from the UV edge up to 2325 nm, as quoted in their data sheets. In the UV range, the low-dispersion crown glasses allow for use down to about 300 nm. A prominent application was in i-line wafer steppers, which were the microlithography work horses in the 1990s, operating at 365 nm. In UV applications, care must be taken due to the solarization effect described in the previous section. High-index glass types, especially the lead-free versions, cannot be applied very far below 400 nm.

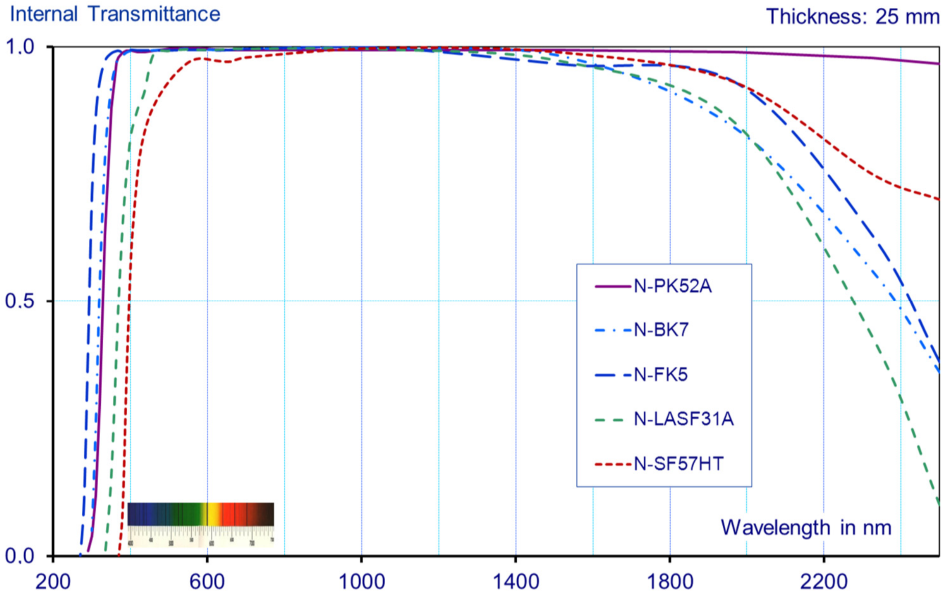

Figure 5.17 Transmittance curves for some glass types from 200 to 2325 nm.

In the NIR, optical glasses maintain high transmittance up to 1800 nm. For most glass types, transmittance falls rapidly when moving to longer wavelengths, eventually becoming opaque at 2400 nm and beyond. However, this does not hold for all glass types. The high fluorine content, low-index, lowest-dispersion glass types such as N-PK52A do not show this transmission drop. This is due to a self-drying effect that occurs during melting, when part of the raw materials' fluorine content evaporates from the melt, taking along the residual water that is the cause of the absorption between 2300 and 2700 nm. The extensive absence of this absorption band can be seen clearly in Fig. 5.17, where the transmittance curve of N-PK52A shows only slight reduction above 1800 nm. Hence, this glass type is one with a very broad application wavelength range, from 320 nm to 4 µm.

References

1. A. Engel, H.-J. Becker, O. Sohr, R. Haspel, and V. Rupertus, "Advanced industrial fluorescence metrology used for qualification of high quality optical materials," *Proc. SPIE* **5188**, 182–189 (2003) [doi: 10.1117/12.506814].
2. A. Engel, R. Haspel, and V. Rupertus, "Fluorescence metrology used for analysis of high quality optical materials," *Proc. SPIE* **5457**, 65–73 (2004) [doi: 10.1117/12.547448].

Chapter 6
Chemical Resistance

6.1. General Remarks on Chemical Resistance of Optical Glasses

The chemical compositions of optical glasses are optimized with highest priority for achieving best dispersion properties. From color-correction aspects, highly desirable glass types are located at the edges of the Abbe diagram glass island and can be produced only with sophisticated melting techniques from unique compositions. In such cases, dispersion properties prevail against all other properties such as thermal expansion, hardness, or chemical resistance.

Glass types for precise pressing must behave in a neutral manner against pressing tool materials and hence are tested and adapted accordingly. If possible, the compositions of optical glasses will be adjusted for better workability. The degrees of freedom for such adaptation, however, are restricted.

Chemical resistance is not a single, well-defined, unambiguous quantity. There is a large manifold of possible environments acting on glass during its processing. Grinding and polishing agents, environmental humidity, and even different quality grades of processing water may lead to different reactions of the glass items.

Glasses with larger contents of sparingly soluble components, such as silicon dioxide (SiO_2), aluminum oxide (Al_2O_3), titanium oxide (TiO_2), or rare-earth oxides, are more resistant to leaching by aqueous and acidic solutions. However, if glasses contain large quantities of more readily soluble substances, such as alkali and possibly also alkaline earth oxides, and relatively readily soluble network formers such as boron and phosphorous oxide, stronger reactions need to be expected. These substances may be sufficient for layer formation or removal of the glass surface.

For a finished optical element, chemical behavior is less important, since, as a rule, the element will be coated and mounted in an objective where it will no longer have contact with environmental media.

6.2 Chemical Resistance: Measurement and Classification

It is not possible to provide data on the chemical resistance for the large variety of processes being used in practice. For orientation, a set of characteristics has been defined by standardized determination methods and classification schemes covering the following processes:

- acid with water in abundance according to the international standard ISO 8424;
- lye with water in abundance according to ISO 10629;

and the following common glass-handling conditions:

- climate resistance for storage in air;
- stain resistance, referring to fingerprints equivalent to attack with water shortfall; and
- phosphate resistance, representing cleaning processes according to ISO 9689.

All methods except climate resistance determine the time required to dissolve 0.1 μm of the glass surface exposed to well-defined liquids. For climate resistance, glass is exposed to 30 hours of temperature cycling in a water-saturated atmosphere. Every hour water condenses on the glass and will be dried off again.

Different intervals of transmission haze change are used for classification. The classification schemes use numbers, with the lowest number indicating highest resistivity.

For sensitive glass types, a code is added describing the appearance of visible surface changes. If more-stable glasses show observable effects, this is also denoted using the code, as given in Table 6.1.

Table 6.1 Chemical resistance code for appearance of surfaces after chemical attack according to the different test methods as used in optical glass data sheets.

0	No visible changes
1	Clear, but with irregular surface (wavy, pockmarked, pitted)
2	Staining and/or interference colors (slight selective leaching)
3	Tenacious, thin, whitish layer (stronger selective leaching, a cloudy/hazy/dullish surface)
4	Loosely adhering thick layer, such as insoluble, friable surface deposit (may be a cracked and/or peelable surface, surface crust, or cracked surface; strong attack)

6.3 Chemical Resistance of the Optical Glass Types: Overview Diagrams

Figure 6.1 shows optical glass types ranked according to their resistance to alkali attack. Most glass types have a high resistance; only few are sensitive. The acid-resistance diagram in Fig. 6.2 shows less-resistant glass types concentrating at the low-dispersion edge. As with alkali resistance, the lead-free flint glass types are much more resistant than the classical lead-containing types. This cannot be seen clearly due to their mostly overlapping positions.

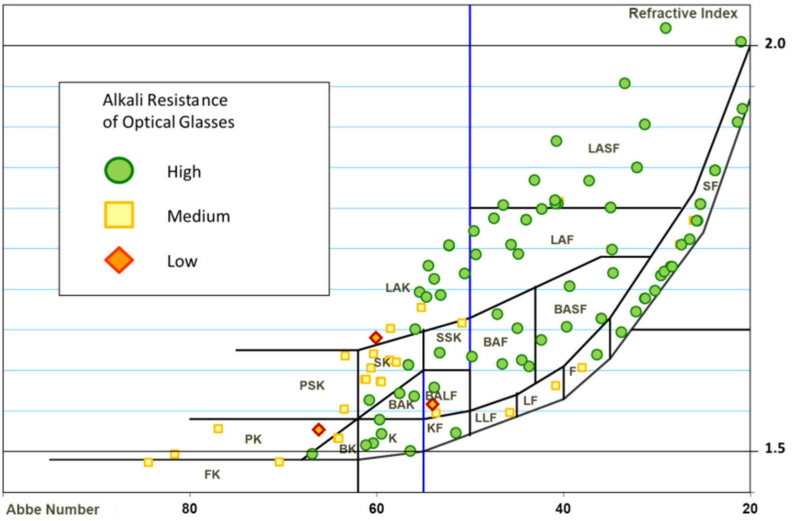

Figure 6.1 Abbe diagram with glass types categorized according to their alkali resistance.

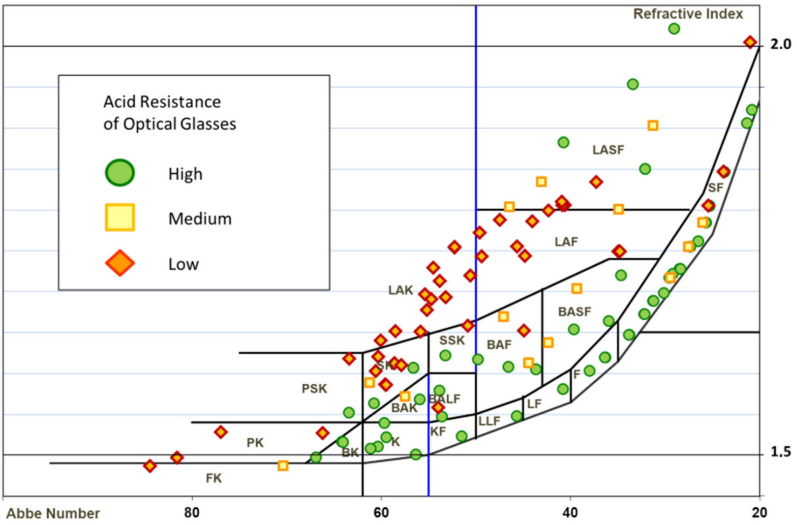

Figure 6.2 Abbe diagram with glass types categorized according to their acid resistance.

Lower phosphate resistance is found primarily at the edges of the glass island, where many glass types lie that are well suited for color correction (Fig. 6.3). Again, the classical flint glasses are more sensitive than the lead-free flints.

Medium- and low-climate-resistant glass types are found mainly at the low-dispersion edge of the medium refractive index range (Fig. 6.4). Polished elements of very climate-sensitive glass types should be stored in dry conditions or immediately coated.

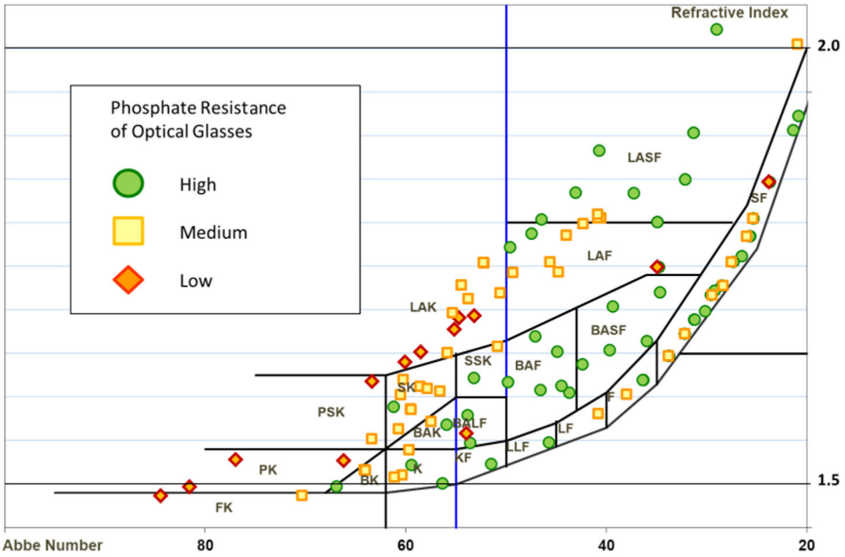

Figure 6.3 Abbe diagram with glass types categorized according to their phosphate resistance.

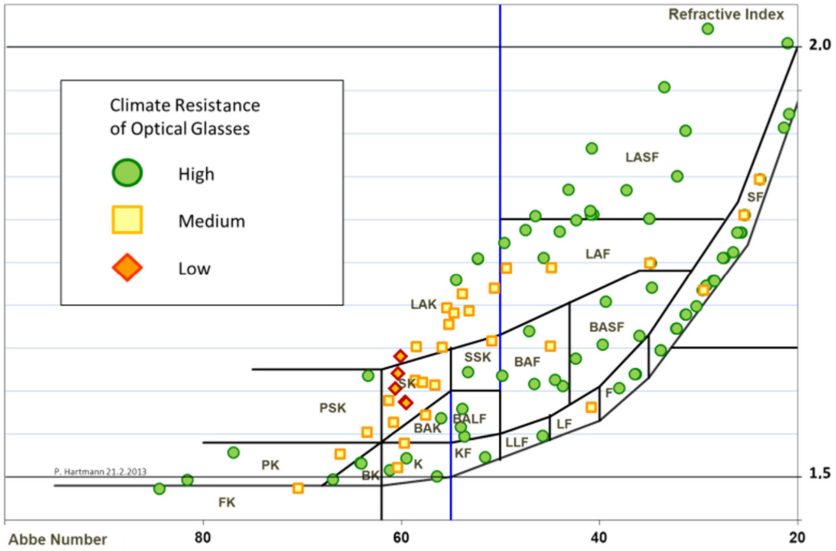

Figure 6.4 Abbe diagram with glass types categorized according to their climate resistance.

Most glass types are highly stain resistant (Fig. 6.5).

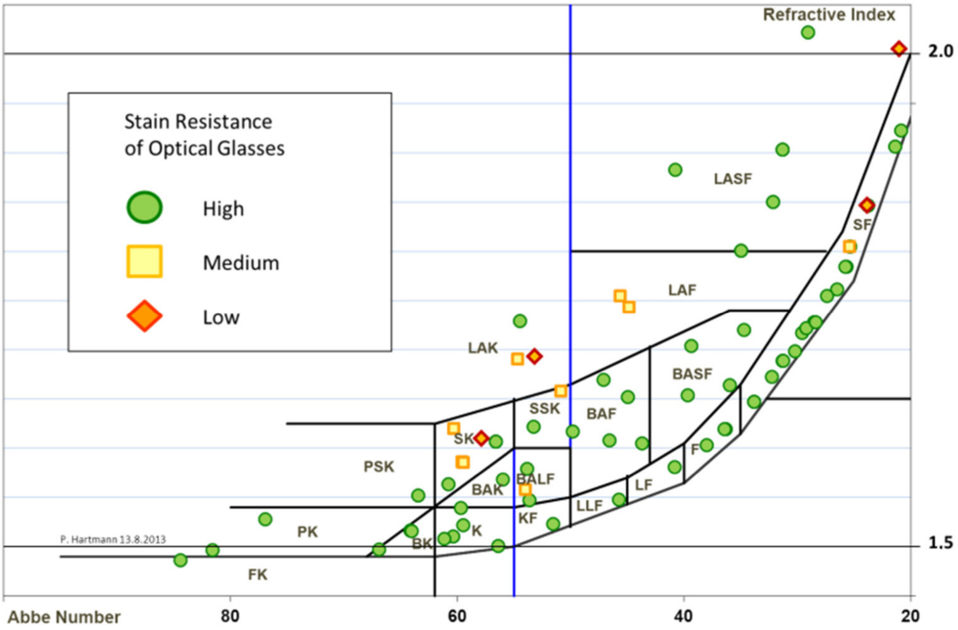

Figure 6.5 Abbe diagram with glass types categorized according to their stain resistance.

Chapter 7
Mechanical Properties

7.1 Density

The density of optical glass lies between 2.4 g/cm^3 and 6.2 g/cm^3. It is measured using a buoyancy force method with uncertainty better than 0.001 g/cm^3. Low-index crown glasses have lowest density. With increasing refractive index, density rises considerably (Fig. 7.1).

The replacement of classical glass types by lead- and arsenic-free glasses has led to lower density. The reduction effect increases with the lead content of the predecessor glass types and hence with its refractive index. The density reduction may amount up to 36% as with N-SF57 (3.53 g/cm^3) and SF57 (5.510 g/cm^3). Table 7.1 gives density values for selected classical glass types and their successor glass types. Low-index crown glasses show no effect since they were already lead free.

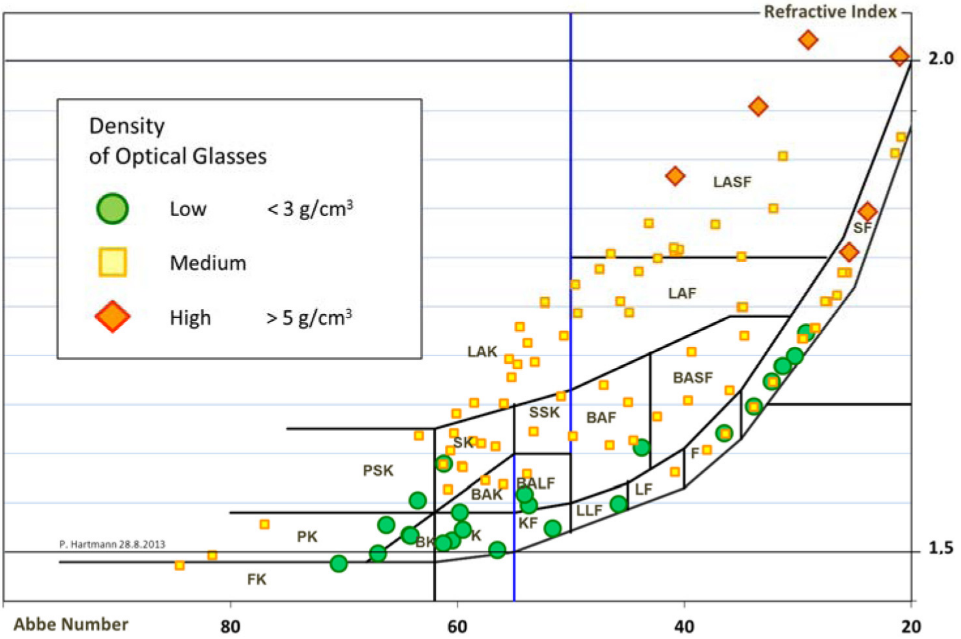

Figure 7.1 Abbe diagram with glass types categorized according to their density.

Table 7.1 Density values for selected classical glass types and their successor glass types.

Glass type	n_d	ν_d	ρ [g/cm^3]
FK5	1.48749	70.41	2.45
N-FK5	1.48749	70.41	2.45
BK7	1.51680	64.17	2.51
N-BK7	1.51680	64.17	2.51
SK15	1.62299	58.06	3.64
N-SK15	1.62296	58.02	3.62
KF9	1.52341	51.49	2.71
N-KF9	1.52346	51.54	2.50
F2	1.62004	36.37	3.60
N-F2	1.62005	36.43	2.65
LAFN7	1.74950	34.95	4.38
N-LAF7	1.74950	34.82	3.73
SF6	1.80518	25.43	5.18
N-SF6	1.80518	25.36	3.37
SF57	1.84666	23.83	5.51
N-SF57	1.84666	23.78	3.53

7.2 Elasticity: Young's Modulus

Below their transformation temperature, glasses behave almost perfectly brittle-elastic, following Hooke's law. The relative elongation $\Delta l/l$ is proportional to the applied stress σ with Young's modulus E as a proportionality constant:

$$\frac{\Delta l}{l} = \frac{\sigma}{E}. \tag{7.1}$$

The lowest values around 50 GPa (giga-Pascals) are found with the classical flint glasses, highest above 120 GPa for lanthanum glasses (Fig. 7.2).

Young's modulus E, torsion modulus G, and Poisson's ratio μ are measured by determining the mechanical resonance frequencies of glass samples. Precisely dimensionally measured and weighed samples are excited to vibration using piezoelectric or electromagnetic systems that are controlled with a precision frequency generator. The sample's vibrations are received and amplified. By scanning the vibration frequency, the resonance frequencies of transversal and torsional vibrations are determined. Measurement uncertainty is better than 1%.

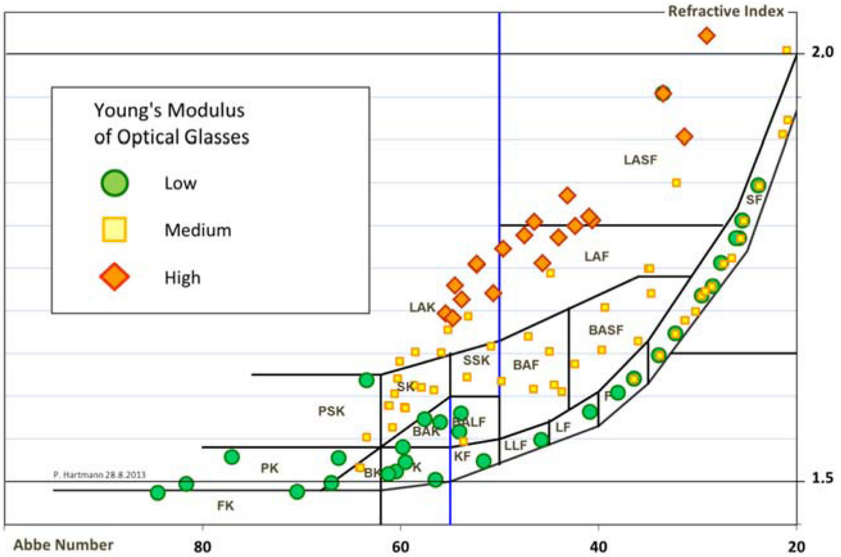

Figure 7.2 Abbe diagram with glass types categorized according to their Young's modulus.

7.3 Knoop Hardness

Knoop hardness is determined according to the international standard ISO 9385. This method evaluates the remaining glass surface change after indentation of a test diamond with a force of 0.9807 Newton applied for 20 sec.

Knoop hardness (HK) is calculated from applied force and the projected area of the microscopic-scale permanent indentation (Fig. 7.3). With the special angles prescribed for the indention diamond, one obtains the formula

$$HK = 14.229 \cdot \frac{0.102F}{d^2}, \tag{7.2}$$

where F is the test force in Newton, and d is the length of the long indentation diagonal in millimeters. The data are denominated with HK 0.1/20, where "0.1" stands for the force given in the obsolete unit kilopond kp (0.1 kp = 0.9807 N).

HK values for optical glasses span from 335 to 810, as shown in Table 7.2. Figure 7.4 ranks optical glass types according to their Knoop hardness. The hardness is a function of the magnitude of the test force and decreases with increasing test force. The data sheet Knoop hardness values before 1992 were lower. This was not because the glasses were softer but because the old determination method generally led to lower numbers.

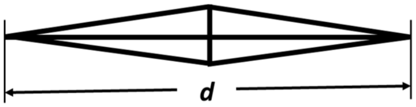

Figure 7.3 Permanent indentation in glass sample.

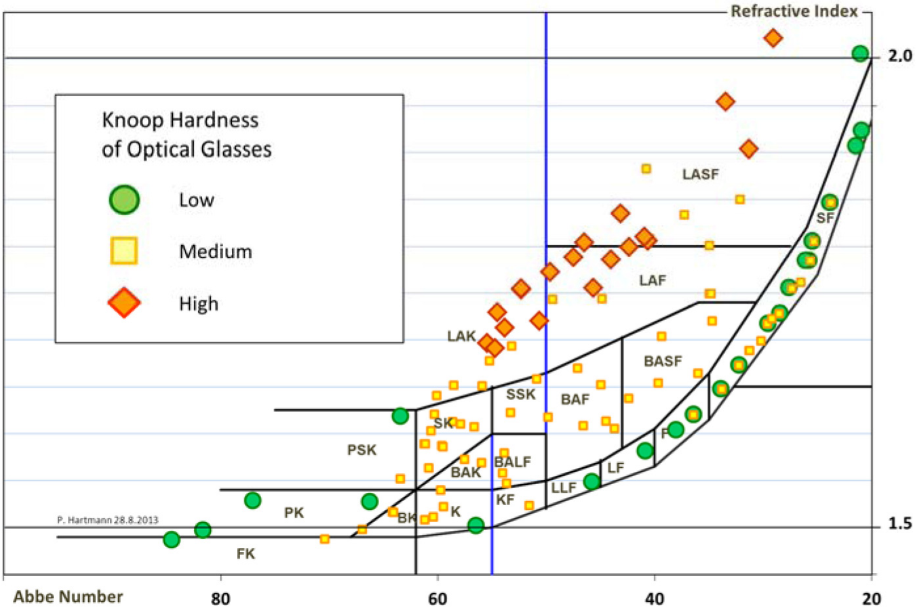

Figure 7.4 Abbe diagram with glass types categorized according to their Knoop hardness.

Table 7.2 Knoop hardness values for selected classical and lead/arsenic-free glass types.

Glass Type	HK	Glass Type	HK	Glass Type	HK
N-FK51A	345	N-KZFS2	490	N-LASF46A	666
SF57	350	N-LAF7	530	N-LAK34	740
SF6	370	N-SSK8	570	N-LASF44	770
N-PK51	415	N-BK7	610	LASF35	810

7.4 Grindability

Grindability was introduced for providing a ranking of glass types with respect to their behavior while being ground. The expression abrasive hardness is deliberately avoided because the removal of glass in a grinding process is not necessarily influenced by hardness as defined, for example, by Knoop hardness. Grinding efficiency can also be reduced by abraded glass dust smearing the grinding tool, as is the case with classical flint glasses.

The determination method for grindability is provided in the standard ISO 12844. The grindability classes are abbreviated by HG. Twenty samples of the glass to be classified are ground for 30 sec in a standardized diamond pellet tool under predetermined conditions. The removed averaged volume of the samples is compared with that of a reference glass, N-SK16 (Table 7.3). According to this scheme, the removal in the lower classes is less, and in the higher classes, is more than in the reference glass N-SK16. The grindability map of Fig. 7.5 ranks glass types according to HG classes 1 and 2, classes 3 and 4, and classes 5 and 6.

Table 7.3 Grindability grades according to ISO 12844.

Grindability class	Grindability limit values in percentage of the reference glass N-SK16
HG 1	≤30
HG 2	>30 and ≤60
HG 3	>60 and ≤90
HG 4	>90 and ≤120
HG 5	>120 and ≤ 150
HG 6	>150

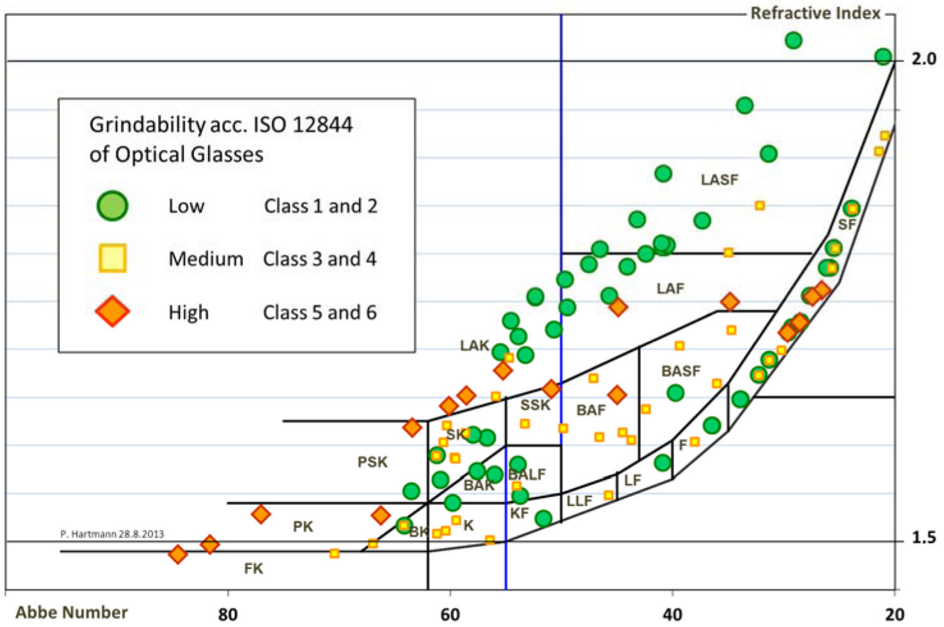

Figure 7.5 Abbe diagram with glass types categorized according to their grindability.

7.5 Bending Strength

The strength of glass as evaluated from its atomic structure is very high. It lies within the range of several giga-Pascals (GPa). In daily practice, this high strength is reduced by about three orders of magnitude due to micro-cracks in glass items' surfaces. Tensile forces opening micro-cracks will be directly effective because there is no ductility that can counteract such forces. Therefore, the decisive influence on the strength of glass is the number and depth of micro-cracks in its surface. Under long-lasting tensile stress loads, glass will fatigue due to is micro-crack growth. Fatigue depends on the effective tensile stress and the initial crack depth. Below a determined threshold value, cracks will not grow at all. Above the threshold value, crack growth velocity rises exponentially with increasing stress. Environmental factors also influence crack growth velocity, and water especially enhances fatigue. Optimum conditions are a dry environment or vacuum.

Generally, in practice, the strength of glass is not primarily a material property such as, e.g., Young's modulus. For evaluation of a tensile load, application case information is needed on:

- surface condition (ground or lapped with defined grain size distribution, or polished or etched—both being best conditions);
- possible presence of micro-cracks from preceding grinding processes (should have been removed);
- tensile stress: spatial distribution, height, and duration; and
- environment (vacuum, dry, or humid).

Optical glasses are weaker than soda lime glass by a scale of 10 to 20% (low-index borosilicate crown glasses) to approximately 60% (extreme fluorophosphate or high-lead-content glasses). This statement is based on evaluations of the same surface preparation lapped with fine-grain SiC-600. With typical applications for optical elements in imaging systems, optical glasses will have no breakage problems. Strength considerations may become necessary when high temperature gradients introduce high thermal stresses, e.g., near strong lamps. For considerably thick glass items, this may be of concern at lower heat loads.

Measurement of strength is done using a set of tile or disk samples carefully prepared with the surface condition to be investigated (see Fig. 7.6). As a final step, a layer of sufficient thickness to include all of the remainder from the preceding grinding steps is removed. A set of samples is loaded with growing forces until they break and are usually evaluated with a Weibull distribution.

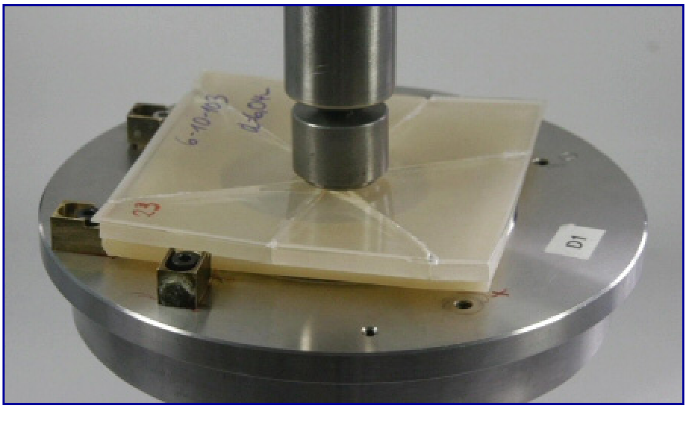

Figure 7.6 Strength test setup with ring-on-ring configuration. The sample (here a glass ceramic sample) rests on a support ring of 90-mm diameter and is loaded in its center with a 18-mm ring with a linearly growing force until its breaks.

For material comparison, the 63% quantile (Weibull characteristic strength) can be used. This is only possible if the same surface preparation has been consistently applied. For strength design of higher-stress-load structures, it is recommended to investigate the surface condition existent in application in more detail and with adequate statistical significance. Such applications, however, are very rare with optical glasses.

7.6 Mechanical Properties of Selected Optical Glass Types

Table 7.4 lists values of the presented mechanical properties for some selected glass types. More data are given in the optical glass data sheets or in a computer readable format in download files provided at glass suppliers' websites. Before usage and comparison, it is recommended to check whether the same definitions have been used as those described in the preceding chapters.

Table 7.4 Mechanical properties of selected optical glasses.

Glass Type	Density in g/cm^3	HK 0.1/20	HG	Young's Modulus in GPa
N-BK7	2.510	610	3	82
N-FK51A	3.675	345	6	73
N-KZFS4	3.002	520	3	78
N-LAF34	4.240	770	2	123
N-LAK10	3.689	780	2	116
N-LASF35	5.410	810	1	132
P-SK57	3.012	535	3	93
F2	3.599	420	2	57
N-F2	2.651	600	2	82
SF57	5.510	350	1	54
N-SF57	3.533	520	4	96

Chapter 8

Thermal Properties

8.1 Viscosity

While cooling down from melting temperatures, the viscosity of glass rises continuously. Cooling down from the liquid state, it is still soft enough to be shaped into the desired forms. Then, viscosity becomes so high that glass items maintain their shape without deformation under their own weight and, in the end, become stiff and brittle. In order to characterize viscosity in a manner suitable for different working processes, some characteristic points have been introduced, such as the following:

- working point: 10^4 dPas (the lower limit for manual glass shaping);
- softening point: $10^{7.6}$ dPas (where a glass fathom starts to lengthen under its own weight);
- annealing point: $10^{13.2}$ dPas (where stresses relax completely within 15 min); and
- strain point: $10^{14.5}$ dPas (where stresses relax within 4 hours).

The unit choice of dPas (deci-Pascal seconds) is slightly unusual. It was chosen in order to result in the same numbers as the obsolete viscosity unit poise.

Glass types differ strongly in viscosity. Characteristic viscosity points lie at considerably different temperatures, and the widths of the temperature differences between such points vary widely among the glass types. With the so-called long glass types, with wide temperature differences between the characteristic viscosity points, temperature does not need to be very precisely controlled while shaping the glass. This is quite opposite for the short glass types. Figure 8.1 shows viscosity curves of the long glass type F2 and of the two short glass types N-FK51A and N-LAF7, which lie at considerably different temperatures. N-BAK4 is an intermediate glass type from the viscosity point of view.

Reheat pressing is done in the viscosity range of 10^4–$10^{7.6}$ dPas, and precise molding in the range above $10^{7.6}$ dPas. At $10^{13.2}$ dPas, internal stress relaxes within 15 min. Above $10^{14.5}$ dPas, glass is solid and brittle.

8.2 Thermal Expansion

The coefficient of thermal expansion α of optical glasses rises almost linearly from room temperature to the transformation range, where glass becomes plastically deformable (Fig. 8.2). Above this range, α rises again almost linearly but with higher slope until deformation occurs. Data sheets contain two α values:

$\alpha_{-30/+70\,°C}$, relevant for room-temperature application and $\alpha_{+20/+300\,°C}$, relevant for higher heat loading. The range of $\alpha_{-30/+70\,°C}$ for optical glasses extends from about 4.5×10^{-6}/K (N-ZK7, N-KZFS2) to more than 12×10^{-6}/K (N-FK51A, N-PK51, N-PK52A, P-PK53). Optical glasses are ranked according to their coefficient of thermal expansion (Fig. 8.3).

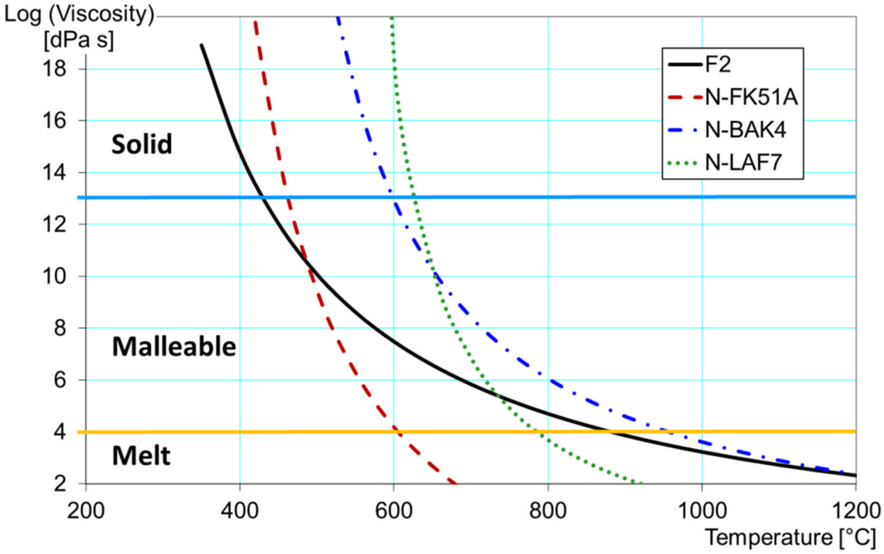

Figure 8.1 Temperature dependence of the viscosity of optical glasses.

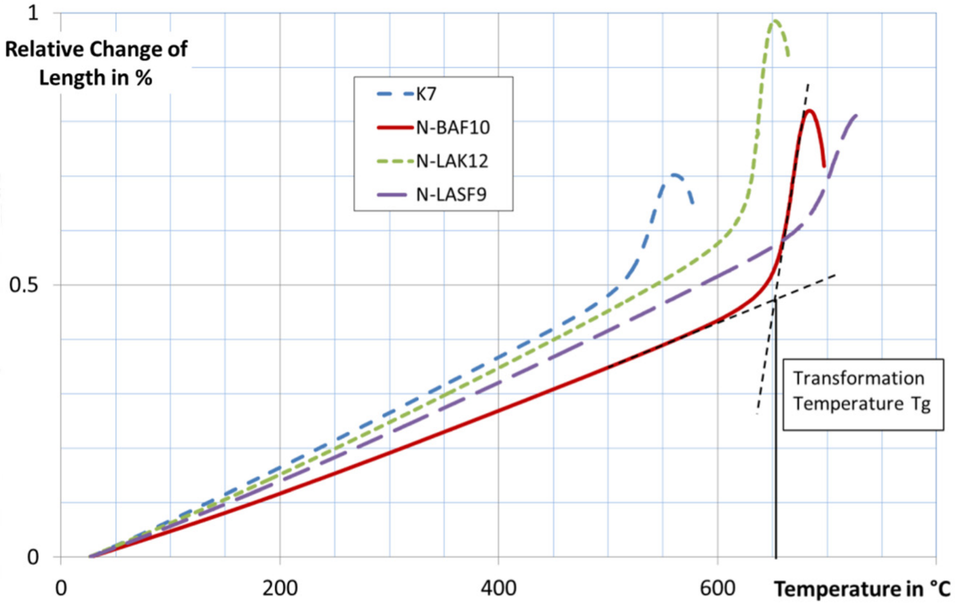

Figure 8.2 Relative change of length with temperature of some optical glasses.

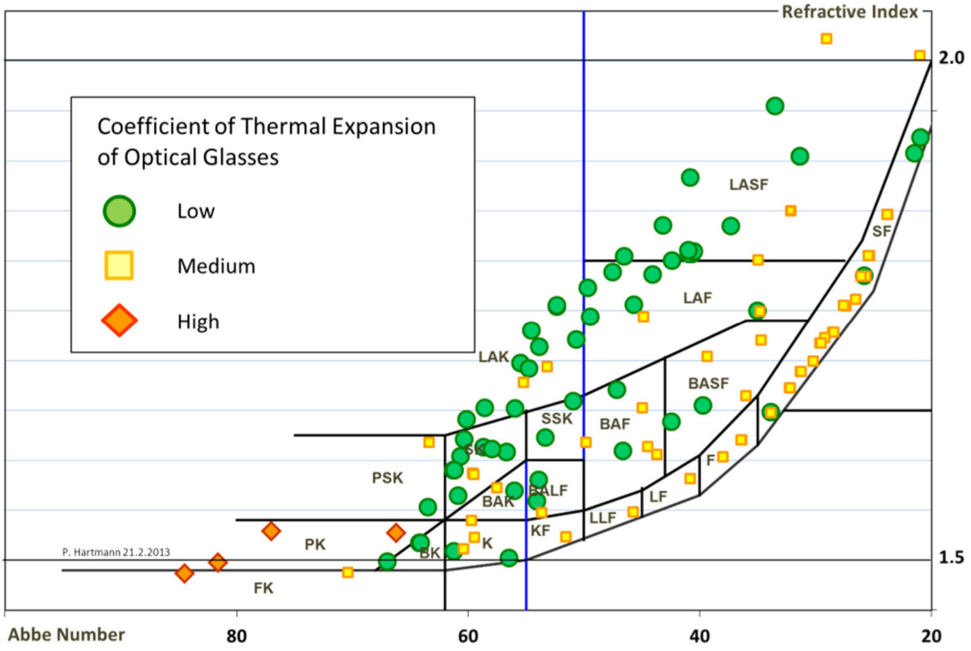

Figure 8.3 Abbe diagram with glass types categorized according to their coefficient of thermal expansion $\alpha_{-30/+70\ °\mathrm{C}}$.

8.3 Transformation Temperature

The transformation temperature T_g is used for marking the temperature range in which glass changes from a highly viscous state to a solid state. In principle, it would be better to use a characteristic viscosity point. However, transformation temperature can be measured more easily than viscosity. T_g is determined according to ISO 7884-8 from the thermal expansion curve obtained from 100-mm glass samples measured with a dilatometer setup. T_g is defined as the temperature where the two extrapolated linear expansion lines meet, as indicated in Fig. 8.2 with the example of N-BAF10. As already explained in Section 2.2 on annealing, the relative length change of glasses depends on the cooling rate. This also holds for the transformation temperature. For this reason, ISO 7884-8 prescribes a pretreatment of samples for the determination of the transformation temperature with a fine annealing using the annealing rate of 2 K/h. Figure 8.4 shows glass types categorized according to their transformation temperature.

As a rule, the transformation temperature lies very close to the annealing point at $10^{13.2}$ dPas, where internal stress in a glass item relaxes within about 15 min. If glass parts need to be tempered due to the requirement of maintaining the refractive index, it is recommended to stay about 200 °C below T_g.

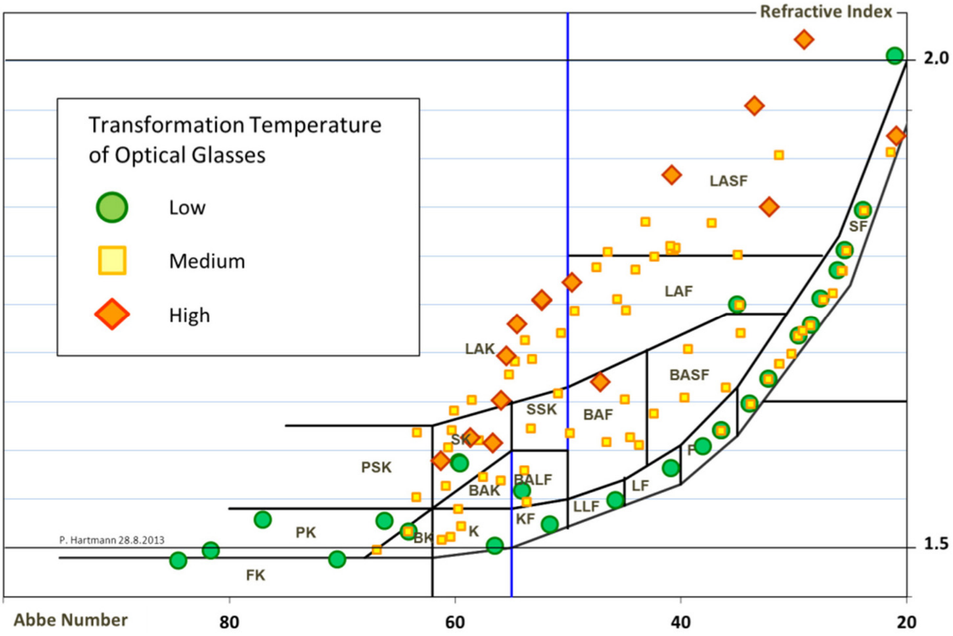

Figure 8.4 Abbe diagram with glass types categorized according to their transformation temperature T_g.

8.4 Thermal Conductivity and Heat Capacity

Glass is a very low-thermal-conducting material. Its heat capacity is similar to that of other common materials, as shown in Table 8.1.

Table 8.1 Thermal conductivity of selected materials.

	Thermal conductivity [W/(m·K)]	Heat capacity [J/(g·K)]
Steel	30–60	0.50
Copper	395	0.38
Borosilicate crown glass N-BK7	1.1	0.86
Dense lead flint glass SF57	0.62	0.36
Common optical glasses	0.9–1.2	0.30–0.89
Low-expansion glass ceramic ZERODUR®	1.46	0.80

Its very low thermal conductivity has many consequences for the production of optical glasses since important properties are determined by the temperature history of the various glass parts. All tempering processes necessarily introduce temperature differences between inner and outer parts of the glass volume. The low thermal conductivity leads to high temperature differences being proportional to the temperature change rate and to the thickness squared. The square law is strictly valid only for an infinite plate with constant thickness. However, considering practical, finite-volume pieces, thermal gradients will depend on thickness with a higher exponent than linear change. This restricts, for example, the thickness of strip glass for crystallization-sensitive glasses. Even chilling glass strips directly after casting will leave enough time for the inner part to crystallize if thickness is high enough to cause high temperature differences.

Another consequence of low thermal conductivity is that precise moldings that are widely used for consumer optics lenses cannot be made thicker than about 4 mm. Otherwise, they will develop stress birefringence and optical inhomogeneity with the short cooling times they need in order to be economic.

8.5 Thermally Induced Stress

Optical glass items exposed to heat loads or rapid temperature changes will develop temperature gradients within their volume, resulting in thermally induced stress. This leads to birefringence and ultimately can cause breakage. Actual stress fields depend on the size and shape of the glass item. For simple geometries, formulas are available in textbooks. Most of these formulae contain a material-dependent term that reads as

$$\varphi = \frac{\alpha E}{1 - \mu}, \tag{8.1}$$

where φ is stress, α is the coefficient of thermal expansion, E is Young's modulus, and μ is Poisson's ratio. This material-specific thermal stress factor varies by a factor of almost three (see Table 8.2). For glass types with a high thermal stress factor, thermal shocks should be avoided since they may develop cracks or ultimately might be broken. Figure 8.5 ranks glass types with respect to their sensitivity to thermal stress calculated from the formula for the thermal stress factor.

8.6 Thermal Properties of Selected Glass Types

Table 8.2 lists values of the presented thermal properties for some selected glass types. More data are given in the optical glass data sheets or in computer-readable format in downloadable files provided at glass suppliers' websites. Before usage and comparison, it is recommended to check if the same definitions have been used as those described in the preceding chapters.

Table 8.2 Thermal properties of selected optical glasses. The thermal stress factor is calculated on the basis of $\alpha_{20/300\ ^\circ\mathrm{C}}$ data since this property is of greater interest at elevated temperatures.

Glass type	$\alpha_{-30/+70\ ^\circ\mathrm{C}}$ in K^{-1}	T_g in °C	$T_{10^{7.6}}$ in °C	Thermal stress factor φ in MPa/K	c_p in J/(g·K)	λ in W/(m·K)
N-BK7	7.1	557	719	0.86	0.86	1.11
N-FK51A	12.7	464	527	1.55	0.69	0.76
N-KZFS4	7.3	536	664	0.84	0.76	0.84
N-LAF34	5.8	668	745	1.22	0.80	0.56
N-LAK10	5.7	636	714	1.11	0.64	0.86
LASF35	7.4	774	n.a.	1.61	0.45	0.92
P-SK57	7.2	493	593	1.10	0.76	1.01
F2	8.2	434	594	0.67	0.56	0.78
N-F2	7.1	557	719	0.86	0.86	1.11
SF57	8.3	414	519	0.66	0.36	0.62
N-SF57	8.5	629	716	1.28	0.66	0.99

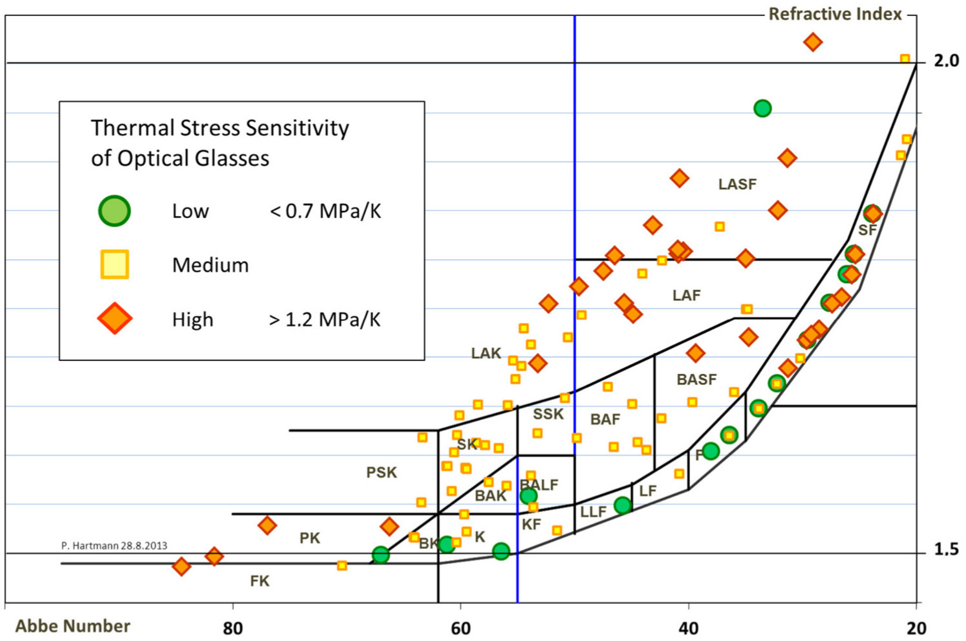

Figure 8.5 Abbe diagram with glass types categorized according to thermal stress sensitivity.

Chapter 9

Environmental Properties

Optical glasses are molten from well-defined mixtures of raw materials. Generally, they are substances of variable compositions, which are expressed by convention as oxides of the constituent elements (for example, SiO_2, Na_2O, CaO, B_2O_3). However, they are not a mixture of individual compounds such as metals or oxides. In fact glass is a noncrystalline inorganic macro-molecular structure. During the melting process, the raw materials react, creating a new chemical substance that is completely different from the starting materials. The physico-chemical, toxicological, and eco-toxicological properties of the substance called glass are totally different from those of the raw materials or oxides from which it is made.

Separation of glasses back into their elements or their oxides is possible only with a high degree of effort and does not occur naturally. All other glass constituents, be they harmless, toxic, or possibly harmful substances such as arsenic oxide, boron oxide, and lead oxide are withdrawn from bioavailability by being melted into glass; thus, they no longer can cause harm to human beings or the biosphere. Raw material supply and melting processes are performed under strictly controlled environmental, health, and safety procedures that are enforced by constant surveillance and regular auditing.

Glass pieces in the bulk state are of no hazard at all. Subsequent transformation to optical elements such as lenses and prisms by grinding and polishing creates grinding sludge, which consists of fine glass powder and a liquid cooling agent. Dry, potentially inhalable powder is prevented from becoming airborne because, while drying, the sludge bakes together, forming bulk waste. This waste must be treated according to local regulations, regardless of its actual composition.

End-of-life optical components, even when removed from their housings and fixtures, will cause no harm because any leakage into waste dumps will be negligibly low, and in incineration plants, glass will be deformed or broken but not disintegrated into its predecessor raw materials.

Recycling of optical glass is not an option because glass types used in an optical system cannot be identified without lengthy investigation. Moreover, collectable amounts of optical glass would be so small that any effort would not be worthwhile from an economic point of view. Additionally, the quality requirements on optical glass are so high that any use of material with properties not precisely known would cause far higher economic losses than what could possibly be saved by recycling.

The regulations restricting or prohibiting the use of chemical elements or their inorganic compounds, such as the European Union (EU) regulation on restriction of certain hazardous substances (EU-RoHS) and the chemical law EU-REACH were not meant to apply to glass.[1,2] To date, possible formal prohibitions, with their potentially adverse consequences on optical technology, have been avoided, and this must continue. For example, lead-containing glass types are absolutely critical for fluorescence microscopy. The glass types with lead-substitution elements have blue–violet transmission so low that their application as replacement glasses is impossible (see Figs. 9.1 and 9.2).

Presently, there exists an exemption of optical glasses from the prohibitions of EU-RoHS that will need to be extended in 2016.[3] Under the EU regulation REACH, glass is classified as a substance of unknown or variable composition, a complex reaction product, or a biological material (UVCB). It is exempt from the REACH registration requirement.

The use of thorium oxide as a raw material was prohibited more than 30 years ago. Since then, substances with elevated radioactivity have no longer been used. Optical glasses have radioactivity levels no higher than those of any currently and commonly used materials.

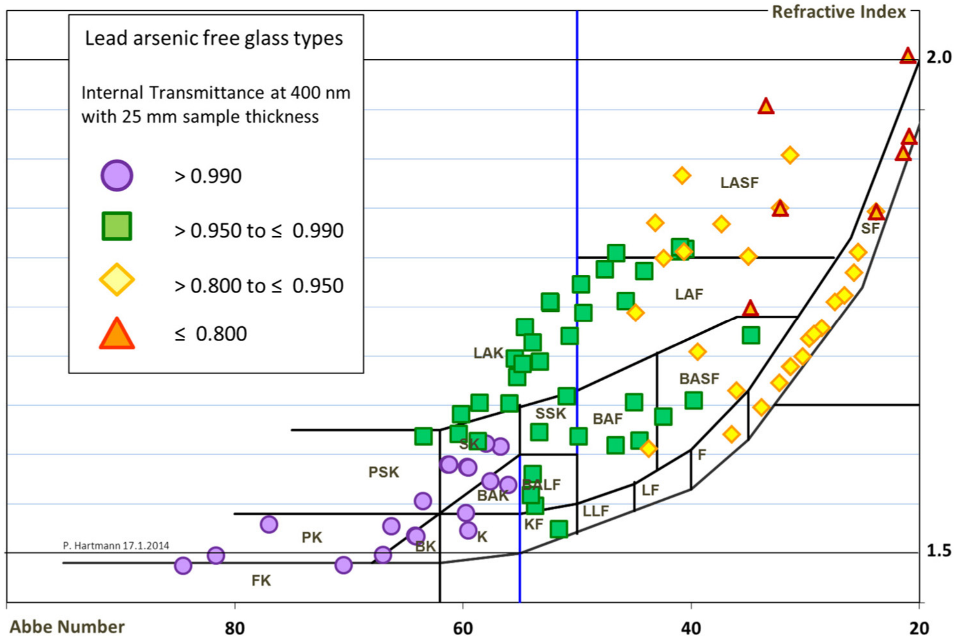

Figure 9.1 Abbe diagram with lead- and arsenic-free glass types ranked according to their internal transmittance.

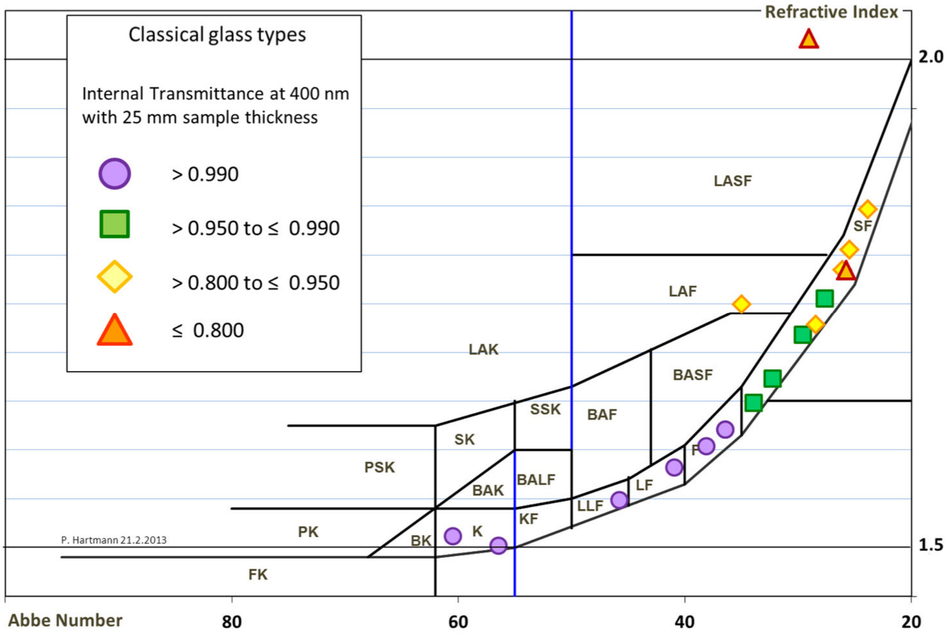

Figure 9.2 Abbe diagram with classical lead- and arsenic-containing glass types ranked according to their internal transmittance. Comparison with Fig. 9.1 shows that the range of high-transmittance glass types extends to higher refractive-index positions than those of lead- and arsenic-free glass types.

References

1. P. Hartmann and U. Hamm, "Optical glass and the EU directive RoHS," *Proc. SPIE* **8065**, 806511 (2011) [doi: 10.1117/12.882922].
2. P. Hartmann, "Optical glass: past and future of a key enabling material," *Adv. Opt. Techn*. **1**, 5–10 (2012).
3. P. Hartmann, "EU regulations threaten availability of raw materials for optics," *SPIE Professional* **4** (April) (2014) [doi: 10.1117/2.4201404.11].

Chapter 10

Specification of Optical Elements: Recommendations for Optical Glass Properties and Optical Element Manufacturing

Some explanation of the way in which optical glass properties change with size will be helpful for finding adequate material specification tolerances of optical elements.[1] Detrimental effects of stress birefringence, bubbles and inclusions, homogeneity, and striae become prominent only for larger glass items. With decreasing item size, especially its thickness, these effects decrease more quickly than linearly. Therefore, for small items some of these effects can simply be ignored (stress birefringence, homogeneity, and striae). This is because the residual wavefront deviations will be, by far, smaller than any requirements, and even smaller than sophisticated measurement methods can detect. Here it is necessary to specify only the use of optical glass in general. The remaining material imperfections, bubbles and inclusions, in small lenses will be treated in a different way than in larger items. They will not be judged by their size and number but just by their presence or absence. In day-to-day business, the value of a small lens will not justify any considerations about allowable bubble content. It will be simply discarded, regardless of the size of the bubble. Thus, this becomes a matter of lens batch yield, not of detailed single lens evaluation. The portion of items to be rejected must remain below a reasonable limit that is agreed upon between the glass supplier and the optical company.

With these size-scaling effects taken into account together with the high-material-quality standard reached by optical glass manufacturers, further simplification of optical element specification can be achieved by introducing default quality levels for the different material characteristics. This has been done in Table 10.1 (see page 148), where information is given for each material characteristic. In order to specify optical elements that are adequate for the functional requirements and for the main manufacturing processes (Fig. 10.1 on page 147), it is appropriate to separate them into three categories with respect to the element's size. The size values discussed do not have precise limits but serve as a guideline.

10.1 Small, thin lenses (diameter <30 mm and thickness <5 mm)

By far, most of these lenses are produced with precise pressing processes. Optical raw glass forms such as strips, blocks, or rods are cut, ground, and polished to preforms (spheres, lenses, disks). An alternative way is to produce preforms with fire-polished surfaces directly from molten glass. These are called precision gobs. These preforms with high-quality surface polish are pressed at the lowest possible temperature into their final lens shape and then rapidly cooled. The objective of this process is to achieve finished lenses in a very cost-effective manner; therefore, the process must exclude additional time-consuming fine-annealing processes. The precise pressing/cooling cycle of less than 30 min puts restrictions on the size—especially the thickness—of the elements. Cooling in such a short timeframe is equivalent to cooling rates of about 1000 K/h and higher. Such coarse annealing cannot be applied to thick glass items because of the high stress birefringence it would introduce.

The restriction of small thickness, on the other hand, has beneficial consequences on the material properties of such lenses. Homogeneity and striae quality are far better than needed for all applications of small lenses. Thus, specific tolerances on these characteristics are not necessary if it is required that these lenses are made from optical glass.

10.2 Medium-sized lenses and prisms (diameter or maximum edge length from 10 to 100 mm and thickness from 5 to 20 mm)

Optical elements in this size category are made following the reheat pressing process. Optical raw glass forms such as strips or blocks are cut or cracked into cubes with slightly higher volume than that of the element. After some preparation (weight adjustment and tumbling), they are heated to temperatures higher than those used for precise pressing and formed to a near-net-shape optical element preform. Directly after pressing, they are cooled rapidly. When the pressing batch is completed, they are collected in a lot and subjected to a subsequent tempering process called fine annealing. Here, cooling rates of about 10 K/h are applied.

Due to the fine-annealing process per se and the still-moderate thickness, low stress birefringence can be expected without any special required tolerance. This also holds for homogeneity and striae quality. The thicker and larger the element, and the higher the functional requirements, the more likely it will be necessary to specify these properties with explicit requirements.

10.3 Large lenses and prisms (diameter or maximum edge length >100 mm and thickness >20 mm)

These elements as a rule are made from fine annealed optical raw glass forms (annealing rate about 1 K/h), such as blocks and prisms, by cutting, grinding, and polishing. For high-precision optics, it is necessary to specify all properties.[2] This is especially required if there is a long light path in the optical element, as frequently occurs with prisms. In prisms, the light path may be much longer than the maximum edge length, whereas, in lenses, it will be not much longer than the lens thickness.

If the net element is still significantly smaller than the raw glass form, some beneficial effects may be exploited. Cutting a raw glass form into pieces smaller by a factor of two in thickness or width significantly reduces the residual mechanical stress and thus the stress birefringence. So, even for elements specified with very low stress birefringence, raw glass can be used with higher stress birefringence since it will collapse while being cut. Such a ratio between gross and net shape also allows for position optimization with respect to striae and bubble and inclusions content. In order to achieve high homogeneity, it is recommended to not position the element for cutting too close to the edge of the original cast surface of the raw glass form. It may be necessary to inspect prisms in two perpendicular directions with respect to striae content.

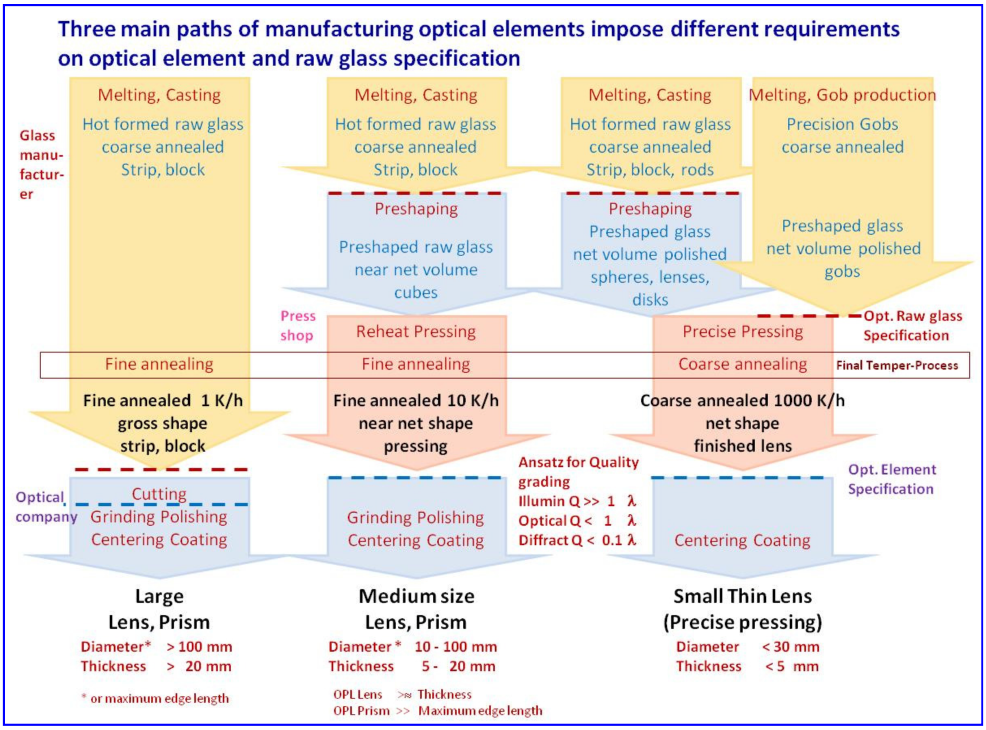
Three main paths of manufacturing optical elements impose different requirements on optical element and raw glass specification
Glass manu-factur-er
Melting, Casting
Hot formed raw glass coarse annealed Strip, block
Melting, Casting
Hot formed raw glass coarse annealed Strip, block
Melting, Casting
Hot formed raw glass coarse annealed Strip, block, rods
Melting, Gob production
Precision Gobs coarse annealed
Preshaping
Preshaped raw glass near net volume cubes
Preshaping
Preshaped glass net volume polished spheres, lenses, disks
Preshaped glass net volume polished gobs
Opt. Raw glass Specification
Press shop
Reheat Pressing
Precise Pressing
Fine annealing
Fine annealing
Coarse annealing
Final Temper-Process
Fine annealed 1 K/h gross shape strip, block
Fine annealed 10 K/h near net shape pressing
Coarse annealed 1000 K/h net shape finished lens
Ansatz for Quality grading
Illumin Q >> 1 λ
Optical Q < 1 λ
Diffract Q < 0.1 λ
Opt. Element Specification
Optical company
Cutting
Grinding Polishing Centering Coating
Grinding Polishing Centering Coating
Centering Coating
Large Lens, Prism
Diameter* > 100 mm
Thickness > 20 mm
* or maximum edge length
Medium size Lens, Prism
Diameter* 10 - 100 mm
Thickness 5 - 20 mm
OPL Lens >≈ Thickness
OPL Prism >> Maximum edge length
Small Thin Lens (Precise pressing)
Diameter < 30 mm
Thickness < 5 mm

Figure 10.1 Schematic diagram of optical element production process from optical raw glass production to the finished element according to three categories with respect to the elements' size (OPL is optical path length).

Table 10.1 Recommendations for raw optical glass specification. Default quality denotes the minimum quality an optical glass supplying company should provide. In cases of doubt, a default quality should be explicitly specified.

Characteristic/ default quality	Large lenses	Medium-sized lenses	Small, thin lenses
Stress birefringence Fine annealing: 10 nm/cm Coarse annealing: 20 nm/cm	From fine annealed strip or block glass with representative or individual inspection. If the raw glass part is much thicker than the element, stress birefringence may be twice as high as specified for the element.	Usually fine annealed optical glass default is sufficient. Special specification is needed only for very critical requirements	Coarse annealed optical glass default is sufficient. Due to the small thickness of the element, no significant stress birefringence will evolve in standard precise pressing process.
Bubbles and inclusions For lenses with diameters up to: 10 mm: 1 × 0.1 32 mm: 1 × 0.15 100 mm: 3 × 0.2 180 mm: 4 × 0.3 320 mm: 4 × 0.4	Fine annealed strip or block glass will be inspected individually. The position of the element in the raw glass form will be optimized for minimum bubble content.	Usually, optical glass default is sufficient. Special specification is needed only for critical requirements.	Optical glass default quality is sufficient.
Striae 60-nm wavefront distortion per 50-mm glass thickness	Fine annealed strip or block glass will be inspected individually. The position of the element in the raw glass form will be optimized for minimum striae content. Large prisms may require inspection in two perpendicular directions.	Usually, optical glass default is sufficient. Special specifications are needed only for critical requirements.	Optical glass default quality is sufficient.
Optical homogeneity Refractive index variation p-v 40×10^{-6} per 50-mm diameter	Fine annealed strip or block glass will be inspected individually. The position of the element in the raw glass form will be optimized for best homogeneity. Usually, interferometric measurements are made at 632-nm wavelength and cannot be made up to the very edge but only to a circular rim zone of 10 mm.	Usually, optical glass default is sufficient. Special specification is needed only for critical requirements.	Optical glass default quality is sufficient.

The optical glass melting process alone does not influence the final material quality of an optical element. The actual melt establishes a quality level in almost all essential characteristics such as refractive index, dispersion, homogeneity, striae, bubbles and inclusions, and stress birefringence. This level is specified, but it is only preliminary since it will be changed by subsequent processes. Only transmittance will be hardly influenced any longer.

The final cooling process of optical glass has decisive influence on the precise values of the refractive index, dispersion, homogeneity, and stress birefringence. In this process, often called the annealing process, optical glass is cooled, usually with a constant rate, within the range of about 150 °C directly below the transformation temperature T_g, which is a glass-type-specific temperature. At T_g a glass completely loses its internal stress within a short time (about 15 min).

For refractive index and dispersion holds, the faster the annealing rate in this special temperature range, the stronger are the changes. For homogeneity and stress birefringence, the temperature gradients occurring within the 150 °C range below T_g are decisive for the values they acquire at room temperature. The temperature gradients are not only determined by the annealing rate (linearly) but also by the thickness of the low-temperature conducting glass item (with thickness squared).

Bubbles and inclusions as well as striae quality can be influenced for given melts only by glass inspection and selection. Hence, for optical element specification it is helpful to take size, thickness, and general manufacturing process types into account.

References

1. P. Hartmann and R. Jedamzik, “Optical glasses and optical elements: Comparison of specification standards ISO DIS 12123 and ISO 10110,” *Proc. SPIE* **7102**, 71020L (2008) [doi: 10.1117/12.797568].
2. P. Hartmann, H. F. Morian, and R. Jedamzik, “Optical glasses and glass ceramics for large lenses and prisms, *Proc. SPIE* **4411**, 6–20 (2002) [doi: 10.1117/12.454884].

Chapter 11

Other Optical Materials

11.1 General Requirements on Materials for Optical Elements

Materials to be used for optical elements must fulfil some general requirements in order to find considerable application. Many of these requirements are also listed in Section 1.4:

- high light transmission,
- precise light deflection,
- high optical homogeneity,
- low birefringence,
- high material homogeneity, clarity (content of bubbles, inclusions, single crystals, clouds of submicroscopic grains: haze, crystallization), and
- suitable behavior in optical element production processes under normal environmental influences (mechanical and chemical resistance).

All of these properties must be:

- well defined as a physical quantity,
- measureable with sufficient accuracy,
- reproducible, and
- constant in minimum piece size and lot size.

Compliance with all of these requirements must be checked before a new material can be introduced for optical element production. Moreover, production and quality assurance costs must be low per element. A lens from optical glass may serve as a comparison measure. If an element replacing one or more of such glass lenses costs considerably more than this lens, the new material will be used only if it is capable of providing a special additional advantage.

11.2 Other Materials Used for Optical Elements

Other materials used for optical elements are plastics, crystals, and fused silica glass.[1,2] The advantages of plastics are:

- low weight,
- high breakage strength,
- low price, and
- versatility in shaping as complex multifunctional elements with mechanical elements for mounting or alignment with low price for large quantities.

Disadvantages of plastics are:

- inferior imaging quality,
- sensitivity to scratching, humidity, temperature, and UV light,
- economic application only for large quantities possible due to high mold costs,
- much smaller ranges of refractive index and Abbe number (color dispersion):
    - maximum refractive index is 1.74,
    - high-index, low-dispersion materials (left upper range) are non-existent,
    - low-index, low-dispersion materials are non-existent; maximum Abbe number is 59,
- refractive index tolerances at least a factor of ten wider,
- low birefringence possible only with additional effort, and
- optical homogeneity unknown and possibly unsuitable for larger elements with higher thickness.

One of the crystals commonly used for optical elements is calcium fluoride. Its advantages are:

- wide transmittance range from 150 nm to 8 μm,
- very low dispersion,
- very high deviation from glass normal lines of partial dispersion; attractive material for color correction,
- precisely defined refractive index and dispersion variations negligible for most applications,
- high homogeneity (10^{-6} and better) possible,
- low birefringence possible, and
- large disks possible.

Disadvantages of calcium fluoride crystal are:

- very high expense and
- very delicate material for handling.

Fused silica is also a glass, but it differs from optical glass in that it is produced by chemical vapor deposition. Its advantages are:

- wide transmittance range from 180 nm to 4 μm,
- very low absorption possible,
- low dispersion,
- precisely defined refractive index and dispersion,
- high homogeneity (10^{-6} and better) possible,
- low birefringence possible,
- large disks possible,
- low thermal expansion,
- high application temperature possible, and
- thermo-shock resistive.

Disadvantages of fused silica are:

- expensive and
- refractive-index/dispersion combination not very attractive.

Although opto-ceramics have attractive refractive-index/dispersion combinations, they have not found significant applications up to now due to the fact that they are produced with high-temperature iso-static pressing in batches. This process is expensive per se and has not yet been shown to be mastered reliably enough to pass inspections of refractive index variations, optical homogeneity, and stray light. This proof would be a necessary precondition to approaching cost regions where one could start considering replacing optical glass elements. Figure 11.1 is an Abbe diagram showing the positions of optical glasses, optical plastics, calcium fluoride (CaF_2), and potential opto-ceramics.

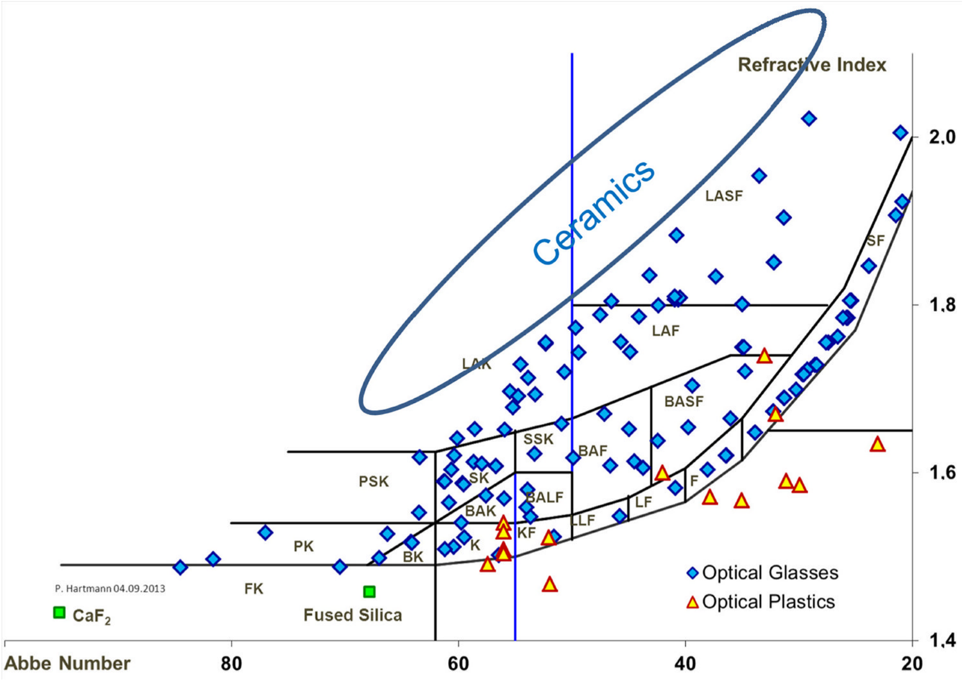

Figure 11.1 Abbe diagram with optical glasses and optical plastics, calcium fluoride, fused silica, and the position range of opto-ceramics.

References

1. I. D. Nikolov and C. D. Ivanov, "Optical plastic refractive measurement in the visible and the near-infrared regions," *App. Opt*. **39**(13), 2067 (2000).
2. T. Westerhoff, K. Knapp, and E. Moersen, "Optical materials for microlithography applications," *Proc. SPIE* **3424**, 10 (1998) [doi: 10.1117/12.323750].

Standards

1. ISO 7884 Part 8, Glass—viscosity and viscosimetric fixed points—Determination of (dilatometric) transformation temperature, International Organization for Standardization, Geneva (1987).
2. ISO 7944 Optics and optical instruments—Reference wavelengths, International Organization for Standardization, Geneva (1998).
3. ISO 8424 Raw optical glass—Resistance to attack by aqueous acidic solutions at 25 °C—Test method and classification, International Organization for Standardization, Geneva (1996).
4. ISO 9385 Glass and glass ceramics—Knoop hardness test, International Organization for Standardization, Geneva (1990).
5. ISO 9689 Raw optical glass–Resistance to attack by aqueous alkaline phosphate-containing detergent solutions at 50 °C–Testing and classification International Organization for Standardization, Geneva (1990).
6. ISO 9802 Raw optical glass—Vocabulary International Organization for Standardization, Geneva (1996).
7. ISO 10110 Part 1: Optics and photonics—Preparation of drawings for optical elements and systems—General, International Organization for Standardization, Geneva (2006).
8. ISO 10110 Part 2: Optics and photonics—Preparation of drawings for optical elements and systems—Material Imperfections—Stress Birefringence, International Organization for Standardization, Geneva (1996).
9. ISO 10110 Part 3: Optics and photonics—Preparation of drawings for optical elements and systems—Material Imperfections—Bubbles and inclusions, International Organization for Standardization, Geneva (1996).
10. ISO 10110 Part 4: Optics and photonics—Preparation of drawings for optical elements and systems—Material Imperfections—Inhomogeneity and Striae, International Organization for Standardization, Geneva (1997).
11. ISO 10629 Raw optical glass—Resistance to attack by aqueous alkaline solutions at 50 °C—Test method and classification, International Organization for Standardization, Geneva (1996).

12. ISO 11455, Raw optical glass—determination of birefringence, International Organization for Standardization, Geneva (1995).
13. ISO 12123 Optics and photonics—Specification of raw optical glass, International Organization for Standardization, Geneva (2010).
14. ISO 12844 Raw optical glass—Grindability with diamond pellets—Test method and classification, International Organization for Standardization, Geneva (1999).
15. ISO/DIS 17411 Draft international standard Optics and photonics—Optical materials and components—Test method for homogeneity of optical glasses by laser interferometry, International Organization for Standardization, Geneva (2013).
16. ANSI / OEOSC OP3.001-2001 American National Standard for Optics and Electro-Optical Instruments—Optical Glass, American National Standards Institute (2001).
17. MIL-G-174B, Military Specification Glass, Optical, U.S. Army Armament Research and Development Center (1986)–obsolete.
18. DIN 3140 Part 2, Inscriptions of dimensions and tolerances for optical component; bubbles, German Institute for Standardization (1978)–obsolete.
19. DIN 3140 Part 3, Inscriptions of dimensions and tolerances for optical component; striae, German Institute for Standardization (1978)–obsolete.
20. DIN 3140 Part 4, Inscriptions of dimensions and tolerances for optical component; strains, German Institute for Standardization (1978)–obsolete.
21. JOGIS—Japanese Optical Glass Industrial Standards (2007).

Bibliography

1. H. Scholze, *Glass—Nature, Structure and Properties*, English translation of German edition, Springer-Verlag, New York, Berlin, Heidelberg (1991).
2. W. Vogel, *Glass Chemistry*, Springer-Verlag, Berlin, Heidelberg, Second edition (1994).
3. H. Bach and N. Neuroth, Eds., *The Properties of Optical Glass*, Springer-Verlag, Berlin, Heidelberg (1998).
4. H. Bach and D. Krause, Eds., *Low Thermal Expansion Glass Ceramics* Springer-Verlag, Berlin, Heidelberg (2005).
5. T. S. Izumitani, *Optical Glass*, Kyoritsu Shuppan Co., Ltd. (1984); English version, Lawrence Livermore National Laboratory (1985).
6. E. Hecht, *Optics*, Addison-Wesley Longman, Reading, MA (2002).
7. F. L. Pedrotti, L. S. Pedrotti, and L. M. Pedrotti, *Introduction to Optics*, Pearson Prentice Hall, Upper Saddle River, NJ (2007).
8. M. Born and E. Wolf, *Principles of Optics: Electromagnetic Theory of Propagation, Interference and Diffraction of Light*, Seventh ed., Cambridge University Press, Cambridge (1999).
9. H. Gross, *Handbook of Optical Systems*, Vol. 1, *Fundamentals of Technical Optics*, Wiley VCH, Berlin (2005).
10. H. Gross, H. Zügge, M. Peschka, and F. Blechinger, *Handbook of Optical Systems*, Vol. 3, *Aberration Theory and Correction of Optical Systems*, Wiley VCH, Berlin (2007).
11. D. Malacara, Ed., *Optical Shop Testing*, Third edition, Wiley, New York (2007).
12. G. Schröder, *Technische Optik: Grundlagen und Anwendungen*, Vogel Industrie Medien GmbH & Co. KG, Würzburg (1998).
13. H. W. McKenzie and R. J. Hand, *Basic Optical Stress Measurement in Glass*, Society of Glass Technology, Sheffield, UK (1999).
14. SCHOTT Technical Information on Optical Glass:
    http://www.us.schott.com/optics_devices/english/download/

Index

Abbe, Ernst, 5
Abbe diagram, 13
Abbe number, 9–11
abrasive hardness, 130
absorption centers, 118
absorption edge, 108
achromatic doublet, 4
acid, 122
acidic solutions, 121
anisotropy, 92
annealing history, 7, 9
annealing line, 47
annealing line diagrams, 46
annealing parameters, 29, 46
annealing point, 27, 135, 138
annealing schedules 28
aqueous solutions, 121
artificial striae, 90
aspheric lenses, 13
aspheric optical elements, 29
atmospheric air pressure, 62
atomic bonds, 105, 115
atomic structure, 131

brittle, 135
brittle elastic, 128
brittle elastic solid, 23
bubbles, 8
bubbles per test volume, number of, 103

calcium fluoride, 152
cerium-doped glass types, 118
characteristic strength, 133
characteristic viscosity point, 138
chemical composition, 9, 47
chromatic aberration, 3
clarity, 105
clay pot, 19
cleaning processes, 122
clear white glass, 3
climate resistance, 122
coarse annealing, 26
coefficient of thermal expansion, 98
compensation method, 95
compressive stress, 24
constant-rate annealing, 45
consumer optics, 30
continuous melting tank, 6, 20
cooling history, 7
cooling process, 149
crack growth velocity, 132
crown glass, 4, 10
crystallization, 8, 14
crystals, 151

data sheet, 9
default quality levels, 145
diffraction, 77
dispersion, 8, 34
dry environment, 132
dual-beam spectral photometer, 106
ductility, 131

edge zones, 82
electron–hole pair, 117
end-of-life optical components, 141
energy dose, 118
environmental humidity, 121
esthetics, 101
EU-RoHS, 142

fatigue, 131–132
figure of merit, 98
fine annealing, 23, 25, 26
fingerprints, 122
flint glass, 4, 10
fluorescence microscopy, 142
fluoro-phosphate crown, 107
fluoro-phosphate glass, 6
focus term, 85
four-edge loading setup, 95
fraction of aperture, 91
Fraunhofer lines, 4
Fresnel reflection, 105
fringe frequency method, 95
fused silica, 151, 152

general requirements, 151
glass composition, 5, 7, 8
glass element sizes, 83
glass homogeneity, 4
glass thickness, 110
glass types, 8
grade denominations, 43
grade number, 104
grain size distribution, 132
grinding and polishing agents, 121
grinding efficiency, 130
grinding sludge, 141

haze, 8
healing effect, 117
heat management, 112
high-refractive-index glasses, 111
high-transmission (HT) grades, 112
homogeneity specification, 79
Hooke's law, 128

i-line microlithography, 6
i-line wafer steppers, 120
immersion oil, 81
incineration plants, 141
inclusions, 8
indentation, 129
index drop, 31
index of refraction, 8
inhomogeneity, 7, 25
initial crack depth, 132
integrating sphere, 106
interference fringes, 80
interferometers, 78
intermelt variation, 66
internal transmittance, 8
ionization, 106
iron straight line, 37
ISO 12123, 11, 78
iso-static pressing, 153

lanthanum glass, 6
large blanks, 85
large glass items, 47
large lenses, 96
large optical elements, 63
large optical glass disks, 99
large pieces, cutting of, 96
large prisms, 92
lateral faces, 85
leaching, 121
lead- and arsenic-free glass types, 6, 51, 127
liquid state, 135
Loewe interferometer, 84
long light path, 82, 147
long working distance, 102
low-T_g glasses, 30
luminescence, 115
lye, 122

material imperfections, 101
measurement uncertainty, 59
mechanical resonance, 128
mechanical stress, 7
metrology, 2
micro-crack growth, 132
micro-cracks, 131
microscope, 1
monochromators, 106

natural cast surfaces, 82
normal glasses, 37

oil-on plates, 81
oil-on-plate method, 80
optical design, 6
optical homogeneity, 8, 78
optical instruments, 1
optical path difference, 93
opto-ceramics, 153

peak-to-valley, 82
phosphate resistance, 122
phosphorescence, 115
plane wavefronts, 77
plastically deformable, 136
plastics, 151
poise, 135
Poisson's ratio, 98
polarization, 99
polarization, elliptical, 98
precise molding technology, 6, 135
precision gobs, 30, 146
preforms, 146
press shops, 103
pressings, 47
principal refractive index, 43
processing water, 121
production batches, 21

quarter-wave plate, 99

raw optical glass, 33
recycling, 141
refining, 20
refining agents, 20
reflection factor, 106
refractive index homogeneity, 77
refractive index variation, 43
reheat pressing, 135, 146
relative partial dispersions, 36
reproducibility, 5
residual water, 106
resistance, mechanical and chemical, 8
resolution, 6
rim zone, 82

satellite optics, 118
Sellmeier coefficients, 61
Sellmeier formula, 41
size-scaling effects, 145
soak annealing, 45
softening point, 135
spectral emission intensity, 115
spectral lines, 35
stabilization, 118
stain resistance, 122
standard air, 33
statistical significance, 133
stitching, 85
strain point, 135
stress birefringence, 7, 8, 25
stress-optical coefficient, 94
stress tensor, 100
striae, 77
striae grades, 91
strip drawing, 89
subapertures, 85
surface condition, 132

tank melting, 89
telescope, 1
temperature change rate, 23
temperature difference, 23
temperature gradients, 63, 139
temperature history, 139
tensile stress, 7, 24, 131–132
thermal conductivity, 23
thermal diffusivity, 97
thermal equilibrium, 7
thermal gradients, 96
thermal lensing, 114
thermal stress coefficient, 98
thermal stress factor, 140
thorium oxide, 142
tilt, 84
torsion modulus, 128
toxicology, 141
transformation range, 23, 136
transformation temperature, 7, 24, 27

transient stress, 27
transmission haze, 122

UV absorption edge, 106
UV cutoff edge, 111

Van Allen radiation belt, 118
variable composition, substances of, 141
vibrations, 107
viscosity, 23
visible surface changes, 122
visual comparison, 91
volume constancy, 77

waste dumps, 141
water, 132
water-saturated atmosphere, 122
wavefront distortion, 77
wavefront shift, 84
wavefront-variation grades, 91
wedge, 82
Weibull distribution, 132
working point, 135

Young’s modulus, 98

Zernike series expansions, 84

Peter Hartmann received his Doctorate in Physics in 1984 from the University of Mainz, Germany. His thesis was on scintillation glasses made at the nuclear physics department of the Max-Planck-Institute for Chemistry in collaboration with Schott Glaswerke. In 1985, after serving as head of a geometrical metrology group in the automotive industry, Dr. Hartmann joined the optics division of Schott. Since then, he has been responsible for quality assurance, metrology development, and advising customers on optical glasses and the zero-expansion glass ceramic ZERODUR®. He has been responsible for projects such as extremely high-quality optical glass for i-line microlithography, and mirror blanks for large astronomical telescopes (Keck I and II, CHANDRA, ESO-VLT, GRANTECAN, and several 4-m telescopes). Since 2007, he has been the Director of Marketing and Customer Relations of Advanced Optics at SCHOTT AG.

Dr. Hartmann served on the Board of Directors of SPIE from 2011 to 2013 and is active in international standardization as a convener of the ISO working group for optical materials. He is a member of the board of the Optics and Photonics Cluster OPTENCE, Hesse/Rhineland-Palatinate, Germany and of the Board of Trustees of the Max-Planck-Institute for Astronomy, Heidelberg, Germany. He is Fellow of SPIE.

OPTICAL GLASS

Peter Hartmann

For more than 400 years, optical glass has provided mankind with a window into both the hidden microcosm and vast outer cosmos of the known universe, transforming philosophy, science, and engineering through its visage and, thus, shaping modern civilization. Its high transmittance, homogeneity, and precisely defined light refraction properties are the preconditions for highly resolved true-color imaging, making it an intrinsic component of technology in general. From consumer products, such as cameras and binoculars, to microscopes and telescopes—the most essential tools of research in many fields—the role of optical glass is integral to the very foundations of modern science and industry.

In contrast to its fundamental importance, there is often a lack of knowledge regarding the properties of optical glass by engineers and designers, causing misunderstandings in purchasing and fabrication, and ultimately limiting the potential and application of this dynamic material. This book will serve as an invaluable resource of technical information, including the index of refraction and its dependence on wavelength (dispersion), optical homogeneity and transmittance (presented together with restrictions imposed by the manufacturing processes and chemical resistance), as well as mechanical, thermal, and environmental properties. Measurement methods with their achievable accuracy are given, along with a wide scope of overview diagrams illustrating properties and main uses, as well as diagrams ranking optical glass types with respect to their properties. The wide scope and lucid organization of this volume will prove to be highly valuable across a wide range of design, engineering, and purchasing applications within the many fields dependent on this incredible material.

ISBN 978-1-62842-1292-5
90000
9 781628 412925

SPIE.

P.O. Box 10
Bellingham, WA 98227-0010

ISBN: 9781628412925
SPIE Vol. No.: PM249